“Humatos de hierro: caracterización, estudio y mejora de la eficacia en la nutrición férrica de plantas de Estrategia I en suelos calizos”

“Iron humates: characterization, evaluation and improvement in iron nutrition of Strategy I plants grown in calcareous soils”

TESIS DOCTORAL

María Teresa Cieschi Villalba

Madrid 2019

Departamento de Química Agrícola y Bromatología
Facultad de Ciencias
Universidad Autónoma de Madrid

TESIS DOCTORAL

"Humatos de hierro: caracterización, estudio y mejora de la eficacia en la nutrición férrica de plantas de Estrategia I en suelos calizos"

"Iron humates: characterization, evaluation and improvement in iron nutrition of Strategy I plants grown in calcareous soils"

Maria Teresa Cieschi Villalba
MADRID, 2019

Departamento de Química Agrícola y Bromatología
Facultad de Ciencias
Universidad Autónoma de Madrid

"Humatos de hierro: caracterización, estudio y mejora de la eficacia en la nutrición férrica de plantas de Estrategia I en suelos calizos"

"Iron humates: characterization, evaluation and improvement in iron nutrition of Strategy I plants, grown in calcareous soils"

Memoria presentada para aspirar al Título de Doctor en Química Agrícola con mención internacional por la Universidad Autónoma de Madrid

Fdo: María Teresa Cieschi Villalba
Licenciada en Química

Director:

Fdo: Juan José Lucena Marotta

Catedrático Universidad Autónoma de Madrid

La presente memoria ha sido financiada por los siguientes proyectos:

- Proyecto Validación de un nuevo producto para la corrección de la clorosis férrica. Financiado por Fertinagro Nutrientes S. L. (2013-2015).
- Proyecto AGL2013-44474-R Fertilización de cultivos a través de empleo de fertilizantes. Ministerio de Economía y Competitividad (MINECO).
- Proyecto AGRISOST-CM S2018/BAA-4330. Tecnología destinada a la sostenibilidad de los sistemas. Financiado por la Comunidad de Madrid.
- Proyecto RTI2018-096268-B-I00. Nuevos fertilizantes de micronutrientes y bioestimulantes: criterios de eficación y mecanismos de acción. Financiado por el Ministerio de Ciencia, Innovación y Universidades (MICINNU).

Y de las siguientes becas:

- Beca de prácticas formativas de posgrado en el Departamento de Química Agrícola Y Bromatología concedida por la Fundación de la Universidad Autónoma de Madrid (FUAM).
- Beca de movilidad internacional para colaborar con la Lomonosov Moscow State University concedida por la Alianza 4 Universidades en el marco del programa Erasmus+ KA107 International Credit Mobility.

Los resultados de la presente tesis fueron expuestos en los siguientes Congresos:

- First Joint Meeting on Soil and Plant System Sciences (SPSS 2019). Natural and Human-induced Impacts on the Critical Zone and Food Production. Attendance and oral Communication: Are iron humates slow iron release fertilizers? September 2019. Bari. Italy.
- 8th International Symposium of the Interactions of Soil Mineral with Organic Components and Microorganisms (ISMOM 2019). Oral Communication: Efficiency of leonardite iron humate/synthetic chelates mixtures in soybean nutrition. June 2019. Sevilla. Spain.
- 19th International Conference of International Humic Substances Society. Attendance and poster presentation: Eco-friendly iron-humic nano-fertilizers tested with ^{57}Fe in calcareous soil. September 2018. Albena Resort. Bulgaria.
- 19th International Symposium on Iron Nutrition and Interaction in Plants (ISINIP 2018). July 2018. Taipei. Taiwan.

Posters presentation:

- Complexation of iron in humates and lignosulfonates.

- Valorization of iron ore tailings as fertilizers (HBED/Fe siderite, HBED/Fe Hematite-Goethite, and HS/Fe siderite, HS/Fe Hematite-Goethite).

- 4th International Conference of CIS IHSS on Humic Innovative Technologies (HIT 2017). Poster presentation: Importance of particle size in synthesis in iron humate fertilizers. October 2017. Moscow. Russia.

- XVI Simposio Hispano-Luso de Nutrición Mineral de las Plantas. Oral communication: Evaluation of the synergic effect of an iron leonardite with chelates in iron nutrition. September 2016. Murcia. Spain.

- 18th International Conference of International Humic Substances Society. Attendance and poster presentation: Role of an iron leonardite fertilizer in plant nutrition. September 2016. Kanazawa. Japan.

- 18th International Symposium on Iron Nutrition and Interaction in Plants (ISINIP). May 2016. Madrid. Spain.

Attendance and posters presentation:

- Kinetics effects of leonardite iron fertilizer in plant nutrition.

- Synthetic chelating and complexing agents as substrates on the ferric chelate reductase activity.

- Implications of the Fe/Ligand ratio and the Fe source on the complexes formation.

AGRADECIMIENTOS

En estos cinco años la vida ha dado muchas vueltas pero lo que empezó con más preguntas que respuestas, al fin se acaba. Hubo muchas personas que me han acompañado, que me han ayudado y alentado. Algunas que ya no están y otras que se han sumado en el camino. Todas han contribuido de diversos modos a que esta Tesis hoy sea una realidad.

Ante todo quiero agradecer al Dr. Juan José Lucena por haberme dado la posibilidad de emprender este desafío. Le agradezco la confianza, el cariño, su saber, su entusiasmo y las discusiones que construyeron nuestra relación profesional y humana.

Le agradezco a la Prof. Irina Perminova la oportunidad de trabajar con ella y su grupo en la Lomonosov Moscow State University. Le agradezco su generosidad, su confianza y su pasión por la ciencia. Fue una experiencia muy desafiante y muy enriquecedora desde lo profesional y lo existencial.

En estos años he aprendido mucho de mis profesores y les agradezco su interés por mi progreso en la tesis, por mi vida en España, por las noticias de Argentina. Gracias Agustín por el buen humor, gracias Eugenio por las charlas de tus viajes, gracias Lourdes por tu forma práctica de ver la vida, gracias Enrique y Elvira por tratar que las cosas sean lo más livianas posibles.

Quiero agradecer a Felipe por todos los cafés que me ha pagado y todas las veces que nos quejamos del sistema educativo y todas las veces que intentamos arreglar el mundo y todas las risas y los delirios compartidos.

Gracias a Sandra L. y Sandra C. por estar a la mano y toda la colaboración en lo cotidiano del laboratorio. Gracias a Silvia por estar pendiente en este tramo final de escritura y alentarme a terminar la tesis cueste lo que cueste.

Mil gracias a Virgi por un montón de momentos compartidos y las veces que me sacó las papas del fuego en mis inicios en el laboratorio. Gracias por las bromas, las confesiones y el cariño.

Gracias a Sam por tantas charlas y tantos silencios. Admiro muchísimo tu dedicación en el trabajo y espero que el futuro te regale las oportunidades que te mereces. Mexicana, ha sido un gran regalo compartir contigo el doctorado.

Quiero agradecer a Alex, Alejandra, Sara, Raquel, Begoña y Rafa por las comidas compartidas con buen humor, sazonadas de algún que otro debate, un poco de tontería y unas cuantas risas. Gracias por todos los aportes de Fernando y la cercanía de Javad. Gracias a Carlos,

Rebeca y Teresa, con los que he compartido parte de este camino y han sido un poco guía para mis pasos.

Quiero agradecer especialmente a Clara, la que considero mi mejor amiga en Madrid, por su apoyo incondicional, por el respeto y el cariño con el que me acompaña desde mis primeros días en España. Gracias por el cine de autor, el Benteveo, el senderismo, la política, el feminismo y las miles de anécdotas que tenemos juntas. Gracias por el ánimo y la alegría. Gracias por ser un poco mi familia y hacerme sentir en casa.

En estos años se han ido personas importantes para mí pero que seguro estarían felices con este logro. En primer lugar quiero agradecer a Rosa e Hilario, mis padres, por dejarnos a mis hermanos a mí la educación como la mejor herencia y por enseñarnos a mirar la vida siempre de frente, con sus luces y sus sombras. Y por supuesto, agradezco especialmente a Isa, que no solo me regaló la posibilidad de compartir la vida y el amor sino que además me alentó muchísimo, creyó en mí más que nadie y me empujó a embarcarme en esta aventura.

Quiero también agradecer a mi familia, a mis sobrinos Germán, Iván y Francisco, a mi cuñado José Luis y en especial a mi hermana, Ma. Rosa, por apoyarme, respetarme y acompañarme siempre en cada una de mis decisiones. Gracias por estar siempre a mi lado.

Por último quiero agradecer a Laurence, porque junto a ella la vida volvió a tener colores, proyectos y el empujón del amor para terminar la tesis. Gracias por ser el oasis en mi caos y por ofrecerme una familia. Gracias por el milagro de habernos encontrado y la osadía de seguir juntas.

“El romper de una ola no puede explicar todo el mar”

Vladimir Navokov (1899-1977)

A mi hermana

RESUMEN

La presente Tesis Doctoral pretende contribuir al estudio de la naturaleza y el mecanismo de acción de los humatos de hierro sintetizados a partir de leonarditas en el sistema suelo-planta, ya que representan una alternativa agroecológica de fertilización férrica a menor costo de plantas de Estrategia I que crecen en suelos calizos; igualmente se estudian vías de mejoras que se pretenden proponer para estos productos.

Los humatos férricos a partir de leonarditas son complejos naturales de hierro usados en la región Mediterránea mediante aplicación foliar o por fertirrigación en cultivos de alto valor económico como, por ejemplo, cítricos, melocotoneros y viñedos, todos ellos plantas de Estrategia I. Su eficiencia en la corrección de la clorosis férrica es inferior a la de los quelatos sintéticos de hierro, dada la complejidad estructural y fisicoquímica de las sustancias húmicas, que dependen del proceso diagenético que las origina. En la actualidad, el mercado de fertilizantes ofrece pocos productos en base a sustancias húmicas como correctores de carencias, dadas las exigencias legales a nivel europeo y español. Sin embargo, las recientes modificaciones en las directivas europeas respecto a fertilizantes de micronutrientes y la necesidad de reducir el impacto ambiental de las prácticas agrícolas actuales, renuevan el debate acerca de la eficacia de estos productos, y abren la posibilidad a un incremento de su uso y comercialización. Por lo tanto, en esta tesis se ha realizado una caracterización exhaustiva de dos tipos de leonarditas, una de origen africano y otra de origen alemán, observándose que ambas presentan hierro en forma de ferrihidrita, compuestos de hierro polinucleares y, en especial la africana, jarosita. Se ha estudiado el comportamiento cinético del humato férrico mediante experimentos de competencia de ligandos con *o,o*EDDHA, HBED y BPDS, observándose la alta estabilidad del humato.

Además, se han preparado complejos de hierro a partir de las leonarditas estudiadas y se han caracterizado los productos obtenidos a fin de evaluar su estabilidad y solubilidad en condiciones de suelo calizo. Se ha observado que los humatos férricos producen un efecto a largo plazo en la fertilización férrica de plantas de Estrategia I tanto en condiciones hidropónicas como en suelo cuando son cultivadas en cámara de cultivo (soja), así como también en experimentos de campo (mandarinos). Inicialmente, en hidroponía se observó la deposición y acumulación de humatos y de formas inorgánicas de hierro en las raíces de plantas de soja que afectó el crecimiento y desarrollo de las plantas, así como también la nutrición férrica. A tal efecto, como primera medida de mejora de estos productos, se estudiaron y corrigieron el modo de aplicación de los humatos férricos y la concentración utilizada, obteniendo a largo plazo resultados similares a los observados con quelatos sintéticos. Además, los humatos de hierro a

partir de la leonardita africana produjeron depósitos de jarosita en las raíces de plantas de soja, lo cual se considera una fuente de hierro potencialmente biodisponible para las necesidades nutricionales de la planta.

Como segunda opción de mejora en la eficiencia, se prepararon mezclas de humatos férricos con quelatos sintéticos de hierro y se aplicaron a plantas de soja que crecían en condiciones de suelos calizos. Se utilizaron isótopos estables de hierro (^{56}Fe y ^{57}Fe) a fin de estudiar la contribución de cada uno de los fertilizantes en la nutrición férrica de la planta. Se observó que el efecto de recarga de los quelatos con el hierro del suelo fue bajo pero mejoró la eficiencia de los humatos férricos y una leve sinergia entre el HBED/Fe^{3+} y los humatos férricos ya que el efecto a largo plazo de este quelato se suma al del humato.

Por último, como otra propuesta de mejora de estos productos por disminución del tamaño de partícula, se sintetizaron nanofertilizantes de humatos férricos. Su aplicación en soja confirmó la contribución de los humatos férricos en la nutrición férrica a largo plazo y se pudo observar su presencia en las vainas ya que los productos se habían preparado con ^{57}Fe. Aunque esta acción no arrojó mejores resultados a los obtenidos, se considera parte de una nueva tecnología dirigida hacia una agricultura sustentable y de precisión que precisa aún ser más investigada.

ABSTRACT

This thesis aims to contribute to the knowledge of the influences of the leonardite iron humates character and their behavior in the soil-plant system as a low-cost and an ecofriendly alternative in iron nutrition for the Strategy I plants when they grow in calcareous soils. Moreover, different methods to improve their efficiency were evaluated.

Leonardite iron humates are natural iron complexes commonly used in the Mediterranean basin to fertilize cash crops such as citrus, peach trees, and vineyards (Strategy I plants) by foliar application or by fertirrigation. They are less efficient in correcting iron chlorosis than synthetic iron chelates because their structural and physicochemical complexity depends on the diagenetic process which originated them. Currently, the fertilizer market offers only a few iron humates as correctors of iron deficiency because of the strict legal requirements at the European and Spanish regulations. However, due to the new European directives in micronutrient fertilizers and the need to reduce the environmental impact of current agricultural practices, the discussion about the effectiveness of these products is renewed as well as the opportunity to increase their use and commercialization. Therefore, two types of leonardite, one of African origin and another of German origin, were exhaustively characterized. Both products presented ferrihydrite and polynuclear iron compounds in their structures. In particular, the African one presented jarosite in its structure. Moreover, iron humates were also characterized to assess their stability and solubility under calcareous conditions. The kinetic behavior of the iron humate has been studied by ligand competition experiments using chelating agents such as o,oEDDHA, HBED, and BPDS. Iron humate presented high stability.

Iron humates exert a long-term effect on the iron fertilization of Strategy I plants in hydroponics (soybean) or soil experiment under controlled conditions as well as in field experiments (tangerines). Deposition and accumulation of humates and iron in the soybean roots were observed in hydroponic assays, and that affected on plant growth as well as in iron nutrition. So, as a first step in improving iron humates, the application mode and the concentration used were studied and corrected. Consequently, iron humates were so efficient at long term as iron synthetic chelates in providing iron ton soybean plants. Furthermore, iron humates from the African leonardite produced jarosite deposits in the soybean roots, which was considered a potentially and bioavailable iron source for the nutritional demands of plants.

As a second option in improving the iron humates efficiency, mixtures of iron humates with synthetic iron chelates in different ratios and doses were prepared and applied to soybean plants that grew in calcareous conditions. The mixtures were prepared using stable iron isotopes

(^{56}Fe and ^{57}Fe) in order to identify the contribution of each fertilizer to the iron nutrition. The iron chelate shuttle effect was low but improved iron humate efficiency and a slight synergy between iron humates and HBED/Fe^{3+} was observed because of its lasting effects fit better to the iron humate long-term effect.

Finally, leonardite iron humate nanofertilizers were prepared as an improvement option by decreasing particle size. Their contribution to iron nutrition was confirmed and their presence in soybean pods was observed. Although the nanofertilizers did not enhance the iron humate efficiency, they are part of novel technology in line with precision and sustainable agriculture so, further research is needed.

ÍNDICE GENERAL

INDEX

ABREVIATURAS \ ABBREVIATIONS

^{13}C-RMN:	Resonancia Magnética Nuclear en estado sólido ^{13}C	^{13}C Nuclear Magnetic Resonance
^{57}Fe-NFs:	Nanofertilizantes de humatos de ^{57}Fe	^{57}Fe humic nanofertilizers
AAS:	Espectroscopía de Absorción Atómica	Atomic Absorption Spectroscopy
BPDS:	Ácido batofenatrolindisulfónico	Bathophenanthroline disulfonic acid
CMC:	Categoría de materiales componentes	Component material categories
DTPA:	Ácido dietilentriaminopentaacético	Diethylenetriaminepentaacetic acid
EDDHA:	Ácido etilendiamino di (o-hidroxifenil-acético)	Ethylenediamine-di (o-hydroxyphenylacetic) acid
EDTA:	Ácido etilendiaminotetraacético	Ethylenediaminetetraacetic acid
EXAFS:		Extended X-ray Absorption Fine Structure
FC-R:	Fe quelato reductasa	Ferric chelate reductase
F-TIR:	Espectroscopía infrarroja con transformada de Fourier	Fourier-transform infrared spectroscopy
HA:	Ácidos húmicos	Humic acids
HBED:		N,N'-bis(2-hydroxybenzyl) ethylened-iamine-N,N'-diacetic acid
HF:	Ácidos fúlvicos	Fulvic acids
HS:	Sustancias húmicas	Humic substances
IC-PMS:	Espectroscopía de masas por plasma de acoplamiento inductivo	Inductively coupled plasma mass spectrometry
IHSS:	Sociedad Internacional de Sustancias Húmicas	International Humic Substances Society
LIH:	Humato férrico procedente de leonardita	Leonardite iron humate
LKH:	Humato potásico procedente de leonardita	Leonardite potassium humate
MA:	Ácido mugineico	Mugineic acid
MCC:	Máxima capacidad de complejación	Máximum complexing capacity
PS:	Fitosideróforos	Phytosiderophores
ROS:	Especies reactivas de oxígeno	Reactive oxygen species
SEM:	Microscopía electrónica de barrido	Scanning electron microscopy
TEM:	Microscopía electrónica de transmisión	Transmission electron microscopy
XAS:	Espectroscopía de absorción de Rayos-X	X-ray absorption spectroscopy
XANES:		X-ray Absorption Near Edge Structure
XRD:	Difracción de rayos X	X-ray diffraction

Capítulo I: Introducción

Chapter I: Introduction

Pág.

I.1 Humatos férricos

La fertilización con humatos de hierro, o complejos de hierro a partir de sustancias húmicas no es nueva, pero la necesidad de reducir el impacto ambiental de las prácticas agrícolas actuales renueva el debate acerca de la eficacia de estos productos.

Muchos artículos resaltan la importancia agrícola de las sustancias húmicas y sugieren el uso de humatos férricos a partir de leonarditas como fertilizantes (*Shenker y Chen* 2005, *Chassapis et al.* 2010, *Colombo et al.* 2012, *Kovács et al*. 2013, *Sorkina et al*. 2014), sin embargo son pocos los estudios agronómicos que se han realizado con humatos férricos en general. *Pinton et al*. (1999) proveyeron evidencias claras de la posibilidad del uso de humatos férricos a partir de turba como fuente de Fe para las plantas tanto en plantas de Estrategia I como en plantas de Estrategia II (*Cesco et al.* 2002). *Alva et al*. (1992) aplicaron con éxito un humato de hierro obtenido como subproducto del proceso de decoloración de agua potable a cítricos desarrollados en suelos calizos y que presentaban clorosis férrica. En 1998, *Alva y Obreza* documentaron el incremento de la concentración de Fe en hoja y la producción de cítricos (naranja y pomelo) debido a la aplicación del mismo humato férrico. *Pérez-Sanz et al*. (2002) observaron el aumento de tamaño de fruto al aplicar un humato férrico del mismo origen que el utilizado por *Alva y Obreza* (1998), a cítricos (naranja) y frutales (melocotón). Sin embargo, hay muy poca literatura referida a la experimentación en campo con humatos férricos a partir de leonardita (*De Santiago y Delgado,* 2007).

Con respecto a la legislación, la Regulación Española vigente sobre productos fertilizantes (RD506/ 2013), permite el uso de sales de potasio, sodio o amonio de sustancias húmicas como agente complejante, las cuales deben contener al menos 60% de ácidos húmicos. Los humatos férricos deben presentar 5% de Fe total soluble, del cual el 50% debe encontrarse complejado. Además, sólo se admite su aplicación foliar y su uso en fertirrigación. Por otro lado, las sustancias húmicas no están incluidas en la Directiva en Fertilizantes de la Unión Europea CE: 2003/2003 como agente complejante y tampoco lo están para la recientemente publicada Directiva CE: 1009/2019, aunque en esta última se contempla el uso de leonardita o lignito como abono orgánico o abono órgano mineral. Además, se establece que los complejos de micronutrientes deben contener como mínimo 5% de hierro total soluble, del cual el 80% debe estar complejado, sin estipular el agente complejante que se puede utilizar, sino las especificaciones que debe cumplir el material. Cabe resaltar que la nueva normativa europea contempla las sustancias o mezclas de sustancias que potencien la disponibilidad a largo plazo

de micronutrientes, dentro de la categoría de materiales componentes (CMC) de fertilizantes, correspondiente a sustancias y mezclas de materiales vírgenes (CMC1, apartado 3, parte II, Anexo II, CE: 1009/2009). Además, en el caso que las sustancias o mezclas de sustancias que potencien la disponibilidad a largo plazo de micronutrientes y que sean preparadas con un agente complejante, el mismo debe ser orgánico, capaz de formar estructura plana o estérica con Fe^{2+} o Fe^{3+} y el producto fertilizante debe permanecer estable en solución acuosa a pH 6-7, como mínimo un día.

Teniendo como base los vademécum de *Liñán* (2001 y 2019) se realizó un estudio de los productos presentes en el mercado español conteniendo sustancias húmicas como correctores de carencia de hierro. En el año 2001 se ofrecían 25 productos de los cuales 13 presentaban el hierro complejado con sustancias húmicas, mientras que el resto de productos presentaban el hierro quelado con agentes quelantes como EDTA, DTPA o EDDHA. Actualmente, los productos a la venta son sólo 6 y en su mayoría solo con hierro complejado. Se entiende que esta fuerte caída de la oferta de humatos férricos se debe en parte a la imposibilidad del cumplimiento de los requisitos legislativos para su comercialización, especialmente la solubilidad del hierro y en parte a que su eficiencia es comparada con la de los quelatos férricos y por lo tanto, son subestimados en su acción nutritiva sin comprender que su comportamiento puede diferir hondamente a la de los productos sintéticos en el sistema suelo-planta.

En la bibliografía constan trabajos de modificación de la estructura de los ácidos húmicos a fin de mejorar su actividad biológica y de ese modo incrementar la producción de biomasa (*Yarkova,* 2011). Además, actualmente se han propuesto nuevas metodologías para la determinación de ácidos húmicos y fúlvicos (*Lamar et al*. 2014, *Fuentes et al*. 2018, *Karpukhina et al*. 2018) a fin de poder valorar de un modo más eficiente la cantidad y calidad de éstos en fertilizantes. Sin embargo, la mejora en la solubilidad del hierro sigue sin resolverse. Cerdán *et al.* (2007) estudiaron el comportamiento cinético de mezclas de quelatos sintéticos de hierro y sustancias húmicas a base de leonarditas (50% p/p) y observaron que las mezclas no incrementaban la solubilidad del hierro en suelos calizos con respecto a la solubilidad del *o,o* EDDHA/Fe^{3+}. *Sorkina et al.* (2014) demostraron la eficiencia de un humato férrico a partir de leonardita sulfonada (Fe–HS-H_2SO_4) como corrector de clorosis férrica en hidroponía pero no evaluaron su eficacia en suelo.

Por lo tanto, la presente tesis doctoral pretende contribuir al estudio de la naturaleza y el mecanismo de acción de los humatos de hierro sintetizados a partir de leonarditas en el sistema suelo-planta, como una alternativa agroecológica de fertilización férrica a menor costo. Además, postula la importancia que existe en la caracterización apropiada de los materiales

originarios y los complejos férricos obtenidos a partir de ellos, a fin de predecir el comportamiento de estos fertilizantes cuando son aplicados, en suelos calizos, para la fertilización de plantas de Estrategia I. Finalmente, propone vías de mejora en la eficiencia de los humatos férricos a partir de modificaciones en su síntesis o en su modo de aplicación.

En esta introducción se exponen aspectos como las funciones del hierro y las sustancias húmicas en el suelo y en el desarrollo de las plantas, las estrategias de absorción de hierro que utilizan las plantas en caso de clorosis férrica y el efecto de las sustancias húmicas en la disponibilidad del hierro. Además, se detallan las técnicas de caracterización de las formas de Fe en las sustancias húmicas y las técnicas de caracterización propias de las sustancias húmicas utilizadas.

I.2 El hierro

El hierro (Fe) es el elemento número 26 de la tabla periódica y pertenece a la familia de los elementos de transición. Es un metal cuya estructura electrónica es [Ar] $4s^2$ $3d^6$. En sistemas naturales sus cationes son Fe^{2+} y Fe^{3+}. El Fe^{3+} se caracteriza por tener orbitales d vacantes ([Ar] $4s^0$ $3d^5$), comportándose como un ácido de Lewis. Su número de coordinación habitual es el seis y sus ligandos (O, N, S) se suelen acomodar en geometría octaédrica u octaédrica distorsionada respecto al Fe^{3+} (*Neilands,* 1994). Además, el hierro es uno de los micronutrientes más importante en la nutrición humana, animal y de los cultivos. Es vital una nutrición férrica propicia de las plantas para proveer concentraciones óptimas de este mineral a los órganos de post cosecha y por lo tanto, garantizar que la alimentación humana y animal sea la adecuada.

I.2.1 El hierro en el suelo

El Fe es el cuarto elemento más abundante en la litosfera (5,1%), después del oxígeno, el silicio y el aluminio (*Lindsay* 1979) y es el tercero más limitante para el desarrollo de los seres vivos (*Yi et al*. 1994). La concentración media del Fe en suelos es de 3,8% en masa (*Lindsay* 1979) por lo que su deficiencia no se debe a su baja concentración en suelo sino a su baja disponibilidad. El Fe se caracteriza por la facilidad con que cambia su estado de oxidación, lo cual determina tanto su presencia en el suelo como su movilidad dentro de la planta:

$$Fe^{3+} + e^- \leftrightarrows Fe^{2+} \qquad logK° = 13{,}04$$

La mayoría del Fe presente en la corteza terrestre se encuentra como silicatos ferro-magnésicos como el olivino, la biotita, etc. cuya descomposición en el suelo se ve favorecida por

procesos de hidrólisis y oxidación debido a su reacción con el agua y el oxígeno del aire. La mayoría del hierro obtenido a partir de procesos de meteorización precipita como óxidos o hidróxidos tales como goetita, hematita y ferrihidrita. Sólo una pequeña parte del Fe es incorporada a silicatos secundarios o es complejada por la materia orgánica (*Schwertmann y Taylor* 1977).

La disolución y precipitación de los óxidos férricos es el factor principal que controla la solubilidad del hierro en el suelo. La solubilidad del Fe^{3+}, a partir de sus óxidos, es altamente dependiente del pH, lo cual se puede observar en la Figura 1.

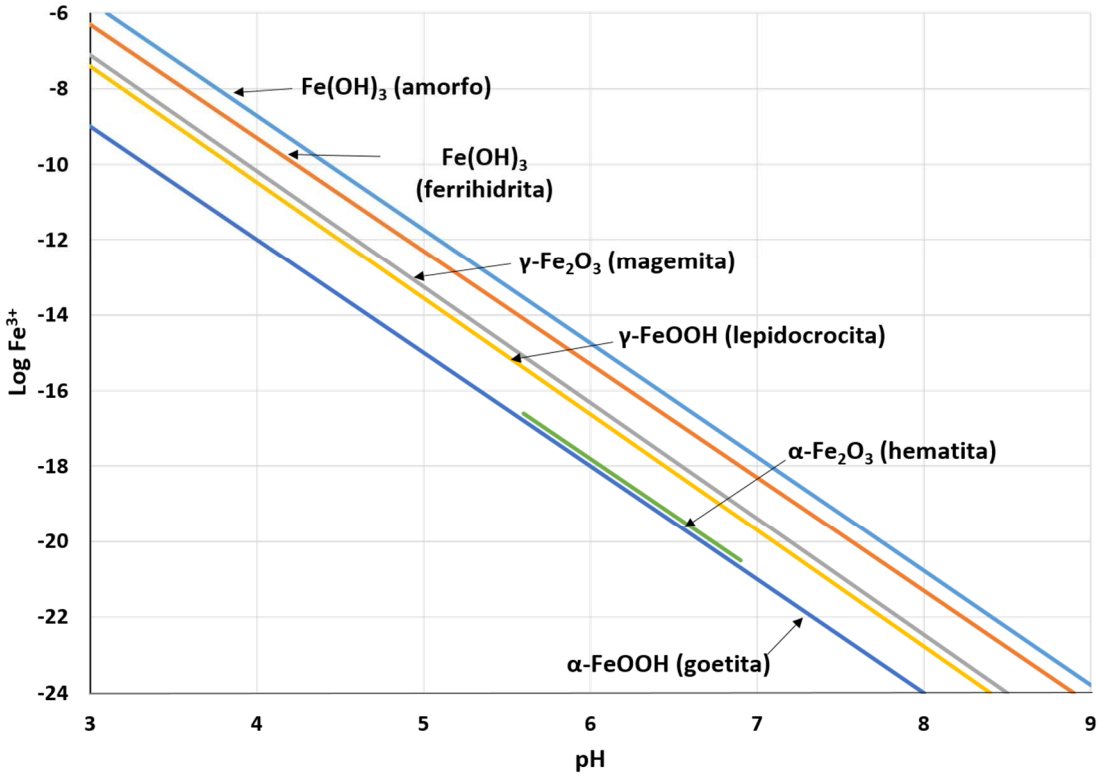

Figura 1: Actividad del Fe^{3+} en equilibrio con varios óxidos de Fe(III) en función del pH (Lindsay, 1979)

Norvell y Lindsay (1982) demostraron que la solubilidad del hierro en suelos bien aireados tiende a comportarse como la del $Fe(OH)_3$ del suelo, que a su vez, corresponde con la de la ferrihidrita. Su solubilidad se representa por la siguiente reacción:

$$Fe(OH)_3 + 3H^+ \leftrightarrows Fe^{3+} + 3H_2O \quad logK° = 2{,}70$$

En la Figura 2 se presenta la actividad de las especies hidroxiladas de Fe(III) en función del pH junto con el Fe^{3+} (para pe +pH = 11,53) en equilibrio con el Fe del suelo. La actividad de la especie Fe^{3+} disminuye 1000 veces al aumentar una unidad de pH. En suelos calizos, el pH se

encuentra en el rango de 7,4 y 8,5 donde la solubilidad del Fe(III) es mínima ($10^{-10.4}$ M) cuando se establece el equilibrio con el hierro del suelo (ferrihidrita). La especie predominante en solución a pH inferior a 7,4 es $Fe(OH)_2^+$, entre pH 7,5 y 8,5 es $Fe(OH)_3°$ y a pH superior a 8,5 es $Fe(OH)_4^-$. En suelos calizos el contenido de caliza ($CaCO_3$) es elevado y, debido a su alto poder tampón, consumirá los protones que se puedan producir por los procesos biológicos o aportes exógenos, evitando así la participación de éstos en la solubilización de los hidróxidos férricos:

$$CO_{2\,gas} + H_2O \leftrightarrows HCO_3^- + H^+ \qquad LogK^0 = -7{,}82$$

$$CO_3Ca_{(calcita)} + 2H^+ \leftrightarrows Ca^{2+} + H_2O + CO_{2\,gas} \qquad LogK^0 = 9{,}74$$

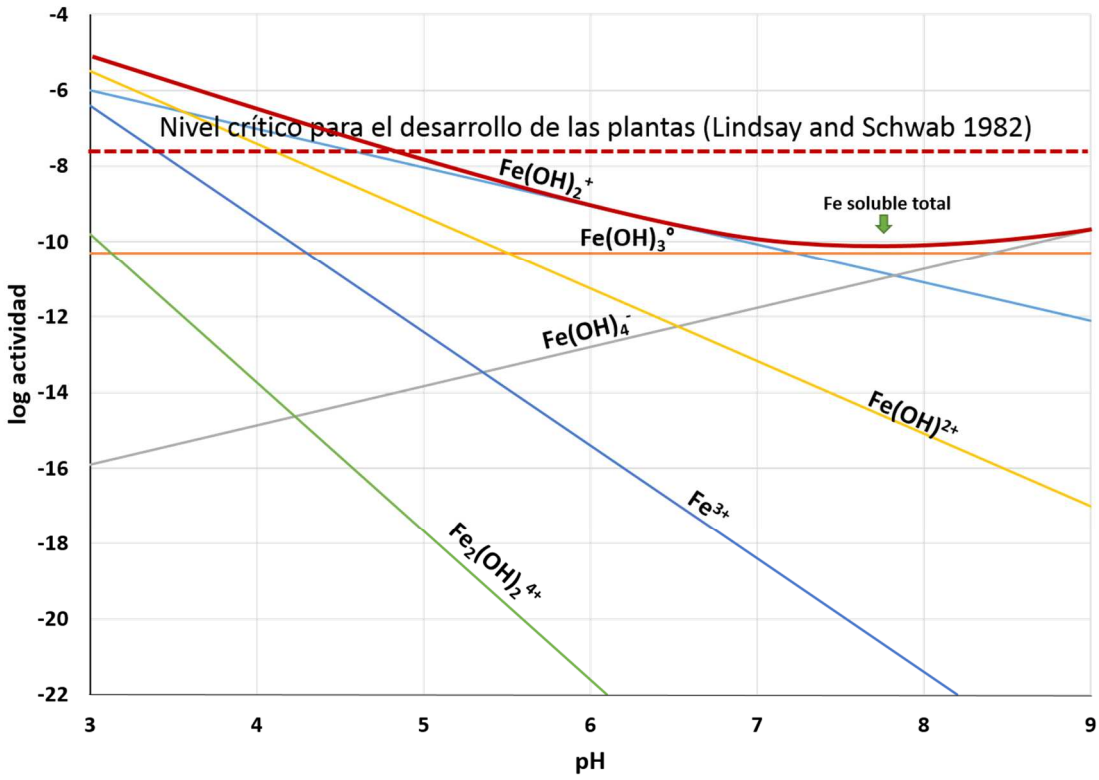

Figura 2: Especies en disolución de Fe (III) en equilibrio con el Fe del suelo ($Fe(OH)_3$). (*Lindsay*, 1979).

El potencial redox (pe +pH) influye en la solubilidad del suelo. En condiciones reductoras (pe+pH <11,53) las especies de Fe (II) son las más abundantes y permitirían mantener suficiente Fe en disolución para un óptimo desarrollo de la planta. Sin embargo, en las condiciones oxidantes (pe+pH >11,53), que se requieren para el crecimiento adecuado de la mayor parte de los cultivos (condiciones aerobias), las especies predominantes son las de Fe (III), las cuales pueden dar lugar a problemas de deficiencia, debido a la facilidad con que pueden pasar a formas insolubles (Figura 2).

I.2.2 El hierro en la nutrición de las plantas

El Fe es un nutriente esencial para casi todos los organismos, dado que juega un rol crítico en procesos bioquímicos importantes como lo son la respiración, la fotosíntesis, la síntesis de ADN y la detoxificación de especies reactivas de oxígeno (ROS). Cualquier impedimento en la disponibilidad del Fe, impacta directamente en el desarrollo de las plantas así como también en la calidad y rendimiento del cultivo (*Briat et al.* 2015). Su deficiencia, la clorosis férrica, afecta a las plantas crecidas de hasta un 30% de los suelos cultivables del mundo. Además, el Fe participa en el metabolismo del nitrógeno y el azufre y juega un rol importante en la síntesis de clorofila. Sin embargo, el Fe abunda en la mayoría de los suelos agrícolas cuya concentración ronda entre 20 y 40 g kg^{-1} (*Cornell y Schwertmann* 2003). La difusión es el principal mecanismo del movimiento del Fe en el suelo y permite su migración desde la disolución del suelo hacia sitios activos de absorción en las raíces (*Oliver y Barber* 1966). Sin embargo, se ha visto en cultivos hidropónicos donde la difusión está ampliamente favorecida, que el nivel crítico de Fe soluble para una adecuada nutrición férrica soja, debe ser $10^{-7.7}$M (*Lindsay y Schwab* 1982), dos órdenes de magnitud mayor a la solubilidad del Fe en el suelo a pH 7.4-8.5 (Figura 2).

El Fe, en general, es tomado del suelo a través de las raíces y transportado en el xilema como un complejo con ácidos orgánicos tales como el citrato y en el floema, el Fe es complejado por la nicotianamina. El hierro se absorbe preferentemente como Fe(II), aunque hay algunas plantas que lo toman como Fe(III) quelado (plantas de Estrategia II). El Fe soluble en el suelo se encuentra principalmente complejado por ácidos orgánicos, fenoles y sustancias húmicas (*Boiteau et al.* 2018, *Zanin et al.* 2019). Cuando la cantidad de Fe a disposición de la planta es suficiente, ésta tiende a utilizar sistemas de transporte de Fe de baja afinidad y absorber sólo la cantidad necesaria para un óptimo crecimiento, previniendo así una posible toxicidad que podría dañar ADN, proteínas, lípidos, etc (*Hell y Stephan* 2003). Sin embargo, en condiciones de deficiencia de Fe, las plantas han desarrollado dos estrategias (Estrategia I y Estrategia II) para adquirir Fe (*Marschner y Römheld* 1994). En ambas estrategias, la adquisición de Fe se realiza en la zona apical del crecimiento radicular y se desarrolla en el transcurso de un día después de la reposición de Fe. En la Figura 3 se describen los mecanismos de adquisición de hierro (Estrategia I y Estrategia II) de las plantas eficientes en situación de deficiencia.

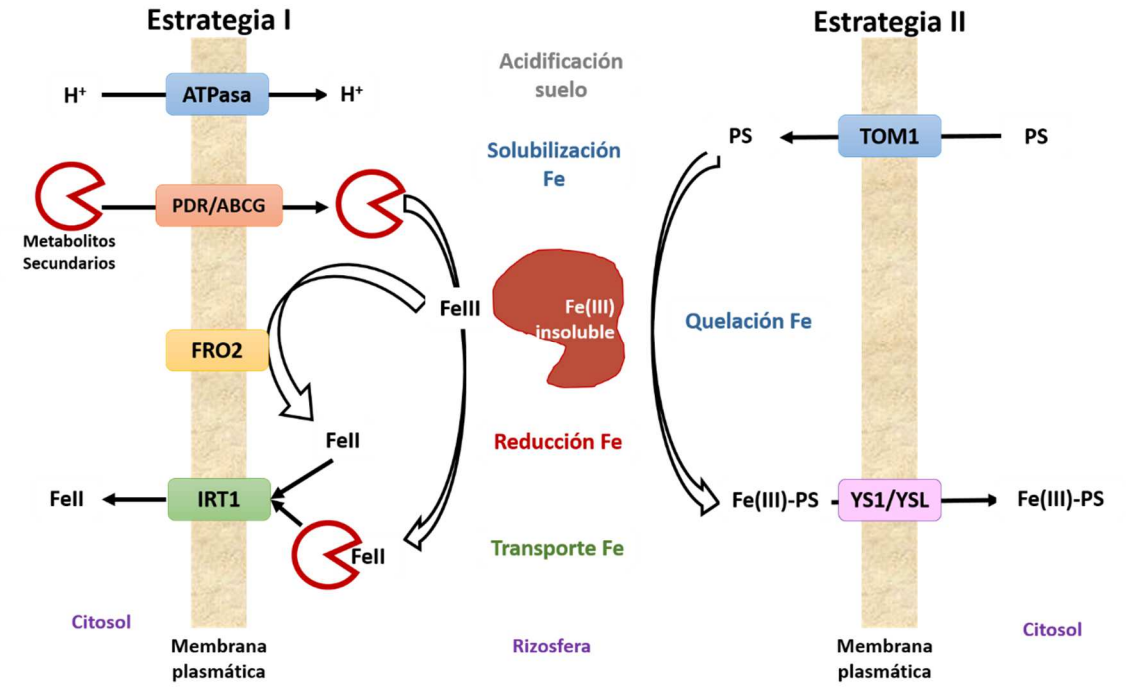

Figura 3: Mecanismos de adquisición de hierro en raíces. Estrategia I y Estrategia II. Diagrama adaptado de Tsai y Schmidt (2017b).

La Estrategia I es típica para plantas dicotiledóneas y monocotiledóneas no-gramíneas. El Fe es movilizado a través de la acidificación de la rizosfera por la actividad de las bombas de protones (H^+-ATPase), en especial la H^+-ATPase 2 (AHA2) (*Santi y Schmidt* 2009) y a través de la quelación del Fe por compuestos de bajo peso molecular como ácidos orgánicos y cumarinas, que son secretados en la rizosfera (*Schmidt et al*. 2014, *Tsai y Schmidt* 2017a). El Fe(III) movilizado se difunde en el apoplasto seguido por la reducción del Fe(III) a Fe (II) por enzimas Fe quelato reductasa de la membrana plasmática (*Robinson et al.* 1999) y cumarinas (*Sisó-Terraza et al.* 2015, *Rajniak et al*. 2018). En *Arabidopsis thaliana*, el Fe(III) rizosférico es reducido por la Ferric Reductase Oxidase 2 (FRO2) (*Robinson et al.* 1999) y luego es transportado como Fe^{2+} dentro de las células epidérmicas por el transportador de metales divalentes IRT1 (Iron-Regulated Transporter) (*Vert et al.* 2002). Ambos componentes (FRO2 e IRT1) son regulados por el factor de transcripción de Fe-inducible FIT/FER (FER-Like Iron deficiency-induced) que forma hetero-dímeros con otros factores de transcripción basic helix – loop - helix (bHLH) (*Colangelo y Guerinot* 2004, *Sivitz et al*. 2012).

La Estrategia II, típica para las plantas que pertenecen a la familia de las gramíneas, se basa en la secreción de las raíces de fitosideroforos (PS), un grupo de agentes quelantes de bajo

peso molecular con una alta afinidad por el Fe^{3+} en respuesta a la deficiencia de hierro y un sistema de absorción específico de los Fe-fitosideroforos. En esta estrategia el hierro no es transportado vía membrana como Fe^{2+}, sino como un complejo de Fe(III) como por ejemplo con ácido mugínico (MA), un derivado de nicotinamina con muy alta afinidad por Fe^{3+} (*Kobayashi y Nishizawa* 2012). Luego, este complejo es introducido a la planta por transportadores YSL que se caracterizaron inicialmente en maíz (*Curie et al.* 2008) y luego en arroz (*Inoue et al.* 2009). La eficiencia de estos mecanismos varía ampliamente entre familia de plantas, especies e incluso entre variedades de una misma especie.

La separación en estas dos Estrategias no es simple. Muchas plantas de Estrategia I liberan en sus exudados radiculares un número de moléculas que pueden solubilizar Fe y algunas de ellas, pueden reducir Fe(III) a Fe(II). Ellas incluyen cumarinas y flavinas así como otros compuestos fenólicos (*González-Guerrero et al.* 2016). Los grupos fenólicos ayudan a solubilizar y reutilizar el Fe apoplástico, lo cual se observó primeramente en el trébol rojo (*Jin et al*. 2007). Además, *Tomasi et al.* (2008) y *Cesco et al.* (2010) propusieron dos funciones para los grupos fenólicos: reducción y complejación. Boyer *et al.* (1989) observó que los ácidos cafeico, clorogénico y ferúlico favorecían la reducción y por lo tanto, la liberación de Fe contenido en la ferrihidrita mientras que *Mira et al.* (2002) demostró que la quercetina y la miricetina quelan el Fe(II) luego de reducir el Fe(III). *Terzano et al.* (2015) también reportaron que la rutina podia extraer grandes cantidades de Fe, principalmente a través de mecanismos de reducción. *Gatullo et al.* (2018) observaron en batch experiments que el citrato y, en especial la rutina, favorecen la movilización del Fe del suelo. La rutina combinada con ácidos orgánicos disuelve las fracciones amorfas de los minerales del suelo y favorece la formación de illita $[(K,H_3O)(Al, Mg, Fe)_2(Si, Al)_4 O_{10}[(OH)_2,(H_2O)]$. Además, los autores observaron en experimentos RHIZOtest con plantas de pepino deficientes de Fe, la disolución de compuestos amorfos en la rizosfera y lo atribuyeron a la liberación de compuestos fenólicos, aminoácidos y ácidos orgánicos aunque no observaron formación de illita.

Aparentemente, las cumarinas juegan un papel crucial en la adquisición de Fe en *Arabidopsis thaliana*, bajo condiciones de pH elevado (*Rodríguez-Celma et al*. 2013, *Fourcroy et al.* 2013, *Schmidt et al.* 2014). La mejora en la exudación de cumarinas en esta especie es relacionada con su adaptación a suelos calizos (*Terés et al.* 2019). Los precursores de las cumarinas pertenecen a la vía del fenilpropanoico. Otras especies de plantas tales como *Medicago truncatula*, segregan flavinas en vez de cumarinas, las cuales también facilitan la disolución de Fe(III) (*Rodriguez-Celma et al*. 2011). Además, la secreción de putrescina favorece la movilización del hierro dentro de las paredes celulares de las planta (*Zhu et al*. 2016).

La mayoría del Fe entra a la planta a través de la raíz y luego es transportado a los tejidos sumideros donde se requiere para las enzimas dependientes de Fe. El hierro se mueve vía simplasto hacia el periciclo para llegar al xilema y desde ahí a las hojas. El Fe(III)-citrato es la forma de hierro principal responsable del transporte a larga distancia en la savia que circula por xilema (*Rellán-Álvarez et al.* 2010). En las hojas, el Fe vuelve a entrar en el simplasto y es reducido a Fe^{2+} por la acción de las proteínas FRO. Una gran parte del Fe es usada en los plástidos. Parte del Fe es removilizado desde las hojas y alcanza otros órganos sumidero a través del floema.

Las semillas son el último destino del transporte de Fe en las plantas. Las reservas de Fe almacenadas en las semillas son importantes durante la germinación, antes de que las plántulas desarrollen un sistema radicular y sean capaces de movilizar y tomar Fe del suelo. Los transportadores YSL están involucrados en la carga de Fe de las semillas (*Jean et al*. 2005) y hay evidencia de que el Fe puede ser liberado a los embriones de guisantes como Fe(III) citrato/malato (*Grillet et al.* 2014). El Fe es dirigido a los tejidos vasculares de los embriones donde es almacenado en las vacuolas de las células endodérmicas (*Roschzttardtz et al.* 2009). Además, el hierro puede almacenarse como ferritina en las semillas. La proporción de Fe total almacenado varía entre las especies, aproximadamente 60% en guisantes y menos del 5% en semillas de *Arabidopsis* (*Zieliñska-Dawidziak* 2015). En las plantas, la ferritina está principalmente localizada en los plástidos. En los granos de cereales como trigo y arroz, el Fe se presenta en la capa aleuronal de las vacuolas. Como esta capa suele ser eliminada durante el procesamiento del grano, los alimentos refinados pueden tener menos concentración de hierro, afectando su valor nutricional (*Kyriacou et al*. 2014).

I.3 Las sustancias húmicas

Las sustancias húmicas (HS), incluyendo los ácidos húmicos (HA) y los ácidos fúlvicos (FA), son los principales compuestos con carbón orgánico (C) en sistemas acuáticos *(Frimmel y Abbt-Braun* 2009) y en suelos (*Stevenson,* 1982). Incluso, se ha detectado sustancias húmicas en la atmósfera (*Salma et al.* 2010). Las HS son generalmente consideradas como la fracción más reactiva del C porque incluye muchos grupos funcionales, la mayoría de los cuales son grupos carboxílicos (–COOH) o fenólicos (–OH). En el suelo, estos grupos unen estrechamente a las HS

con los minerales (complejo arcillo-húmico), controlando la especiación de los metales y su solubilidad (*Tipping,* 2002).

Las HS son mezclas complejas y heterogéneas de materiales poli-dispersos formados por reacciones químicas y bioquímicas, durante la descomposición y transformación de restos vegetales y microbianas (humificación). La lignina y sus productos de transformación así como polisacáridos, proteínas, lípidos, ácidos nucleicos, etc., son componentes importantes que participan del proceso de humificación. Las HS tienen alta reactividad química aún recalcitrante con respecto a la degradación. Las propiedades y estructuras de una dada HS dependen de la procedencia del suelo o el agua que la contienen, la vegetación de origen y las condiciones específicas de extracción. Además, el peso molecular de las HS en general varía en un rango de cientos a decenas de miles de Dalton (*Bolea et al.* 2006).

Existen dos teorías acerca de la estructura de las HS. La teoría más tradicional las define como grandes moléculas poliméricas (*Swift* 1999), mientras que la teoría más moderna, las considera como un conjunto supra-molecular heterogéneo y de unidades de bajo peso molecular (<1000 Da) (*Piccolo,* 2001), formado por asociaciones dinámicas que son estabilizadas por interacciones hidrofóbicas y puentes de hidrógeno (*Sutton y Sposito* 2005). Por lo tanto, según esta última teoría, las HS son macromoléculas de estructura polimérica que presentan su propia organización (*Piccolo,* 2002) y están formadas de cientos de diferentes moléculas de diferente tamaño con múltiples posibilidades de orientación: torsión, flexión, compresión y extensión (cambios conformacionales). Se sostienen unidas por fuerzas lábiles en estado coloidal y cualquier cambio en el pH de la solución, la concentración o la presencia de iones metálicos, especialmente los iones calcio, causará cambios importantes en la constitución física de las moléculas húmicas.

La composición de las HS ha sido materia de estudio y controversia por más de 200 años dado que son mezclas coloidales complejas que nunca han sido separadas en compuestos puros. Tradicionalmente, las HS han sido separadas por su solubilidad en ácidos o bases y de acuerdo a ello, se obtienen HA, ácidos FA y humina. En la Figura 4 se expone un esquema de fragmentación de la materia orgánica a partir de la que se obtienen estos componentes. La mayoría de los datos de cada fracción, se refieren al promedio de las propiedades y estructuras de un conjunto de compuestos de diversa estructura y peso molecular. Las propiedades y estructura precisas de una HS dada dependen de la fuente acuática o edáfica y las condiciones específicas de extracción. Sin embargo, las propiedades promedio de los HA, FA y de la humina procedente de diferentes fuentes son notablemente similares (*IHSS* 2007).

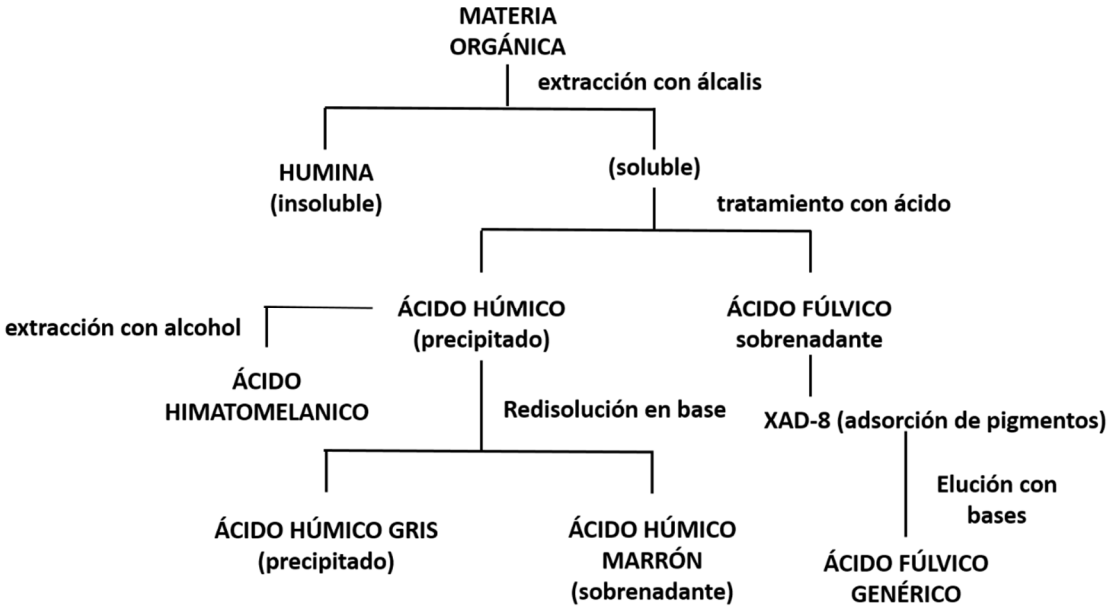

Figura 4: Esquema de la fragmentación de la materia orgánica del suelo (*Stevenson,* 1994)

Los HA comprenden las sustancias orgánicas que son solubles en medio alcalino e insoluble en medio ácido (pH 1–2), mientras que los FA son sustancias orgánicas que son solubles a cualquier valor de pH. Las huminas son insolubles a cualquier valor de pH (*Bolea et al.*, 2006). Los HA son considerados polímeros lineales flexibles que existen como hélices al azar unidos de forma entrecruzada. El 35% de las unidades en HA son grupos aromáticos mientras que el resto se compone de cadenas alifáticas. El peso molecular varía entre 10.000 Da y 100.000 Da. En la Figura 5 se presenta la estructura hipotética de un HA.

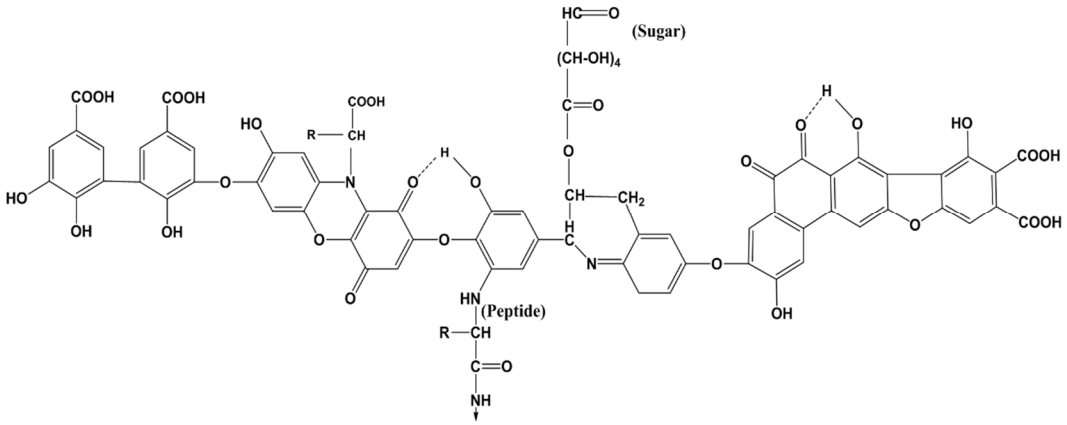

Figura 5: Estructura hipotética de un ácido húmico. (*Stevenson*, 1994)

Schulten y Schnitzer (1993) desarrollaron la estructura de un HA a partir de resultados obtenidos con resonancia magnética nuclear ^{13}C (^{13}C-RMN), análisis pirolítico y datos de degradación oxidativa. La estructura propuesta se expone en la Figura 6 y se compone de anillos aromáticos unidos por largas cadenas alifáticas, formando una red flexible con huecos que

atrapan y unen otros compuestos orgánicos. La composición elemental de la estructura representada en la Figura 6 es $C_{308}H_{328}O_{90}N_5$ (66.8% de C, 6% de H, 26% de O y 1.3% de N) y su peso molecular es 5540Da.

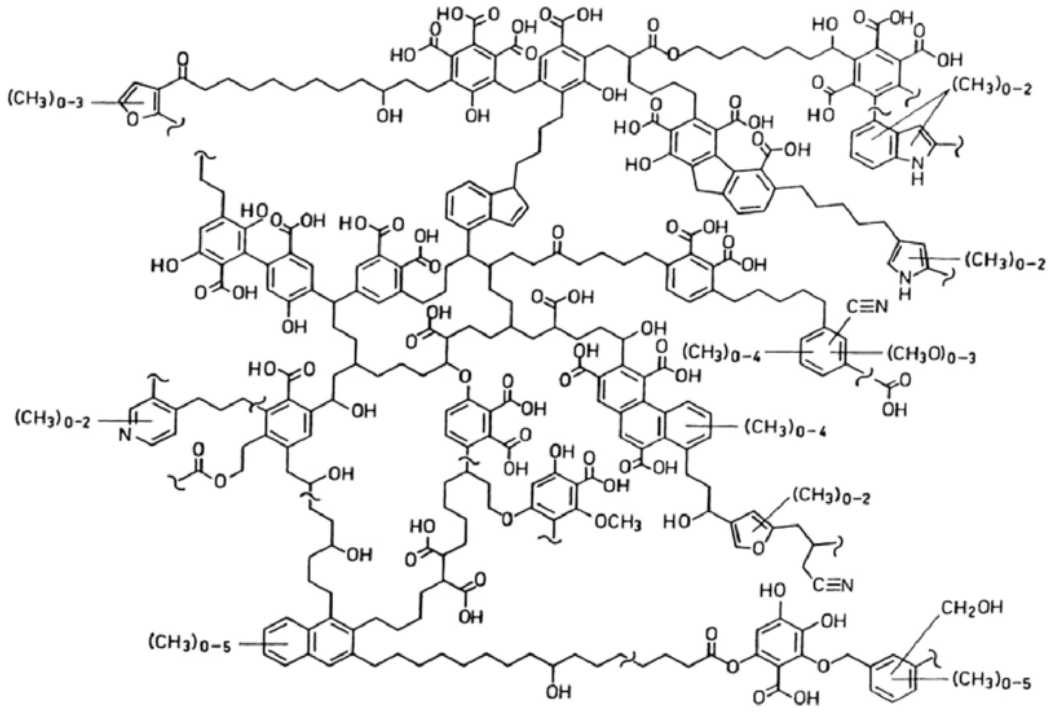

Figura 6: Estructura de un ácido húmico propuesta por *Schulten y Schnitzer* (1993).

Shulten propuso en 1996 un modelo tridimensional para ácidos húmicos en sistemas acuáticos y terrestres a partir de datos de espectroscopía de masas acoplada a pirólisis y pirólisis con cromatografía de gases acoplada a espectroscopía de masas con la posterior optimización geométrica y molecular de los complejos húmicos considerando, entre otros factores, las conformaciones de menor energía y los puentes de H inter e intramoleculares. Posteriormente, en el año 2000, *Schulten y Leinweber* publican la simulación de la estructura de un coloide natural formado por 22 moléculas de ácido húmico cuya composición elemental sería $C_{6932}H_{7662}O_{1970}N_{110}$.

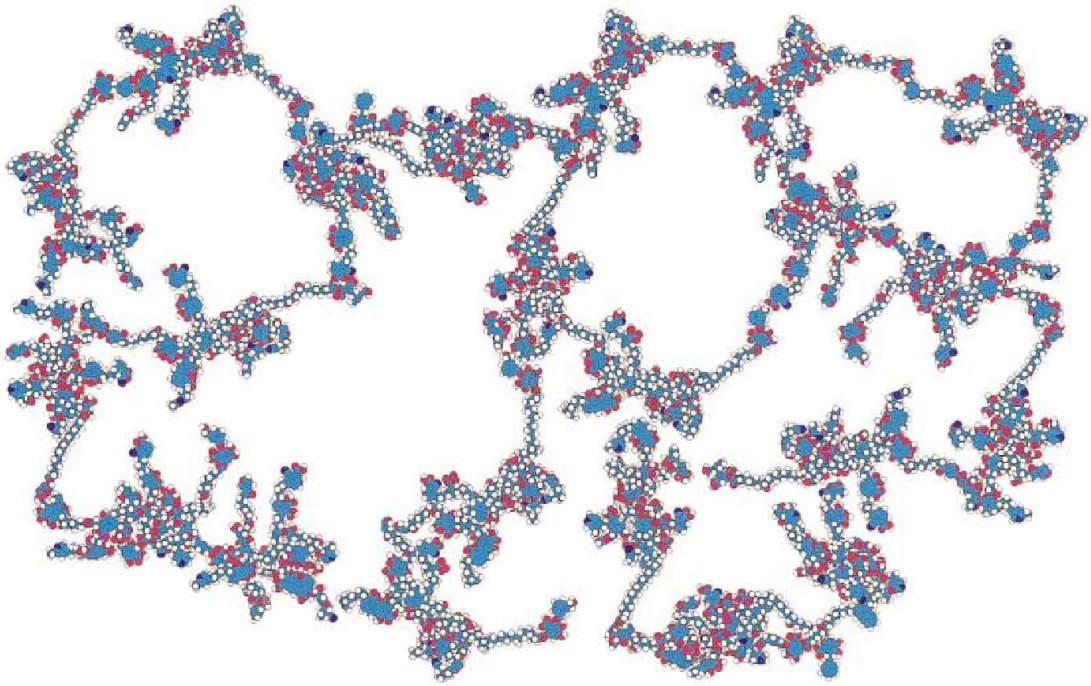

Figura 7: Ejemplo de coloide natural de ácidos húmicos desarrollado por *Schulten y Leinweber* (2000)

Los FA poseen el doble de contenido de oxígeno que los HA. Su peso molecular varía entre 1.000 y 10.000. Son más reactivos químicamente ya que poseen abundantes grupos carboxilos e hidroxilos. La capacidad de intercambio catiónico de los FA es más del doble que la de los HA debido a la gran abundancia de los grupos carboxílicos (entre 520 y 1120 cmol kg^{-1}, *Pettit,* 2004). Además, presentan bajo contenido de fenoles y menor contenido de compuestos aromáticos respecto de los HA. En la Figura 8 se presenta la estructura parcial de un FA.

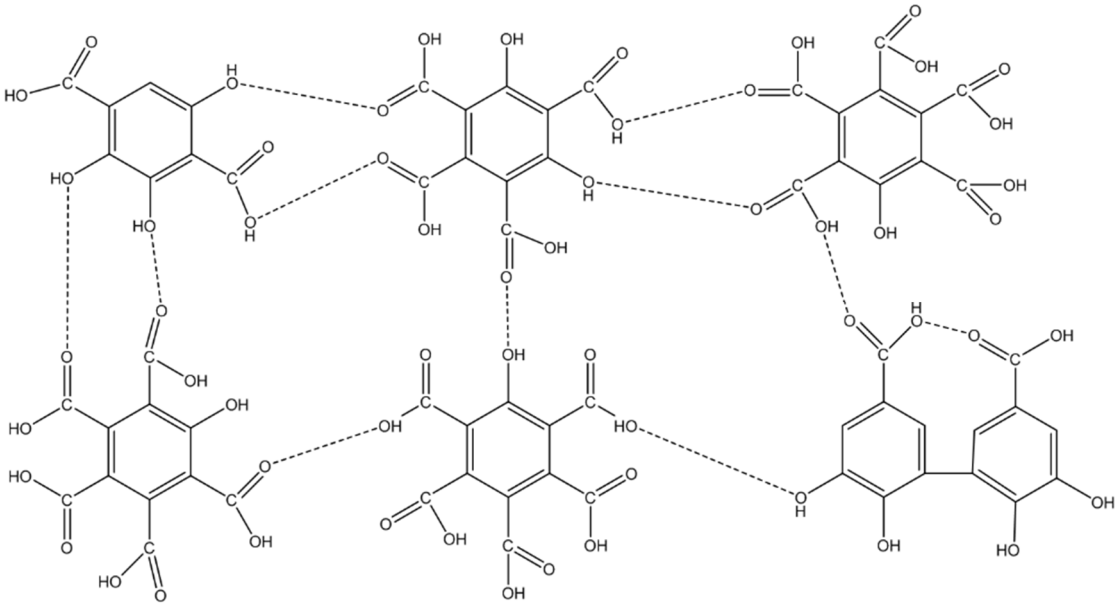

Figura 8: Estructura parcial de un ácido fúlvico propuesta por *Schtnizer* (1978)

Por otro lado, *Piccolo* (2002) redefinió los FA como asociaciones de pequeñas moléculas hidrofílicas en las cuales hay suficientes grupos funcionales ácidos como para mantener dispersos clasters fúlvicos en soluciones que se encuentran a cualquier valor de pH, mientras que los HA están formados de asociaciones donde predominan los compuestos hidrofóbicos (cadenas polimetílicas, ácidos grasos, esteroides) que son estables a pH neutro por fuerzas hidrofóbicas dispersantes. Sus conformaciones crecen progresivamente en tamaño cuando los puentes de hidrógeno inter-moleculares aumentan a pH bajo hasta que la sustancia húmica flocula.

Recientemente, la Sociedad Internacional de Sustancias Húmicas (*IHSS*) ha definido a los FA como el material que es soluble tanto en medio básico como ácido y que queda adsorbido a una resina no-iónica, distinguiéndolo de este modo de la fracción de materia orgánica natural que es muy hidrofílica aún a pH bajo y que no es adsorbida por resina (*IHSS* 2007).

La humina es la fracción húmica menos estudiada y presenta el mayor peso molecular de las tres, ya que varía entre 100.000 Da y 10.000.000 Da. Por lo tanto, estaría constituida por ácidos húmicos de alta condensación que se encuentran fuertemente unidos a la parte mineral del suelo. La humina tiene menor reactividad química y geológica que los HA y FA. Es la fracción más resistente a la descomposición (*Pettit,* 2004).

Ayuso et al. (1997), realizaron un estudio comparativo de HA extraídos de desechos orgánicos (aguas de depuradora y compost) y aquellos comercializados por las empresas de HA (extractos de leonarditas y turba). Observaron que los HA procedentes de materia orgánica menos evolucionada (aguas de depuradora y compost) mostraban alto contenido alifático, alto contenido de nitrógeno, bajo grado de oxidación y composición más heterogénea que aquellos HA extraídos de materia orgánica más evolucionada (leonarditas y turba).

A medida que las HS envejecen, su estructura química se vuelve progresivamente más aromática y contiene menos polisacáridos y derivados de ligninas. Un ejemplo de ello es la evolución de las HS procedentes de turba, leonarditas y lignitos, cuya composición química se encuentra fuertemente influenciada por el proceso de diagénesis (*González-Vila et al*. 1994). Por lo tanto, las HS que provienen de carbones de baja calidad son parte de la formación del carbón y son altamente solubles en soluciones básicas, mientras que las que se originaron a partir de carbones maduros vía un proceso de oxidación tienen una estructura similar a la de los carbones originarios y no son solubles. La diagénesis de cada carbón difiere radicalmente entre sí, dependiendo de los residuos orgánicos y las condiciones de generación del carbón (*Francioso et al*. 2005).

La formación de la leonardita se remonta a la Era Carbonífera del Paleozoico. Durante este período geológico se produce la mineralización de grandes depósitos de materia orgánica por la acción de calor del subsuelo, la presión de acumulación de residuos de plantas y animales y las condiciones reductoras, formándose los principales depósitos de turba, lignito y carbón en Europa y Estados Unidos. Más tarde, en el Cenozoico, especialmente durante el Terciario, por la acción de importantes plegamientos y formación de cordilleras, parte de los depósitos que se encontraban a distintas profundidades emergen, quedando expuestos a humedad y condiciones oxidantes. Por lo tanto, la leonardita es una forma oxidada de lignito, un material intermedio entre turba y lignito, con apariencia similar al carbón y que en general se encuentra en la superficie de minas de carbón (*Qian et al.* 2015). Debe su nombre a A. G. Leonard, en reconocimiento de sus contribuciones científicas en la investigación de la materia orgánica humificada. Contiene entre un 30 y un 80% de HA y puede usarse como fertilizante orgánico o como enmienda (*Ayuso et al.*, 1997). La leonardita que se encuentra en Dakota del Norte (EEUU) fue la primera en describirse pero existen otros yacimientos naturales disponibles en el mundo. En la tabla 1 se presentan las diez naciones más importantes en la producción de carbón de baja calidad, dentro de los cuales se encuentra la leonardita. Los datos corresponden al año 2016 y fueron recogidos por el Instituto Geológico de España.

Tabla 1: Principales países productores de carbones de baja calidad

País	Producción (millones de toneladas)
Alemania	171
Estados Unidos	66,5
Rusia	73,5
Polonia	60,3
Australia	63,6
Turquía	56,8
Grecia	32,7
India	45,1
Serbia	37,6
Bulgaria	29,3
Rumania	23,0
España	0,38

El método de extracción de leonardita más utilizado es por medio del uso de disoluciones alcalinas. Se lleva a cabo con disoluciones de 0,1 a 0,5 M de NaOH o KOH con una relación (leonardita: disolución) 1:5 a 1:2 g ml^{-1}. Este método permite hasta un 80% de extracción pero puede producir cambios químicos en la estructura húmica original y adicionar impurezas inorgánicas (*Juárez et al*. 2006). La principal explotación y comercialización de leonardita en España se encuentra en la Comunidad Autónoma de Aragón, en las Provincias de Teruel y Zaragoza (Panorama Minero 2017).

Respecto del uso de la leonardita como fertilizante, *Akinremi et al.* (2000) demostraron que la leonardita incrementa la producción y la absorción de nutrientes (N, P, K y S) en cultivos de colza. En condiciones de invernadero, la leonardita es capaz de mejorar la resistencia de las plantas de tomate al stress salino (*Casierra-Posada y Fischer,* 2009). Además, se ha observado el aumento de producción y floración de *Arnica montana* L., cuando fue tratada con leonardita (*Sugier et al.* 2013). Actualmente está siendo también estudiada por sus posibles propiedades bioestimulantes (*Barone et al*. 2019). *Mora et al*. (2012), observaron que la leonardita afecta el desarrollo de raíces de plantas de pepino incrementando la concentración de óxido nitroso, ácido indolacético y etileno aunque no se detectaron en su estructura la presencia de hormonas vegetales. Además, observaron el incremento de la actividad de citoquininas en parte aérea de plantas y la asociaron con la capacidad de la leonardita de promover el crecimiento de las plantas (*Mora et al*. 2010). Sin embargo, *Canellas y Olivares* (2014) observaron que las plantas presentan mayor respuesta fisiológica cuando se les aplica HA extraídos de compost o vermicompost que cuando se les aplica ácidos húmicos procedentes de leonarditas.

I.3.1 Las sustancias húmicas en el suelo

Parte de las HS que se encuentran en los suelos forman complejos húmicos-arcillosos que mejoran la porosidad, aireación, retención de humedad y transporte de nutrientes en los suelos (*Stevenson,* 1982). Además, las HS son fuente de energía para los microorganismos del suelo, mejoran la estructura y la formación de agregados, inactivan o estabilizan la actividad enzimática, regulan la temperatura del suelo y la velocidad de evaporación del agua (*Pettit*, 2004). Igualmente, actúan como tampón del pH del suelo y son buenos absorbentes de contaminantes y pesticidas (*Stevenson,* 1982).

Las HS son consideradas complejantes naturales de cationes de micronutrientes (Fe, Mn, Cu y Zn) cuyo orden de estabilidad para divalentes sigue la serie de *Irving-Williams* (1953): Mn(II) < Fe(II) < Co(II) < Ni(II) < Cu(II) > Zn(II) mientras que su orden de solubilidad es el inverso

(*García-Mina,* 2006). La estabilidad y solubilidad de los complejos están condicionadas por el pH y la relación molar entre el micronutriente y la HS. Una alta estabilidad sería favorable en un rango de pH 5-9 para una relación metal-HS baja, mientras que una alta solubilidad sería favorable a pH alcalinos (*García-Mina* 2006). El mismo autor confirmó que el orden de estabilidad de los complejos metálicos formados a partir de HS de distinto origen, es el siguiente: HS de sedimentos marinos > FA de sedimentos marinos > HS de aguas naturales > HA de suelos > FA de suelos. Estos resultados indican que las HS acuáticas tienden a formar complejos más estables que las HS terrestres, que los FA tienden a formar complejos metálicos menos estables que los HA y que las HS no fraccionada tiende a formar complejos metálicos con una estabilidad mayor que los HA o FA extraídos de las HS. Además, la evaluación de las constantes de estabilidad de complejos Fe-HS (*García-Mina et al.* 2004) muestra valores más bajos que los que se obtienen para quelatos sintéticos de Fe como el HBED/Fe^{3+} (*López-Rayo et al.* 2009) o el EDDHA/Fe^{3+} (*Yunta et al*. 2003) o compuestos orgánicos de origen biológico como ácidos orgánicos o sideróforos (*Mimmo et al*. 2014).

Uno de los diversos factores de los que depende la eficacia de los complejos metálicos es la relación molecular metal: HS. En el caso particular del Fe, a bajas relaciones moleculares de Fe:HS, se favorece la movilización del complejo soluble desde la fase sólida hacia las raíces. Por el contrario, a altas relaciones moleculares Fe:HS, la solubilidad del complejo disminuye y por lo tanto su movilidad, produciéndose la precipitación de los mismos (*García-Mina et al.* 2006).

Nuzzo et al. (2013), utilizando cromatografía de exclusión molecular observaron cambios conformacionales en los ácidos húmicos y fúlvicos inducidos por la complejación con Fe. A medida que se incrementa la complejación con Fe, la distribución del tamaño molecular de los HA se reduce y la de los FA aumenta. Según estos autores, el Fe^{3+} forma complejos fuertes con los FA hidratados ya que éstos son más ácidos e hidrofílicos mientras que los HA son menos ácidos y más hidrofóbicos. El alto contenido de iones carboxilo en los FA favorece la formación de puentes intra o intermoleculares entre las moléculas de FA cargadas negativamente y de cadenas más compactas y de mayor tamaño que las que se forman con HA. En cambio la complejación de los HA con Fe, altera los arreglos conformacionales de los HA estabilizados sólo por puentes hidrofóbicos débiles, formando agregados de pequeño tamaño que poseen mayor estabilidad conformacional.

I.3.2 Las sustancias húmicas y las plantas

El efecto de las HS en el crecimiento de las plantas depende de la procedencia, la concentración, el peso molecular de la fracción húmica y principalmente de los componentes químicos que contiene (*Muscolo et al.* 2013). Además, se ha demostrado que las HS pueden estimular la liberación de H^+ de las raíces y la actividad de la H^+-ATPasa de vesículas aisladas de la membrana plasmática (*Zandonadi et al., 2016*), se ha observado a nivel transcripcional y post-transcripcional la activación de la bomba de protones de la membrana plasmática, relacionada con la extrusión protónica y toma de iones tales como nitrato (*Canellas et al.* 2015), fosfato (*Jindo et al.* 2016) y sulfato (*Jannin et al*. 2012). Además, se ha observado que las HS promueven el metabolismo del C mediante la glicólisis y el ciclo de Krebs (*Trevisan et al.* 2011) y la síntesis de metabolitos secundarios tales como los fenilpropanoides (*Jannin et al.* 2012).

El tratamiento de las plantas con HS induce cambios en la morfología de la raíz y modula las actividades de la membrana plasmática: adquisición de nutrientes, rutas de metabolismo primario y secundario, balance hormonal y de ROS (*Olaetxea et al*. 2018, *Zanin et al.* 2019). Estos efectos, sugieren que las HS son promotoras del crecimiento y de la resistencia al stress de las plantas. Varios autores (*Canellas et al.* 2015, *Nardi et al.* 2017) observaron que las plantas tratadas con HS de diferente origen son capaces de inducir proliferación de raíces laterales y pelos radiculares. *Canellas et al.* (2019) observaron que el crecimiento de raíces de plantas de maíz tratadas con HS es acompañado de liberación de exudados que contienen ácidos orgánicos de bajo peso molecular. Además, este comportamiento se relacionó con la activación de señales que involucran fitohormonas, en especial auxina, óxido nítrico, Ca^{2+} y ROS (*Zandonadi et al*. 2010, *Mora et al.* 2012, *García et al.* 2016). Los trabajos publicados por *Trevisan et al.* (2011) y *Zanin et al*. (2018) sugieren que las HS pueden influir en el equilibrio del estado estacionario de diferentes hormonas de plantas. Sin embargo, el crecimiento de las raíces también se observa independientemente de los cambios hormonales, sugiriendo que en las modificaciones morfológicas producidas por las HS pueden estar involucradas otras señales (*Mora et al.* 2012).

Nardi et al. (2002) informaron que, de las HS marcadas con ^{14}C y aplicadas a plantas de guisantes, entre un 10 y un 12% se trasladó de la raíz a las hojas, sugiriendo de este modo, que las HS ingresan a la planta. Recientemente, esta información fue confirmada por *Kulikova et al.* (2014) utilizando autorradiografía con tritio en plántulas de trigo fertilizadas con HS procedentes de leonardita.

Dentro de los beneficios que aportan las sustancias húmicas a las plantas, se reconoce que éstas pueden contribuir a la nutrición férrica mediante la formación de complejos Fe-HS solubles a través de grupos funcionales que contienen O como grupos carboxílicos y fenólicos (*Schenker y Chen*, 2005) que pueden difundir en el suelo y alcanzar las raíces.

Uno de los efectos beneficiosos de las HS se explica por la presencia de grupos donadores de electrones, que pueden intervenir en la respiración de las células e incrementar el suministro de energía a las células:

$$HS^- + O_2 + FADH_2/NADH \rightarrow HS + H_2O + FAD/NAD^+$$

Esta capacidad reductora posibilita la absorción de Fe de plantas de Estrategia I ya que éstas liberan sustancias reductoras (fenoles) para transformar Fe (III) en Fe (II). La concentración de compuestos fenólicos en las HS varía entre 700 mmol kg^{-1} para HA y entre 300–5700 mmol kg^{-1} para FA (*Sánchez-Sánchez et al.* 2002).

En los últimos años se ha estudiado en profundidad la participación de los humatos férricos de distinto origen en colaboración con la homeostasis del Fe en plantas de Estrategia I. *Pinton et al.* (1999) obtuvieron el complejo Fe-WEHS por medio de la reacción de complejación de una fracción húmica soluble (WEHS), purificada a partir de un extracto soluble de turba *sphagnum* (un FA), con $FeCl_3$. El Fe-WEHS se utilizó para corregir la clorosis férrica inducida en plantas de pepino. *Aguirre et al*. (2009) demostraron que HS purificadas de leonardita inducen un aumento pasajero en la regulación de los genes CsHA2, CsFRO1 y CsIRT1 de la raíz de plantas de pepino y relacionaron estos efectos con un incremento de la actividad de la enzima Fe quelato reductasa en raíz. *Tomasi et al*. (2009) observaron el aumento en la expresión génica de LeFRO1, LeIRT1 y Ferritin2 en hoja, después de la aplicación foliar de Fe-WEHS a plantas de tomate crecidas en hidroponía. *Colombo et al.* (2012) comprobaron la formación de ferrihidrita en la síntesis de complejos de Fe insolubles a partir de leonardita y confirmaron su eficacia en la corrección de la clorosis férrica en plantas de pepino cultivadas en hidroponía a pH 7,5. *Kovács et al*. (2013) obtuvieron resultados similares en pepino para un complejo férrico soluble a partir de leonardita. En plantas de tomate fertilizadas con Fe-WEHS se observó la inducción de la regulación génica de LeFRO1, LeIRT1 y LeIRT2 (*Tomasi et al.* 2013). Además, *Zamboni et al*. (2016) concluyeron que la respuesta transcripcional de las raíces a la nutrición férrica depende de la naturaleza del agente complejante. Recientemente, *Di Iorio et al*. (2019) han demostrado que los ácidos húmicos de leonardita influyen en el tamaño de partícula y la cristalinidad de la

goetita y magnetita que co-precipita con la sustancia húmica, cuando se aplican como fuente de hierro en hidroponía para la corrección de clorosis férrica de plantas de pepino.

Además, las dinámicas de movilización de Fe por acción de las HS dependen de las condiciones en la rizosfera, tales como pH y potencial redox, así como de la presencia de otros agentes quelantes de origen microbiano (sideróforos) o vegetal (ácidos orgánicos y PS). Por otro lado, las fracciones de HS de alto peso molecular pueden afectar la disponibilidad del Fe mediante la estabilización de los óxidos amorfos de Fe. Las fases de Fe amorfo co-precipitan con las fracciones insolubles de las HS y se mantienen por largo tiempo en esta forma, representando una reserva de Fe para la nutrición férrica de las plantas (*Colombo et al.* 2012, 2014, 2015). *Kulikova et al*. (2017) prepararon dos humatos de hierro a partir de leonardita con distintas relaciones Fe: HS, uno con exceso de HS y el otro con exceso de Fe. En el primer caso, obtuvieron nanoparticulas (< 11 nm) de un complejo polinuclear de Fe atrapado en la matriz húmica mientras que en el segundo, obtuvieron nanopartículas (35±20 nm) de feroxihita (δ'-FeOOH) estabilizadas por la HS. El complejo más eficiente en la corrección de la clorosis férrica en plantas de trigo fue el preparado con exceso de HS.

Todos estos resultados se resumen en la Figura 9, diagrama extraído y modificado para plantas de Estrategia I del trabajo publicado por *Zanin et al.* (2019).

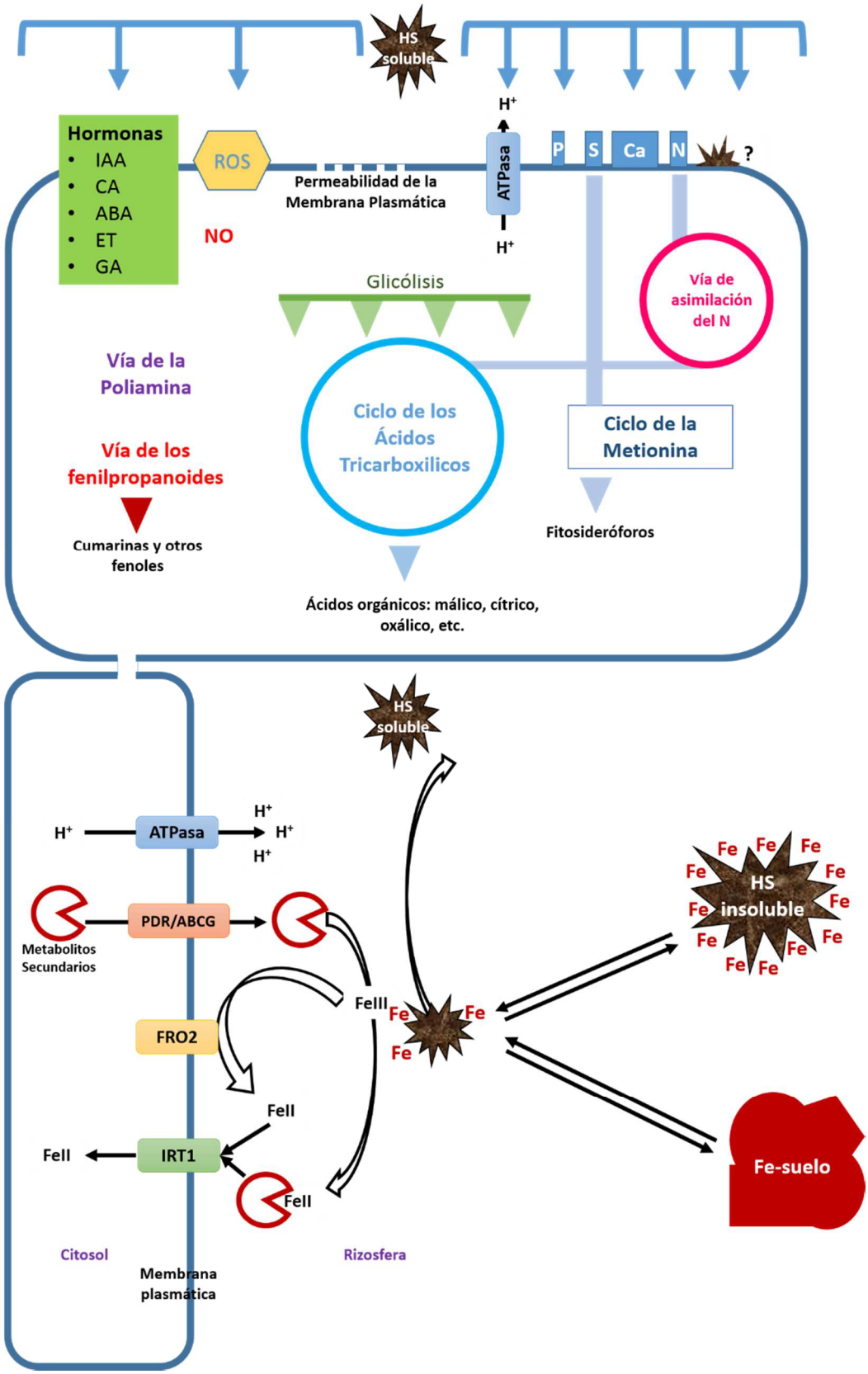

Figura 9: Respuesta fisiológica y molecular de las plantas de Estrategia I a la acción de las sustancias húmicas (parte superior) y el rol de los humatos de Fe en la nutrición (parte inferior). Diagrama modificado de *Zanin et al.* (2019).

I.4 Caracterización de los humatos férricos

La caracterización de los humatos férricos implica el análisis específico de la sustancia húmica y, además, la de las formas de hierro en su estructura, por lo cual, cuanto más completa sea, más datos proporcionará acerca de la estabilidad y solubilidad del producto fertilizante en las condiciones de pH del suelo y de su disponibilidad para las plantas.

En esta tesis se han aplicado técnicas analíticas de diversa complejidad en la determinación de Fe y sustancias húmicas que a continuación se detallan:

I.4.1 Caracterización relacionada con las formas de hierro

I.4.1.1 Determinación del hierro soluble y complejado

Es un requisito de la legislación para la comercialización de los complejos de Fe, contener como mínimo 5% de Fe soluble total del cual el 50% (RD506/ 2013) o el 80% (CE: 2019/1009) del elemento se debe encontrar complejado. Por lo tanto, la determinación analítica de dichos contenidos es imprescindible.

La determinación del Fe soluble en agua se realiza según el Método 9.3 y 9.4 del Reglamento CE: 2003/2003, recientemente modificado por la norma UNE-EN 16962:2018.

El contenido de Fe complejado se determina mediante el método incluido en la norma (UNE-EN 15962:2011). Si bien este método se ha desarrollado para lignosulfonatos, es aplicable a otro tipo de complejos, como por ejemplo, los obtenidos a partir de sustancias húmicas.

I.4.1.2 Microscopía electrónica

La microscopía electrónica se basa en la producción de imágenes a partir de la interacción de un haz de electrones con la materia. Algunas de sus múltiples aplicaciones son la determinación del tamaño de partícula de un material, su heterogeneidad química y su morfología (*Pansu y Gautheyrou* 2007). Según la aplicación que se necesite, será la técnica adoptada y la resolución del microscopio a elegir. Por ejemplo, la microscopía electrónica de barrido (SEM) produce imágenes tridimensionales de magnitud moderada mientras que la microscopía electrónica de transmisión (TEM) proporciona imágenes bidimensionales de cristales cuyo tamaño varía de unos pocos nanómetros hasta uno o dos micrómetros (*Cornell y Schwertman* 2003). Ambas técnicas fueron utilizadas en esta tesis y se describen a continuación:

- *Microscopía electrónica de barrido (SEM)* Es la técnica más utilizada para estudiar morfologías y superficies de minerales ya que se pueden determinar

los elementos constituyentes de las mismas y su proporción en las mismas (análisis semicuantitativo). La preparación de las muestras es relativamente fácil. Las muestras se colocan en un porta-muestra y se recubren con una capa de carbono o una capa delgada de un metal, como el oro, para darle carácter conductor. La resolución se encuentra entre 2 y 10 nm (*Pansu y Gautheyrou* 2007), dependiendo del elemento observado y para su identificación es necesario comprobar toda la familia de picos del elemento en estudio, dentro del espectro analizado. Esta técnica ha sido utilizada para determinar la naturaleza del Fe depositado sobre la superficie de las raíces, la cual se puede confirmar mediante difracción de Rayos X y espectroscopía Mössbauer. De este modo, *Amils et al.* (2007) determinaron la presencia de jarosita en raíces de *Imperata cylindrica* y *López-Rayo et al.* (2015) observaron cristales de hierro en las raíces de plantas de viña.

- *Microscopía electrónica de transmisión (TEM)* Esta técnica permite la observación de la muestra en cortes ultrafinos. La muestra debe tener al menos una micra de espesor y debe ser un ensamble de finas películas conductoras (*Pansu y Gautheyrou* 2007). La técnica ha sido utilizada en la determinación de tamaño de partículas de humatos férricos (*Polyakov et al*. 2012, *Sorkina et al*. 2014, *Angelico et al*. 2014, *Colombo et al*. 2015, *Kulikova et al*. 2017)

I.4.1.3 Espectroscopía Mössbauer

La espectroscopía Mössbauer es una técnica robusta de análisis no destructivo de sólido que provee información acerca del campo magnético en el núcleo, la valencia del Fe y el tipo de coordinación con el ligando (*Cornell y Schwertman* 2003). Esta técnica ha sido utilizada para identificar una amplia gama de fases de hierro en suelos (*Parfitt y Childs* 1988) y fases amorfas de hierro como ferrihidrita a bajas concentraciones (*Cornell y Schwertmann* 2003). Además, esta técnica se ha utilizado para la caracterización de humatos férricos (*Kovács et al.* 2013, *Polyakov et al.* 2013, *Sorkina et al.* 2014, *Kulikova et al.* 2017) y en el estudio de la química de las plantas utilizando ^{57}Fe (*Kilcoyne et al*. 2000). Sin embargo, la concentración de Fe en los tejidos vegetales es generalmente muy baja para ser detectada por esta técnica debido a la baja abundancia del ^{57}Fe en la naturaleza (2,12%) y a la baja sensibilidad de la técnica. Se ha observado mediante la espectroscopía Mössbauer que el Fe presente en plantas de lenteja de agua, alelí, soja y guisante (*Goodman y DeKock* 1982) se encuentra en la forma férrica, la mayoría como ferritina y una

pequeña fracción (<15%) complejado. *Kilcoyne et al.* (2000) observaron diferentes componentes de Fe(III) precipitados en las paredes de las células de raíces de plantas de arroz, además de ferritina y de otras especies complejadas que los autores no pudieron identificar. *Amils et al.* (2007) identificaron jarosita ($KFe_3(SO_4)_2(OH)_6$) en las raíces y los rizomas de una planta hiperacumuladora de Fe (*Imperata cylindrica*) mientras que *Fuente et al*. (2016) detectaron jarosita en sus tallos y hojas. *Kovács et al.* (2016) observaron Fe-carboxilato y oxi-hidróxido de Fe en el apoplasto y la superficie de raíces de plantas de pepino nutridas con $^{57}Fe^{3+}$.

I.4.1.4 Difracción de Rayos-X en muestras policristalinas

Esta técnica es ampliamente utilizada para identificar formas cristalinas de Fe (*Cornell y Schwertmann* 2003) presentes originalmente en las sustancias húmicas y las formadas durante la preparación de humatos férricos. Ejemplo de esto son los trabajos de *Angelico et al*. (2014) que caracterizaron ferrihidrita co-precipitada con ácidos húmicos (*Colombo et al.* 2015) y que utilizaron esta técnica para identificar los óxidos de Fe que precipitan con las sustancias húmicas en función del pH y de condiciones redox.

I.4.1.5 Espectroscopía de absorción de Rayos-X (XAS)

La espectroscopía de absorción de rayos X es una poderosa técnica estructural que permite investigar la vecindad de un átomo incrustado en un medio condensado y cuya teoría básica fue desarrollada a inicios de 1970 *(Filipponi et al*. 1995). Esta técnica utiliza la radiación generada por un acelerador de partículas (Sincrotrón). *Polyakov et al*. (2012) y *Sorkina et al.* (2014) han utilizado esta técnica en la caracterización de humatos de Fe mientras que *Fuente et al.* (2016) han analizado Fe en raíces y rizomas de plantas de *Imperata cylindrica.*

- *EXAFS (Extended X-ray Absorption Fine Structure)* Esta técnica es muy útil para muestras complejas donde el uso de XAS es insuficiente (*Lee y Beni* 1977) y provee información complementaria a otras técnicas como F-TIR, RMN y Difracción de Rayos-X (*Newton et al.* 2002). Es una técnica con selectividad elemental y es local. Se puede utilizar para obtener información estructural en sistemas amorfos muy complejos. Esta técnica es menos precisa que los métodos difractométricos, aunque se puede utilizar para el estudio de gases, líquidos y sólidos amorfos (*Filipponi,* 2001, *Guo et al.* 2010).

- *XANES (X-ray Absorption Near Edge Structure)* Es una técnica muy relacionada con el EXAFS pero solo se analiza la zona de absorción que rodea el átomo (*Pansu y Gautheyrou* 2007) y permite principalmente el estudio de los estados de oxidación de los diferentes elementos aunque no tiene gran utilidad para abarcar estudios estructurales. Es muy utilizada para la caracterización de los estados de oxidación del Fe.
- *EELS (Electron Energy Loss Spectroscopy)* Es una técnica relacionada con las anteriores que se utiliza para determinar las vibraciones de los átomos y las moléculas adsorbidos en las superficies metálicas (*Backx et al*. 1980). El detector EELS se sitúa habitualmente al final de la columna de un microscopio TEM. El análisis de la estructura de un espectro de EELS ofrece la posibilidad de determinar importantes características cristaloquímicas: estado de oxidación, número de coordinación, valencia, ángulos de enlace, posición de simetría, etc. y es además, una herramienta útil para el microanálisis elemental a escala nanométrica y para investigaciones relacionadas con la estructura electrónica (*Abad et al.* 2001). Parte de los electrones incidentes causan la ionización de electrones de capa internas del átomo con la consecuente emisión de fotones de Rayos X. Estos electrones incidentes pierden parte de su energía en el proceso inelástico. Los espectros resultantes, de pérdida de energía, se han aplicado principalmente a elementos de bajo número atómico para los que las pérdidas de energía son pequeñas.

I.4.2 Caracterización de las sustancias húmicas

Debido a la heterogeneidad de las sustancias húmicas y dado que la composición y estructura de las mismas varía de acuerdo a su origen geológico, es de vital importancia una adecuada y detallada caracterización química y espectroscópica de las mismas. Es de destacar que por la complejidad de la matriz es necesario aplicar diversas técnicas analíticas que se complementen entre sí a fin de obtener resultados consistentes. A continuación se detallan las determinaciones químicas y espectroscópicas utilizadas en esta tesis.

I.4.2.1 Caracterización química

- *Análisis elemental*

Según *Rice y Mac Carthy* (1991), el análisis elemental es una herramienta útil para la caracterización de materiales no-estequiométricos como las sustancias húmicas. Esta técnica provee información acerca de la distribución de los elementos mayoritarios (C, H, N, S y O) en las sustancias húmicas (*Schnitzer* ,1978). El contenido de C de los HA del suelo, en general, oscila entre 53,8 y 58,7%, el contenido de O entre 32,8 y 38,3%; los porcentajes de H y N varían desde 3,2 a 6,2% y 0,8 a 4,3%, respectivamente. El contenido de S varía de 0,1 a 1,5%. Comparado con los HA, los FA contienen más O y S pero menos C, H y N que los HA. El contenido de C de los FA varía desde 40,7 a 50,6% y el O desde 39,7 a 49,8%. Por lo tanto, los HA contienen 10% más de C pero 10% menos de O que los FA. Las sustancias húmicas acuáticas contienen menos C y N que las extraídas del suelo. El contenido elemental de las HS está condicionado por el pH, el material de origen, la vegetación y la edad del suelo (*Schnitzer,* 1978).

Una forma de obtener información acerca de la composición elemental de las HS es mediante el uso de relaciones atómicas (*Stevenson, 1994*). La relación O/C para HS extraída del suelo es de 0,5 mientras que para FA es de 0,7. La diferencia se debe a que los FA contienen mayor cantidad de COOH y/o de carbohidratos. La relación H/C para HS extraída del suelo y para FA es alrededor de 1,0.

La *IHSS* ha registrado en su página web (*IHSS* 2019a) los resultados del análisis elemental para una muestra de leonardita obtenida de una mina en Gascoyne (Bowman County, North Dakota, Estados Unidos) libre de cenizas con los siguientes valores, C: 63,81%, H: 3,70%, O: 31,27%, N: 1,23%, S: 0,76% y P:<0,01%.

- *Acidez total, contenido de ácidos carboxílicos y fenólicos*

La mayoría de los grupos funcionales que contienen las sustancias húmicas son carboxilos, hidroxilos y carbonilos. Los FA contienen más grupos funcionales de carácter ácido, especialmente carboxilos.

La acidez total de una HS se compone del contenido de grupos fenólicos más grupos carboxilos. La acidez total se determina por el método absorción con hidróxido de bario y el contenido de grupos carboxilos por el método del acetato de calcio, ambos métodos desarrollados por *Schnitzer* (1972). El contenido de grupos fenólicos se determina por diferencia entre la acidez total y el contenido de grupos carboxilos.

La acidez total en los FA (900-1400 mmol $100g^{-1}$) es considerablemente mayor que en los HA (400-870 mmol $100g^{-1}$). El contenido de carboxilos varía ampliamente, especialmente en el caso de los HA (*Peña-Méndez et al*. 2005).

Los valores registrados por la *IHSS* (2019b) para grupos funcionales ácidos de una muestra de leonardita corresponden a la densidad de carga de 7,46 mmol g C^{-1} para carboxilos a pH 8 y de densidad de carga de 2,31 mmol g C^{-1} para grupos fenólicos entre pH 8 y 10.

- *Máxima capacidad de complejación*

La máxima capacidad de complejación de Fe(II) o Fe(III) de un agente complejante se realiza para poder determinar la máxima cantidad de Fe que admite el agente complejante a un determinado pH sin que el complejo de Fe flocule. El método utilizado se basa en el trabajo realizado por *Villén et al.* (2007). Brevemente, se adicionan volúmenes crecientes de una solución de $FeSO_4 \cdot 7H_2O$ para la determinación de Fe (II) o de una solución de $FeCl_3 \cdot 6H_2O$ en el caso de Fe (III), a una alícuota de una solución de humato férrico. Luego, se lleva a pH 9, se centrifuga, se filtra y se mineraliza en medio ácido (HCl y H_2O_2). El Fe complejado se mide en espectroscopía de absorción atómica (AAS). En la Figura 10 se presenta un ejemplo de una gráfica de la determinación de la MCC de Fe (III) de un humato potásico utilizado en esta tesis. El punto de intersección de las dos rectas proporciona el valor de la máxima complejación del agente complejante. Esta técnica ha sido utilizada para la preparación de complejos de Fe por *Kovács et al*. (2013).

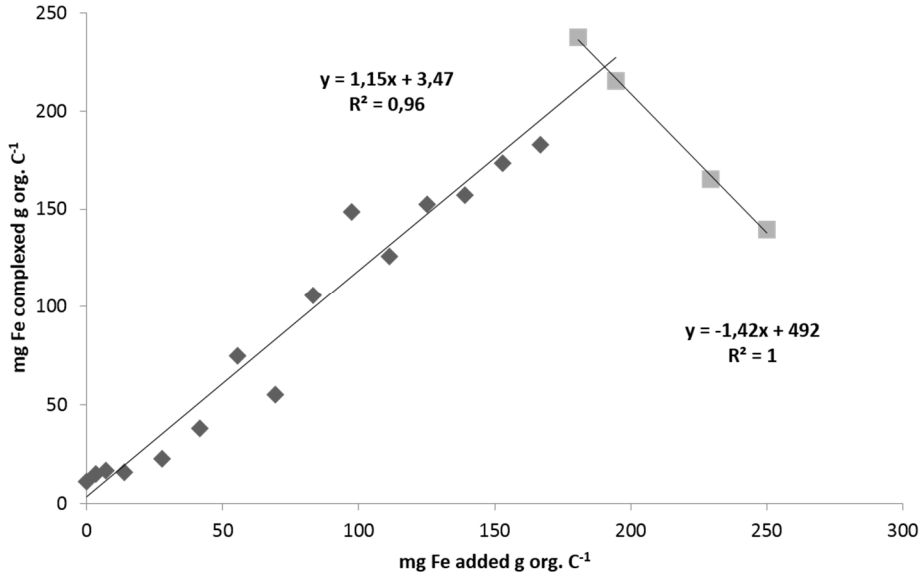

Figura 10: Ejemplo de gráfica de máxima capacidad de complejación de Fe(III) con leonardita

I.4.2.2 Caracterización espectroscópica

Las medidas espectroscópicas en diferentes regiones del espectro electromagnético proveen información valiosa acerca de la naturaleza de las sustancias húmicas (*Stevenson,* 1982), apoyan los resultados del análisis químico y son requerimientos esenciales para la caracterización de los humatos férricos. Sin embargo, ninguna de estas técnicas por sí solas es suficiente para elucidar la complejidad estructural de las moléculas húmicas.

- *Espectroscopía ultravioleta-visible*

Las HS no poseen un espectro característico en las regiones del ultravioleta y visible. El espectro de absorción de soluciones alcalinas y neutras de HA y FA, y las soluciones ácidas de FA no poseen rasgos distintivos ya que no muestran ni máximos ni mínimos. La densidad óptica disminuye en general, a medida que aumenta la longitud de onda.

La absorción de luz de las sustancias húmicas aumenta con:

1. el grado de condensación de los anillos aromáticos (*Kononova* 1966)
2. la relación entre el C presente en los núcleos aromáticos y el C lateral en las cadenas alifáticas (*Kasatochkin et al.* 1964)
3. el contenido de C total
4. el peso molecular

- *Relación E4/E6*

La relación de las densidades ópticas o absorbancias de soluciones diluidas de HA y FA a 465 y 665 nm (abreviada como relación E4/E6), se utiliza ampliamente para caracterizar la materia orgánica. Ésta consiste en la relación entre la absorbancia a 465 y 665 nm, de una solución de HA o FA en $NaHCO_3$ a pH 8,2; donde, valores bajos (E4/E6 < 5) indican un alto grado de aromaticidad; mientras que los altos (E4/E6 > 5) señalan un mayor contenido de cadenas alifáticas. *Chen et al.* (1977) observaron que esta relación presenta una alta correlación con el contenido de radicales libres, contenido de O, C y CO^2H, la acidez total y el peso molecular del material, los cuales están relacionados con el grado de madurez y estabilidad de las enmiendas orgánicas. La relación H/C de una HS está directamente relacionada con la relación E4/E6 que a su vez es inversamente proporcional al grado de condensación. Una baja relación E4/E6, es indicativa de un alto grado de condensación de estructuras aromáticas. Inversamente, una alta relación E4/E6 reflejará un bajo grado de condensación aromática e infiere la presencia de

proporciones relativamente grandes de estructuras alifáticas (*Stevenson*, 1994). Para los HA de suelos, el autor indica valores comprendidos entre 3 y 5,5 y para los FA de suelos el intervalo se encuentra entre 6 y 8,5.

- *Espectroscopía infrarroja (F-TIR)*

Los espectros infrarrojo (IR) de las HS y sus derivados contienen una variedad de bandas que diagnostican la estructura molecular específica. Según *Stevenson* (1982), la espectroscopía infrarroja con transformada de Fourier (F-TIR) proporciona información clave sobre la naturaleza, reactividad y distribución estructural de grupos funcionales que contienen oxígeno. Además, revela la presencia de proteínas, carbohidratos e impurezas inorgánicas (metales, iones, arcillas) en fracciones húmicas aisladas. La F-TIR es una técnica adecuada para análisis cuantitativo. De acuerdo a la *IHSS* (2019c) para el espectro de leonardita se esperarían los picos de absorción que se observan en la Figura 11.

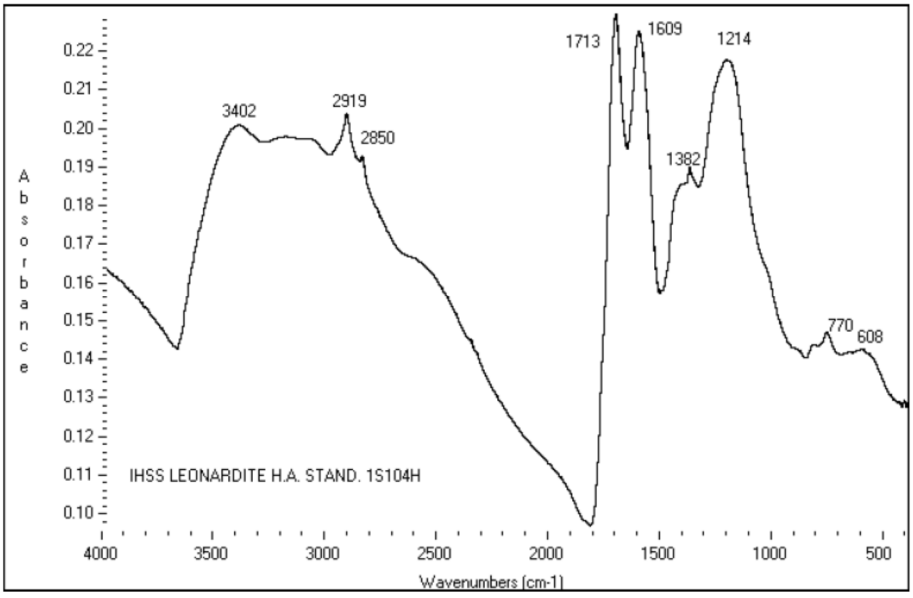

Figura 11: Espectro de absorción FTIR de una muestra estándar de leonardita analizada por la *IHSS* (2019c)

La tabla 2 resume la información recogida por *Karpukhina et al*. (2018) a partir de distintas fuentes bibliográficas de asignación de grupos funcionales a las correspondientes bandas de absorción de humatos secos y en solución acuosa.

Además, debemos mencionar las bandas de absorción correspondientes a Fe, que en la mayoría de los casos, son asociadas a ferrihidrita. A 3450−3300 cm^{-1} corresponden a tensiones O−H de Fe-OH mientras que las bandas que se observan a 1383, 1032 y 539 cm^{-1} son asignadas a uniones Fe−O (*Colombo et al.* 2012).

Tabla 2: Asignación de las bandas de absorción de humatos secos y en solución acuosa (*Karpukhina et al.*, 2018)

Nº de onda (cm^{-1})	**Asignación**
3691	Tensión O-H de la estructura de grupos hidroxílicos de la caolinita
3400-3300	Tensión O-H, tensión N-H (trazas), uniones H en OH
2935-2925,2850	Tensión simétrica y asimétrica C-H de grupos CH_2
1725-1710	Tensión asimétrica C=O de -COOH
1640-1600	Vibraciones estructurales de uniones C=C aromático, tensión C=O de grupos de amidas (banda de amida primaria), C=O de quinonas y/o H unidos a cetonas conjugadas
1560	Tensión estructural de uniones C=C aromáticos, C=O de quinonas y/o H unidos a cetonas conjugadas; $-COO^-$ tensión simétrica
1460-1450	Flexión asimétrica C-H de grupos CH_2
1420-1410	Torsión O-H y tensión C-O de OH fenólicos
1380	Flexión C-H de grupos CH_2 y CH_3, tensión asimétrica $-COO^-$
1308	CO de fenoles, CO y OH de ácidos carboxílicos, C-C alifáticos
1184	Tensión C-O-C (vibraciones estructurales) de residuos de celulosa
1170-950	C-O de polisacáridos; Si-O de silicatos
1130-1110	Tensiones C-O de alcoholes secundarios y/o ésteres
1070-1020	Tensión CO de alcohol y polisacárido, deformación OH; torsión Si-OH en impurezas de silicatos
1015	Si-OH de silicatos
938	Torsión OH de superficie interna de grupos hidroxílicos de caolinita
910	Torsión OH de superficie interna de grupos hidroxílicos de caolinita (en soluciones acuosas)
875	Flexión de salto de plano de calcita.

- *Resonancia magnética nuclear en estado sólido (^{13}C-RMN)*

Esta técnica ofrece una descripción de las principales clases de grupos que contienen carbono en su estructura; de una manera simple ha contribuido considerablemente a la información en cuanto a la naturaleza química de las HS (*Mao et al.* 2000) ya que proporciona información sobre los grupos funcionales presentes en la sustancia húmica y su aromaticidad. La tabla 3 muestra los grupos funcionales asignados a cada rango del espectro de ^{13}C-NMR según *Mao et al*. 2000.

De acuerdo a la *IHSS* (2019c) para el espectro de ^{13}C-RMN de leonardita se esperaría el espectro que se observa en la Figura 10. El pico entre 190 y 220 ppm corresponde a carbonilos, entre 190 y 165 ppm corresponde a carboxilos, entre 165 y 110 ppm a C aromáticos y entre 60 y 0 ppm a C alifáticos.

Table 3: Asignación grupos funcionales a cada intervalo (ppm) en espectros de **^{13}**C-RMN (*Mao et al*. 2000)

Intervalo (ppm)	Rango químico	Grupos funcionales
190-220	cetonas, quinonas, aldehidos	C=O, HC=O
162-190	Carboxilos, ésteres, quinonas	COO, COOH
145-162	Fenólicos	C-O-, C-OH
120-145	Aromáticos	CH, C
108-120	Aromáticos	CH
96-108	Anoméricos, carbón aromático cercano a carbones fenólicos	O-CH-O, CH
60-96	sacáridos, alcoholes, ésteres	CHOH, CH_2OH, CH_2-O-
50-60	metoxilos, metano, cuaternario	CH_3O-, CH-NH, CH, C
35-50	Complejos alifáticos	CH_2, CH, C
25-35	Metilenos de alifáticos simples	CH_2
0-25	Metilos	CH_3

De acuerdo a la *IHSS* (2019c) para el espectro de ^{13}C-RMN de leonardita se esperaría el espectro que se observa en la Figura 10. El pico entre 190 y 220 ppm corresponde a carbonilos, entre 190 y 165 ppm corresponde a carboxilos, entre 165 y 110 ppm a C aromáticos y entre 60 y 0 ppm a C alifáticos.

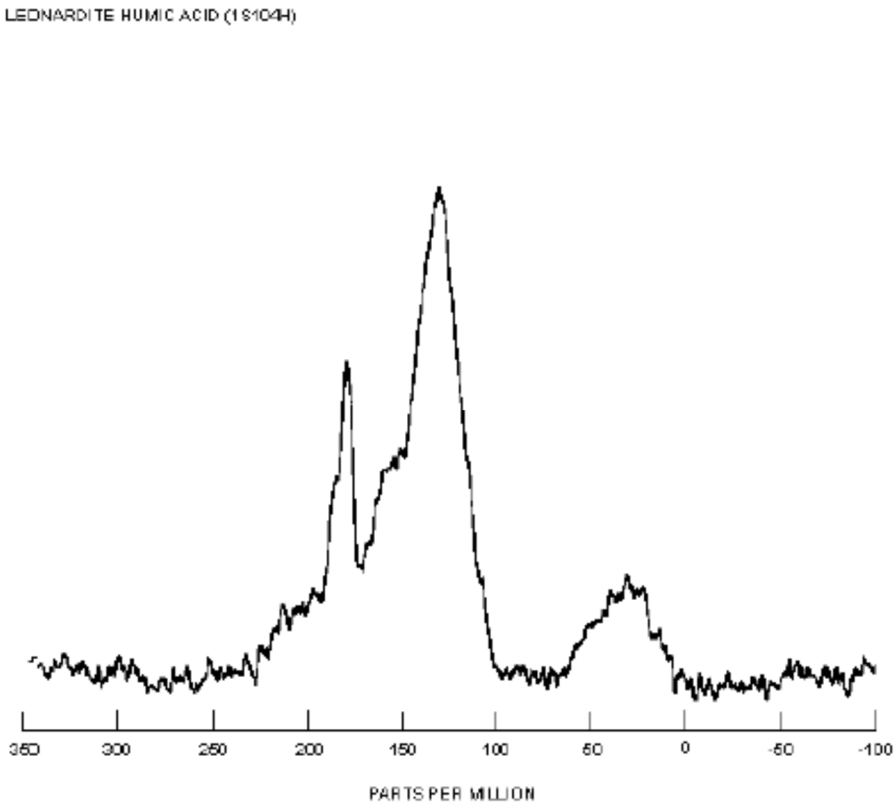

Figura 12: Espectro de ^{13}C-RMN para una muestra de leonardita analizada por la *IHSS* (2019c).

Esta información se suele contrastar con la obtenida de compuestos carboxílicos y fenoles por titulación potenciométrica y la máxima capacidad de complejación para predecir la estabilidad del complejo de Fe obtenido.

I.5 Uso de isótopos estables de Fe

En la naturaleza, el Fe es una mezcla de cuatro isótopos estables: ^{54}Fe, ^{56}Fe, ^{57}Fe y ^{58}Fe cuyas respectivas abundancias naturales son: 5,85%, 91,75%, 2,12% y 0,28% (*Isoflex* 2019). La aplicación de Fe marcado en experimentos de fertilización en suelo permite conocer en detalle la absorción, el transporte y la acumulación del Fe en la planta. Además, el desarrollo de técnicas analíticas de alta sensibilidad como la espectroscopía de masas por plasma de acoplamiento inductivo (ICP-MS) de cuadrupolo, favorece el uso de los isótopos estables. La alta precisión y los bajos límites de detección que se obtienen con las técnicas isotópicas permiten encontrar diferencias que normalmente no son detectadas con las técnicas convencionales. Varios autores (*Cesco et al*. 2002, *Nikolic et al.* 2003, *Chen et al*. 2004, *Tomasi et al*. 2013) han utilizado el isótopo radioactivo ^{59}Fe en sus estudios de evaluación de humatos férricos y su disponibilidad en suelos calizos. Sin embargo, el uso de isótopos estables, a diferencia del uso de radioactivos, ofrece alta flexibilidad en los diseños experimentales incluso en estudios de campo porque las mediciones se pueden realizar en condiciones seguras y sin necesidad de personal entrenado para tal fin. El ^{57}Fe es ampliamente utilizado en espectroscopía Mössbauer para caracterizar muestras de humato férrico y de tejidos vegetales, como se ha detallado previamente, y en estudios de eficacia de complejos de Fe (*Kovács et al.* 2009, *Rodríguez-Lucena et al*. 2011) gracias al cálculo de la deconvolución isotópica desarrollada por *Rodriguez-Castrillón et al*. (2008). En esta tesis se ha contribuido al estudio de la eficiencia de los humatos de Fe mediante el uso de isótopos estables de Fe.

Capítulo II: Objetivos

Chapter II: Objetives

Actualmente, los quelatos sintéticos de hierro son los fertilizantes más eficientes en la corrección de la clorosis férrica y los más utilizados en cultivos extensivos en suelos calizos. Sin embargo, su costo es elevado, pueden ralentizar los mecanismos naturales de absorción de Fe por las plantas y son persistentes en el medioambiente. Todo ello sugiere la necesidad de desarrollar nuevos fertilizantes que despierten el interés de los agricultores que apuestan por un manejo sostenible y agroecológico de sus cultivos.

Los humatos férricos son complejos naturales de hierro que se aplican en la Región Mediterránea desde hace décadas pero se ha observado que en los últimos veinte años su oferta como correctores de deficiencia de hierro ha disminuido en el mercado español. En parte, esa disminución se debe a los requerimientos impuestos por la Regulación Española y Europea y en parte, a su menor eficiencia respecto de los quelatos de hierro. Además, la composición y estructura de los humatos férricos presentan una alta complejidad y dependen de las características geológicas de donde son extraídos, por lo cual, precisan una caracterización fisicoquímica adecuada tanto de la materia orgánica que los compone como del estado de agregación del hierro y su cristalinidad, a fin de garantizar la calidad del fertilizante.

En los últimos años se ha avanzado ampliamente en la comprensión de la homeostasis del hierro y la influencia de las sustancias húmicas en la expresión génica de los transportadores de hierro en la rizosfera, proporcionando mayor información acerca de los mecanismos que gobiernan la nutrición férrica en presencia de sustancias húmicas. Además, nuevas tecnologías que se encuentran en fase experimental como la producción de nanopartículas, prometen mejorar la eficiencia de los fertilizantes y convertirse en herramientas claves de la agricultura de precisión y sustentable. A todo esto debemos sumar también el uso de isótopos estables de hierro como el ^{57}Fe y el ^{56}Fe que permiten identificar los fertilizantes en los órganos de la planta y los avances en la caracterización química, espectroscópica y microscópica del hierro y las sustancias húmicas que permiten obtener información detallada de la composición de los humatos férricos.

Por todo ello, la presente Tesis Doctoral pretende vincular las características físico-químicas de los humatos de hierro a partir de leonarditas con su mecanismo de acción en la nutrición de plantas de Estrategia I, cultivadas en suelos calizos, y propone modificaciones en la preparación y en el modo de aplicación de los humatos férricos a fin de mejorar su eficiencia en la nutrición férrica, y como una alternativa agroecológica de fertilización a menor costo.

Los trabajos que se detallan en esta Tesis Doctoral se han realizado a fin de responder a los siguientes objetivos:

1. *Establecer la relación entre algunas de las características físico-químicas de los humatos de hierro sintetizados a partir de leonardita y su eficiencia en la nutrición de plantas de Estrategia I cultivadas en suelos calizos.*

Para concretar este objetivo se realizaron las siguientes tareas:

- Se prepararon humatos de hierro a partir de leonarditas que se caracterizaron química y espectroscópicamente, se estudiaron su reactividad en suelo y su comportamiento cinético en la liberación de hierro a fin de predecir su eficiencia en la nutrición férrica.
- Se estudió la relación entre acumulación de ácidos húmicos, hierro y bio-mineralización de hierro sobre las raíces de plantas de soja cultivadas en condiciones calizas y sus efectos en la nutrición férrica.
- Se evaluó la eficiencia de los humatos férricos en la nutrición férrica de plantas de Estrategia I por medio de su aplicación a plantas de soja en experimentos hidropónicos y en suelo calizo en cámara de cultivo, así como también en ensayos de campo, a cultivos de cítricos en la Región Mediterránea.

2. *Proponer posibilidades de mejora en la eficiencia en la nutrición de plantas de Estrategia I cultivadas en suelos calizos.*

Para lograr este objetivo se realizaron las siguientes tareas:

- se prepararon mezclas de humatos férricos y quelatos sintéticos de hierro mediante el uso de isótopos estables de hierro (^{56}Fe y ^{57}Fe), se eligió el quelato de hierro más conveniente para la mezcla, se estudió la relación más adecuada entre ambos productos y se evaluó el efecto de distintas dosis en la nutrición férrica de plantas de soja cultivadas en suelo calizo.
- Se prepararon nano-fertilizantes de humato férrico marcados con ^{57}Fe, se caracterizaron, y se evaluó la eficiencia de distintas dosis en la nutrición férrica de plantas de soja cultivadas en suelo calizo.

The objectives of this Doctoral Thesis are:

1. To study the relationship between the physicochemical characterization of leonardite iron humates and their efficiency in iron nutrition of Strategy I plants in calcareous soils.

In order to achieve this objective, the following tasks were carried out:

- Leonardite iron humates were prepared, characterized, their reactivity in soil tested and their kinetic behavior in iron release was studied in order to predict their efficiency in iron nutrition.
- The relationship among iron and humic acid accumulation, iron biomineralization on soybean roots and their effects in iron nutrition of soybean plants under calcareous conditions was assessed.
- The iron humates efficiency in iron nutrition of Strategy I plants was evaluated by their application in hydroponics and soil pot experiments to soybean plants and in a field experiment carried out in a citrus orchard of the Mediterranean basin.

2. To propose methods for improvements of iron leonardite humate efficiency in iron nutrition of Strategy I plants grown in calcareous soils

In order to achieve this objective, the following tasks were carried out:

- Iron humate/iron chelate mixtures by using iron isotopes (^{56}Fe y ^{57}Fe) were prepared, the most convenient iron synthetic chelate was chosen, the most adequate iron humate: iron chelate ratio was tested and the dose effect in soybean iron nutrition in calcareous soils was evaluated.
- Leonardite iron humates nanofertilizers labeled with ^{57}Fe were synthesized, characterized and the efficiency of different doses in providing iron to soybean plants in calcareous soils, was evaluated.

Capítulo III: Relación entre caracterización y eficiencia de los humatos férricos

Chapter III: Relationship between characterization and iron humates efficiency

RESUMEN

Los humatos férricos procedentes de leonardita son fertilizantes de bajo costo y amigables con el medioambiente. En este capítulo se estudia la vinculación entre las características fisicoquímicas y espectroscópicas de los humatos férricos y su eficiencia en la nutrición férrica. Específicamente, se estudia la relación entre caracterización, perdurabilidad y comportamiento de la cinética de liberación del hierro. Además, se estudia la relación entre acumulación de humatos férricos y de hierro en raíces de plantas de Estrategia I, bio-mineralización de hierro en raíces y nutrición.

Los humatos férricos utilizados en estos trabajos (LIH) son principalmente ácidos húmicos con una estructura de alta condensación donde el hierro se encuentra en forma de ferrihidrita, compuestos polinucleares férricos estabilizados por la materia orgánica y uno de ellos presenta jarosita que puede bio-mineralizarse en los puntos ácidos de la rizosfera. La relación humato: hierro debe ser la adecuada a fin de evitar la floculación del hierro debido a la formación de agregados con la materia orgánica. Además, los humatos férricos presentan una cinética lenta que favorece que la corrección de la clorosis férrica se realice a largo plazo y en función de la demanda de la planta durante todo su ciclo vegetal.

Este capítulo se divide en dos apartados con sus correspondientes trabajos:

3.1 Long-term effect of a leonardite iron humate improving Fe nutrition as revealed *in silico*, in vivo, and in field experiments. (Efecto a largo plazo de un humato de hierro procedente de leonardita que mejora la nutrición férrica según experimentos de modelización, con plantas y en campo). Este trabajo se publicó en *Journal of Agricultural and Food Chemistry* 2017, 65, 6554-6563.

3.2 Iron and humic acid accumulation on soybean roots fertilized with leonardite iron humates under calcareous conditions. (Acumulación de hierro y ácidos húmicos en raíces de plantas de soja, fertilizadas con humatos férricos en condiciones calizas). Este trabajo se publicó en *Journal of Agricultural and Food Chemistry* 2018, 66, 13386-13396.

III.1 Long-term effect of a leonardite iron humate improving Fe nutrition as revealed in silico, in vivo, and in field experiments.

JOURNAL OF AGRICULTURAL AND FOOD CHEMISTRY

Article

pubs.acs.org/JAFC

Long-Term Effect of a Leonardite Iron Humate Improving Fe Nutrition As Revealed in Silico, in Vivo, and in Field Experiments

María T. Cieschi,[†] Marcos Caballero-Molada,[‡] Nieves Menéndez,[§] Miguel A. Naranjo,[‡] and Juan J. Lucena*[,†]

[†]Department of Agricultural Chemistry and Food Science, Autonomous University of Madrid, c/Francisco Tomás y Valiente, 7 Ciudad Universitaria de Cantoblanco, 28049 Madrid, Spain

[‡]Institute for Plant Molecular and Cellular Biology, CSIC, Polytechnic University of Valencia, Camino de Vera s/n, 46022 Valencia, Spain

[§]Department of Applied Physical Chemistry, Autonomous University of Madrid, c/Francisco Tomás y Valiente, 7 Ciudad Universitaria de Cantoblanco, 28049 Madrid, Spain

Supporting Information

ABSTRACT: Novel, cheap and ecofriendly fertilizers that solve the usual iron deficiency problem in calcareous soil are needed. The aim of this work is to study the long-term effect of an iron leonardite fertilizer on citrus nutrition taking into account a properly characterization, kinetic response with a ligand competition experiment, efficiency assessment using *Saccharomyces cerevisiae* strain and finally, in field conditions with citrus as test plants. Its efficiency was compared with the synthetic iron chelate FeEDDHA. Leonardite iron humate (LIH) is mainly humic acid with a high-condensed structure where iron is present as ferrihydrite and Fe^{3+} polynuclear compounds stabilized by organic matter. Iron and humic acids form aggregates that decrease the iron release from these kinds of fertilizers. Furthermore, LIH repressed almost 50% of the expression of *FET3*, *FTR1*, *SIT1*, and *TIS11* genes in *Saccharomyces cerevisiae* cells, indicating increasing iron provided in cells and improved iron nutrition in citrus.

KEYWORDS: *humic acids, iron complexes, ligand competition, citrus clementine*

INTRODUCTION

Citrus is one of the most important horticultural Mediterranean crops. Tangerines represented 34% of total Spanish citrus production during 2014.[1] Iron deficiency is a widespread problem in these areas because fruit trees grow on calcareous soils. The normal growth of chlorotic trees is affected, decreasing yield and fruit quality. Iron fertilizers based on humic substances such as leonardite are used in the Mediterranean area (as liquid concentrates) in drip irrigated fruit tree plantations.[2] Leonardite is a coal-like substance similar in structure to lignite but significantly different in its oxygen and ash contents.[3] Moreover, its humic materials are complex organic molecules that contain a wide variety of functional groups (carboxyl, hydroxyl, and carbonyl) involved in chemical binding.[4] Leonardite iron humate (LIH) is obtained by the complexation of potassium humate with diverse iron salts,[5−7] mainly $Fe_2(SO_4)_3{\cdot}9H_2O$, $FeSO_4$, or $Fe(NO_3)_3{\cdot}9H_2O$. The Spanish Regulation on Fertilizers and Soil Amendments[8] allows the use of humic and fulvic acids in fertigation and foliar applications, while in the EU Fertilizer Directive use is under discussion. In general, iron complexes fertilizers are cheaper and more ecofriendly than iron synthetic chelates as Fe-*o*,*o*EDDHA (iron ethylenediamine-di(*o*,*o* -hydroxyphenylacetic acid)) although less effective in correcting iron chlorosis.[9]

According to Francioso et al.,[10] diagenesis of each coal differs radically depending on plant residues and coal generating conditions. Furthermore, it is important to characterize correctly the iron humate fertilizer in order to obtain an understanding of its physical-chemical nature. New analytical methods allow a detailed profile of the humic substances to be obtained and thus apply them more adequately. Analytical techniques such as FT-IR, Mössbauer, or X-ray diffraction are essential requirements for characterizing a humic substance-Fe complex.

Chen et al.[11] suggested that humic substances enhance iron uptake by plants because of their ability to form metal complexes, although it depends, among another factors, on their stability and solubility.[12] Ligand competition is a general method proposed by Stevenson[13] and is applied to evaluate the stability of metal complexes when the calculation of relative constants by potentiometric and photometric methods is difficult to carry out due to the chemical nature of the metal complex. This method was used with iron chelates by Lucena and Chaney,[14] and it can be adapted for iron complexes and thus, approximating to the iron humate kinetic behavior at ideal conditions of pH and ionic strength.

Iron is an essential nutrient for nearly all organisms because it plays a critical role in important biochemical processes such as respiration and photosynthesis. Yeast, like plants, reduces iron before uptake via a plasma membrane-bound Fe(III) reductase. Similarly, yeast like plants, appears to have an Fe(II)

Received: April 19, 2017
Revised: July 9, 2017
Accepted: July 17, 2017
Published: July 17, 2017

DOI: 10.1021/acs.jafc.7b01804
J. Agric. Food Chem. 2017, 65, 6554−6563

transporter.[15] *Saccharomyces cerevisiae* has been proposed as a model organism for the study of iron metabolism, since the mechanisms that regulate the homeostasis of this metal are highly conserved in this strain and plants.[16] Moreover, *S. cerevisiae*, a nonpathogenic single-celled fungus, provides an ideal model system for studying the molecular and cellular biology of eukaryotes as it has, among other advantages, rapid growth and an easily manipulated genome,[17] which was sequenced[18] and highly characterized.[19] In addition, the use of yeasts to evaluate the iron fertilizers efficiency avoids hydroponic and greenhouse expenses, reduces the time process of studying of a new fertilizer, completes the appropriate characterization, and predicts their possible behavior in plant nutrition.

In spite of the high agricultural importance of the humic substances originating from low-rank coals as fertilizers, few studies have been carried out on these humic substances compared with studies on soil or water-derived humic substances.[10] Shenker and Chen[9] have indicated that investigations carried out with coal materials had shown that Fe-deficiency in various crops grown on calcareous soils and had been alleviated over a long period of time. Alva et al.[20] observed a slow but increasing recovery of iron from Fe-sludge products in a batch experiment and suggested that these products were able to provide available iron for crop uptake slowly over an extended period following their application to soil. Alva and Obreza[21] showed that usage of iron humate increased leaf iron concentration as well as yield in citrus and in grape fruit after the first year of application. Pérez-Sanz et al.[22] investigated the efficiency of iron-enriched sewage sludge as a substitute for synthetic chelates in a remedy for citrus and peach chlorosis and observed that despite the absence of increased yield, the size and quality of fruits were improved. Several authors[23,24] have observed improved yield, mineral uptake, and fruit quality when leonardite was applied in the field but there are few agronomical studies about iron leonardite application to orange trees in calcareous soils. The aim of this work is to study the kinetic conditionings related to the chemical characteristics of a leonardite iron humate that produce a long-term effect in citrus nutrition in calcareous soils.

MATERIALS AND METHODS

Reagents. All reagents used were of recognized analytical grade, and solutions were prepared with type-I grade water according to ISO 3696:1987,[25] free of organic contaminants (Millipore, Milford).

Chemical and spectroscopic characterization of LIH. The LIH used in this work is a commercial humic material generously provided by the Spanish company, Fertinagro S.L. It was characterized using standard methods as indicated in the Supporting Information.

Reactivity of LIH. In order to test the amount of soluble Fe available to plants under various agronomic conditions, the effect of pH in Ca solutions and the interaction with soil and soil components of the LIH were carried out following the method described by Álvarez-Fernández et al.[26] For both experiments, blanks of LIH solution and blanks of soils and soil components were prepared and taken into consideration for the calculations. Samples (two replicates) were stored in the dark to avoid the possible photodecomposition of the complex. After the respective time periods supernatants of the samples were filtered through a 0.45 μm Millipore membrane, and pH was measured using an Orion Research Ion Analyzer (EA920). A 0.2 mL aliquot of 6.0 M HCl was added to 2.0 mL of each filtrate, and the soluble Fe was quantified using AAS.

Effect of pH in Ca Solutions. An amount of 5.0 mL of 2.0 mM LIH solution and 5.0 mL of a universal buffer solution (10.0 mM HEPES + 10.0 mM MES + 10.0 mM CAPS + 10.0 mM AMPSO + 100 mM $CaCl_2$ at pH 5) was dissolved in 25.0 mL of water. The pH of each solution was then adjusted from 4.0 to 13.0 with HCl or NaOH and the volume raised to 50 mL. Samples were placed in a shaker bath at 25 °C and 11 min^{-1} for 3 days and then analyzed as previously indicated.

Interaction with Soil and Soil Components. Various materials (see the Supporting Information for their description) were allowed to interact with 5.0 mL of 0.40 mM solutions of LIH and 5.0 mL in 20 mM $CaCl_2$ and 2.0 mM HEPES (pH = 8) in sterile polyethylene flasks. The flasks were shaken at 11 min^{-1} for 1 h, then allowed to stand for 3 days in an incubator at 25 °C, and finally analyzed as previously indicated.

Ligand Competition of LIH with the Synthetic Chelating Agents EDDHA, HBED, and BPDS. LIH may retain Fe(II) or Fe(III) in different forms of different reactivity. In order to study the stability of LIH at pH 7, two ligand competitions (LIH + EDDHA + BPDS and LIH + HBED + BPDS) were carried out for 97 days, measuring every 2 or 3 days the changes in absorbance from 350 to 650 nm. The chelate agents used were EDDHA (ethylenediamine-di(*o-o* hydroxyphenylacetic acid)) obtained from LGC Standards, Teddington, U.K. (93.12%); bathophenanthrolinedisulfonic acid disodium salt trihydrate (BPDS) obtained from Sigma-Aldrich, Alcobendas, Spain (98.0%) and *N*,*N*′-di(2-hydroxybenzyl)-ethylenediamine-*N*,*N*′-diacetic acid monohydrochloride (HBED) generously provided by ADOB PPC, Poznan, Poland (93.72%). The chelated agents EDDHA and HBED were chosen as specific Fe(III) chelators and BPDS as a Fe(II) chelator. The following solutions 100.0 μM were prepared: leonardite humic acid (LHA), LIH, EDDHA, HBED, BPDS, FeEDDHA, FeHBED, $FeBPDS_3$, LIH + EDDHA + BPDS, and finally LIH + HBED + BPDS. All the solutions were prepared in three replicates with an ionic strength of 0.1 M with KNO_3. In all cases, pH was then adjusted to 7 with KOH 0.1 M, buffered with 2.0 mL of HEPES 0.1 M and made up to 100.0 mL. The solution labeled LHA corresponds to the original leonardite obtained by potassium hydroxide extraction previously complexed with iron and which was used as a blank solution. Afterward, the solutions were kept at room temperature in the dark until measurement. The chelating agents EDDHA, HBED were dissolved previously with 3 mol of NaOH per mol of chelating agent, and the pH was then adjusted to 7. The UV/vis spectra of samples from 350 to 650 nm were recorded on a Jasco V-650 spectrophotometer every 2 or 3 days for 97 days.

Taking into account the iron contribution of each component, for example, in the solution LIH + FeEDDHA + $FeBPDS_3$, the total iron concentration in this solution would be

$$[Fe_{total}]_{LIH+EDDHA+BPDS} = [Fe]_{LIH} + [Fe]_{FeEDDHA} + [Fe]_{FeBPDS_3} = 100\ \mu M$$

The theoretical results were calculated as the sum of contributions of each component absorbance at each wavelength measured from 350 to 650 nm.

$$A_{\lambda i=} \sum_i A_\lambda = \sum_i [i]_\lambda \varepsilon_\lambda + e_\lambda$$

where A is the absorbance, λ is every wavelength measured from 350 to 650 nm, ε is the absorptivity calculated for each wavelength for these experimental conditions. Each component is represented by i and, for this example, the components are LHA, LIH, EDDHA, BPDS, FeEDDHA, and $FeBPDS_3$. The best concentration of each component at each wavelength from 350 to 650 nm was found by least-squares fitting of the error vector e (minimizing the square sum of errors) and mathematical deconvolution was applied among the experimental and the theoretical results. The same procedure was applied for the solution LIH + HBED + BPDS.

Prediction of the LIH Efficacy in Iron Nutrition Using a *Saccharomyces cerevisiae* Strain. The yeast strain BY4741 (*MATa*, *his3Δ1*, *leu2Δ0*, *met15Δ0*, *ura3Δ0*) was used in this work as a model of Fe(III) reducing organism, so the iron assimilation from LIH can be

DOI: 10.1021/acs.jafc.7b01804
J. Agric. Food Chem. 2017, 65, 6554−6563

conveniently studied. It was obtained from the European *Saccharomyces cerevisiae* Archive for Functional Analysis.[27] For the experiments with and without iron, yeast cells were grown in synthetic dextrose (SD) defined media (glucose, mineral salts, and vitamins) buffered with 0.5 M MES at pH 6 according to Sherman[17] with agitation at 28 °C. For experiments without iron, yeast nitrogen base (YNB) without amino acids and iron (Formedium, Norfolk, U.K.) was added to SD and BPDS 6 μM as an extracellular chelating agent was used. Experiments were designed to study the cell growth rate after FeEDDHA and LIH additions at several doses including a Fe control, the quantification of mRNA of cells grown in the presence of FeEDDHA and LIH and for the determination of intracellular iron content of cells grown in presence or absence of FeEDDHA and LIH. More detailed information on the *Saccharomyces cerevisiae* experiments is included in the Supporting Information.

Field Experiment. Besides the studies done "in silico" and "in vivo" to understand the Fe release pattern from the LIH, a field experiment was designed so LIH behavior could be corroborated. A chlorotic orange (*Citrus clementine Hort. ex Tanaka*, ClemenRubí PRI 23) orchard situated in Bétera (Valencia, Spain) was fertilized by drip irrigation with LIH and FeEDDHA from May to August, 2014. The iron content in leaves was analyzed along the entire process. During September and October 2014, the crop was harvested and the yield was calculated. Orange trees were 6 years old, grafted on Citrange Carrizo rootstocks and grown on a calcareous soil that was properly characterized (Table 1). According to Soltanpour and Schwab,[28] the calcareous soil presented adequate iron nutrition. The experiment was arranged in a randomized block design, with 5 replicates per treatment and 27 trees per row. The FeEDDHA applied was Facile PLUS (Agrofit, S. Coop, Valencia, Spain) and was analyzed according to EN 13368-2:2012[29] (soluble Fe, 5.96%; chelated with *o,o* EDDHA, 4.72% and 0.85% *o,p* EDDHA). All treated trees received the same Fe(III) rate of 0.25 g of Fe tree^{-1} in the first application and 0.10 g of Fe tree^{-1} for all of the following applications, every 2 weeks. Control trees without Fe-treatment were also included.

Table 1. Soil Characterization (Bétera, Valencia, Spain)

pH H_2O (1:2.5 w/v)	8.01 ± 0.02
pH KCl (1:2.5 w/v)	7.90 ± 0.03
EC (extract 1:5) (dS m^{-1})	0.26 ± 0.01
sand[a] (g kg^{-1})	600
silt[a] (g kg^{-1})	240
clay[a] (g kg^{-1})	160
texture[a]	Sandy loam
OM (oxidizable)[b] (g kg^{-1})	21 ± 0.6
N total[c] (g kg^{1-})	1.4 ± 0.1
P (assimilable)[d] (g kg^{-1})	0.15 ± 0.01
$CaCO_3$ total[e] (g kg^{-1})	107 ± 5.09
active lime[f] (g kg^{-1})	26 ± 1.3
Macronutrients[g] (cmol$_c$ kg^{-1})	
Ca	6.6 ± 0.2
Mg	1.2 ± 0.1
K	1.2 ± 0.1
Micronutrients[h] (mg kg^{-1})	
Fe	28.0 ± 0.05
Zn	6.3 ± 0.1
Mn	39.0 ± 0.47
Cu	5.21 ± 0.06

[a]Densitometry. Bouyoucos's method. [b]Walkley-Black's method. [c]Kjeldahl's method. [d]Olsen's method. [e]Williams's calcimeter. [f]Droineau's method. [g]Exchengeable cations extracted with NH_4Ac pH = 7. [h]Soltanpour and Swab's method.[28] EC: Electrical conductivity. OM: Organic matter.

In order to evaluate the influence of Fe on leaves, the Soil-Plant Analysis Development (SPAD) Index was measured using a Minolta Chlorophyll Meter SPAD-502 (Minolta, Osaka, Japan) before the first application of the Fe fertilizers and at 15, 45, and 75 DAT (Days After Treatment initiation). This is a green color index related to chlorophyll content. The average of 2 determinations per tree and 25 trees per row was recorded.

Four samplings of leaves were carried out, one before to apply the Fe fertilizers and the other three, after the first treatment application. Two young spring leaves, in the opposite position of the tree and at 1 m high, were sampled per tree and row[30] except for the border trees. Leaves were then washed with Tween-80 and HCl 0.1 M for 20 s with distilled water to wash off dust particles[26] and dried in a forced air oven at 60 °C for 3 days. Samples were mill ground, and after a dry digestion in a muffle furnace (480 °C) the ashes were digested using HCl 1:1. Iron was determined by AAS.

Statistical Analysis. In order to verify the homogeneity of the data, the Levene test was used first. Then, differences between treatments were tested for significance by one-way analysis of variance (ANOVA). Means were compared using the Duncan multiple range test ($P < 0.05$). All calculations were performed using SPSS 24.0 software.

RESULTS AND DISCUSSION

Chemical and Spectroscopic Characterization of LIH. The chemical characterization of LIH is presented in Table 2.

Table 2. Chemical LIH Characterization

parameter			elemental analysis (mg kg^{-1} dw[a])
moisture (g kg^{-1} fw[a])	100 ± 0.01	C	148 ± 0.35
total OM (g kg^{-1} dw)	249 ± 0.06	H	16 ± 0.6
ashes (%)	751 ± 0.06	N	4.7 ± 0.1
THE (g kg^{-1} dw)	249 ± 0.31	S	17.8 ± 8.97
HA (g kg^{-1} dw)	174 ± 1.39	O[c]	571 ± 1.31
FA[b] (g kg^{-1} dw)	75 ± 1.6	C/N ratio	31 ± 0.4
pH (1:2.5) H_2O	10		
EC (1:2.5) dS m^{-1}	23		
E4/E6 ratio	2.34 ± 0.04		
macronutrient concentration (mg kg^{-1} dw)		micronutrient concentration (mg kg^{-1} dw)	
Ca	11.3 ± 1.47	total Fe	65.7 ± 0.07
K	177 ± 0.91	soluble Fe	34.9 ± 0.18
Na	12.6 ± 0.73	complexed Fe	31 ± 0.3
Mg	1.90 ± 0.05	complexed Fe fraction (complexed/soluble × 100)	92 ± 2.4
		Cu	0.104 ± 0.002
		Mn	0.645 ± 0.001
		Zn	0.20 ± 0.01

[a]fw = fresh weight; dw = dry weight. [b]FA was determined as the difference between THE and HA. [c]O = 1000 − (C + H + N + S + K + Fe+ Mn + Cu + Zn). OM: Organic Matter. THE: Total humic extract. HA: Humic acid. FA: Fulvic acid. EC: Electrical conductivity.

Total OM is coincident with the THE. A high K content is observed as a consequence of the production procedure that includes a strong base extraction. Chemical changes may occur using high alkaline extractants and long extraction periods.[13]

Almost 70% of the content of THE are humic acids that correspond with the E4/E6 ratio obtained (<5). According to Stevenson,[13] the ratio E4/E6 decreases with increasing weight and humus condensation, serving as an index of humification. In our case, LIH presents a low ratio which may indicate a high molecular weight and a relative high degree of condensation of aromatics constituents from ancient origin. Moreover, a high

DOI: 10.1021/acs.jafc.7b01804
J. Agric. Food Chem. 2017, 65, 6554−6563

Journal of Agricultural and Food Chemistry Article

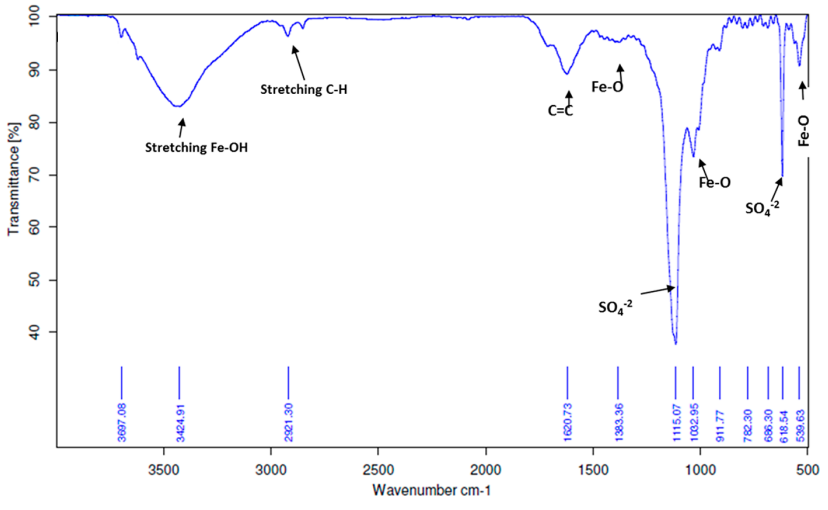

Figure 1. FT-IR spectra of LIH powder in a KBr matrix.

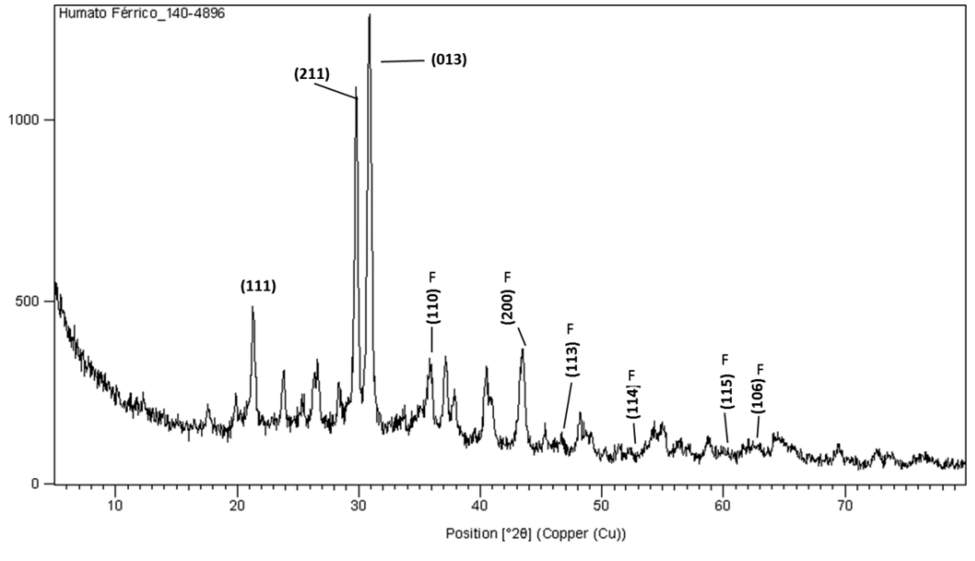

Figure 2. X-ray diffraction pattern of LIH. The horizontal index corresponds to K_2SO_4 (JCPDS-No. 24-0703) and the vertical index agrees with ferrihydrite (F), syn. $Fe_5O_7(OH)\cdot 4H_2O$ (JCPDS-No. 29-0712).

C/N ratio (>10) indicates that the humification process is favored with respect to the mineralization.

The FT-IR spectra of LIH (Figure 1) presents a broad band at 3424 cm^{-1} that, according to Stevenson,[13] can be attributed to O−H and N−H stretching of carboxylic, phenolic, and alcoholic groups. The band at 2923 cm^{-1} can be ascribed to aliphatic C−H stretching vibrations. The band at 1625 cm^{-1} can be due to aromatic C═C, strongly H bonded to C═O of conjugated ketones. The band at 1383 cm^{-1} designates OH deformation and C−O stretching of phenolic OH, C−H deformation of CH_2 and CH_3 groups, and COO^- antisymmetric stretching. Furthermore, according to Colombo et al.,[31] the absorption bands at 3450−3300 cm^{-1} correspond to O−H stretching of Fe−OH while the bands observed at 1383, 1032, and 539 cm^{-1} can be assigned to Fe−O bonds for samples of Ferrihydrite. As this product was obtained from the complexation of potassium humate with iron sulfate, LIH presents two marked peaks at 1115 and 618 cm^{-1} that can be associated with sulfate vibrations.[32]

The LIH X-ray diffraction pattern (Figure 2) presents a high signal/noise ratio for the diffraction lines of relevant intensity for the potassium sulfate (JCPDS-No. 24-0703). The wide lines at 21.3, 29.8, and 30.9 in 2θ, characteristic of potassium sulfate, were identified with high intensity with indexes (111), (211), and (013). Iron is presented in LIH as ferrihydrite by six lines (JCPDS No. 29-0712) at 35.9, 40.8, 46.3, 53.2, 61.3, and 62.7 in 2θ with indexes (110), (200), (113), (114), (115), and (106).

A Mössbauer spectrum of LIH at 298 K is shown in Figure 3 and can be interpreted as the sum of two quadrupole doublets with the same width at middle height that are characteristic of Fe(III) high spin.[33] One of these doublets (64%) corresponds to distorted Fe^{3+} octahedral forms (δ = 0.34(1) mm s^{-1} and ΔE_Q = 0.60(5) mm s^{-1}) that can be associated with ferrihydrite. The other doublet (36%) is compatible with Fe^{3+} polynuclear structures (δ = 0.34(1) mm s^{-1} and ΔE_Q =

DOI: 10.1021/acs.jafc.7b01804
J. Agric. Food Chem. 2017, 65, 6554−6563

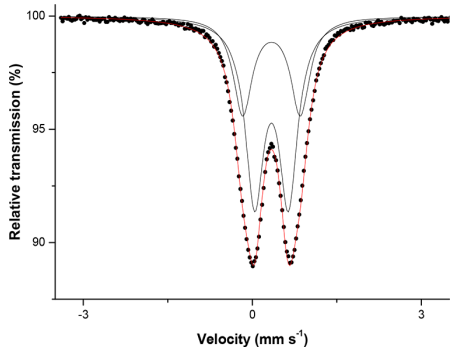

Figure 3. Mössbauer spectra at room temperature (298 K) for LIH sample. Dots represent experimental spectra. Black lines indicate the components of the calculated spectra. Red line is the calculated spectra.

1.02(10) mm s^{-1}) that can be related to Fe^{3+} stabilized structures by the OM present in the LIH. Similar results were obtained by Sorkina et al.[6]

The FT-IR spectra and the X-ray diffraction pattern of LIH are consistent in showing the presence of peaks relevant to K_2SO_4 and ferrihydrite. These spectroscopic results correspond with the high concentration of K in its composition and the high EC (Table 2). Mossbaüer spectra confirms the presence of Fe(III) in the LIH structure, mainly as an iron oxyhydroxide that can be attributed to ferrihydrite and Fe^{3+} stabilized by the OM. Similar results were obtained by Colombo et al.[31]

Reactivity of LIH. *Effect of pH in Ca Solutions.* Figure 4 shows the percentage of Fe remaining after 3 days of

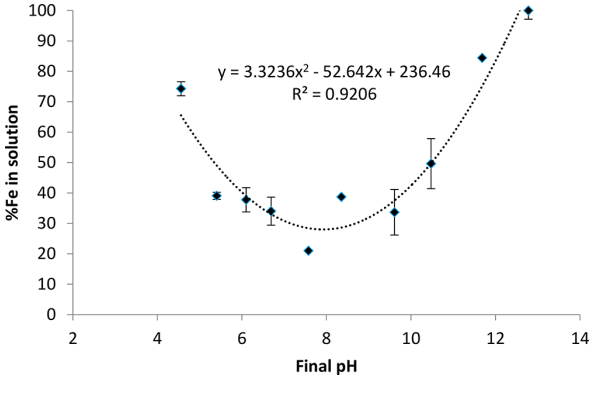

Figure 4. Effect of pH on the percentage of Fe remaining in solution with respect to the amount of iron added as LIH. Error bars indicate standard deviation (n = 2).

interaction in 10.0 mM $CaCl_2$ solution. The pH dropped from the initial values due to the proton release during iron hydroxide formation. As the solution pH changed, data are presented versus final pH (considered as the equilibrium pH). The percentage of Fe remaining in solution for LIH reduced to 21% at pH 7.6, subsequently increasing again up to 100% at pH 13. Therefore, in calcareous soil conditions (pH ≥ 8) LIH would be more than 30% soluble.

Interaction with Soil and Soil Components. The percentage of the complexed iron remaining in solution after LIH interaction with soil and soil components for 3 days is shown in Figure 5. High Fe amounts (100%) were recovered

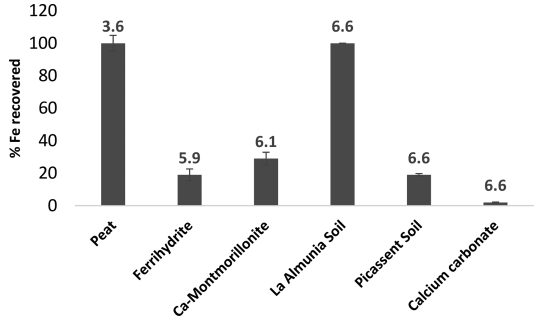

Figure 5. Iron percentage remained in solution after 3 days of interaction of LIH with soils (Picassent and La Almunia) and different soil components (peat, ferrihydrite, Ca-montmorillonite, and calcium carbonate). Final pH is indicated for each interaction, and error bars denote standard deviation (n = 3).

after interaction of LIH with peat and La Almunia calcareous soil. La Almunia soil (a sandy loam) presents lower clay content than Picassent soil (a sandy clay soil). A low percentage of clay in soils allows a low aggregation of clay-Fe-humic substances. Thus, La Almunia soil allows more iron to remain in solution to be taken by the plants. In general, the final pH decreased for all tested material from eight at around six, except for peat that shifted from 4 to 3.6.

Metal complexes of humic acids are less soluble than those of fulvic acids because of their low acidities and high molecular weights.[13] Therefore, the low solubility of LIH in calcareous conditions is in agreement to its chemical structure. The LIH remains highly retained in Ca-montmorillonite and a sandy clay soil such as Picassent soil due to the sorption of humic acids by clay minerals occurring mainly when polyvalent cations are present on the exchange complex. Polyvalent cations, as Ca^{2+} or Fe^{3+}, work as bridges between the acidic functional groups of the organic matter (e.g., COO−) and the negative charges of the clays. In this regard, iron is a stronger binding cation between organic molecules and clays than calcium. With the sandy loam soil (La Almunia soil), this effect is less pronounced and with the peat, negligible. In the presence of calcium carbonate, humic acids tend to form aggregates. This aggregation is possible because Ca^{2+} binding decreases the zeta potential of humic acids and because it is able to form bridges between humic acid molecules when its concentration is above 1.0 mM.[34] Therefore, the iron solubility was the lowest. Interaction with ferrihydrite showed precipitation with the LIH although, at the final pH (5.9), 20% of iron remained in solution which is expected according to Lindsay.[35] In general, the LIH presents low solubility in soil unlike the iron synthetic chelates that can pose environmental concerns due to their high leachability.

Ligand Competition of LIH with the Synthetic Chelating Agents EDDHA, HBED, and BPDS. Since the LIH has a high-condensed structure, it is not possible to study its stability through the calculation of relative constants by potentiometric and photometric methods. Therefore, two ligand competition experiments were carried out for 97 days at pH 7. Different solutions were prepared, as explained above, and measured every 2 or 3 days. Changes in absorbance were registered in the 350−650 nm wavelength range. Figure 6A,B shows the mathematical deconvolution at day 73 of the experiment for the solution LIH + HBED + BPDS and for LIH + EDDHA + BPDS, respectively, and the experimental

DOI: 10.1021/acs.jafc.7b01804
J. Agric. Food Chem. 2017, 65, 6554−6563

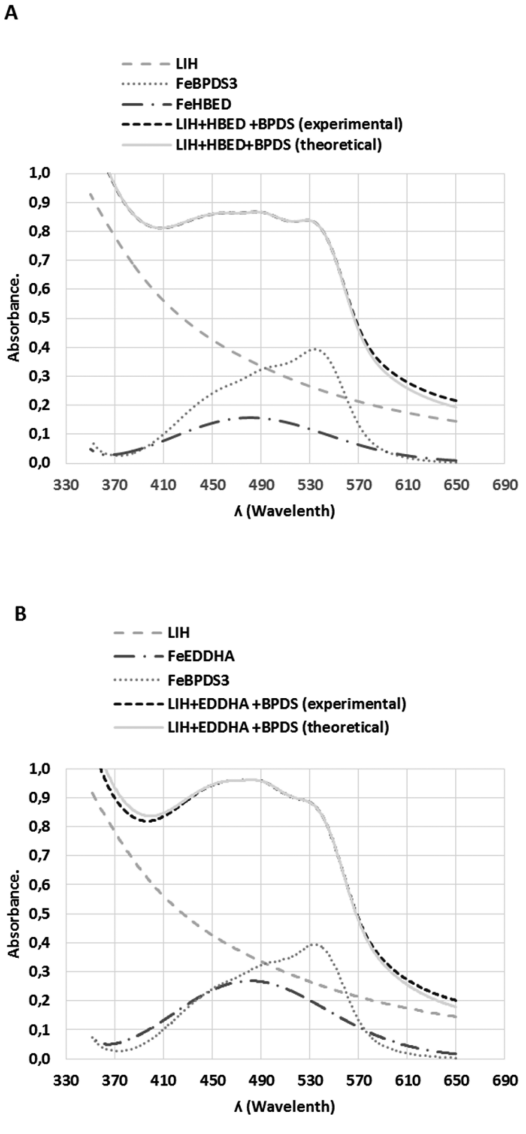

Figure 6. Mathematical deconvolution of the mixture LIH + HBED + BPDS (A) and the mixture LIH + EDDHA + BPDS (B) at 73 days of the experiment.

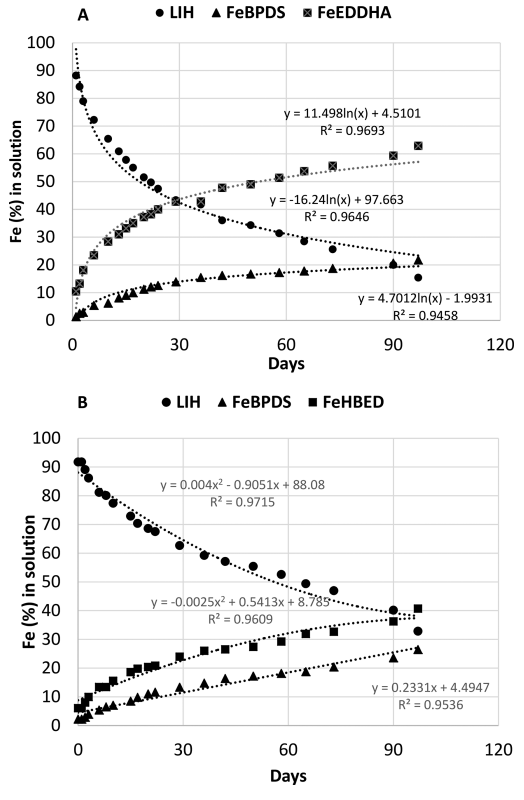

Figure 7. Time course of LIH in competition with EDDHA + BPDS (A) and with HBED + BPDS (B) for 97 days.

contributions of the different components individually. In this way, we studied indirectly the stability of LIH and its kinetic capacity to retain Fe(III) in solution in the presence of different chelating agents. As the experiment progressed, EDDHA or HBED chelated Fe(III) released by LIH and BPDS chelated Fe(II) obtained by the Fe(III) reduction at that pH condition. Figure 7A,B shows the formation rate of FeEDDHA and FeHBED, respectively. Also, Figure7A,B shows the formation of $Fe(BPDS)_3$ and the decrease of LIH. At the end of the experiment, EDDHA had chelated the 63% of Fe(III) and HBED the 41% of Fe(III); meanwhile, BPDS had chelated 22% of Fe(II) for the solution LIH + EDDHA + BPDS and 26% of Fe(II) for the solution LIH + HBED + BPDS. With respect to the LIH, it remained at 15% when reacted with EDDHA and BPDS and 33% when reacted with HBED and BPDS. On the basis of these results, LIH presented, in general, a slow kinetic behavior since in more than 3 months, LIH released between 67% of Fe (in the presence of HBED) and 85% of Fe (in the presence of EDDHA). Both chelating agents are strong Fe(III) chelators with high stability constants. For FeEDDHA, the log *K* is 35.09[36] and for FeHBED the log *K* is 39.02,[37] while for an iron humate obtained through iron complexation of humic acids from leonardite the log *K* (apparent stability constant) is 4.67.[38] According to the high affinity of the chelating agent for Fe(III), a fast iron release was expected from the LIH, but in our study the kinetics is quite slow. Piccolo[39] suggested a new conformational nature of humic substances, defining them as supramolecular associations of heterogeneous and relative small (<1000 Da) molecules, which are held together in only apparently large molecular sizes by weak forces, such as hydrogen and hydrophobic bonds. Then as humic substance is complexed with iron, its conformational structure changes. Fulvic acids tend to form a compact network of intra- and intermolecular complexes with iron cations while humic acids used to form small aggregates and thermodynamically stable associations.[40] Hence, the LIH is formed by 70% of humic acids and 30% of fulvic acids; the kinetic reaction would depend mainly on the ability of the chelating agents to produce the disaggregation of the humic acids in order to chelate the Fe(III). According to our results (Figure 7), the most stable chelate (FeHBED) is formed slower than FeEDDHA. Moreover, part of the Fe(III) has been reduced to Fe(II) at pH 7 by the reducing capacity of humic substances and the Fe(II) chelated by BPDS. Under these experimental conditions, BPDS showed similar behavior independently of the Fe(III) chelating agent in solution.

DOI: 10.1021/acs.jafc.7b01804
J. Agric. Food Chem. 2017, 65, 6554−6563

Prediction of the LIH Efficacy in Iron Nutrition Using a *Saccharomyces cerevisiae* Strain. *Cell Growth Rate.* Figure 8 shows the cell growth rate that was evaluated in the presence

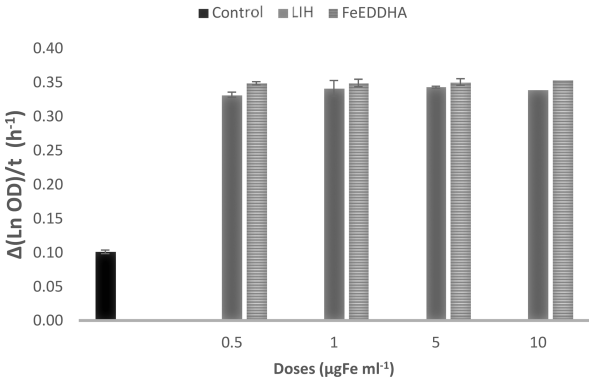

Figure 8. Cellular growth rate of *Saccharomyces cerevisiae* strain expressed as the increment of the Neperian logarithm of the optic density (OD) with time (h^{-1}) in the presence of different doses of LIH or FeEDDHA, measured during the exponential phase (48 h later): The results are averages ± standard deviation of three independent biological replicates, each performed in three technical repetitions.

of LIH and FeEDDHA treatments at different doses (0.5, 1.0, 2.0, and 10.0 μg mL^{-1}) and absence of iron treatments (Control) for cells cultivated in SD media without iron. The cell growth rate was mainly inhibited for the Control-Fe cultures. Comparing the Fe sources, the growth rate for the yeast culture treated with FeEDDHA was 5% higher than when treated with LIH. This result indicates a slow kinetic effect of LIH in the *Saccharomyces cerevisiae* cells growth.

Quantification of mRNA Using RT-qPCR. The expression of four genes involved in the high-affinity iron transport system in cultures treated with LIH and FeEDDHA (10.0 mg L^{-1}) were analyzed and compared with the expression of genes in cultures without treatments (Control). The results are presented in Figure 9. The genes analyzed were *FET3*, *FTR1*, *SIT1*, and *TIS11*. The genes *FET3* and *FTR1* encode transporters that are part of the so-called Iron Transport Reducing Route while

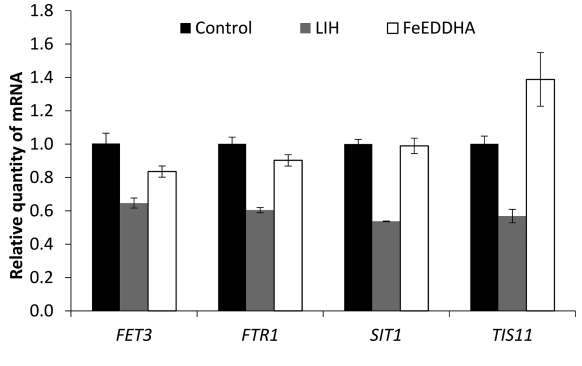

Figure 9. Effects of LIH and FeEDDHA on *Saccharomyces cerevisiae* strain by the expression of genes involved in the high-affinity iron transport system (*FET3*, *FTR1*; *SIT1*, *TIS11*) using quantitative real time PCR (RT-qPCR). The results are averages ± standard deviation of three independent biological replicates, each performed in three technical repetitions.

S1T1 encodes an iron siderophore transporter and *TIS11* codifies a regulatory protein of the degradation of mRNAs that encode proteins requiring iron.

The LIH addition promoted a decrease of 40 and 50% of expression for the four genes analyzed in the cells treated. These results suggest that the iron levels are increasing in the LIH treated cells due to the gene expression in the high-affinity iron transport system regulated for Aft1, a transcriptional factor whose activity increases in conditions in the absence of iron and decreases when the iron concentration in the cell increases. Therefore, LIH provides iron to being taken up by the cells. With respect to the effect of the addition of FeEDDHA, a slight repression in the genes *FET3* and *FTR1* was observed. Moreover, a small induction of the gene *TIS11* was detected indicating that the chelate promoted some effect over the gene expression in these experimental conditions.

Determination of Iron Intracellular Content. The results of Fe intracellular content in cells grown in SD media YNB without iron and treated with LIH and FeEDDHA (1.0 mg L^{-1}) and untreated are presented in Figure 10. Cells treated

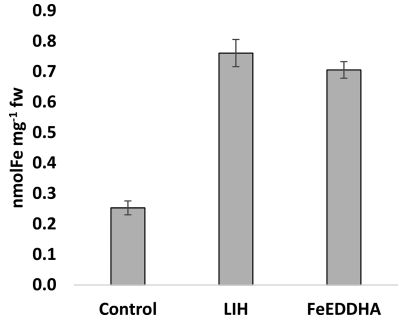

Figure 10. Intracellular Fe content measured in *Saccharomyces cerevisiae* cells grown in SD media YNB without iron and treated with LIH and Fe EDDHA. The results are averages ± standard deviation of three independent biological replicates, each performed in three technical repetitions.

with LIH and FeEDDHA presented almost three times more iron content than the control cells, and no significant differences were observed between iron treatments. Therefore, LIH showed to be as efficient as the iron chelate providing iron to the yeast cells.

Field Experiment. The relative increase of SPAD (%) with respect to the Control, calculated at 15, 45, and 75 DAT is shown in Figure 11. No significant differences were observed among treatments. The chlorophyll index presented a general increase of 9.4% in trees treated with LIH and 10.5% in trees treated with FeEDDHA. The SPAD values for the Control were high during all the assessment.

The Fe concentration in citrus leaf for the different samplings is presented in Table 3. Before the treatment applications, the plants presented 54 mg kg^{-1} of iron in leaves, indicating iron deficiency since an adequate iron nutrition for citrus is considered over 60 mg kg^{-1}, according to Legaz et al.[30] The deficiency was corrected during application of treatments. Trees treated with FeEDDHA showed the highest results at the first sampling, indicating a short-term effect in correcting the deficiency while orange trees treated with LIH presented and incremented concentration tendency of iron in each sampling, confirming the kinetic results obtained for the ligand competition experiment and the experiments with *Saccharo-*

DOI: 10.1021/acs.jafc.7b01804
J. Agric. Food Chem. 2017, 65, 6554−6563

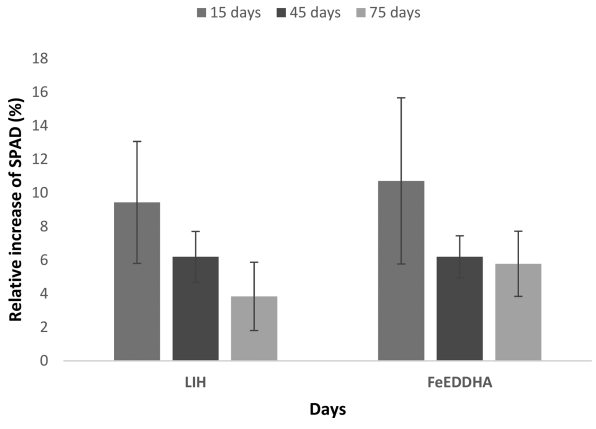

Figure 11. Relative increase of soil plant analysis development index (SPAD)% calculated for plants treated with LIH or FeEDDHA, with respect to the Control at 15, 45, and 75 days after treatments application. The results are averages ± standard error.

Table 3. Iron Concentration (mg kg^{-1}) in Citrus Leaf for Three Samplings and Relative Yield (%) at the End of the Field Experiment[a]

	Fe (mg kg^{-1})			
treatment	1st sample	2nd sample	3rd sample	relative yield increase (%)[b]
Control	58 ± 3 b	66 ± 2 ab	60 ± 5 b	
LIH	58 ± 2 b	73 ± 5 a	84 ± 2 a	6 b
FeEDDHA	71 ± 2 a	56 ± 2 a	68 ± 0 b	18 a

[a]The a, b, and ab indicate significant differences among the treatments or the samplings according to Duncan's Test ($P < 0.05$). [b]Percentage of yield per tree increase calculated respect to the Control yield.

myces cerevisiae strain. This iron behavior is associated with a long-term effect of LIH in correcting iron chlorosis.

The orchard soil has a sandy loam texture (Table 1), similar to La Almunia soil, with a low clay percentage that favors iron release from LIH and thus avoids Fe-humic substances aggregation. According to Stevenson,[13] the main polyvalent cations responsible for the binding of humic and fulvic acids to soil clays are Ca^{2+}, Fe^{3+}, and Al^{3+}. The divalent Ca^{2+} ion does not form strong coordination complexes with organic molecules unlike Fe^{3+} that form coordination complexes with the organic compounds, so strong bonding of humic substances is possible through this mechanism.

In September and October 2014, two successive harvests were made, and the yield (total fruit weight) was evaluated. The percentage of yield per tree increase was calculated with respect to the control and significant differences between the treatments were observed. Orange trees treated with FeEDDHA showed the highest production (Table 3).

The LIH is mainly a humic acid (70%) with a high condensed complexed Fe(III) structure. Iron is presented in the product as Ferrihydrite and Fe^{3+} polynuclear forms, according to the spectroscopic characterization. The iron slow release of this iron humate is attributed to the small stable aggregates and the thermodynamically stable associations formed by the humic acids with iron that limits the kinetic behavior. In spite of its structural complexity, the LIH repressed among 40−50% of the expression of *FET3*, *FTR1*, *SIT1*, and *TIS11*, iron homeostasis genes analyzed in *Saccharomyces cerevisiae* cells unlike the iron chelate and provided iron to these cells similar to iron chelate. The slow kinetic effect in iron release (5% less than the FeEDDHA) was confirmed with the cell growth rate experiment. Although longer agronomic studies are needed, LIH has provided slow and increasing iron nutrition to citrus growth in calcareous conditions and has corrected the iron deficiency for the first year of application with similar results to the FeEDDHA fertilization. Finally, the LIH is a cheap and ecofriendly fertilizer that exerts a long-term effect in providing iron to citrus trees due to their own kinetic limitation in calcareous soils.

■ ASSOCIATED CONTENT

Supporting Information

The Supporting Information is available free of charge on the ACS Publications website at DOI: 10.1021/acs.jafc.7b01804.

Methods for LIH characterization, soils and soil components used in the interaction experiment, and procedures used in the experiments using a *Saccharomyces cerevisiae* strain (PDF)

■ AUTHOR INFORMATION

Corresponding Author

*E-mail: juanjose.lucena@uam.es. Phone: +34 914973968. Fax: +34 914973826.

ORCID

Juan J. Lucena: 0000-0001-9130-2909

Author Contributions

M.T.C. carried out the chemical LIH characterization, the reactivity assessment, the ligand competition, and the field experiment. Furthermore, M.T.C. analyzed the plant and soil material, did the mathematical deconvolution, and performed the statistical study. M.C.-M. carried out the *Saccharomyces cerevisiae* assays with the subsequent statistical analysis, and M.A.N. led those assays. N.M. carried out the Mössbauer Spectroscopy analysis. J.J.L. conceived the study. M.T.C. wrote the manuscript together with the revision of J.J.L. J.J.L. designed the manuscript and supervised all the experimental work presented. All the authors read and approved the final manuscript.

Funding

This work was financially supported by the Project AGL2013-44474-R of the Spanish Ministry of Science and Innovation and partially by Fertinagro SL.

Notes

The authors declare no competing financial interest.

■ ACKNOWLEDGMENTS

Thanks to Fertinagro S L for providing the iron humate and the leonardite humate acid used in this work.

■ ABREVIATIONS USED

LIH, leonardite iron humate; LHA, leonardite humic acid; OM, organic matter; THE, total humic extract; HA, humic acids; FA, fulvic acids; EC, electrical conductivity; HBED, *N*,*N*′-bis(2-hydroxybenzyl) ethylened-iamine-*N*,*N*′-diacetic acid acid; EDDHA, ethylenediamine-di (*o*-hydroxyphenylacetic acid); Na_2BPDS, bathophenanthrolinedisulfonic acid disodium salt trihydrate; EDTA, ethylene diamine tetraacetic acid; HEPES, *N*-(2-hydroxyethyl) piperazine *N*′-(2-ethanesulfonic acid); MES, 2-(*N*-morpholino) ethanesulfonic acid; CAPS, 3-(cyclo-

DOI: 10.1021/acs.jafc.7b01804
J. Agric. Food Chem. 2017, 65, 6554−6563

hexylamino)-1-propanesulfonicacid; AMPSO, *N*-(1,1-dimethyl-2-hydroxyethyl)-3-amino-2-hydroxy- propanesulfonic acid; YNB, yeast nitrogen base; AAS, atomic absorption spectroscopy; FTIR, Fourier transform infrared spectroscopy; RT-qPCR, real-time quantitative reverse transcription polymerase chain reaction; SD, synthetic dextrose; SPAD, soil-plant analysis development; DAT, days after treatments; ANOVA, analysis of variance

REFERENCES

(1) Ministry of Agriculture, Food and Environement. *Statistical Yearbook*. Government of Spain. Madrid, Spain. 2016. http://www.mapama.gob.es/estadistica/pags/anuario/2015/AE15.pdf, (accessed June 7, 2017).

(2) Kovács, K.; Czech, V.; Fodor, F.; Solti, A.; Lucena, J. J.; Santos-Rosell, S.; Hernández-Apaolaza, L. Characterization of Fe-leonardite complexes as novel natural iron fertilizers. *J. Agric. Food Chem.* **2013**, *61*, 12200−12210.

(3) Kołodziej, B.; Sugier, D.; Bielińska, E. The effect of leonardite application and various plantation modalities on yielding and quality of roseroot (*Rhodiola rosea* L.) and soil enzymatic activity. *J. Geochem. Explor.* **2013**, *129*, 64−69.

(4) Sugier, D.; Kołodziej, B.; Bielińska, E. The effect of leonardite application on *Arnica montana* L. yielding and chosen chemical properties and enzymatic activity of the soil. *J. Geochem. Explor.* **2013**, *129*, 76−81.

(5) Horner, C. K.; Burk, D.; Hoover, S. R. Preparation of humate iron and other humate metals. *Plant Physiol.* **1934**, *9*, 663−669.

(6) Sorkina, T. A.; Polyakov, A. Y.; Kulikova, N. A.; Goldt, A. E.; Philippova, O. I.; Aseeva, A. A.; Veligzhanin, A. A.; Zubavichus, Y. V.; Pankratov, D. A.; Goodilin, E. A.; Perminova, I. V. Nature-inspired soluble iron-rich humic compounds: New look at the structure and properties. *J. Soils Sediments* **2014**, *14*, 261−268.

(7) Krizenecka, S.; Hejda, S.; Machovic, V.; Trogl, J. Preparation of iron, aluminium, calcium, magnesium, and zinc humates for environmental applications. *Chem. Pap.* **2014**, *68*, 1443−1451.

(8) Royal Decree 506/2013 on fertilizers (In spanish). *BOE (Official Bulletin of the State)* **2013**, *164*, 51119−51207.

(9) Shenker, M.; Chen, Y. Increasing iron availability to crops. Fertilizers, organo-fertilizers, and biological approaches. *Soil Sci. Plant Nutr.* **2005**, *51*, 1−17.

(10) Francioso, O.; Montecchio, D.; Gioacchini, P.; Ciavatta, C. Thermal analysis (TG−DTA) and isotopic characterization (13C−15N) of humic acids from different origins. *Appl. Geochem.* **2005**, *20*, 537−544.

(11) Chen, Y.; Clapp, C. E.; Magen, H. Mechanisms of plant growth stimulation by humic substances: The role of organo-iron complexes. *Soil Sci. Plant Nutr.* **2004**, *50*, 1089−1095.

(12) García-Mina, J. M. Stability, solubility and maximum metal binding capacity in metal-humic complexes involving humic substances extracted from peat and organic compost. *Org. Geochem.* **2006**, *37*, 1960−1972.

(13) Stevenson, F. J. *Humus chemistry: Genesis, composition, reactions*. 2nd ed.. J. Willey and sons. New York, USA., 1994.

(14) Lucena, J. J.; Chaney, R. L. Synthetic iron chelates as substrates of root ferric chelate reductase in green stressed cucumber plants. *J. Plant Nutr.* **2006**, *29*, 423−439.

(15) Guerinot, M. L.; Yi, Y. Iron: nutritious, noxious, and not readily available. *Plant Physiol.* **1994**, *104*, 815−820.

(16) Jeong, J.; Guerinot, M. L. Homing in on iron homeostasis in plants. *Trends Plant Sci.* **2009**, *14*, 280−285.

(17) Sherman, F. Getting started with yeast. *Methods Enzymol.* **2002**, *350*, 3−41.

(18) Goffeau, A.; Barrell, B. G.; Bussey, H.; Davis, R. W.; Dujon, B.; Feldmann, H.; Galibert, F.; Hoheisel, J. D.; Jacq, C.; Johnston, M.; Louis, E. J.; Mewes, H. W.; Murakami, Y.; Philippsen, P.; Tettelin, H.; Oliver, S. G. Life with 6000 genes. *Science* **1996**, *274*, 546−567.

(19) Botstein, D.; Fink, G. R. Yeast: an experimental organism for 21st century biology. *Genetics* **2011**, *189*, 695−704.

(20) Alva, A. K. Solubility and iron release characteristics of iron chelates and sludge products. *J. Plant Nutr.* **1992**, *15*, 1939−1954.

(21) Alva, A. K.; Obreza, T. A. By-product iron-humate increases tree growth and fruit production of orange and grapefruit. *HortScience* **1998**, *33*, 71−74.

(22) Pérez-Sanz, A.; Álvarez-Férnandez, A.; Casero, T.; Legaz, F.; Lucena, J. J. Fe enriched biosolids as fertilizers for orange and peach trees grown in field conditions. *Plant Soil* **2002**, *241*, 145−153.

(23) Olego, M. A.; Cordero, J.; Quiroga, M. J.; Garzón-Jimeno, J. C.; Álvarez, E. Effect of leonardite application on soil organic matter and micronutrient levels in an inceptisol soil cultivated with vine (*Vitis vinifera* L.). (In spanish). *Inf. Técnica Económica Agraria* **2015**, *111*, 210−226.

(24) Eshghi, S.; Garazhian, M. Improving growth, yield and fruit quality of strawberry by foliar and soil drench applications of humic acid. *Iran Agric. Res.* **2015**, *34*, 14−20.

(25) ISO *3696:1987 Water for analytical laboratory use. Specification and test methods*.International Organization for Standardisation. Geneva. Switzerland..

(26) Álvarez-Fernández, A.; Pérez-Sanz, A.; Lucena, J. J. Evaluation of effect of washing procedures on mineral analysis of orange and peach leaves sprayed with seaweed extracts enriched with iron. *Commun. Soil Sci. Plant Anal.* **2001**, *32*, 157−170.

(27) EUROSCARF. European *Saccharomices cerevisiae* Archive for Functional Analysis http://web.uni-frankfurt.de/fb15/mikro/euroscarf (accessed June 7, 2017).

(28) Soltanpour, P. N.; Schwab, A. P. A new soil test for simultaneous extraction of macro and micronutrients in alkaline soils. *Commun. Soil Sci. Plant Anal.* **1977**, *8*, 195−207.

(29) UNE-EN 13368−2:2012 Fertilizers- Determination of chelating agents in fertilizers by chromatography. Part 2: Determination of Fe chelated by *o,o*-EDDHA, *o,o*-EDDHMA and HBED by ion pair chromatography. 2012. AENOR ed.s. Madrid. Spain.

(30) Legaz, F.; Serna, M. D.; Ferrer, P.; Cebolla, V.; Primo-Millo, E. Analysis of leaves, soils and waters for the nutritional diagnosis of citrus orchards. Sampling procedure. (Spanish). *Generaitat Valenciana, Conselleria d'Agricultura, Pesca i Alimentació* **1995**, *741*, 70.

(31) Colombo, C.; Palumbo, G.; Sellitto, V. M.; Rizzardo, C.; Tomasi, N.; Pinton, R.; Cesco, S. Characteristics of insoluble, high molecular weight iron-humic substances used as plant iron sources. *Soil Sci. Soc. Am. J.* **2012**, *76*, 1246−1256.

(32) Periasamy, A.; Muruganand, S.; Palaniswamy, A. Vibrational studies of Na_2SO_4, K_2SO_4, $NaHSO_4$ and $KHSO_4$ crystals. *Rasayan J. Chem.* **2009**, *2*, 981−989.

(33) Greenwood, N.; Gibb, T. *Mössbauer Spectroscopy*. Springer. London, UK, 1971.

(34) Kloster, N.; Brigante, M.; Zanini, G.; Avena, M. Aggregation kinetics of humic acids in the presence of calcium ions. *Colloids Surf., A* **2013**, *427*, 76−82.

(35) Lindsay, W. L. *Chemical equilibrium in soils*; J. Wiley and sons. New York, 1979.

(36) Yunta, F.; García-Marco, S.; Lucena, J. J.; Gómez-Gallego, M.; Alcázar, R.; Sierra, M. A. Chelating agents related to ethylenediamine bis (2-hydroxyphenyl) acetic acid (EDDHA): Synthesis, characterization, and equilibrium studies of the free ligands and their Mg^{2+}, Ca^{2+}, Cu^{2+}, Fe^{3+} chelates. *Inorg. Chem.* **2003**, *42*, 5412−5421.

(37) López-Rayo, S.; Hernández, D.; Lucena, J. J. Chemical evaluation of HBED/Fe^{3+} and the novel HJB/Fe^{3+}. Chelates as fertilizers to alleviate iron chlorosis. *J. Agric. Food Chem.* **2009**, *57*, 8504−8513.

(38) Fuentes, M.; Olaetxea, M.; Baigorri, R.; Zamarreño, A. M.; Etienne, P.; Laîné, P.; Ourry, A.; Yvin, J.-C.; Garcia-Mina, J. M. Main binding sites involved in Fe(III) and Cu(II) complexation in humic-based structures. *J. Geochem. Explor.* **2013**, *129*, 14−17.

(39) Piccolo, A. The supramolecular structure of humic substances. *Soil Sci.* **2001**, *166*, 810−832.

DOI: 10.1021/acs.jafc.7b01804
J. Agric. Food Chem. 2017, 65, 6554−6563

(40) Nuzzo, A.; Sánchez, A.; Fontaine, B. Conformational changes of dissolved humic and fulvic superstructures with progressive iron complexation. *J. Geochem. Explor.* **2013**, *129*, 1−5.

DOI: 10.1021/acs.jafc.7b01804
J. Agric. Food Chem. 2017, 65, 6554−6563

III.2 Iron and humic acid accumulation on soybean roots fertilized with leonardite iron humates under calcareous conditions

JOURNAL OF AGRICULTURAL AND FOOD CHEMISTRY

Article

Cite This: J. Agric. Food Chem. 2018, 66, 13386−13396

pubs.acs.org/JAFC

Iron and Humic Acid Accumulation on Soybean Roots Fertilized with Leonardite Iron Humates under Calcareous Conditions

María Teresa Cieschi and Juan José Lucena*

Department of Agricultural Chemistry and Food Science, Autonomous University of Madrid, c/Francisco Tomás y Valiente, 7, Ciudad Universitaria de Cantoblanco, 28049 Madrid, Spain

ABSTRACT: Iron humates are eco-friendly fertilizers that are less efficient than iron synthetic chelates at correcting iron chlorosis. The aim of this work was to improve the efficiency of a leonardite iron humate (LIH), by studying the relationship among humic acid (HA) accumulation, iron biomineralization on soybean roots, and iron nutrition in soybean plants under calcareous conditions. Two hydroponic experiments were performed: a short-term bioassay (21 days) with several doses (10, 20, 50, and 100 μmol of Fe pot^{-1}) of LIH applied once a week and a long-term bioassay (60 days) with just one application of LIH (250 μmol of Fe pot^{-1}). When LIH was applied several times, it precipitated on the root, blocking the cell wall pores and reducing iron transport in plants, while these effects decreased when LIH was applied just once, thus favoring iron uptake by the plants and avoiding HA accumulation. Jarosite was observed on the surface of soybean roots.

KEYWORDS: *complex fertilizer, maximum complexing capacity, jarosite*

INTRODUCTION

Despite leonardite iron humates being less efficient than iron synthetic chelates at correcting iron chlorosis, they are a natural iron complex fertilizer that is commonly applied to crops cultivated in calcareous soils. They are mainly used in soilless horticulture, applied by drip irrigation or foliar applications.[1] However, their main benefit in comparison to iron synthetic chelates is their low cost and eco-friendly behavior due to their natural raw materials.

One of the most important characteristics of humic substances (HS) is their ability to improve plant growth in diverse plant species and growth conditions.[2] The biological effects of HS on plant metabolism are influenced by the origin, age, and decomposition processes of the parent organic material and are related to the chemical composition of each HS.[3] However, not all HS produce the same biologic effects in all plants. According to Canellas and Olivares,[4] the growth response of monocotyledonous plants to exogenously applied HS appears to be greater than that for dicotyledonous plants, although the molecular and physiological basis for this difference remains unclear. Moreover, according to these authors, the plant physiological responses to HS isolated from brown coal (e.g. lignite, leonardite, and subbituminous coals) are less pronounced than those observed in response to the addition of HS isolated from peat, composts, or vermicomposts. However, there have been no reports on the relationship between their structure and effectiveness.

The storage form of iron and the organelles in which it is accumulated in plants have been only partially defined. Thomine et al.[5] propose that most of the iron is stored as ferritin in the plastids (chloroplasts contain up to 90% of the leaf cell iron), with about half in the stroma and the rest in the thylakoid membranes. In cucumber plants supplied with ^{57}Fe(III) citrate, Kovács et al.[6] observed a transient presence of Fe carboxylates in removable forms and the accumulation of partially removable, amorphous hydrous ferric oxide/hydroxide that were identified in the apoplast and on the root surface, respectively. They did not observe ferritin accumulation at optimal iron supply. Under Fe deficiency, they suggest that the root xylem is the major site of accumulation of Fe(III) citrate.

Iron accumulation in roots (iron plaque) is generally related to halophytes such as *Oryza sativa*,[7] wetlands such as *Typha latifolia* L.[8] and iron hyperaccumulator plants such as *Imperata cylindrica*.[9] Biomineralization of iron, under reducing conditions, has been observed in the roots of *Imperata cylindrica*, mainly as jarosite, ferrihydrite, hematite, and maghemite/magnetite phases, with a greater presence of ferromagnetic phases in roots and rhizomes. Longnecker and Welch[10] documented iron accumulation in soybean roots for some soybean genotypes when plants were fertilized with FeEDTA 25.0 μM, and Asli and Neumann[11] studied the effects of HA accumulation on roots. Iron biominerals in roots, jarosite and ferritin, were observed in *Imperata cylindrica* (L.) P. Beauv. cultivated under hydroponic conditions at pH 3 for 60 days.[12] The relationship between iron biomineralization and HA accumulation in roots has been less studied.

In previous research,[13] it has been demonstrated that LIH exerts a long-term effect by providing iron to citrus trees cultivated in calcareous soils. Thus, it was deemed appropriate to perform a long-term hydroponic experiment to obtain more information that would be closer to agronomical situations.

The aim of this work was to improve LIH efficiency, studying the relationship among HA accumulation, iron biomineralization on the soybean root, and iron nutrition in soybean plants under calcareous conditions.

Received: July 30, 2018
Revised: November 7, 2018
Accepted: December 3, 2018
Published: December 3, 2018

MATERIALS AND METHODS

Reagents. All of the reagents used were of recognized analytical grade, and solutions were prepared with type I grade water according to ISO 3696:1987[14] free of organic contaminants (Millipore, Milford, MA, USA).

Humates. The leonardite potassium humate (LKH) was chemically and spectroscopically characterized using standards. Moisture was measured after heating the humic material overnight at 105 °C.[15] Ash was determined by weight loss after calcination for 4 h at 540 °C, and oxidizable organic matter (OM) was analyzed by wet oxidation with potassium dichromate.[16] Elemental composition (C, H, N, and S) was established by total oxidation of the samples through instant and complete combustion in a LECO CHNS-932 elemental analyzer. The total humic extract (THE), humic acid (HA), and fulvic acid (FA) contents were measured in the soluble fraction of the leonardite iron humate (LIH). For THE, the sample was extracted in 0.1 M NaOH and 0.1 M $Na_2P_2O_7$. The HA was then obtained by precipitation with H_2SO_4 at pH 1.0. The carbon contents in THE and HA were determined after oxidation with $K_2Cr_2O_7$ and determination of excess $Cr_2O_7^{2-}$ with $Fe(NH_4)_2(SO_4)_2{\cdot}6H_2O$. Conversion of C to THE and HA was calculated using a factor of 1.724. The FA content was determined by the difference between THE and HA.[17] The pH and the electrical conductivity (EC) were measured in a humic material/water mixture at a ratio of 1/2.5 (w/v).

The ratio of absorbance at 465 to 665 nm (ratio E4/E6) was determined according to Chen et al.,[18] by dissolving 3.0 mg of LKH in 10.0 mL of 0.05 M $NaHCO_3$ and adjusting the pH to 8.3 with 0.02 M NaOH. Absorbances at 465 and 665 nm were measured using a Jasco V650 spectrophotometer.

The total acidity of the LKH samples was determined by baryta adsorption, the content of carboxyl groups was determined by the Ca acetate method, and the content of phenolic groups was calculated as the difference between total acidity and the content of the carboxyl groups.[19]

Macro- and micronutrient concentrations in LKH were analyzed by inductively coupled plasma mass spectrometry (ICP MS; NexION 300XX, PerkinElmer) after nitric acid digestion. The LKH was characterized by X-ray diffraction (XRD), Fourier transform infrared spectroscopy (FT-IR), Mössbauer spectroscopy, and ^{13}C nuclear magnetic resonance (^{13}C NMR). The XRD pattern was obtained using a Panalytical X'Pert PRO with Ge (111) as a primary monochromator and graphite as a secondary monochromator, which allowed the selection of the Cu Kα_1 radiation that was analyzed with an X'Celerator detector. The FT-IR spectrum of a mixture of LKH and KBr (1.0 mg of sample + 99.0 mg of dry KBr) from 7000 to 560 cm^{-1} was recorded on a Bruker IFS66v FT-IR spectrophotometer fitted with an apparatus for diffuse reflectance. Mössbauer spectra were recorded in triangular mode using a conventional spectrometer with $^{57}Co(Rh)$ source. The analysis of the spectrum was performed by a nonlinear fit using the NORMOS program,[20] and the energy calibration was conducted using α-Fe (6 mm) foil. The ^{13}C NMR spectrum was recorded at 100.32 MHz with a rotation speed of 10 kHz in a Bruker WB-400-V spectrometer 4 mm triple-channel probe with ZrO_3 rotors and a Kel-F cap at room temperature.

The iron complex was prepared in the laboratory. Its chemical characterization is presented in Table 1. A stock solution (1000 μmol L^{-1}) of LIH was prepared by the complexation of LKH with an iron standard solution of 1000 mg L^{-1} of $Fe(NO_3)_3$ obtained from Merck KGaA, Darmstadt, Germany, in such a way that the final solution reached 90% of the MCC (maximum complexing capacity) of the LKH (see below for MCC determination). The final pH (7) was obtained by the careful addition of KOH 1 M. The main chemical characteristics of LKH and LIH are summarized in Table 1.

Determination of the MCC of LKH with Fe(II) and Fe(III). To determine the Fe MCC of LKH, the official method EN 15962:2011,[21] based on the work of Villén et al.,[22] was used. In brief, increasing volumes of a c_{Fe} = 200 g L^{-1} solution of $FeSO_4{\cdot}7H_2O$ for Fe(II) and $FeCl_3{\cdot}6H_2O$ for Fe(III) were added to 20 mL of the LKH solution (c_{LKH} = 100 g L^{-1}). After the addition of two drops of H_2O_2 (33% w/v), the pH was raised to 9.0 with NaOH solution. After 1 day in the dark, the pH was increased again to 9.0. After 2 h, the solutions were transferred to a 100 mL volumetric flask and the volume made up to 100 mL. The solutions were subsequently centrifuged at 7500 min^{-1} at room temperature for 10 min, and the supernatants were filtered using 0.45 μm filters (Millipore). After removal of the organic compound in accordance with EU method 9.3,[23] using H_2O_2 (33% w/v) and 0.5 M HCl for the digestion, the complexed element was determined by atomic absorption spectrometry (AAS) with an AAnalyst 800 Spectrometer (PerkinElmer, Shelton, CT, USA) using 0.5% La, 0.2% Cs, and 5% HCl as a matrix modifier. MCC determinations were made in triplicate.

Table 1. Chemical LKH and LIH Characterization

	LKH	LIH
moisture (g kg^{-1} fw[a])	136 ± 6.11	100 ± 0.01
total OM (g kg^{-1} dw[a])	363 ± 0.04	249 ± 0.06
ash (%)	637 ± 0.04	751 ± 0.06
THE (g kg^{-1} dw)	332 ± 2.50	249 ± 0.31
HA (g kg^{-1} dw)	202 ± 92.2	174 ± 1.39
FA (g kg^{-1} dw)[b]	130 ± 3.00	75.0 ± 1.60
EC (1:25 dS m^{-1})	13.0	23.1
total acidity (mol kg^{-1} dw)	2.05 ± 0.30	1.33 ± 0.21
carboxyl groups (mol kg^{-1} dw)	0.22 ± 0.07	0.14 ± 0.02
phenolic OH (mol kg^{-1} dw)	1.84 ± 0.23	1.19 ± 0.22
E4/E6	2.47 ± 0.01	2.34 ± 0.04
C (mg kg^{-1} dw)	220 ± 0.32	148 ± 0.35
H (mg kg^{-1} dw)	21 ± 1.2	16 ± 0.6
N (mg kg^{-1} dw)	7.0 ± 0.1	4.7 ± 0.1
S (mg kg^{-1} dw)	12 ± 2.9	18 ± 9.0
O[c] (mg kg^{-1} dw)	555 ± 7.85	571 ± 1.31
C/N ratio	30.9 ± 0.04	31.2 ± 0.40
Ca (mg kg^{-1} dw)	11 ± 1.0	11 ± 1.5
K (mg kg^{-1} dw)	124 ± 5.29	177 ± 0.91
Na (mg kg^{-1} dw)	4.1 ± 0.7	12.6 ± 0.73
Mg (mg kg^{-1} dw)	1.53 ± 0.07	1.90 ± 0.05
Fe[d] (mg kg^{-1} dw)	18.0 ± 0.69	34.9 ± 0.18

[a]Abbreviations: fw = fresh weight; dw = dry weight. [b]FA was determined as the difference between THE and HA. [c]O = 1000 − (C + H + N + S + K + Fe). [d]Abbreviations: Fe, soluble iron; LKH, leonardite potassium humate; LIH, leonardite iron humate; OM, organic matter; THE, total humic extract; HA, humic acid; FA, fulvic acid; EC, electrical conductivity.

Ferric Chelate Reductase (FC-R) Experiment. The behavior of LIH as substrate for FC-R in Fe-stressed cucumber plants was evaluated. Cucumber plants (strategy I) were used because they are efficient and induce FC-R when iron is limited. Cucumber seeds (*Cucumis sativus* L. cv. Ashley) were germinated in the dark at room temperature for 5 days on papers moistened with distilled water. Uniform seedlings were selected, and the stems of two individual plants wrapped together with polyurethane foam and placed in a 12 L polypropylene bucket (12 pairs of plants per bucket). The buckets contained a continuously aerated Fe-limited and EDTA-buffered nutrient solution[24] of the following composition: macronutrients (mM) 1.0 $Ca(NO_3)_2$, 0.9 KNO_3, 0.3 $MgSO_4$, and 0.1 KH_2PO_4; cationic micronutrients (μM) 5.0 FeEDTA, 2.5 $MnSO_4$, 1.0 $CuSO_4$, 10.0 $ZnSO_4$, 1.0 $CoSO_4$, 1.0 $NiCl_2$, and 115.5 $EDTANa_2$; anionic micronutrients (μM) 35.0 NaCl, 10.0 H_3BO_3, and 0.05 Na_2MoO_4; 0.1 mM HEPES. The pH was adjusted to 7.5 with KOH 1.0 M.

Plants were grown for 14 days in this nutrient solution in a Dycometal-type CCK growth chamber provided with fluorescent and sodium vapor lamps with a 16 h, 25 °C and 40% humidity day and 8 h, 20 °C, and 60% humidity night regime. Water was added every 2 days, and the nutrient solution was renewed every 7 days.

DOI: 10.1021/acs.jafc.8b04021
J. Agric. Food Chem. 2018, 66, 13386−13396

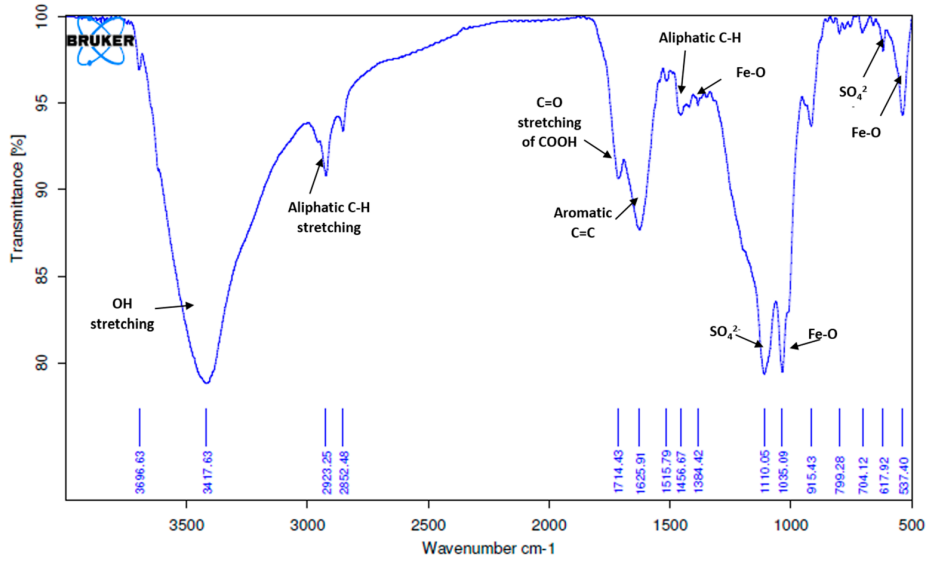

Figure 1. Infrared spectrum of LKH powder in a KBr matrix (1.0 mg of sample + 99.0 mg of dry KBr).

The measurement of FC-R activity was performed as in Lucena and Chaney[25] at pH 6 due to FC-R activity being higher at pH 6 than at pH 7.5.[26] A solution of Na_2BPDS (300 μM) was used as the Fe(II) trapping and colorimetric reagent. The experiment began 2 h after the start of the daylight period. The treatments applied were FeEDTA and LIH. At time zero, 5 mL of the corresponding treatment solution was added so that the final iron concentration was 100 μM. Aliquots of 3.0 mL were withdrawn at 0, 10, 20, 60, and 120 min, and seven replicates were prepared for each treatment. Two replicate blanks per treatment, consisting of solutions without plants, were included in order to correct reduction rates for slow photoreduction. The $Fe(BPDS)_3$ concentration was calculated as in Lucena and Chaney[25] by absorbance determination at 535 nm (maximum absorbance of $Fe(BPDS)_3$).

The fresh weight of the roots was measured at the end of the experiment. The slope of the plots of Fe(II) (μmol g^{-1} fresh root) plotted against time (h) was used as the Fe(III) reduction rate for each pair of plants.

Hydroponic Assays. *Plant Material.* Soybeans (Glycine max W316N, Wensman Seed Co.) were germinated in the dark at room temperature on filter paper moistened with distilled water. After germination (7 days), seedlings were transferred to the growth chamber, where they grew until the end of the experiment under the same controlled climatic conditions as in the FC-R experiment. Seedlings were placed on containers filled with 1/5 diluted nutrient solution with the same composition as for the FC-R experiment, although the iron concentration was 2 μM FeHBED. After 8 days, the diluted nutrient solution was replaced by a full-strength solution without Fe. Seedlings were kept in this solution for 2 days in order to induce iron deficiency. The iron-deficient plants were then transferred to polyethylene pots (three pairs of plants per pot) containing 2.0 L of full-strength nutrient solution without iron. In order to simulate calcareous conditions, $CaCO_3$ (0.1 g L^{-1}) was added to each pot. To evaluate the influence of Fe on leaf chlorophyll, the soil-plant analysis development (SPAD) index was measured every 2 or 3 days, using a Minolta Chlorophyll Meter SPAD-502 (Minolta, Osaka, Japan) after the first application of the Fe fertilizers.

Short-Term Bioassay. Stock solutions of LIH and FeEDDHA of 1000 μM were used in this bioassay. The LIH was prepared as explained above. The FeEDDHA stock solution was prepared by chelation with an iron standard solution of 1000 mg L^{-1} (Merck KGaA, Darmstadt, Germany) of EDDHA (ethylenediaminebis(*o*-*o*-hydroxyphenylacetic acid)) obtained from LGC Standards, Teddington, U.K. (93.12%). Prior to the iron chelation, EDDHA was dissolved with 3 mol of NaOH/mol of chelating agent. To ensure that all the Fe added to the chelate agent (EDDHA) was chelated, an extra 5% amount of Fe was added. The LIH and FeEDDHA solutions were adjusted at pH 7 with KOH 1 M. Four doses of LIH (10, 20, 50, and 100 μmol Fe pot^{-1}) and one dose of FeEDDHA (10 μmol Fe pot^{-1}), as a positive control treatment, were applied to the nutrient solution in which the chlorotic soybean seedlings were growing. The nutrient solution and the treatments were renewed weekly. The iron content in the nutrient solution of plants treated with LIH (20 and 100 μmol Fe pot^{-1}) and FeEDDHA was measured at 7, 14, and 21 days after the first treatment application (DAT). Three replicates (three pots) per treatment were used. Two pairs of plants were harvested at 7 DAT, and the rest of the plants were sampled at 21 DAT.

Long-Term Bioassay. The iron treatments applied just once were FeEDDHA (50 μmol Fe pot^{-1}) and LIH (250 μmol Fe pot^{-1}). The FeEDDHA was prepared as explained above. The pH was then adjusted to 7.0 for both solutions. Three replicates (three pots) per treatment were used. Two plants per pot were harvested in each sampling that was carried out at 10, 30, and 60 DAT.

Analytical Procedures. The sampled roots, stems, and leaves were separated, weighed, and washed with 0.1% HCl and 0.01% nonionic detergent (Tween 80) solution, rinsed with ultrapure water,[27] and dried in a forced air oven at 65 °C for 3 days. Thereafter, samples were milled and calcined in a muffle furnace (480 °C). The ashes were digested using HCl 1/1. Total iron was determined by AAS for the plant samples.

Electron Microscopy Analysis. Fresh root material was cut and mounted on stubs and sputters, coated with gold, and examined with a Philips XL30 (FEI, Eindhoven, The Netherlands) scanning electron microscope (SEM). The qualitative element composition of the samples was determined using energy-dispersive X-ray microanalysis (Dx4i and Si-Li Econ 4 detector).

Statistical Analysis. In order to verify the homogeneity of the data, the Levene test was used first, prior to testing the differences between Fe treatments for significance by one-way analysis of variance (ANOVA). Means were compared using the Duncan multiple range test (α < 0.05). All of the calculations were performed using SPSS v.24.0 software.

RESULTS AND DISCUSSION

Chemical and Spectroscopic Characterization. The LKH was physically and chemically characterized in order to obtain a detailed profile of the humic substance used in this

DOI: 10.1021/acs.jafc.8b04021
J. Agric. Food Chem. 2018, 66, 13386−13396

work. The chemical characterization is presented in Table 1. High K and low C contents were observed because of the strong base extraction. The iron content in this parental material was remarkable.

Almost 61% of the content of THE belonged to the humic acids, with a high molecular weight obtained corresponding to the E4/E6 ratio (<5.0), in line with the findings of Stevenson.[28] Moreover, a high C/N ratio (>10) indicated that the humification process was favored over mineralization.

The FT-IR spectrum of LKH is presented in Figure 1. According to Stevenson,[28] the spectrum mainly responds to HA extracted with alkali. Consistent with Colombo et al.,[29] the absorption bands at 3450−3300 cm^{-1} also corresponded to O−H stretching of Fe−OH, while the bands observed at 1384, 1035, and 537 cm^{-1} could be assigned to Fe−O bonds, indicating the presence of ferrihydrite. Moreover, LKH presented two marked peaks at 1110 and 617 cm^{-1}, which could be associated with sulfate vibrations.[30,31] The ^{13}C NMR spectrum is presented in Figure 2. Three main signals were

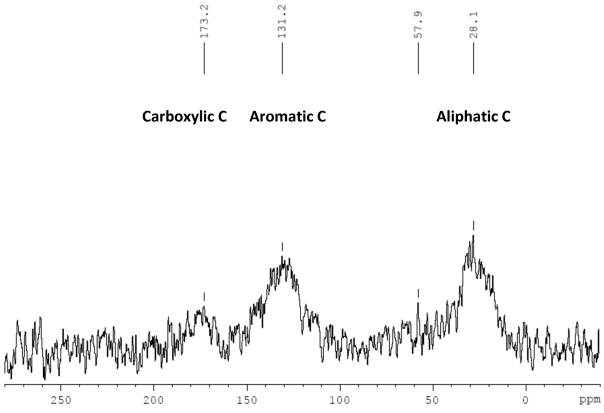

Figure 2. ^{13}C NMR spectrum of solid LKH.

obtained at 28.1, 131.2, and 173.2 ppm. The signal at 28.1 ppm is attributed to the aliphatic carbons, the signal at 131.2 ppm to the aromatic carbons, and the signal at 173.2 ppm to the carboxylic carbons. The results were compared with the database of the International Humic Substances Society (IHSS) for a leonardite sample, observing that aromatic and carboxylic carbon signals were smaller and the aliphatic carbons greater than those indicated by the database. These differences were attributed to the strong base extraction. Similar results have been obtained by Gao et al.[32] In addition, these results were confirmed with the carboxylic and phenolic group content (Table 1). The LKH showed that its total acidity corresponded mainly to the phenolic acidity. The results obtained for the total acidity expressed that LKH has a structure mainly formed by HA.[28]

The Mössbauer spectrum of LKH is shown in Figure 3. At 298 K, the Mössbauer spectrum can be interpreted as the sum of three quadrupole doublets with the same width at middle height and are characteristic of Fe(III) high spin.[33] One of these doublets, with δ = 0.37(1) mm s^{-1} and ΔE_Q = 1.26(3) mm s^{-1} at 298 K, was characteristic of a jarosite-type compound, $MFe_3(OH)_6(SO_4)_2$ (M = K^+, H_3O^+, Na^+, ...).[34] The rest of the Mössbauer spectrum area (62.9%) could be fitted as two quadrupole doublets. One of these (31.7%) could be associated with distorted iron octahedral forms, probably

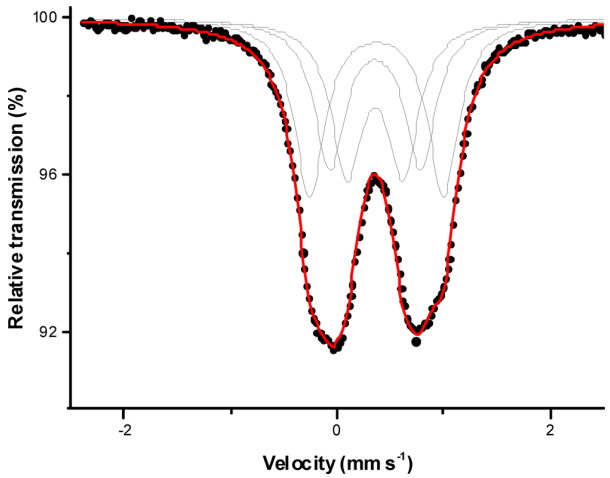

Figure 3. Mössbauer spectrum at room temperature (298 K) for the LKH sample. Dots represent experimental spectra. Black lines indicate the components of the calculated spectra. The red line is the calculated spectrum.

ferrihydrite (δ = 0.35(1) mm s^{-1} and ΔE_Q = 0.53(5) mm s^{-1}), and the other (31.2%) could be related to iron polynuclear structures (δ = 0.36(1) mm s^{-1} and ΔE_Q = 0.85(7) mm s^{-1}). No Fe(II) was found.

In Figure 4, the LKH XRD pattern presents a high signal/noise ratio for the diffraction lines of intensity relevant for

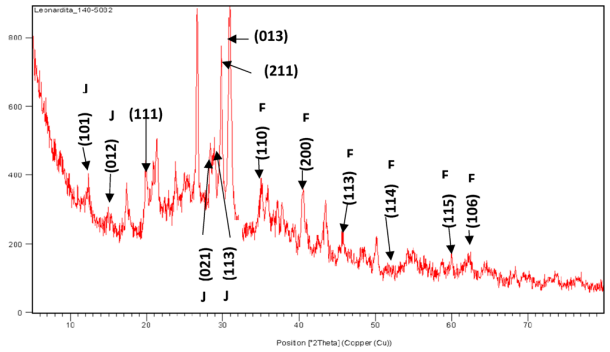

Figure 4. X-ray diffraction pattern of LKH. The horizontal index corresponds to K_2SO_4 (JCPDS No. 24-0703), and the vertical index agrees with jarosite (J) $KFe_3(SO_4)_2(OH)_6$ (JCPDS No. 4-015-0713) and ferrihydrite (F), syn. $Fe_5O_7(OH)\cdot 4H_2O$ (JCPDS No. 29-0712).

potassium sulfate (JCPDS No. 24-0703). The wide lines at 21.3, 29.8, and 30.9° in 2θ, which are characteristics of potassium sulfate, were identified with high intensity with indexes (111), (211), and (013). Iron was present in LKH mainly as jarosite (JCPDS No. 4-015-0723), with 14.9, 17.4, 28.7, and 28.9° in 2θ with indexes (101), (012), (021), and (113). In addition, iron was observed at a low intensity as ferrihydrite with six lines (JCPDS No. 29-0712) at 35.9, 40.8, 46.3, 53.2, 61.3, and 62.7° in 2θ with indexes (110), (200), (113), (114), (115), and (106).

In summary, LKH was found to be a soluble humic acid with a high molecular weight and it was in the process of natural humification. Iron (1.8%) was present in the LKH structure as jarosite, ferrihydrite, and polynuclear structures. Most of the acidic groups in LKH corresponded to phenolic groups that

DOI: 10.1021/acs.jafc.8b04021
J. Agric. Food Chem. 2018, 66, 13386−13396

would be available for being complexed with more iron, as demonstrated in the Fe-MCC test.

Determination of MCCs of LKH with Fe(II) and Fe(III). The importance of the complexing capacity of DOM on the availability of micronutrients including iron has long been acknowledged, especially under adverse soil conditions.[35] Maximum complexing capacity corresponds to the maximum iron content, Fe(II) or Fe(III), that can be bound to the LKH structure without clotting at pH 9, where the principal functional groups involved in the complexing process are the carboxylic and phenol groups[36] (see Figure 5). An initial

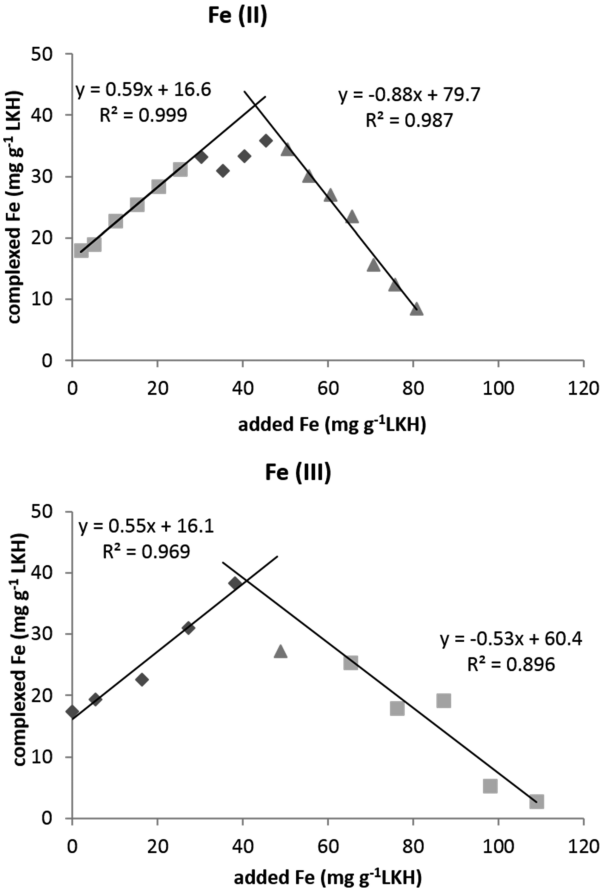

Figure 5. Typical titration curves for the determination of the maximum complexing capacities (MCCs) of LKH with Fe(II) (top) and Fe(III) (bottom).

amount of iron (1.8%) in the LKH was confirmed (Table 1). Moreover, it was observed that 42.7 mg of Fe(II)/g of LKH was necessary to obtain 41.9 mg of complexed Fe(II)/g of LKH, while 40.8 mg of Fe(III)/g of LKH was necessary to obtain 38.7 mg of complexed Fe(III)/g of LKH. Similar results were obtained for Fe(II) and Fe(III), probably because the Fe(II) has been oxidized to Fe(III) under this pH conditions (pH 9). It is noteworthy that the MCC for LKH is less than half of that for leonardites from other origins,[37] and this is because of the high molecular weight of LKH that favors the rapid clotting of the iron added.

The result obtained for Fe(III) was used to prepare LIH with 90% of MCC (Table 1) in order to obtain a soluble product, since the solubility of the iron humates increases with high pH and decreases in line with the increase in Fe/HS ratio.[36] The product LIH was applied to the ferric chelate reductase and the hydroponic experiments.

Ferric Chelate Reductase (FC-R) Experiment. It is very well known that, in order to alleviate Fe deficiency, "strategy I" plants (nongraminaceous monocot and dicot) develop an ensemble of root responses such as (i) the release of protons by plasma membrane H^+-ATPase into the rhizosphere to increase iron solubility, (ii) the induction of both a plasma membrane bound Fe(III) chelate reductase, to reduce chelated Fe(III) to Fe(II), (iii) the development of subapical swelling with abundant root hairs and transfer cells, and finally, (iv) the release of organic molecules with reducing and complexing capacity.[38] Therefore, LIH was prepared from the LKH and its behavior as a substrate for FC-R in Fe-stressed cucumber (a quite efficient strategy I plant and a model plant for the studies of the Fe reduction) at pH 6 was evaluated, since the reduction of Fe(III) to Fe(II) on root surfaces is an essential step for iron uptake in strategy I plants.[39] The results obtained are presented in Figure 6. A low reduction of Fe(III) to Fe(II)

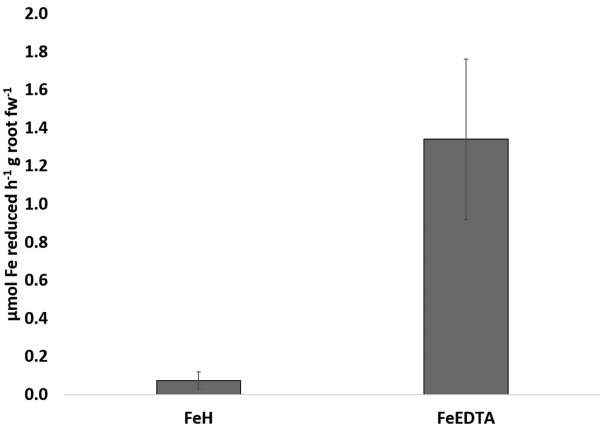

Figure 6. Ferric chelate reductase activity (μmol Fe reduced h^{-1} g root fw^{-1}) obtained when LIH and FeEDTA were used as substrates in iron-stressed cucumber plants at pH 6. Error bars represent standard deviations.

was observed after 2 h of the treatment application and was attributed to a fast accumulation of HA on the roots, which probably inactivated functional sites and/or further delayed the FC-R activity because of the nature (high-molecular-weight humic acid) and capability of LKH in activating Fe uptake mechanism and translocation. Moreover, in a previous work,[13] LIH was demonstrated to exert a slow kinetic effect in iron release when it was tested in a cell growth rate experiment. Furthermore, Kulikova et al.[40] observed a period of rapid (60 min) and linear accumulation of HA on wheat root seedlings from a solution containing 50 mg L^{-1} coal HA, followed by a slower accumulation (after 3 h until 24 h). The slower rate of HA accumulation represented a membrane-mediated process. Other studies have reported the capacity of HA to reduce Fe(III) on the root surface of Fe-deficient cucumber plants.[38,41] Aguirre et al.[38] have reported the increment of transcription of genes encoding Fe(III) chelate reductase (CsFR01) in purified leonardite humic acid treated cucumber roots after 48 h from the onset of the treatment, and the maximum effect was observed after 72 h of treatment with the higher doses. However, Tomasi et al.[42] observed high

DOI: 10.1021/acs.jafc.8b04021
J. Agric. Food Chem. 2018, 66, 13386−13396

expression levels of LeFRO1 (coding for an isoform of the PM Fe(III) chelate reductase), in root tissues of Fe-deficient tomato plants treated with Fe complexed by peat water-extractable humic substances (Fe-WEHS) at 1 h after the beginning of the treatment.

It is possible that the results also depend on the dicotyledonous species used for the bioassay, since in a previous FC-R experiment with soybean (a inefficient strategy I model plant), FC-R activity was not detected (data not shown). Similar results were obtained by Martín-Fernández et al.[43] for soybean plants tested with another leonardite iron humate.

Hydroponic Assays. Two hydroponic assays, short-term (21 DAT) and long-term (60 DAT), were carried out in order to evaluate the relationship between iron accumulation on soybean roots and iron nutrition when the fertilizer was applied several times or just once. In both bioassays, an additional iron synthetic chelate treatment was carried out (FeEDDHA10 or FeEDDHA50) as a positive Fe control treatment.

Short-Term Experiment. Iron-deficient soybean seedlings were fertilized with four LIH doses—LIH10, LIH20, LIH50, and LIH100 (10, 20, 50, and 100 μmol Fe pot^{-1})—applied three times (once a week) and compared with FeEDDHA10 (10 μmol Fe pot^{-1}). Table 2 shows the SPAD index measured during the experiment. Only high concentrations (LIH50 and LIH100) revealed symptoms of regreening at 21 DAT. Dry weight (g) and Fe content (μmol pot^{-1}) were measured at 7 and 21 DAT (Figure 7). At 7 DAT (Figure 7A), no significant differences were observed among treatments for shoot dry weight. At 21 DAT (Figure 7B), shoot and root weight increased with the dose, and significant differences were observed among treatments. The highest shoot and root dry weight was observed for plants fertilized with FeEDDHA10, although the shoot weight of plants treated with the LIH50 and LIH100 showed 60% and 40% less weight, respectively, in comparison to plants treated with FeEDDHA10.

Table 2. SPAD Index at the Last Level of Trifoliate Well Developed Soybean Leaves in Both Hydroponic Experiments[a]

First Hydroponic Experiment			
treatment	7 days	14 days	21 days
FeEDDHA10	28.9 ± 0.95^{a}	30.8 ± 3.90^{a}	33.9 ± 1.15^{a}
LIH10	2.3 ± 1.10^{b}	5.23 ± 0.78^{c}	10.2 ± 3.76^{b}
LIH20	8.83 ± 1.43^{b}	8.30 ± 2.26^{c}	8.23 ± 2.53^{b}
LIH50	21.3 ± 1.20^{a}	21.5 ± 0.80^{b}	24.0 ± 5.15^{a}
LIH100	23.5 ± 6.50^{a}	24.4 ± 2.74^{ab}	25.0 ± 3.31^{a}
Second Hydroponic Experiment			
treatment	10 days	30 days	60 days
FeEDDHA50	25.4 ± 1.03^{ns}	23.2 ± 1.59^{ns}	38.0 ± 3.28^{ns}
LIH250	22.8 ± 2.02	25.8 ± 2.41	35.8 ± 0.70

[a]Results are expressed as averages ± standard error. SPAD denotes soil-plant analysis development.

With respect to the Fe content in the shoots and roots (Figure 7), it was noticeable that iron accumulation in the roots increased with the LIH doses at 7 and 21 DAT, while a small proportion of the iron was translocated to the shoots. At 7 DAT (Figure 7C) and 21 DAT (Figure 7D), no significant differences were observed between LIH50 and LIH100 for iron accumulation on the roots. At 7 DAT, the plants treated with FeEDDHA10 presented the maximum iron content in shoots, while at 21 DAT no significant differences were observed in iron content in the shoots of plants treated with FeEDDHA10 or LIH100.

An aliquot (50 mL) of the nutrient solution of two LIH doses (LIH20 and LIH100) and FeEDDHA10 had been taken before to renew them and the residual iron content was analyzed (Figure 8). The iron removed from the nutrient solution was calculated, and significant differences were observed. In all cases, the iron in the nutrient solution for plants treated with LIH was almost 30% lower than for the plants treated with FeEDDHA at 7 DAT and almost 15% lower at 14 and 21 DAT. A different behavior was observed for plants fertilized at a low iron concentration (LIH20) in comparison to a high concentration (LIH100). The iron remaining in the nutrient solution for plants treated with LIH20 and FeEDDHA increased over time, while for plants treated with LIH100 the iron content in the nutrient solution increased up to 14 DAT and then remained constant until the end of the experiment (21 DAT). These results corresponded to the high accumulation of iron content in the roots of plants treated with LIH (Figure 7D). Between the first and the second samplings, iron accumulation increased in the roots of plants fertilized with LIH50 by more than 60%, while for the LIH100 it increased by more than 200% (Figure 7C,D). Figure 9A shows a dark brown covering observed on all the roots, which was removed during the washing process at the end of the experiment.

The weekly application of LIH caused a decreasing trend in the water transport from root to shoot as the LIH doses increased. While the water content in shoots for LIH10 did not vary between both sampling times (no significant increment, from 85.9 to 86.5%), for LIH100 there is a significant (α = 0.068) diminution (variation from 87.1 to 83.0% of water content). Then high LIH doses applied frequently may have caused partial blockage of root cell-wall pores. According to Asli and Neumann,[11] the physical accumulation of supramolecular agglomerates of HA on roots causes reductions in root hydraulic conductivity, leaf growth, transpiration, and root to shoot water transport. Moreover, Nardi et al.[44] have reported that the amount of a low molecular weight of humic acid transferred from pea roots to shoots was only 10−12%, whereas HS were mainly tightly bound to the cell walls of the roots. Recently, Olaetxea et al.[45] have concluded that the effects caused by a root-applied modeled sedimentary humic acid from leonardite on shoot growth are probably integrated into a primary physicochemical interaction of the humic acid molecular complex with pores in cell walls at the root surface, which have consequences on shoot growth (beneficial or detrimental) that would depend on the humic acid concentration in the rhizosphere.

In addition, possibly as a consequence of an increasing of LIH concentration in the rhizosphere, suspected partial blockage of the root cell-wall pores was produced, the transcription levels of the genes involved in the iron transport and shoot growth decreased, and so the iron transport from root to shoot decelerated (Figure 7D). The iron detected in the roots would be in two fractions, one taken up by the roots and the other adsorbed on the root surface. The iron taken up by the roots may have come from the dissolution of polynuclear structures and ferrihydrite, because they were

DOI: 10.1021/acs.jafc.8b04021
J. Agric. Food Chem. 2018, 66, 13386−13396

Journal of Agricultural and Food Chemistry Article

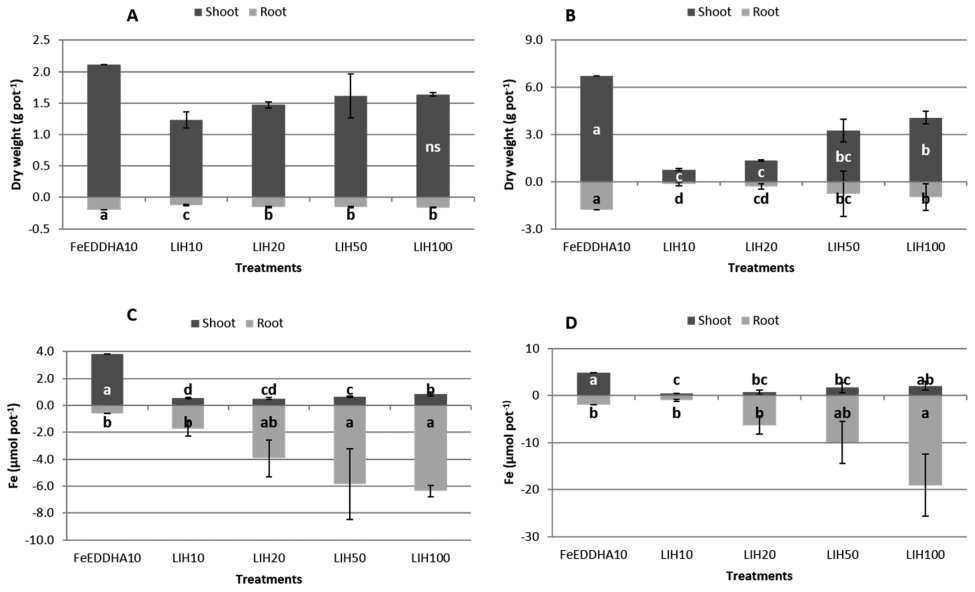

Figure 7. Dry weight (g pot[1]) at 7 DAT (A) and at 21 DAT (B) and Fe content (μmol pot^{-1}) at 7 DAT (C) and at 21 DAT (D) in soybean shoot (positive values) and root (negative values) fertilized with FeEDDHA 10.0 μmol pot^{-1} (FeEDDHA10) and LIH 10.0, 20.0, 50.0, and 100.0 μmol pot^{-1} (LIH10, LIH20, LIH50, and LIH100) for the first hydroponic experiment. The results are average ± standard error. For each series, different letters denote significant differences between the treatments according to Duncan's test (α < 0.05) (ns, not significant).

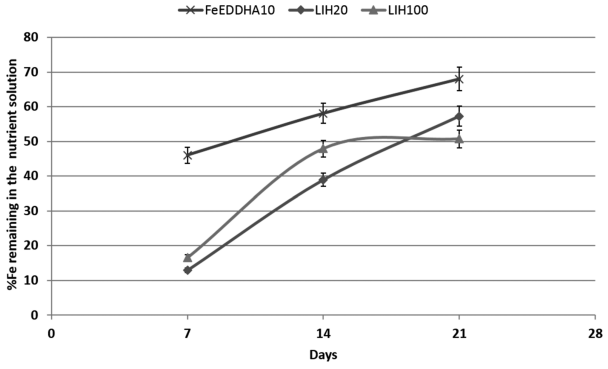

Figure 8. Percentage of iron remaining in the nutrient solution of plants treated with FeEDDHA (10 μmol Fe pot^{-1}) and LIH (20 and 100 μmol Fe pot^{-1}) at 7, 14, and 21 DAT for the first hydroponic experiment. The results are average ± standard error.

Figure 9. Photograph of soybean roots treated with LIH100 at 21 DAT in the short-term experiment (A), and a photograph of soybean roots treated with LIH250 at 60 DAT in the long-term experiment (B)

detected in the LKH structure by Mössbauer spectroscopy (Figure 3) and also because the plants fertilized with iron humates only take up iron from very small and amorphous particles of ferric polymers incorporated into the HS matrix, whereas crystalline iron (hydr)oxide nanoparticles are readily adsorbed on roots but not translocated to the shoots.[46] In fact, for soybean roots, only macromolecules with Stokes radii ≤3.3 nm may penetrate the cell wall unhindered.[47] Thus, the iron adsorbed by roots may have a crystalline structure, but this was not studied in the present experiment.

Long-Term Bioassay. Taking into account the results obtained in the previous hydroponic assay, a long-term (60 DAT) hydroponic experiment was carried out with only one LIH dose, LIH250 (250 μmol Fe pot^{-1}), applied once in an amount 5 times higher than that for FeEDDHA50 (50 μmol Fe pot^{-1}).

Dry weight (g) and Fe content (μmol pot^{-1}) in the shoot and root obtained in this experiment are plotted in Figure 10. It was observed that plants fertilized with LIH did not present significant differences in shoot dry weight in comparison to plants treated with FeEDDHA50 at 10 and 60 DAT, but at 30 DAT LIH250 presented a higher yield than FeEDDHA50. No significant differences were observed in root weight between treatments throughout the bioassay (Figure 10A).

The iron content (Figure 10B) in shoots presented significant differences between treatments at 10 DAT, while no significant differences were observed subsequently. Iron accumulation was detected in the roots of plants treated with LIH250, although no significant differences were observed between treatments.

Table 2 shows the SPAD index measured for the last level of trifoliate well-developed soybean leaves at 10, 30, and 60 DAT. The soybean plants treated with LIH250 presented regreening of their leaves and no significant differences with respect to the plants fertilized with FeEDDHA50.

DOI: 10.1021/acs.jafc.8b04021
J. Agric. Food Chem. 2018, 66, 13386−13396

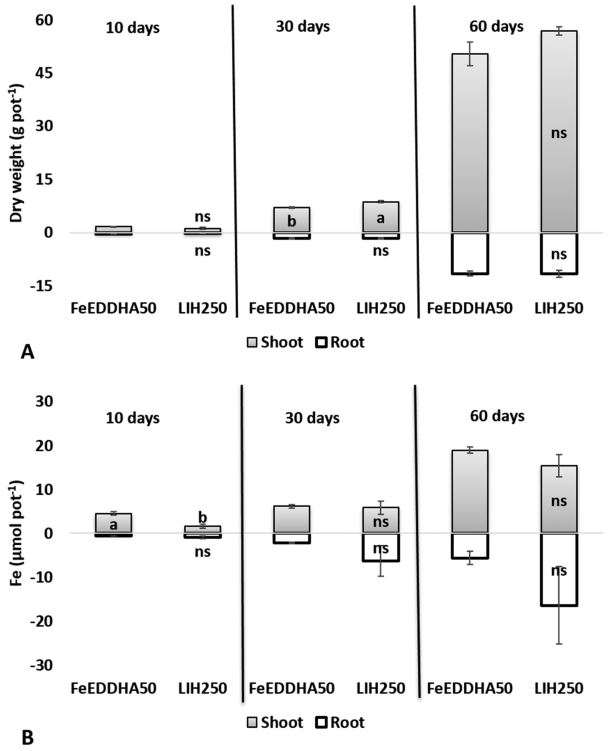

Figure 10. Dry weight (g plant^{-1}) (A) and Fe content (μmol plant^{-1}) (B) at 10 DAT, 30 DAT, and 60 DAT in soybean shoots and roots fertilized with FeEDDHA 50 μmol pot^{-1} (FeEDDHA50) and LIH 250 μmol pot^{-1} (LIH250) for the second hydroponic experiment. Negative values refer to dry weight and Fe content in roots. The results are average ± standard error. For each series, different letters denote significant differences between the treatments according to Duncan's test (α < 0.05) (ns, not significant).

The dark brown cover on the roots was observed less and just in their upper part (Figure 9B). Iron accumulation in roots was also observed (Figure 10B), although better transport of iron from the shoot to the root was observed than in the first hydroponic assay. When treatments are applied only once, HA deposition on the root surface is avoided, progressive iron release is favored, and thus the iron transport from shoot to root is improved.

The fresh soybean root material of plants treated with LIH250, obtained at 10, 30, and 60 DAT, was analyzed by SEM. Figure 11 shows the distribution of crystals of jarosite deposited over the root surface in each micrograph with the corresponding spectrum. The jarosite deposits increased over time, indicating a possible source of available iron for the soybean plants under calcareous conditions. According to Bigham and Kirk Norstrom,[48] jarosite tends to form at low pH (<5), at high sulfate ion concentrations (>3000 mg L^{-1}), and in the presence of base cations. Thus, the jarosite formation was not expected under calcareous conditions (nutrient solutionat pH >7), although it was one of the components of the LKH. The jarosite deposits were evidence of high acidic points on the root surfaces and probably a slow-release iron source that provided iron as the plant needed it. In order to confirm this pH decrease in the soybean rhizosphere, produced by the iron humate accumulation, changes in pH along the roots of intact soybean plants were measured using the agar-dye method and a glass microelectrode as described by Marshner et al.[50] Figure 12 shows that pH in the rhizosphere decreases up to 4.32 (yellow area) by the LIH accumulation, while in the rest of the agar medium the pH is 6.5 (red area) within 5 h around the roots embedded in agar medium with bromocresol purple, adjusted to pH 6. Soybean roots growing in liquid culture release amino acids into the medium in which they are growing and can reabsorb them.[49] The rhizosphere pH has been reported to be up to 1−2 pH units below nutrient solution pH.[51] Crabbe et al.[52] studied the crystallization of jarosite in the presence of amino acids and observed that glycine significantly affects the jarosite nucleation rate. Glycine is one of the amino acids exudates from the soybean roots[53] and may have enabled the jarosite nucleation on some points of the soybean roots.

When the LIH is prepared at pH 7 and applied to the nutrient solution at pH 7.5, according to Lindsay[54] the jarosite, as a component of LKH, is dissolved, although as soon as LIH

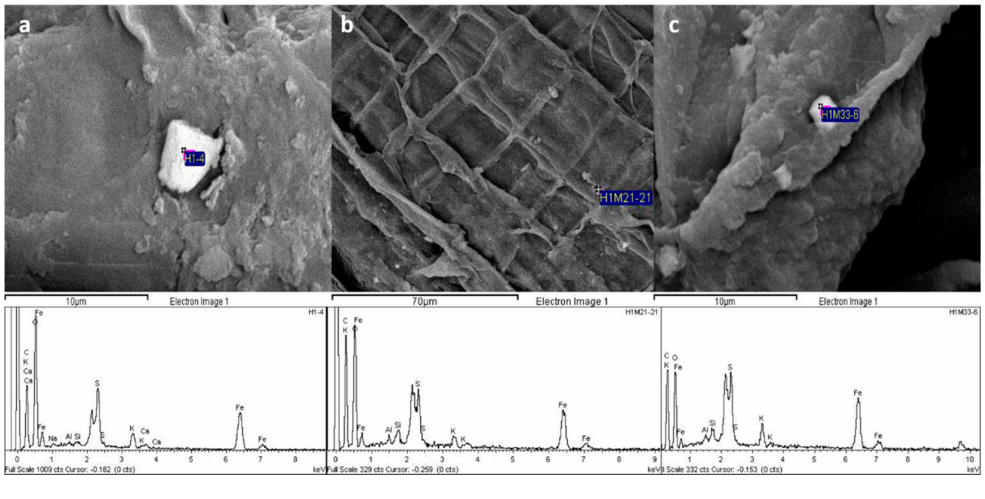

Figure 11. SEM micrographs of sections of soybean root treated with LIH250 (μmol pot^{-1}) at 10 (a), 30 (b), and 60 DAT (c) for the second hydroponic experiment, showing the distribution of jarosite deposits with the corresponding spectra. The reference scale is shown in each micrograph.

DOI: 10.1021/acs.jafc.8b04021
J. Agric. Food Chem. 2018, 66, 13386−13396

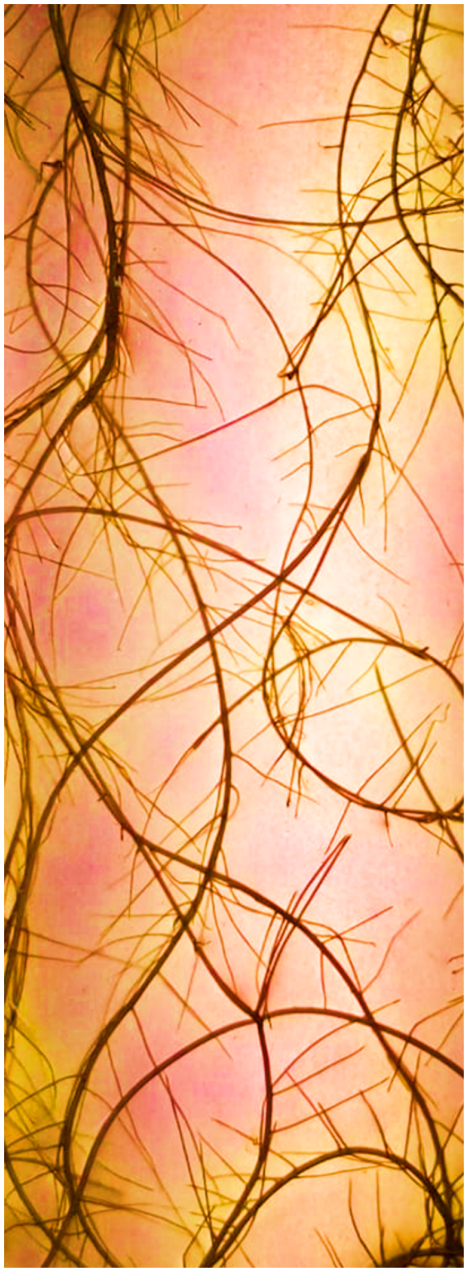

Figure 12. Effect of LIH accumulation on pH changes within 5 h around the intact soybean roots embedded in agar medium with bromocresol purple, adjusted to pH 6.0 (red). Yellow areas along the roots reflect acidification of the medium to pH 4.32, while the rest of the agar medium presents pH 6.5. The pH values were measured by inserting a glass microelectrode into the agar media.

approaches the rhizosphere, the pH decreases and the iron-deficient soybean roots release amino acids, mainly glycine that favors jarosite nucleation. Jarosite crystals, smaller than 20 nm, may have been taken up by the roots, while the rest would be adsorbed at the root surface and would continue growing on it (Figure 11).

The physicochemical characteristics and origin of HA limit its efficiency in agronomical uses whereby its characterization is crucial for diagnosis of its efficiency and improvement in its agronomical application. In general, HA presents an inhomogeneous structure with several particle sizes, mainly larger than 100 nm. Moreover, if the iron concentration is increased, more aggregates will be obtained and the HA accumulation on roots will be promoted. Thus, in this study, LIH (a soluble leonardite iron humate) was properly prepared by taking in account its MCC and by iron complexation of LKH, a high-molecular-weight humic acid. When LIH is applied to iron-deficient soybean plants, the roots are covered with a dark brown coating. This HA accumulation, due to the multiple applications of LIH, may produce partial blockage of root cell-wall pores, which may lead to a reduction in water and iron transport from root to shoot. As demonstrated by other authors,[38,42,45] the accumulation of humic acid in the rhizosphere most likely promotes a decrease of transcription of genes encoding Fe(III) chelate reductase (LeFRO1) and encoding for Fe^{2+} transporters (LeIRT1 and LeIRT2). However, if LIH is applied only at the beginning, HA accumulation is avoided in the roots growing after the application and the iron transport from root to shoot is improved by a cycling process of precipitation and dissolution of LIH that releases iron. Moreover, LKH contains in its structure ferrihydrite, polynuclear structures, and jarosite. Ferrihydrite and iron polynuclear structures are sources of available Fe for plants, while jarosite, due to the low rhizospheric pH, is deposited on the root surface. Although further research is required, the present study revealed the consequences of HA accumulation on soybean roots in the iron transport from root to shoot and the iron biomineralization to form jarosite on the soybean root surface. Moreover, a cycling process of iron availability to improve iron nutrition is proposed.

AUTHOR INFORMATION

Corresponding Author

*J.J.L.: e-mail, juanjose.lucena@uam.es; tel, +34 914973968; fax, +34 914973826.

ORCID

Juan José Lucena: 0000-0001-9130-2909

Author Contributions

J.J.L. conceived the study. M.T.C. carried out the chemical LKH characterization, MCC and FC-R determinations, and the hydroponic bioassays. Furthermore, M.T.C. analyzed the plant material and performed the statistical study. J.J.L. designed the manuscript and supervised all the experimental work presented. M.T.C. wrote the manuscript, which was revised by J.J.L. Both authors read and approved the final manuscript.

Funding

This work was financially supported by the project AGL2013-44474-R of the Spanish Ministry of Science and Innovation.

Notes

The authors declare no competing financial interest.

ACKNOWLEDGMENTS

We thank Dr. Nieves Menéndez for conducting the Mössbauer studies.

ABBREVIATIONS USED

LIH	leonardite iron humate
LKH	leonardite potassium humate
OM	organic matter

DOI: 10.1021/acs.jafc.8b04021
J. Agric. Food Chem. 2018, 66, 13386−13396

THE	total humic extract
HA	humic acids
FA	fulvic acids
EC	electrical conductivity
EDDHA	ethylenediaminebis(*o*-hydroxyphenylacetic acid)
Na_2BPDS	bathophenanthrolinedisulfonic acid disodium salt trihydrate
EDTA	ethylenediaminetetraacetic acid
HEPES	*N*-(2-hydroxyethyl)piperazine-*N*′-(2-ethanesulfonic acid)
FC-R	ferric chelate reductase
AAS	atomic absorption spectroscopy
FTIR	Fourier transform infrared spectroscopy
ICP MS	inductively coupled plasma mass spectrometry
XRD	X-ray diffraction
^{13}C NMR	^{13}C nuclear magnetic resonance
SEM	scanning electronic microscope
SPAD	soil-plant analysis development
DAT	days after treatments
ANOVA	analysis of variance

REFERENCES

(1) Lucena, J. J.; Hernández-Apaolaza, L. Iron nutrition in plants: an overview. *Plant Soil* **2017**, *418*, 1−4.

(2) Chen, Y.; Clapp, C. E.; Magen, H. Mechanisms of plant growth stimulation by humic substances: the role of organo-iron complexes. *Soil Sci. Plant Nutr.* **2004**, *50*, 1089−1095.

(3) Muscolo, A.; Sidari, M. Carboxyl and phenolic humic fractions affect callus growth and metabolism. *Soil Sci. Soc. Am. J.* **2009**, *73*, 1119−1129.

(4) Canellas, L. P.; Olivares, F. L. Humic and fulvic acids as biostimulants in horticulture. *Sci. Hortic.* **2015**, *196*, 15−27.

(5) Thomine, S.; Lèlievre, F.; Debarbieux, E.; Schroeder, J. I.; Barbier-Brygoo, H. AtNRAMP3, a multispecific vacuolar metal transporter involved in plant responses to iron deficiency. *Plant J.* **2003**, *34*, 685−695.

(6) Kovács, K.; Pechoušek, J.; Machala, L.; Zbořil, R.; Klencsár, Z.; Solti, Á.; Tóth, B.; Müller, B.; Pham, H. D.; Kristóf, Z.; Fodor, F. Revisiting the iron pools in cucumber roots: identification and localization. *Planta* **2016**, *244*, 167−179.

(7) Fu, Y. Q.; Yang, X. J.; Ye, Z. H.; Shen, H. Identification, separation and component nalysis of reddish brown and non-reddish brown iron plaque on rice (*Oryza sativa*) root surface. *Plant Soil* **2016**, *402*, 277−290.

(8) Koch, I.; Nearing, M. M. A Barrier to metal movement: synchrotron study of iron plaque on roots of wetland plants. *J. Environ. Sci. (Beijing, China)* **2016**, *44*, 1−3.

(9) Amils, R.; de la Fuente, V.; Rodríguez, N.; Zuluaga, J.; Menéndez, N.; Tornero, J. Composition, speciation and distribution of iron minerals in *Imperata Cylindrica*. *Plant Physiol. Biochem.* **2007**, *45*, 335−340.

(10) Longnecker, N.; Welch, R. M. Accumulation of apoplastic iron in plant roots. A factor in the resistance of soybeans to iron-deficiency induced Chlorosis ? *Plant Physiol.* **1990**, *92*, 17−22.

(11) Asli, S.; Neumann, P. M. Rhizosphere humic acid interacts with root cell walls to reduce hydraulic conductivity and plant development. *Plant Soil* **2010**, *336*, 313−322.

(12) Franco, A.; Rufo, L.; de la Fuente, V. Fe absorption and distribution of *Imperata cylindrica* (L.) P. Beauv. under controlled conditions. *J. Environ. Anal. Toxicol.* **2015**, *05*, 1−7.

(13) Cieschi, M. T.; Caballero-Molada, M.; Menéndez, N.; Naranjo, M. A.; Lucena, J. J. Long-term effect of a leonardite iron humate improving Fe nutrition as revealed in silico, in vivo, and in field experiments. *J. Agric. Food Chem.* **2017**, *65*, 6554−6563.

(14) *ISO 3696:1987 Water for analytical laboratory use. Specification and test methods*; International Organization for Standardization: Geneva, Switzerland; 6563.

(15) AFNOR. *NF U44-171 Sludge. Organic soils conditioners. Growth media. Determination of dry matter*; Association Francaise de Normalisation ed.s: Paris, France, 1982; p 3.

(16) AFNOR. *NF U44-160 Organic soil conditioners and organic material for soil. Determination of total organic matter. Calcination method*; Association Francaise de Normalisation: Paris, France, 1985; p 3.

(17) Royal Decree 1110/1991 *Oficial methods for organic fertilizers analysis*. (In spanish). BOE (Official Bulletin of the State). 1991, *170*, 23725−23730.

(18) Chen, Y.; Senesi, N.; Schnitzer, M. Information provided on humic substances by E4/E6 Ratios. *Soil Sci. Soc. Am. J.* **1977**, *41*, 352−358.

(19) Schnitzer, M. Organic matter characterization. In *Methods of Soil Analysis Part 2. Chemical and Microbiological Properties*; Page, B. L., Miller, R. H.; Keeney, D. R.; Agronomy Society of America: Madison, WI, 1982; Agronomy Monograph 9, pp 581−594.

(20) Brand, R. A. Improving the validity of hyperfine field distributions from magnetic alloys. *Nucl. Instrum. Methods Phys. Res., Sect. B* **1987**, *28*, 398−416.

(21) UNE-EN 15962:2011. *Fertilizers: Determination of the complexed micronutrient content and of the complexed fraction of micronutrients*; AENOR: Madrid, Spain, 2011.

(22) Villén, M.; Lucena, J. J.; Cartagena, M. C.; Bravo, R.; García Mina, J. M. Comparison of two analytical methods for the evaluation of the complexed metal in fertilizers and the complexing capacity of complexing agents. *J. Agric. Food Chem.* **2007**, *55*, 5746−5753.

(23) Regulation (EC) No 2003/2003 of the European Parliament and of the Council of 13 October 2003 relating to fertilizers. *Official Journal of the European Union L304*, 1−194.

(24) Degryse, F.; Smolders, E.; Parker, D. R. Metal complexes increase uptake of Zn and Cu by plants: implications for uptake and deficiency studies in chelator-buffered solutions. *Plant Soil* **2006**, *289*, 171−185.

(25) Lucena, J. J.; Chaney, R. L. Synthetic iron chelates as substrates of root ferric chelate reductase in green stressed cucumber plants. *J. Plant Nutr.* **2006**, *29*, 423−439.

(26) Susín, S.; Abadia, A.; González-reyes, J. A.; Lucena, J. J.; Abadia, J.; Córdoba, D.; San, A.; Magno, A.; De Química, D. The pH requirement for in vivo activity of the iron- deficiency-induced " turbo " ferric chelate reductase. *Plant Physiol.* **1996**, *110*, 111−123.

(27) Álvarez-Fernández, A.; Pérez-Sanz, A.; Lucena, J. J. Evaluation of effect of washing procedures on mineral analysis of orange and peach leaves sprayed with seaweed extracts enriched with iron. *Commun. Soil Sci. Plant Anal.* **2001**, *32*, 157−170.

(28) Stevenson, F. J. *Humus chemistry: genesis, composition, reactions*, 1st ed.; Wiley-Interscience: New York, USA, 1982.

(29) Colombo, C.; Palumbo, G.; Sellitto, V. M.; Rizzardo, C.; Tomasi, N.; Pinton, R.; Cesco, S. Characteristics of insoluble, high molecular weight iron-humic substances used as plant iron sources. *Soil Sci. Soc. Am. J.* **2012**, *76*, 1246−1256.

(30) Bishop, J. L.; Murad, E. The visible and infrared spectral properties of jarosite and alunite. *Am. Mineral.* **2005**, *90*, 1100−1107.

(31) Periasamy, A.; Muruganand, S.; Palaniswamy, A. Vibrational studies of $Na_2SO_4K_2SO_4NaHSO_4$ and $KHSO_4$ Crystals. *Rasayan J. Chem.* **2009**, *2*, 981−989.

(32) Gao, T.-G.; Jiang, F.; Yang, J.-S.; Li, B.-Z.; Yuan, H.-L. Biodegradation of leonardite by an alkali-producing bacterial community and characterization of the degraded products. *Appl. Microbiol. Biotechnol.* **2012**, *93*, 2581−2590.

(33) Greenwood, N.; Gibb, T. In *Mössbauer spectroscopy*; Springer Netherlands: London, U.K., 1971.

(34) Rothstein, Y. *Spectroscopy of jarosite minerals, and implications for the mineralogy of mars*; Mount Holyoke College: 2006.

(35) García-Mina, J. M.; Antolín, M. C.; Sánchez-Díaz, M. Metal-humic complexes and plant micronutrient uptake: a study based on different plant species cultivated in diverse soil types. *Plant Soil* **2004**, *258*, 57−68.

DOI: 10.1021/acs.jafc.8b04021
J. Agric. Food Chem. 2018, 66, 13386−13396

(36) García-Mina, J. M. Stability, solubility and maximum metal binding capacity in metal−humic complexes involving humic substances extracted from peat and organic compost. *Org. Geochem.* **2006**, *37*, 1960−1972.
(37) Kovács, K.; Czech, V.; Fodor, F.; Solti, A.; Lucena, J. J.; Santps-Rosell, S.; Hernández-Apaolaza, L. Characterization of Fe−leonardite complexes as novel natural iron fertilizers. *J. Agric. Food Chem.* **2013**, *61*, 12200−12210.
(38) Aguirre, E.; Leménager, D.; Bacaicoa, E.; Fuentes, M.; Baigorri, R.; Zamarreño, A. M.; García-Mina, J. M. The root application of a purified leonardite humic acid modifies the transcriptional regulation of the main physiological root responses to Fe deficiency in Fe-sufficient cucumber plants. *Plant Physiol. Biochem.* **2009**, *47*, 215−223.
(39) Yi, Y.; Guerinot, M. Lou. Genetic evidence that induction of root Fe(III) chelate reductase activity is necessary for iron uptake under iron deficiency. *Plant J.* **1996**, *10*, 835−844.
(40) Kulikova, N.; Badun, G. A.; Korobkov, V. I.; Chernysheva, M. G.; Tsvetkova, E. A.; Abroskin, D. P.; Konstantinov, A. I.; Zaitchik, B. T.; Ruzhitsky, A. O.; Perminova, I. V. Accumulation of coal humic acids by wheat seedlings: direct evidence using tritium auto-radiography and occurrence in lipid fraction. *J. Plant Nutr. Soil Sci.* **2014**, *177*, 875−883.
(41) Pinton, R.; Cesco, S.; Santi, S.; Agnolon, F.; Varanini, Z. Water-extractable humic substances enhance iron deficiency responses by Fe-deficient cucumber plants. *Plant Soil* **1999**, *210*, 145−157.
(42) Tomasi, N.; De Nobili, M.; Gottardi, S.; Zanin, L.; Mimmo, T.; Varanini, Z.; Römheld, V.; Pinton, R.; Cesco, S. Physiological and molecular characterization of Fe acquisition by tomato plants from natural Fe complexes. *Biol. Fertil. Soils* **2013**, *49*, 187−200.
(43) Martín-Fernández, C.; Solti, Á.; Czech, V.; Kovács, K.; Fodor, F.; Gárate, A.; Hernández-Apaolaza, L.; Lucena, J. J. Response of soybean plants to the application of synthetic and biodegradable Fe chelates and Fe complexes. *Plant Physiol. Biochem.* **2017**, *118*, 579−588.
(44) Nardi, S.; Pizzeghello, D.; Muscolo, A.; Vianello, A. Physiological effects of humic substances on higher plants. *Soil Biol. Biochem.* **2002**, *34*, 1527−1536.
(45) Olaetxea, M.; Mora, V.; Bacaicoa, E.; Garnica, M.; Fuentes, M.; Casanova, E.; Zamarreño, A. M.; Iriarte, J. C.; Etayo, D.; Ederra, I.; Gonzalo, R.; Baigorri, R.; García-Mina, J. M. Abscisic acid regulation of root hydraulic conductivity and aquaporin gene expression is crucial to the plant shoot growth enhancement caused by rhizosphere humic acids. *Plant Physiol.* **2015**, *169*, 2587−2596.
(46) Kulikova, N. A.; Polyakov, A. Y.; Lebedev, V. A.; Abroskin, D. P.; Volkov, D. S.; Pankratov, D. A.; Klein, O. I.; Senik, S. V.; Sorkina, T. A.; Garshev, A. V.; Veligzhanin, A. A.; Garcia Mina, J. M.; Perminova, I. V. Key roles of size and crystallinity of nanosized iron hydr(oxides) stabilized by humic substances in iron bioavailability to plants. *J. Agric. Food Chem.* **2017**, *65*, 11157−11169.
(47) Baron-Epel, O.; Gharyal, P. K.; Schindler, M. Pectins as mediators of wall porosity in soybean cells. *Planta* **1988**, *175*, 389−395.
(48) Bigham, J. M.; Kirk Nordstrom, D. Iron and aluminum hydroxysulfates from acid sulfate waters. *Rev. Mineral. Geochem.* **2000**, *40*, 351−403.
(49) Sargent, P. A.; King, J. Investigations of growth-promoting factors in conditioned soybean root cells and in the liquid medium in which they grow: ammonium, glutamine, and amino acids. *Can. J. Bot.* **1974**, *52*, 1747−1755.
(50) Marschner, H.; Römheld, V.; Ossenberg-Neuhaus, H. Rapid method for measuring in pH and reducing processes along roots of intact plants. *Z. Pflanzenphysiol.* **1982**, *105*, 407−416.
(51) Römheld, V.; Marschner, H. Plant-induced pH changes in the rhizosphere of Fe-efficient and Fe-inefficient soybean and corn cultivars. *J. Plant Nutr.* **1984**, *7*, 623−630.
(52) Crabbe, H.; Fernandez, N.; Jones, F. Crystallization of jarosite in the presence of amino acids. *J. Cryst. Growth* **2015**, *416*, 28−33.
(53) Kuzmicheva, Y. V.; Shaposhnikov, A. I.; Petrova, S. N.; Makarova, N. M.; TychinskayaJan, I. L.; Puhalsky, V.; ParahinIgor, N. V.; Tikhonovich, A.; Belimov, A. A. Variety specific relationships between effects of rhizobacteria on root exudation, growth and nutrient uptake of soybean. *Plant Soil* **2017**, *419*, 83−96.
(54) Lindsay, W. L. *Chemical equilibrium in soils*; Wiley: New York, 1979.

DOI: 10.1021/acs.jafc.8b04021
J. Agric. Food Chem. 2018, 66, 13386−13396

Capítulo IV: Propuestas de mejora de la eficiencia de los humatos férricos en la nutrición vegetal

Chapter IV: Methods proposed for improvements of leonardite iron humate efficiency in plants nutrition

RESUMEN

En los últimos veinte años la oferta de humatos férricos como correctores de deficiencia de hierro en el mercado español de fertilizantes, ha disminuido considerablemente a pesar de ser productos de bajo costo y respetuosos con el medioambiente. En parte se debe a los requerimientos legales para su comercialización ya que su contenido en hierro soluble suele ser inferior al de hierro total, así como a su baja eficiencia respecto de los quelatos sintéticos de hierro. Es por tal motivo que se estudiaron posibilidades de mejorar la solubilidad del hierro en estos productos, preparando mezclas de humatos férricos y quelatos sintéticos de hierro, así como también preparando nanofertilizantes de humatos férricos, realizando una caracterización exhaustiva de los mismos, así como estudios cinéticos de liberación de hierro. Además, los productos obtenidos fueron marcados con isótopos estables de hierro (^{57}Fe y ^{56}Fe) a fin de estudiar su contribución real a la nutrición férrica de plantas de Estrategia I cuando son aplicados en suelos calizos.

Los humatos de hierro y los quelatos sintéticos de hierro poseen cinéticas diferentes en la nutrición de las plantas. Mientras los quelatos entregan el hierro a la planta en forma rápida y a corto plazo, los humatos férricos lo hacen en forma lenta y a largo plazo. Las mezclas de humatos y quelatos pueden producir un efecto sinérgico en la nutrición férrica debido al efecto de recarga de los quelatos, especialmente si se utiliza HBED/Fe^{3+} ya que aumenta el hierro soluble disponible para las plantas. Con respecto a los experimentos realizados con nanofertilizantes, se ha confirmado que el hierro procedente del humato llega a todos los órganos de la planta, en especial al fruto, además de presentar un efecto a largo plazo en la nutrición férrica. No se observó que la aplicación de nanofertilizantes mejore la solubilidad del hierro aunque por tratarse de una nueva tecnología, se necesita más investigación al respecto.

Este capítulo se divide en dos apartados con sus correspondientes trabajos:

4.1 Efficiency of leonardite iron humate and iron synthetic chelates mixtures in *Glycine* max nutrition. (Eficiencia de mezclas de humato férrico procedente de leonardita y quelatos sintéticos de hierro en la nutrición de plantas Glycine max). Este trabajo ha sido enviado para su publicación en Julio de 2019 a *Journal of Plant Nutrition and Soil Science.*

4.2 Eco-friendly iron-humic nanofertilizers synthesis for the prevention of iron chlorosis in soybean (*Glycine* max) grown in calcareous soil. (Síntesis de nanofertilizantes de hierro-sustancias húmicas como prevención de la clorosis férrica de plantas de soja cultivadas en suelo calizo. Este trabajo se publicó en *Frontiers in Plants Science* 2019, 10: 413.

IV.1 Efficiency of leonardite iron humate and iron synthetic chelates mixtures in *Glycine* max nutrition

Abstract

It has been proposed that humic substances may help iron acquisition by plants when iron chelates are used to correct iron chlorosis. The aim of this work is to study the possible synergic effect between mixtures of an iron leonardite humate (L/Fe^{3+}) with iron synthetic chelates (*o,o*EDDHA /Fe^{3+} or HBED/Fe^{3+}) and to reevaluate the classical chelate shuttle effect model. Different ratios, doses and sampling times were used in hydroponic and soil experiments using soybean (*Glycine* max) as model Strategy I crop in calcareous conditions. The isotopes ^{56}Fe and/or ^{57}Fe were used as tracers in the soil experiments. Also ligand competition between the humate and chelating agents were done. Results suggest that the initially iron humate participates in the chelate shuttle mechanism providing available Fe to the chelating agent and then to the plants, showing a slight synergic effect. After few days the contribution of the chelates to the Fe nutrition decreases substantially, but the one from the humates is maintained. The most efficient ratio was two parts of iron humates and one part of iron chelate, in particular, HBED/Fe^{3+} because of its lasting effect that fits better to the iron humate kinetics. The soluble iron in soil increased and the shoot to root iron translocation improved due to a synergic effect by a shuttle effect exerted by iron chelate in the mixture.

Introduction

Iron, the fourth most widespread element in the Earth's crust and soils, was among the very first elements to be identified as an essential nutrient for plants (*Shenker and Chen*, 2005). Iron chlorosis is a nutritional disorder in plants growing in calcareous soils, characterized by a significant decrease of chlorophyll in leaves that reduces the yield and quality of many crops. Iron synthetic chelates such as *o,o*EDDHA/Fe^{3+} and HBED/Fe^{3+} are the most efficient soil fertilizers to treat iron chlorosis in plants. A problem related to Fe synthetic chelates is their low persistence under field conditions because they are leached from the rhizosphere due to their high solubility (*Tagliavini and Rombolà*, 2001; *Hernández-Apaolaza and Lucena*, 2011).

The positive effect of humic substances (HS) on the growth of numerous plants is well documented (*Nardi and Pizzeghello*, 2002; *Trevisan et al.*, 2010; *Vaccaro et al.*, 2015). Leonardite is a coal-like substance similar in structure to lignite, but significantly different in its oxygen and ash contents. Some of the effects of HS contained in leonardite are ascribed to a general improvement of soil fertility, leading to a higher nutrient availability for plants. Moreover, HS exert a positive

influence on the metabolic and signaling pathways involved in plant development (*Kołodziej et al.*, 2013).

In the last years, new Fe fertilizers have been developed, focusing on their slow-release, environmental-friendly and high purity properties (*Abadía et al.*, 2011; *Monreal et al.*, 2016). Humic substances are promising materials due to their variable structure, high content of functional groups, easy preparation and environmental compatibility. Because of the presence of these functional groups, mainly carboxylic and phenolic groups, humic acids are attractive chelating agents for Fe(III) ions and convenient to prepare eco-friendly materials that can be applied as fertilizers (*Chassapis et al.*, 2010). The leonardite iron humates are less effective for the correction of iron chlorosis than iron synthetic chelates since they provide slowly and increasingly the iron to the plants because of their kinetic limitations in calcareous soils (*Cieschi et al.*, 2017).

According to *Sánchez-Sánchez et al.* (2002), the application of a 1:1 (w/w) mixture of commercially available *o,o*EDDHA/Fe^{3+} and HS can improve Fe uptake by lemon trees in calcareous soils. Moreover, *Cerdán et al*. (2007) have proposed a partial substitution of iron chelates by HS as an ecological and economical option. However, no references were found in the literature about mixtures of iron humates and iron synthetic chelates application in calcareous soil.

Lindsay and Schwab (1982) proposed a mechanism for the action of iron chelates in soils in which the chelating agent works ideally as a shuttle iron transporter between soil and plant roots. This mechanism was later referred to as the "shuttle effect" (*Lucena*, 2003) but it has not been fully demonstrated. On the other hand, *Cesco et al*. (2000) and Colombo et al. (2011) have described the mechanism of iron Fe acquisition of Strategy I and Strategy II plants and the pathways of Fe mobilization at the rhizosphere when the iron sources applied are iron humic substances. According to *Senesi et al*. (1977), there are two different binding sites for Fe^{3+} in humic materials: (1) Fe^{3+} is strongly bound and protected by tetrahedral and/or octahedral arrangements, that resist to a significant extent not only chemical complexing but also chemical reduction and (2) Fe^{3+} is adsorbed on external surfaces of humic acids as leonardite, weakly bound octahedral easily complexed and reduced. Thus, exhibiting high chemical reactivity. Then, we have hypothesized that the labile iron bonded to the leonardite can be easily chelated by the synthetic ligand and transport it to the roots by the shuttle effect, ameliorating the soybean iron nutrition (*Lucena*, 2003; *Schenkeveld et al.*, 2014). Therefore, in order to study a possible synergy between fertilizers by the chelate agent-shuttle effect, two mixtures (L/Fe^{3+}+ Ch/Fe^{3+}) of an iron leonardite humate (L/Fe^{3+}) with iron

synthetic chelates (Ch: *o,o*EDDHA /Fe^{3+} or HBED/Fe^{3+}) were prepared and their efficiency was tested in one hydroponic assay and two soil experiments using soybean (*Glycine* max) iron-deficient plants as a model Strategy I crop in calcareous conditions. Moreover, the contribution of both fertilizers in soil conditions was evaluated by labeling them with iron stable isotopes (^{56}Fe, ^{57}Fe).

Materials and methods

Iron synthetic chelate (Ch/Fe^{3+}) and the leonardite iron humate (L/Fe^{3+}) preparation

The (L/Fe^{3+}) used in this work was prepared according to *Cieschi and Lucena*, 2018. In brief, a stock solution (1000µml L^{-1}) of L/Fe^{3+} was prepared by the complexation of a leonardite potassium humate (LKH), provided by Fertinagro S.L, with an iron standard solution of 1000 mg L^{-1} of $Fe(NO_3)_3$ obtained from Merck KGaA, Darmstadt, Germany. The final solution reached 90% of its iron maximum complexing capacity (40.8 mg Fe (III) g LKH) that was previously determined by *Cieschi and Lucena*, (2018). The pH (7.0) was obtained by the careful addition of 1.0M KOH.

The *o,o*EDDHA/Fe^{3+} was prepared by chelation with Fe^{3+} from $Fe(NO_3)_3$ and *o,o*EDDHA (ethylenediamine-di (*o-o* hydroxyphenylacetic acid)) obtained from LGC Standards, Teddington, U.K. (93.12%), previously dissolved with 3.0 mol of NaOH per mol of the chelating agent. The HBED/Fe^{3+} was prepared in the same way as to *o,o*EDDHA /Fe^{3+} although using HBED (N,N'-di(2-hydroxybenzyl)-ethylenediamine-N,N'-diacetic acid monohydrochloride) kindly provided by ADOB PPC, Poznan, Poland (93.72%).

Plant material

Three bioassays (one hydroponic and two pot soil experiments) were carried out using soybean seeds (*Glycine* max W316N, Wensman Seed Co), which were germinated in the dark at room temperature on filter paper moistened with distilled water. After germination (7 days), seedlings were transferred to a Dycometal-type CCK growth chamber where they grew until the end of the experiments under controlled climatic conditions: day/night photoperiod, 16/8 h; temperature (day/night) 30/25 ºC, relative humidity (day/night) 50/70 %. After that, seedlings were placed on containers filled with 1/5 diluted nutrient solution (NS). The composition of NS was the following: (macronutrients in mM) 1.0 $Ca(NO_3)_2$, 0.9 KNO_3, 0.3 $MgSO_4$, and 0.1 KH_2PO_4; (cationic micronutrients in µM) 2.0

HBED/Fe^{3+}, 2.5 $MnSO_4$, 1.0 $CuSO_4$, 10.0 $ZnSO_4$, 1.0 $CoSO_4$, 1.0 $NiCl_2$, and 115.5 $EDTANa_2$; (anionic micronutrients in µM) 35.0 NaCl, 10.0 H_3BO_3, and 0.05 Na_2MoO_4 and 0.1mM HEPES. The pH was adjusted to 7.5 with 1.0M KOH. After 5 days, the diluted NS was replaced by the full-strength NS without Fe. Seedlings were kept in this solution for two days to induce iron deficiency. To simulate calcareous conditions, $CaCO_3$ (0.1g L^{-1}) was added to every pot.

Hydroponic assay

The deficient seedlings were transferred to polyethylene pots (three pairs of plants per pot) containing 2.0L of full-strength NS and 10µmol pot^{-1} in Fe of the L/Fe^{3+}+ Ch/Fe^{3+} (*o,o*EDDHA/Fe^{3+} or HBED/Fe^{3+}) mixes were applied every seven days to the NS, in different molar ratios of L/Fe^{3+}:Ch/Fe^{3+} (0:10, 3:7, 5:5, 6:4, 7:3, 8:2, 9:1, 10:0). Two pairs of plants were harvested at 7 days after treatments (DAT) were applied, and the remaining plant was harvested at 21DAT.

Soil pot experiments

For both soil pot experiments, deficient iron soybean plants were transferred to polystyrene pots filled with 600g of a soil/sand 70/30% (w/w) mixture. The calcareous soil (pH-H_2O: 7.9, active $CaCO_3$ g Kg^{-1}: 89) was obtained from the first 20 cm of a citrus farm at Picassent, Valencia, Spain (39º21'41.28'' N, 0º27'42.58'' W). Physicochemical characteristics of this soil are described in *Cieschi et al*. 2016. Standardized calcareous sand (2–4 mm) was used. Before transferring the seedlings, pots were irrigated till field capacity. The pots were watered weekly with a macronutrient solution prepared as in the hydroponic assays.

Short-term experiment: different L/Fe^{3+}: Ch/Fe^{3+} ratios. This soil pot experiment finished 13 DAT and different L/Fe^{3+}: Ch/Fe^{3+} ratios were applied. Labeled L/$^{57}Fe^{3+}$ was prepared complexing LKH with ^{57}Fe according to the 90% of the MCC of LKH (See 2.1). The iron isotope was provided by Isoflex with the following isotopic distribution (atom %): ^{54}Fe (0.01), ^{56}Fe (1.17), ^{57}Fe (96.66) and ^{58}Fe (2.16).

Three plants per pot were placed and only one sampling was carried out at 13 DAT. The treatments consisted of mixes of L/$^{57}Fe^{3+}$ and Ch/Fe^{3+} (*o,o*EDDHA/Fe^{3+} or HBED/Fe^{3+}) with a total Fe^{3+} amount of 54.0 µmol pot^{-1}. The mixes L/$^{57}Fe^{3+}$+Ch/Fe^{3+} were prepared in six different ratios of L/$^{57}Fe^{3+}$:Ch/Fe^{3+} (µmol L/$^{57}Fe^{3+}$ pot^{-1} : µmol Ch/Fe^{3+} pot^{-1}): 0:54, 12:42, 24:30, 30:24, 42:12 and 54:0, that were applied over the soil surface and then irrigated with the Fe-free nutrient solution.

Long-term experiment: different doses. This pot experiment lasted till 60 DAT and was designed to compare the efficiency in iron nutrition among the mixtures (L/Fe^{3+}: *o,o*EDDHA/Fe^{3+} or L/Fe^{3+}: HBED/Fe^{3+}), using a 2:1 ratio. The iron treatments were prepared using ^{56}Fe to label L/Fe^{3+} (L/$^{56}Fe^{3+}$) and ^{57}Fe to label *o,o*EDDHA/Fe^{3+} (*o,o*EDDHA/$^{57}Fe^{3+}$) or HBED/Fe^{3+} (HBED/$^{57}Fe^{3+}$). The ^{57}Fe isotopic distribution was specified above. The ^{56}Fe was also provided by Isoflex and its isotopic distribution (atom %) was the following: ^{54}Fe (0.01), ^{56}Fe (99.94), ^{57}Fe (0.04) and ^{58}Fe (0.01). Different doses (µmol pot^{-1}) of the mixtures L/$^{56}Fe^{3+}$: *o,o*EDDHA/$^{57}Fe^{3+}$ or L/$^{56}Fe^{3+}$: HBED/$^{57}Fe^{3+}$ (40:20; 60:30; 90:45) were added over the soil surface. Pots without iron exogenous sources were used as a negative control treatment. Four iron-deficient soybean seedlings per pot were set and five replicates (five pots per treatment) were done. Two samplings were carried out at 7 DAT (3 plants per pot) and 60 DAT (the remaining plant).

Ligand competition of L/Fe^{3+} with the synthetic chelating agents *o,o*EDDHA and HBED

In order to study the stability of L/Fe^{3+} at pH 7, two ligand competitions (L/Fe^{3+} + *o,o*EDDHA and L/Fe^{3+} + HBED) were carried out for 97 days, measuring every two or three days the changes in absorbance from 350 to 650nm. The following solutions 100 µM were prepared: LKH, L/Fe^{3+}, *o,o*EDDHA, *o,o*EDDHA/Fe^{3+}, HBED, HBEDFe^{3+}, L/Fe^{3+} + *o,o*EDDHA and finally, L/Fe^{3+} + HBED. All the solutions were prepared in three replicates with an ionic strength of 0.1M with KNO_3. In all cases, pH was buffered with 2.0ml HEPES 0.1M, then adjusted to 7.0 with KOH 0.1M, and volume made up to 100.0mL. The solution named LKH was used as a blank solution. Afterward, the solutions were kept at room temperature (21-23ºC) in the dark until measurement. The chelating agents *o,o*EDDHA and HBED were

previously dissolved with 3 mol of NaOH per mol of chelating agent and the pH was then adjusted to 7.0. The UV/Vis Spectra of samples from 350 to 650nm were recorded on a Jasco V-650 spectrophotometer every two or three days for 97 days.

Taking into account the iron contribution of each component, for example, in the solution L/Fe^{3+} + *o,o* EDDHA, the total iron concentration in this solution would be:

$$[Fe_{Total}]_{L/Fe^{3+}+o,o\ EDDHA} = [Fe]_{L/Fe^{3+}} + [Fe]_{o,o\ EDDHA/Fe^{3+}} = 100\mu M$$

, the theoretical results were calculated as the sum of contributions of each component absorbance at each wavelength measured from 350 to 650nm.

$$A_{\lambda i=} \sum_i A_\lambda = \sum_i [i]_\lambda \, \varepsilon_\lambda + e_\lambda$$

, where A is the absorbance, λ is every wavelength measured from 350 to 650nm, ε is the absorptivity calculated for each wavelength for these experimental conditions. Each component is represented by i and, for this example, the components are LKH, L/Fe^{3+}, *o,o*EDDHA and *o,o*EDDHA/Fe^{3+}. The best concentration of each component at each wavelength from 350 to 650nm was found by least-squares fitting of the error vector *e* (minimizing the square sum of errors) and mathematical deconvolution was applied among the experimental and the theoretical results.

The same procedure was applied for the solution L/Fe^{3+}+ HBED.

Analytical procedures

For all the bioassays, the sampled roots, stems and leaves were separated, weighed and washed with 0.1% HCl and 0.01% non-ionic detergent (Tween 80) solution and rinsed with ultrapure water (*Álvarez-Fernández et al.*, 2001). Then samples were dried in a forced-air oven at 65ºC for 3 days. After that, samples were mill ground and calcined in a muffle furnace (480ºC). The ashes were digested using 5ml of HCl 1:1 and 5 ml of H_2O_2 30%, according to *Gárate et al*. (1984). Total Fe was measured by atomic absorption spectrometry (AAS) for the hydroponic samples.

Soil soluble fraction was obtained at the end of the experiment by washing the complete soil: sand mixture of each pot with distilled water (600mL) and then stirred for 10

min with a rotary stirrer at 90 min^{-1}. An aliquot of 40mL was centrifuged for 5 min at 6000 min^{-1} (Rotofix 32 Hettich), the supernatant was filtered using a cellulose filter (Filter Lab 1238) and then, filtered using a Millipore 0.45µm syringe filter. Enough HNO_3 (Suprapur, Merck) was added up to achieve a 1% acid matrix. Soil available fraction was obtained from the remaining solid in the centrifuge tube by extraction for 20 min with 25mL of *Soltanpour and Schwab* (1977) extractant (DTPA + ammonium bicarbonate). After, the samples were filtered. The extraction was made in triplicate, the extracts were joined, and volume made up to 100 ml. Nitric acid was added to eliminate the excess of bicarbonate and to allow an acid media for the analytical determinations. Isotope quantification in the plant organs and soil fractions (soluble and available) were determined by ICP-MS (NexIon 300XX, Perkin-Elmer, Waltham, Massachusetts, USA) using ^{57}Fe standards and correcting Ca and Ar interferences using a collision cell quadrupole ICP-MS instrument. The specific contribution of each iron fertilizer to the soil and plant nutrition was calculated by isotope pattern deconvolution analysis considering the three iron sources, with a modification of the method proposed by *Rodríguez-Castrillón et al.* (2008). In brief, the mass balance for all the Fe natural isotopes Fe can be expressed as shown by matrix notation when L/Fe^{3+} is prepared with ^{57}Fe:

$$\begin{bmatrix} {}^{54}A_{Total} \\ {}^{56}A_{Total} \\ {}^{57}A_{Total} \\ {}^{58}A_{Total} \end{bmatrix} = \begin{bmatrix} {}^{54}A_{L/Fe^{3+}} & {}^{54}A_{Nat+Ch/Fe^{3+}} \\ {}^{56}A_{L/Fe^{3+}} & {}^{56}A_{Nat+Ch/Fe^{3+}} \\ {}^{57}A_{L/Fe^{3+}} & {}^{57}A_{Nat+Ch/Fe^{3+}} \\ {}^{58}A_{L/Fe^{3+}} & {}^{58}A_{Nat+Ch/Fe^{3+}} \end{bmatrix} \times \begin{bmatrix} x_{L/Fe^{3+}} \\ x_{Nat+Ch/Fe^{3+}} \end{bmatrix} + \begin{bmatrix} {}^{54}e \\ {}^{56}e \\ {}^{57}e \\ {}^{58}e \end{bmatrix}$$

where each $A_{Total,}$ is the isotope abundance of each Fe isotope in the vegetal or soil sample. A_{LIH} indicates the isotope abundance in the tracer and $A_{Nat+Ch/Fe}{}^{3+}$ corresponds with the natural isotope abundance and includes the contribution of the Ch/Fe^{3+}. The same concept is applied for the molar fraction $x_{Nat+Ch/Fe}{}^{3+}$.

When the L/Fe^{3+} is prepared with ^{56}Fe and the iron synthetic chelates (Ch/Fe^{3+}) with ^{57}Fe, the mass balance is expressed as the following matrix notation:

$$\begin{bmatrix} {}^{54}A_{Total} \\ {}^{56}A_{Total} \\ {}^{57}A_{Total} \\ {}^{58}A_{Total} \end{bmatrix} = \begin{bmatrix} {}^{54}A_{Ch/Fe^{3+}} & {}^{54}A_{L/Fe^{3+}} & {}^{54}A_{Nat} \\ {}^{56}A_{Ch/Fe^{3+}} & {}^{56}A_{L/Fe^{3+}} & {}^{56}A_{Nat} \\ {}^{57}A_{Ch/Fe^{3+}} & {}^{57}A_{L/Fe^{3+}} & {}^{57}A_{Nat} \\ {}^{58}A_{Ch/Fe^{3+}} & {}^{58}A_{L/Fe^{3+}} & {}^{58}A_{Nat} \end{bmatrix} \times \begin{bmatrix} x_{Ch/Fe^{3+}} \\ x_{L/Fe^{3+}} \\ x_{Nat} \end{bmatrix} + \begin{bmatrix} {}^{54}e \\ {}^{56}e \\ {}^{57}e \\ {}^{58}e \end{bmatrix}$$

$A_{Ch/Fe}^{3+}$ and $A_{L/Fe}^{3+}$ are the corresponding isotope abundance in the tracer, and A_{Nat} is the natural isotope abundance. Moreover, $x_{Ch/Fe}^{3+}$, $x_{L/Fe}^{3+}$ and x_{Nat} denote the molar fractions of iron in the isotopically altered sample arising from the two or three different sources of the element (fertilizers or natural). The best values of x_{Nat}, $x_{L/Fe}^{3+}$ and $x_{Ch/Fe}^{3+}$ are found by least-squares fitting of the error vector *e* (minimizing the square sum of errors) using the SOLVER application in Excel®

Since the use of iron isotopes (^{57}Fe, ^{56}Fe) allow the evaluation of the distribution of L/Fe^{3+} ($L/^{56}Fe$ or $L/^{57}Fe$) in soybean plants and soil, the L/Fe^{3+} percentage was calculated, applying the following equation:

$$\%L/Fe^{3+} = \frac{L/Fe^{3+}\ (\mu mol\ pot^{-1})}{Total\ L/Fe^{3+}\ (\mu mol\ pot^{-1})} \times 100$$

where, the Total L/Fe^{3+} (µmol pot^{-1}) = L/Fe^{3+} in shoot (µmol pot^{-1}) + L/Fe^{3+} in root (µmol pot^{-1}) + L/Fe^{3+} in soil available fraction (µmol pot^{-1}) + L/Fe^{3+} in soil soluble fraction (µmol pot^{-1}).

Statistical analysis.

With the purpose of ensuring the assumptions for statistical analysis were fulfilled, the equality of variances and the normality of the data were tested. Differences between Fe treatments were tested for significance by one-way analysis of variance (ANOVA). Means were compared using the Duncan multiple range test ($P < 0.05$). All calculations were performed using SPSS software v. 24.0.

Results

Hydroponic assay

The aim of this hydroponic assay was to study the iron uptake by soybean plants in calcareous conditions using different L/Fe^{3+} : Ch/Fe^{3+} (10 µmol Fe pot^{-1}) ratios (0:10, 3:7, 5:5, 6:4, 7:3, 8:2, 9:1 and 10:0). Plants fertilized with ratios 0:10 and 10: 0 were considered as control plants (Ch/Fe^{3+} or L/Fe^{3+} respectively). Figure 1 summarizes the results obtained for the shoot and root dry weight (g pot^{-1}). In a short term (7 DAT), plants fertilized with the mixtures showed a slight synergic effect with respect to the control plants (L/Fe^{3+}) or HBED/Fe^{3+} but not with respect to *o,o*EDDHA/Fe^{3+} while in a long term (21 DAT) the synergic effect was relevant with respect to L/Fe^{3+} for both mixtures.

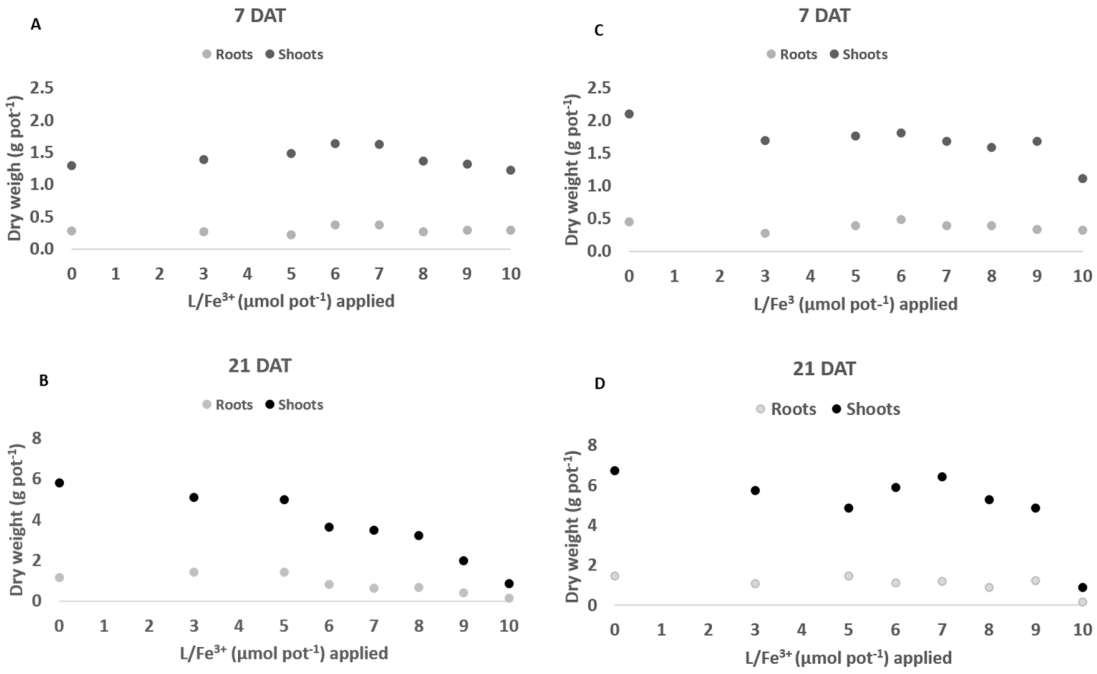

Figure 1: Dry weight (g pot^{-1}) of soybean shoot and root for the mixture L/Fe^{3+}+HBED/Fe^{3+} (A and B) and L/Fe^{3+}+o,oEDDHA/Fe^{3+} (C and D) at 7DAT (at the top) and at 21 DAT (at the bottom) for the hydroponic assay.

Figure 2 presents the Fe content (µmol pot^{-1}) in the soybean shoot at 7 and 21 DAT. The linear-plateau model was applied to evaluate the most efficient L/Fe^{3+}: Ch/Fe^{3+} ratio in providing iron to iron-deficient soybean plants. In the short term (7DAT) for the mix L/Fe^{3+}+HBED/Fe^{3+} the ratio obtained by the mathematical adjustment was 7:3 while for the

mix L/Fe^{3+}+ *o,o*EDDHA/Fe^{3+} the ratio was 6:4 so, the ratio most convenient would be 2 parts of L/Fe^{3+} and 1 part of Ch/Fe^{3+}. However, in the long term (21DAT) the ratios observed were close to 9:1 for both mixtures.

Soil pot experiments

Short-term experiment: different L/Fe^{3+}: Ch/Fe^{3+} ratios. This soil pot experiment aimed to study the contribution of L/$^{57}Fe^{3+}$ in iron soybean nutrition and determine what L/Fe^{3+}: Ch/Fe^{3+} ratio is the most efficient.

Dry weight (g pot^{-1}) at 13 DAT of soybean shoot and root fertilized with the mixes L/$^{57}Fe^{3+}$+HBED/$Fe^{3+}$and L/$^{57}Fe^{3+}$+ *o,o*EDDHA/Fe^{3+} is presented in Figure 3. Slight increments in plant biomass respect to the Ch/Fe^{3+} control plants were observed for plants treated with the mix L/$^{57}Fe^{3+}$+HBED/Fe^{3+} as the ratio increased and minimal differences between mix-ratios were observed for plants fertilized with the mix L/$^{57}Fe^{3+}$: *o,o*EDDHA/Fe^{3+}.

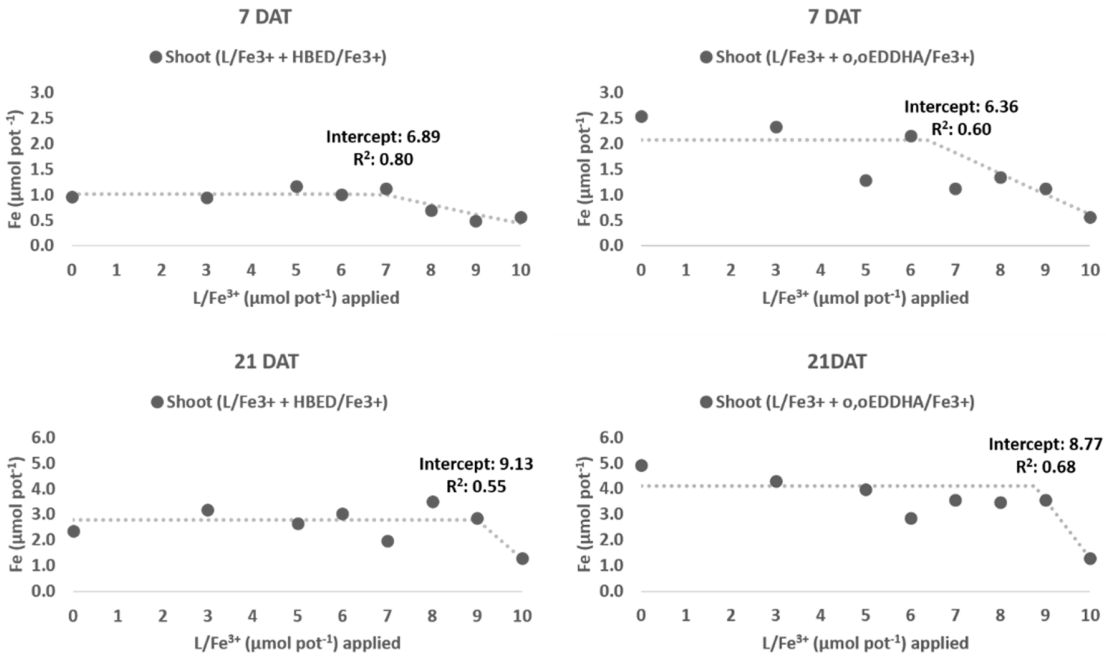

Figure 2: Total Fe content (µmol pot^{-1}) in soybean shoot for the mixture L/Fe^{3+}+HBED/Fe^{3+} or L/Fe^{3+}+o,oEDDHA/Fe^{3+} at 7 DAT (at the top) and 21 DAT (at the bottom) for the hydroponic assay. The dot lines correspond to the linear-plateau model.

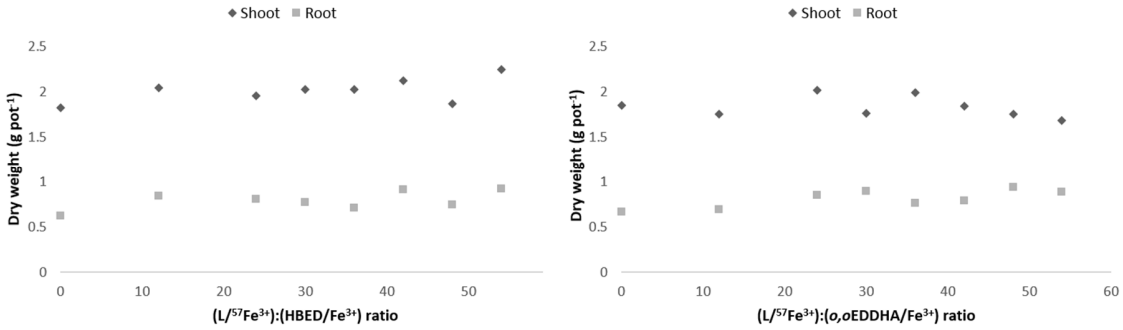

Figure 3: Dry weight (g pot^{-1}) of soybean shoot and root for the mixture L/$^{57}Fe^{3+}$+HBED/Fe^{3+} (A) or L/$^{57}Fe^{3+}$+ *o,o*EDDHA/Fe^{3+} (B) at 13 DAT for the short-term soil experiment.

In Figure 4, the $^{57}Fe^{3+}$ content (µmol pot^{-1}) in the shoot, root, soluble and available soil fraction were plotted for soybean plants treated with mixes L/$^{57}Fe^{3+}$+HBED/Fe^{3+} or L/$^{57}Fe^{3+}$+ *o,o*EDDHA/Fe^{3+} at 13 DAT. In general, for both mixes, the maximum L/$^{57}Fe^{3+}$ contribution to the $^{57}Fe^{3+}$ content in the shoot was between the ratio 30:24 and 42:12, almost the ratio 35:14 or in other words 2 parts of L/Fe^{3+} and 1 part of Ch/Fe^{3+}, according to the regression curves. The highest $^{57}Fe^{3+}$ content was observed in the shoot from plants fertilized with the mixture L/$^{57}Fe^{3+}$+ *o,o*EDDHA/Fe^{3+} (0.42 µmol pot^{-1}). Moreover, the $^{57}Fe^{3+}$ content in root increased as the L/Fe^{3+}: Ch/Fe^{3+} ratio was increased. Humic and iron accumulation were observed on the roots as well as iron crystalline deposits (jarosite) adsorbed on them, in a previous hydroponic assay (*Cieschi and Lucena*, 2018). For the soluble soil fraction, two maximums were also observed between the ratios 24:30 and 30:24. In this case, the mixture L/$^{57}Fe^{3+}$+HBED/Fe^{3+} presented the highest $^{57}Fe^{3+}$ content in the soluble soil fraction (0.22 µmol pot^{-1}).

The iron content in the available soil fraction presented a similar behavior to the iron content in the root which was previously observed in *Cieschi et al*., 2019. In general, iron complexes tend to remain available in the soil for plant requirements (*Colombo et al*., 2014).

Long-term experiment: different doses. In order to approach agronomical conditions, a long-term pot experiment (60DAT) was carried out. Taking into account the results obtained in the short term experiment, the ratio 2:1 (two parts of L/Fe^{3+} and one part of Ch/Fe^{3+}) was chosen and three (20:40, 30:60 and 45:90) doses (µmol Ch/$^{57}Fe^{3+}$ pot^{-1}: µmol L/$^{56}Fe^{3+}$ pot^{-1}) were prepared. To observe the L/Fe^{3+} and Ch/Fe^{3+} behaviors in the soil-plant system, HBED/Fe^{3+} and *o,o*EDDHA/Fe^{3+} were prepared with ^{57}Fe while L was labeled with ^{56}Fe (L/$^{56}Fe^{3+}$). In the figures, the letter H indicates the $^{57}Fe^{3+}$ content (µmol pot^{-1}) applied with HBED/$^{57}Fe^{3+}$, the letter E refers to the $^{57}Fe^{3+}$content added with *o,o*EDDHA/$^{57}Fe^{3+}$ and the letter L denotes the $^{56}Fe^{3+}$ content applied with L/$^{56}Fe^{3+}$.

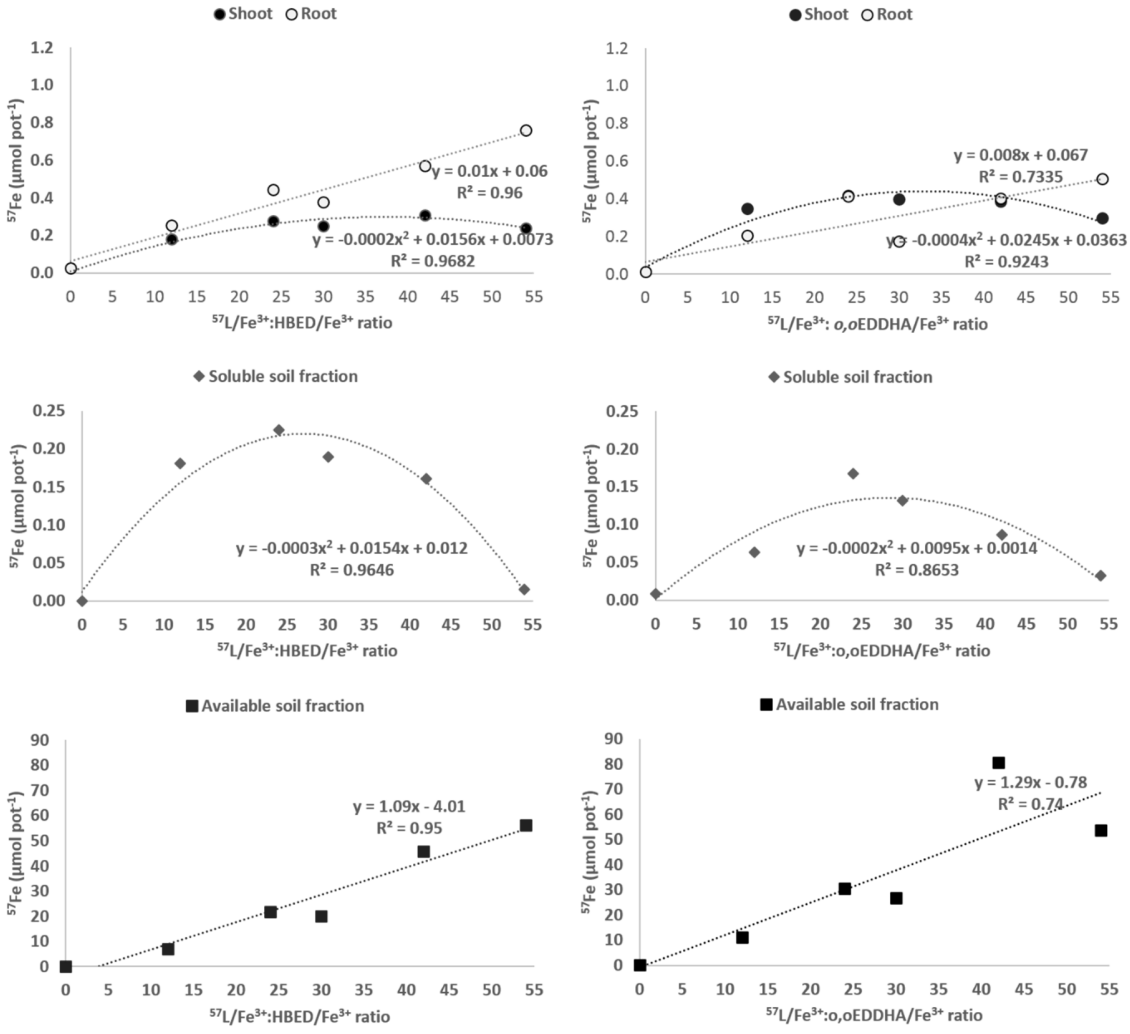

Figure 4: Iron content (µmol pot^{-1}) from L/$^{57}Fe^{3+}$ in shoot and root (top), soluble (center) and available soil fraction (bottom) for the mixture L/$^{57}Fe^{3+}$+HBED/Fe^{3+} (left) or L/$^{57}Fe^{3+}$+*o,o*EDDHA/Fe^{3+} (right), measured at 13 DAT for the short-term soil experiment. Trend lines for each mixture behavior were plotted.

In Table 1, the dry weight of soybean shoot at 7 DAT as well as the dry weight of soybean shoot and root at 60 DAT is exhibited. At short-term (7 DAT) significant differences were observed between the L40:H20 and the L90:H45 for the plants treated with the mix L/$^{56}Fe^{3+}$+HBED/$^{57}Fe^{3+}$ but no significant differences were observed with the control plants. However, at long-term (60 DAT) these differences disappeared, and both mixes presented similar behavior, regardless of the doses.

Table 1: Dry weight (g pot^{-1}) of shoot at 7 DAT and shoot and root at 60 DAT of soybean plants treated with the mixture L/$^{56}Fe^{3+}$ + HBED/$^{57}Fe^{3+}$ (L40:H20, L60:H30, L90:H45) or L/$^{56}Fe^{3+}$ + *o,o*EDDHA/$^{57}Fe^{3+}$ (L40:E20, L60:E30, L90:H45) for the second pot experiment.

	7 DAT	**60DAT**	
	Shoot (g pot^{-1})	**Shoot (g pot^{-1})**	**Root (g pot^{-1})**
Control	0.91±0.06^{ab}	4.75±0.21^{ns}	2.09±0.26^{ns}
L40:E20	0.94±0.10^{ab}	4.92±0.24	2.06±0.22
L60:E30	1.00±0.18^{ab}	5.02±0.13	2.23±0.07
L90:E45	0.83±0.18^{b}	4.86±0.27	1.88±0.23
L40:H20	1.05±0.07^{ab}	5.20±0.26	1.95±0.21
L60:H30	1.00±0.11^{ab}	4.82±0.27	2.46±0.10
L90:H45	0.86±0.09^{b}	5.03±0.18	2.34±0.44

For each series, different letters denote significant differences among treatments according to Duncan's Test ($p < 0.05$). ns: not significant

The iron content (µmol plant^{-1} or µmol pot^{-1}) from L/$^{56}Fe^{3+}$, Ch/$^{57}Fe^{3+}$ and Fe_{Nat} in the shoot at the first sampling (7 DAT) and the second sampling (60 DAT), root, soluble and available soil fraction was plotted in Figure 5 for soybean plants treated with mixes L/$^{56}Fe^{3+}$+HBED/$^{57}Fe^{3+}$ or L/$^{56}Fe^{3+}$+ *o,o*EDDHA/$^{57}Fe^{3+}$.

In general, the total iron content (L/$^{56}Fe^{3+}$+ Ch/$^{57}Fe^{3+}$ + Fe_{Nat}) in the shoot was much higher in plants treated with L/$^{56}Fe^{3+}$+ Ch/$^{57}Fe^{3+}$ respect to the control plants at 7 and 60 DAT. At 7 DAT the soybean shoot presented higher Fe^{3+} contents from the iron chelates than from other Fe^{3+} sources while at 60 DAT the main contribution to the Fe in the shoot was from the soil as an indicator of the kinetic of the Fe delivery processes from the three sources. Figure 6 shows the percentage contribution (%) in Fe uptake between 7 and 60 DAT for each treatment and dose. This contribution was calculated according to the following equation:

$$\Delta Fe\ uptake\ (\%) = \frac{Fe_{60DAT} - Fe_{7DAT}}{Fe_{60DAT}} \times 100$$

where Fe_{60DAT} is the Fe content (µmol plant^{-1}) at 60 DAT and Fe_{7DAT} is the Fe content (µmol plant^{-1}) at 7 DAT.

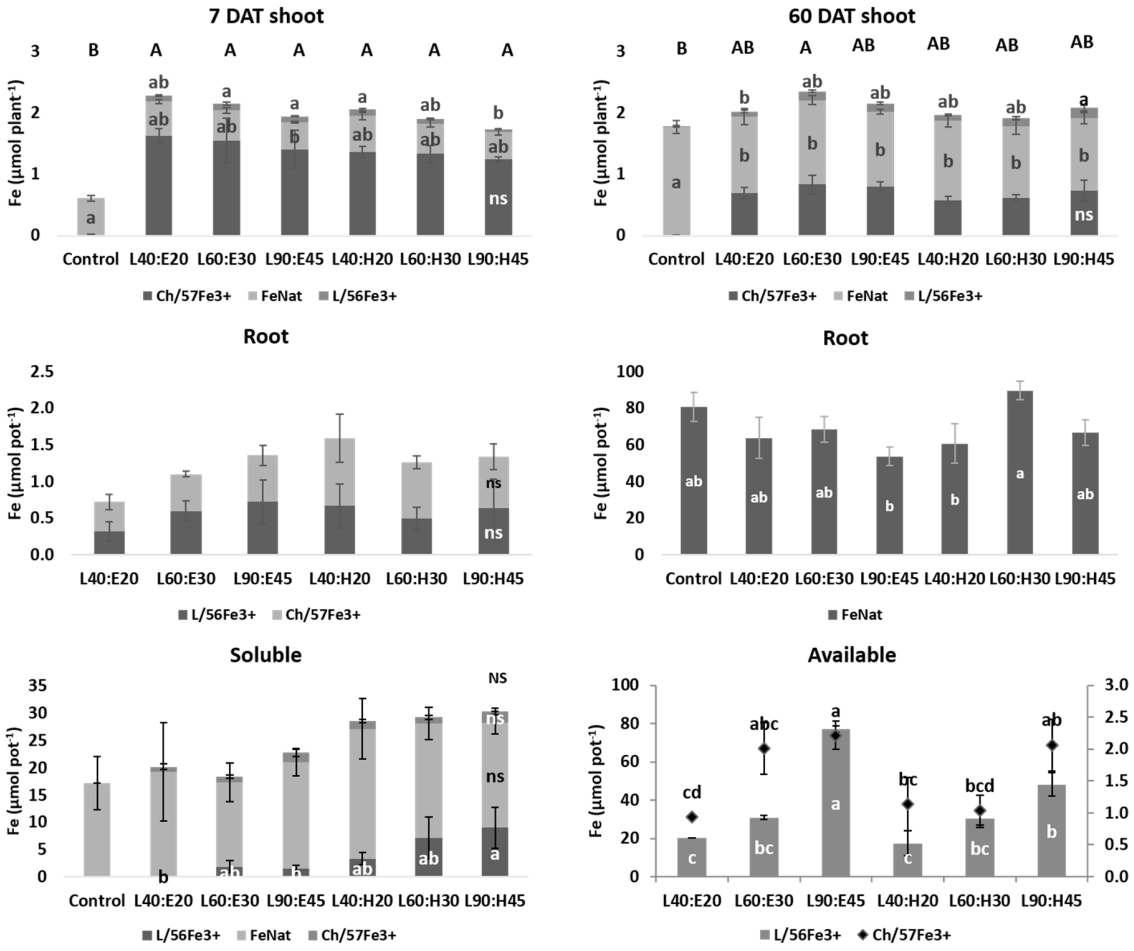

Figure 5: Fe content (µmol pot^{-1}) from the L/$^{56}Fe^{3+}$, Ch/$^{57}Fe^{3+}$ and natural sources (Fe_{Nat}) in soybean shoots, roots, soluble and available soil fraction of plants treated with the mixture L/$^{56}Fe^{3+}$+ HBED/$^{57}Fe^{3+}$ (L40:H20, L60:H30, L90:H45) or L/$^{56}Fe^{3+}$+ *o,o*EDDHA/$^{57}Fe^{3+}$ (L40:E20, L60:E30, L90:E45) at 60DAT for the second soil experiment: For each series, different letters denote significant differences among the treatments according to Duncan's Test ($p < 0.05$). Capital letters correspond to Fe_{Total} statistical results. ns: not significant.

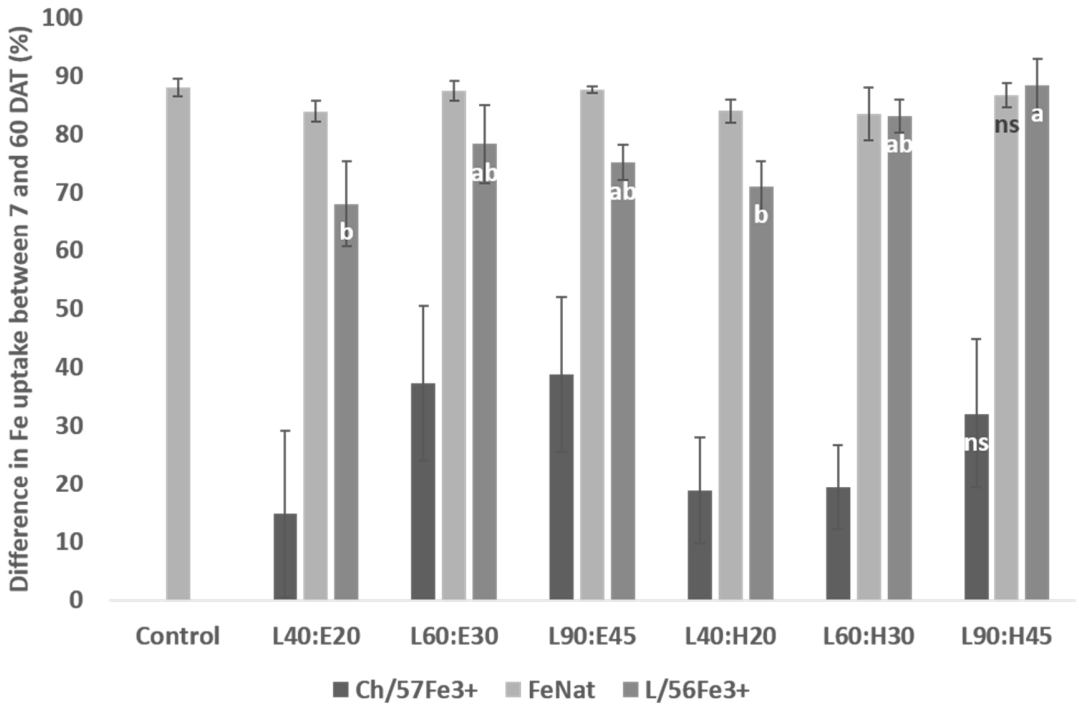

Figure 6: Contribution in Fe uptake (%) between 7 and 60 DAT in soybean shoot fraction of plants treated with the mixture L/$^{56}Fe^{3+}$+ HBED/$^{57}Fe^{3+}$ (L40:H20, L60:H30, L90:H45) or L/$^{56}Fe^{3+}$+ *o,o*EDDHA/$^{57}Fe^{3+}$ (L40:E20, L60:E30, L90:E45). For each series, different letters denote significant differences among the treatments according to Duncan's Test ($p < 0.05$). ns: not significant.

It was observed that plants took up Fe from the L/$^{56}Fe^{3+}$ in a higher percentage than the Ch/$^{57}Fe^{3+}$ and increasingly with the dose during the 7-60DAT period. These results are consistent with those obtained in previous soil experiments (*Cieschi et al.* 2019) since the iron synthetic chelate provides iron so fast and in a short time (15 days).

Concerning the root (Figure 5), the iron content increased with the doses when the mix L/$^{56}Fe^{3+}$+ *o,o*EDDHA/$^{57}Fe^{3+}$ was used, while for plants treated with L/$^{56}Fe^{3+}$+HBED/$^{57}Fe^{3+}$, the iron showed a decreasing tendency with increasing doses. However, no significant differences were observed among treatments or doses respect to the iron content from L/$^{56}Fe^{3+}$ or Ch/$^{57}Fe^{3+}$. The highest total Fe content (L/$^{56}Fe^{3+}$ + Ch/$^{57}Fe^{3+}$ + Fe_{Nat}) in the soluble soil fraction was observed for plants fertilized with the mixture L/$^{56}Fe^{3+}$+HBED/$^{57}Fe^{3+}$ as in the short-term experiment, and an increasing tendency of the

iron content from HBED/$^{57}Fe^{3+}$ with the dose was detected. For the available soil fraction, the Fe content from the L/$^{56}Fe^{3+}$ increased with the doses with for both mixes but the highest L/$^{56}Fe^{3+}$ content was for the pots treated with the mix L/$^{56}Fe^{3+}$+ *o,o* EDDHA/$^{57}Fe^{3+}$ (L90:E45).

Ligand competition of L/Fe^{3+} with the synthetic chelating agents *o,o*EDDHA and HBED

Two ligand competition experiments were carried out for 97 days at pH 7. Different solutions were prepared, as explained above, and visible spectra obtained every 2 or 3 days. Changes in absorbance were registered in the 350−650 nm wavelength range.

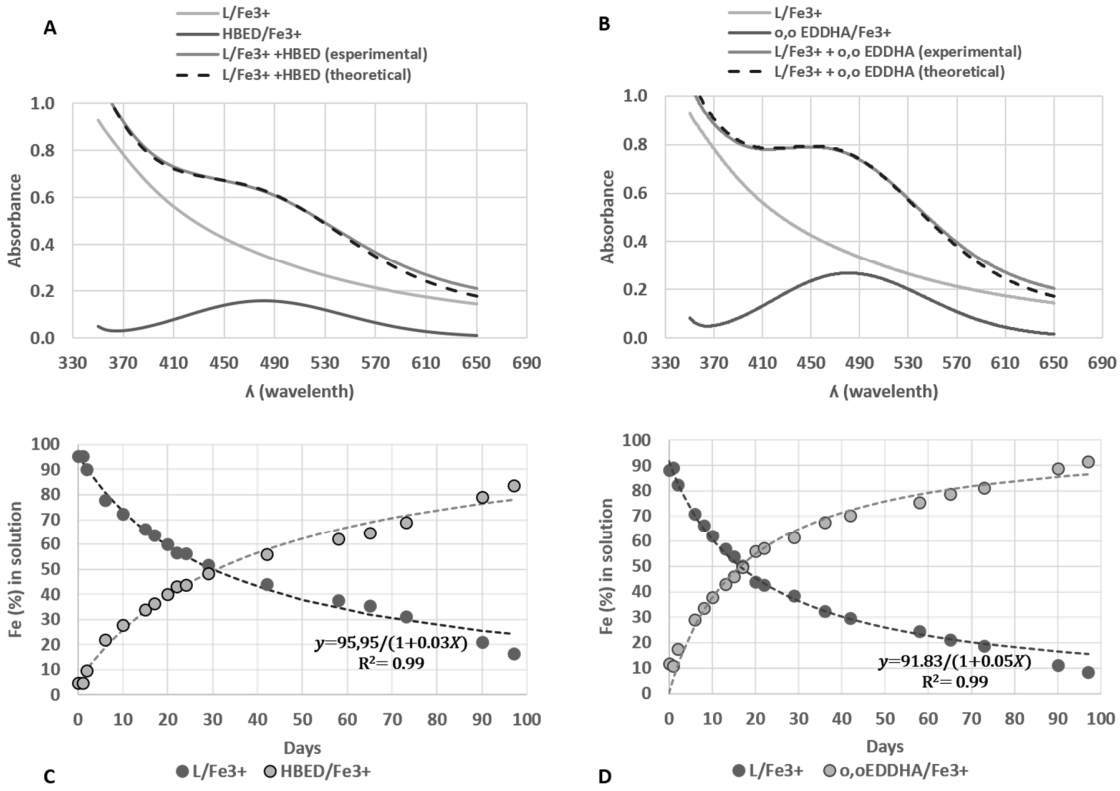

Figure 7: Example of mathematical deconvolution of the mixture L/Fe^{3+} + HBED (A) and the mixture L/Fe^{3+} + *o,o*EDDHA at 73 days of the experiment. Percentage of L/Fe^{3+} remaining in solution in the mixture with HBED (C) and with *o,o*EDDHA (D) during 97 days. Curve-fitting were plotted with dot lines.

Figure 7A and B show the mathematical deconvolution at day 73 of the experiment for the solutions L/Fe^{3+} + HBED and L/Fe^{3+} + o,oEDDHA, respectively, and the experimental

contributions of the different components individually. The curve-fittings were obtained by application of the formula for the kinetic second-order reaction:

$$[Fe] = \frac{[Fe]_{max}}{1 + [Fe]_{max} kt}$$

where $[Fe]_{max}$ is the maximum percentage of Fe in solution, k is the kinetic second-order constant and t is time (days). The best values of $[Fe]_{max}$ and k were found by least-squares fitting and minimizing the square sum of errors, using the SOLVER application in Excel®.

In this way, we studied indirectly the stability of L/Fe^{3+} and its kinetic capacity to retain Fe(III) in solution in the presence of different chelating agents. As the experiment progressed, o,oEDDHA or HBED chelated Fe(III) released by LIH. Figure 7C and D show the formation rate of o,oEDDHA/Fe^{3+} and HBED/Fe^{3+}, respectively. At 17 days, o,oEDDHA had chelated the 50% of Fe(III), while HBED chelated the same percentage at 30 days. Longer times were observed in previous work (*Cieschi et al*, 2017) when the ligand competition was carried out in mixtures of L/Fe^{3+}, o,oEDDHA + BPDS or L/Fe^{3+} + HBED + BPDS. In any case, the slow kinetic behavior of the L/Fe^{3+} was confirmed and the most stable chelate (HBED/Fe^{3+}, *log K*: 39.02 (López-Rayo et al, 2009)) was formed slower than o,oEDDHA/Fe^{3+}.

4.1.4 Discussion

Three bioassays (one hydroponic and two soil experiments) were carried out to test two mixtures prepared with L/Fe^{3+} and Ch/Fe^{3+} (*o,o* EDDHA/Fe^{3+} or HBED/Fe^{3+}) at different ratios and concentrations. For the soil experiments, L/Fe^{3+} and Ch/Fe^{3+} were labeled with stable iron isotopes (^{56}Fe or ^{57}Fe).

Concerning the dry weight, for the hydroponic bioassay, it decreased with the increment of the L/Fe^{3+}: Ch/Fe^{3+} ratio but it presented slight synergic effect respect to the control L/Fe^{3+} plants, mainly at 21 DAT (Figure 1). However, for the soil experiments, in the short-term, a slight improvement was observed respect to the control Ch/Fe^{3+} plants (Figure 3) while at long term no significant differences were observed (Table 1) for the control

plants in neither of both samplings (at 7 and 60DAT). Therefore, the presence of the iron chelates has improved the soybean growth in hydroponic and soil conditions at short term respect to the control L/Fe^{3+} plants but this beneficial improvement is negligible in the long term. According to *Stevenson* (1982), depending on the molecular size and solubility of HS fractions, the mobility of HS complexes with metals like Fe in the soil varies. The HS applied in these bioassays, L/Fe^{3+}, was properly characterized in previous work (*Cieschi and Lucena* 2018) and it was defined as a humic acid with a high molecular weight that may produce accumulation of humic acid on root and, thus, restriction in shoot and root growth. In that work, soybean plants were grown under hydroponic conditions with an iron humate concentration five times higher than the iron chelate and they obtained similar plant dry weight to the soybean plants fertilized with *o,o*EDDHA/Fe^{3+} at 60DAT. Likewise, in a recent work (*Cieschi et al*, 2019) soybean plants treated with different doses of three different nano-iron humates (35, 75 and 150 µmol ^{57}Fe pot^{-1}) did not present significant differences in biomass respect to the control plants (natural iron and *o,o*EDDHA/^{57}Fe 50 µmol pot^{-1}). In addition, it is important to consider that soybean is an optimal plant for studying iron chlorosis and iron plant metabolism in calcareous conditions (*Vasconcelos and Grusak,* 2014; *Vasconcelos et al.* 2014; *Santos et al.* 2015) but it presents a low growth response when leonardite is applied as an exogenously HS source *(Canellas and Olivares*, 2014; *Canellas et al*. 2015). Moreover, *Vallini et al.* (1993) have reported that the stimulatory effects of humic acid on biomass have dissipated with increments in humic acids concentration and have produced reductions in the laurel plant's growth. Also, *Muscolo and Sidari* (2009) have shown that the positive effects of HS on callus growth may depend on the relative content of specific classes of humic components. They have suggested that the biological effects of HS on plant metabolism are influenced by the origin, age, and decomposition processes of the parent organic material and are related to the chemical composition of HS.

Whit respect to the iron content in plants, for the hydroponic assay, it was observed synergic effect respect to the control plants that decreased with the increment of the L/Fe^{3+}: Ch/Fe^{3+} ratio (Figure 2). According to the results obtained for the plants fertilized with the

mix L/Fe^{3+}+HBED/Fe^{3+} the most efficient ratio was 7:3 while for the mix L/Fe^{3+}+ *o,o*EDDHA/Fe^{3+} the ratio was 6:4 so, in the short term, the ratio most convenient would be roughly 2 parts of L/Fe^{3+} and 1 part of Ch/Fe^{3+}. However, in the long term (21DAT) the ratios observed were close to 9:1 for both mixtures. This synergic effect may be explained by the shuttle effect since the iron uptake would be the result of the contribution of the Ch/Fe^{3+} and the labile Fe^{3+} remobilized from L/Fe^{3+} on the roots by the chelating agent that has previously released Fe^{3+}. Figure 8 presents a proposed shuttle model for the L/Fe^{3+}+ Ch/Fe^{3+} mixes for Strategy I plants in hydroponic conditions.

The proposed mechanism consist of the following reactions:

1) The iron chelates (Ch/Fe^{3+}) applied to the nutrient solution dissociates itself into Fe^{3+} and Ch. Thus, Fe^{3+} is reduced to Fe^{2+} by the iron chelate reductase (FRO2) with the plasma membrane of the root cells and then and finally Fe^{2+} is transported across the plasma membrane of root epidermal cells via the iron transporter IRT1, to the soybean plants (Jeong and Connolly, 2009).

2) The labile Fe^{3+} in the soluble L/Fe^{3+} is chelated by HBED or o,oEDDHA and carried it to the rhizosphere.

3) The Fe^{3+} bonded to the L/Fe^{3+} adsorbed on the soybean roots is chelated by HBED or o,oEDDHA and carried it to the rhizosphere.

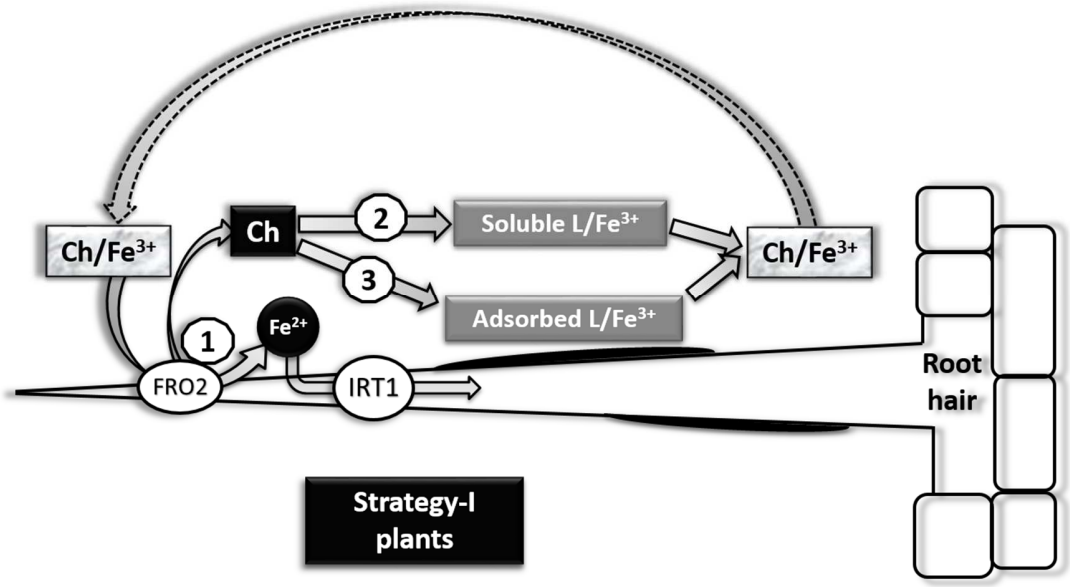

Figure 8: Schematic representation of the reactions of an iron chelate in hydroponic conditions**:** (1) Fe^{3+} and Ch (chelating agent) release;(2) Ch binds to soluble and labile Fe^{3+} from L (leonardite); (3) Ch binds to the Fe^{3+} adsorbed on the roots and complexed by L (ligand competition)

Then, this shuttle effect would be faster as the iron chelate content in the mixture increased. Moreover, the soluble L/Fe^{3+} in the solution and the adsorbed L/Fe^{3+} on the soybean surface provided iron to the plant but in lesser quantities than the iron chelates. The long term effect was confirmed once again since the soybean plants fertilized only with L/Fe^{3+} were affected by the multiple applications of L/Fe^{3+} and so the iron transport from root to shoot was decelerated. Similar results were observed in *Cieschi and Lucena*, 2018.

For the soil pot experiment at 13 DAT (Figure 4), the $^{57}Fe^{3+}$ content from the humate in the shoot was higher than in control L/$^{57}Fe^{3+}$ plants. Highest $^{57}Fe^{3+}$ content was observed between 30:24 and 42:12 L/$^{57}Fe^{3+}$: Ch/Fe^{3+} ratios. Figure 9 presents a proposed shuttle model for the L/Fe^{3+}+ Ch/Fe^{3+} mixes for Strategy I plants under calcareous soil conditions and it completes the hydroponic model with the following reactions:

1) The iron chelates (Ch/Fe^{3+}) applied to the nutrient solution dissociates itself into Fe^{3+} and Ch. Thus, Fe^{3+} is reduced to Fe^{2+} by the iron chelate reductase (FRO2) with the plasma membrane of the root cells and then and finally Fe^{2+} is transported across

the plasma membrane of root epidermal cells via the iron transporter IRT1, to the soybean plants (Jeong and Connolly, 2009).

2) The labile Fe^{3+} in the soluble L/Fe^{3+} is chelated by HBED or o,oEDDHA and carried it to the rhizosphere by diffusion.

3) The Fe^{3+} bonded to the L/Fe^{3+} adsorbed on the soybean roots is chelated by HBED or o,oEDDHA and carried it to the rhizosphere by diffusion.

The soil natural Fe^{3+} is in equilibrium with the available L/Fe^{3+} chelated by HBED or o,oEDDHA and carried it to the rhizosphere by diffusion.

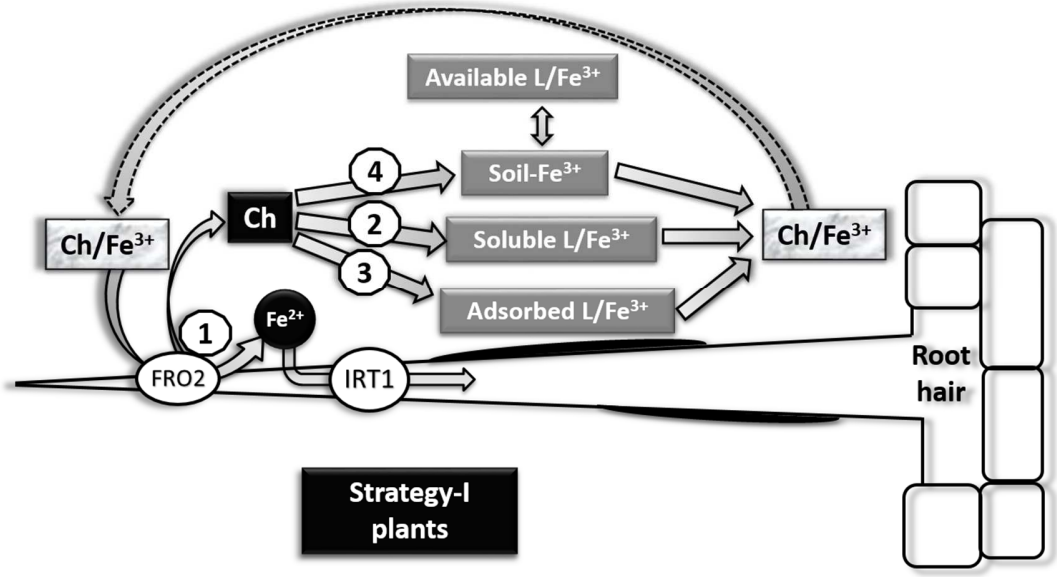

Figure 9: Schematic representation of the reactions of an iron chelate in calcareous soil conditions: (1) Fe^{3+} and Ch (chelating agent) release; (2) Ch binds to soluble and labile Fe^{3+} from L (leonardite); (3) Ch binds to the Fe^{3+} adsorbed on the roots and complexed by L (ligand competition); (4)Ch reacts with the solid phases and extract native Fe^{3+} from the soil that is in equilibrium with the available L/Fe^{3+}.

We must take into account for this model that L/Fe^{3+} is providing Fe^{3+} to the soybean plants but in lesser quantities than the iron chelates. For the soil experiment at 60 DAT and ratio L/$^{56}Fe^{3+}$: Ch/$^{57}Fe^{3+}$ 2:1 (Figure 5), the doses and the chelated agents used (HBED or o,oEDDHA) did not exert a significant influence into the results obtained. However, it is remarkable that at 7 DAT the soybean shoot mainly contained iron from the synthetic

chelates while at 60 DAT the natural iron is the main contributor to the shoot Fe. In spite of L/$^{56}Fe^{3+}$ contains the double Fe^{3+} amount than the synthetic chelates, shoot contains mainly Fe^{3+} from the synthetic iron chelate and Fe^{3+} from the soil but low quantities of Fe^{3+} from the iron humates after 60 DAT.

However, soybean plants took up iron increasingly and in a higher percentage from the iron humates than from the iron chelates between the samplings, meaning that L/Fe^{3+} provides iron slowly and progressively while the Ch/Fe^{3+} makes it fast and at once. Similar results were obtained by *Cieschi et al*., 2019.

The models here presented include the formation of the Ch/Fe^{3+} using Fe from L/Fe^{3+}. Ligand competition is a general method proposed by *Stevenson* (1982) and is applied to evaluate the stability of metal complexes when the calculation of relative constants by potentiometric and photometric methods is difficult to carry out due to the chemical nature of the metal complex. It has been also applied successfully for chelates (*Lucena and Chaney*, 2003). Figure 7 shows the competition results and they demonstrate that under controlled conditions (pH 7, ionic strength of 0.1 M and mixtures L/Fe^{3+}:Ch) after 97 days, *o,o*EDDHA chelated the 50% of Fe^{3+} present in the iron leonardite humate in 17 days while HBED chelated the same percentage in almost 30 days. It is foreseeable that under soil conditions the kinetic would be different than in solution. Then, we can identify an order of priority in iron uptake by the soybean plants may be related to a kinetic effect: 1) Fe^{3+} from the iron synthetic chelate, 2) Fe^{3+} from the soil and 3) Fe^{3+} from the HS. According to *Chen and Aviad* (1990) and *Varanini* and *Pinton* (1995), HS has selective actions on ion uptake, and the magnitude of their effect is related to the HS concentration, the individual plant species, and the soil composition and pH. Moreover, *Nardi et al.* (2017) and *Olaetxea et al.* (2018), propose the presence of a plant soil cross-talk through plants exudates and HS created by plants in the rhizosphere zone, in order to adapt and to survive to different environments.

With respect to the iron accumulation in soybean roots, *Abros'kin et al.* (2016) have reported a similar effect in wheat roots and they have attributed it to the predominant adsorption of iron humate on the surface of roots and the limited input of adsorbed iron into the vascular system of plants.

The mixes L/$^{57}Fe^{3+}$ + HBED/Fe^{3+} and L/$^{56}Fe^{3+}$ + HBED/$^{57}Fe^{3+}$ improved the presence of soluble L/Fe^{3+} in soil while the iron humate availability in soil increased with the dose when the mix L/$^{57}Fe^{3+}$+ *o,o*EDDHA/Fe^{3+} or the mix L/$^{56}Fe^{3+}$+ *o,o*EDDHA/$^{57}Fe^{3+}$ are applied (Figures 4 and 5) because the *o,o* EDDHA/Fe^{3+} is retained due to the meso *o,o*EDDHA/Fe^{3+} is adsorbed by the organic matter unlike the HBED/Fe^{3+}. According to *López-Rayo et al*. (2009), HBED/Fe^{3+} is able to maintain 90% of Fe in soil solution while almost 60% of Fe remains soluble with meso *o,o*EDDHA/Fe^{3+} and 90% with racemic *o,o* EDDHA/Fe^{3+} in a long time interaction with peat.

The purpose of mixing Ch/Fe^{3+} with L/Fe^{3+} was to improve the L/Fe^{3+} efficiency and in this way, favoring the iron mobilization from soybean root to shoot, avoiding the iron accumulation in roots. According to our research, the synergic effect between fertilizers is observed in hydroponic or soil because of the iron chelate shuttle effect when the ratio 2:1 iron humate: iron chelates for Strategy I plants.

Sánchez-Sánchez et al. (2006) has suggested a replacement of between 30% and 50% of the iron chelate with humic substances in order to improve Fe, P and Na nutrition while *Cerdán et al*. (2007) informed that a replacement of 67% of o,oEDDHA/Fe^{3+} by HS citrus fertilization has improved leaf P and leaf Fe as well as vitamin C content and peel thickness. Although more research is needed, we consider that the iron chelates dose can be only slightly reduced while the iron humate dose is double. Moreover, it should be advisable to test these mixtures with less sensitive crops to the iron chlorosis than soybeans to obtain results closer to agronomical situations.

4.1.5 Conclusions

Iron chelates and iron humates present different kinetic behavior in providing iron to the plants. According to our results, after few days the contribution of the chelates to the Fe nutrition decreases substantially, but the one from the humates is maintained. The mixtures can produce a synergic effect in iron uptake and improve in the shoot to root iron translocation due to a slow shuttle effect. Moreover, the application ratio should be two parts of iron humates and one part of iron chelate and the iron chelate used is HBED/Fe^{3+}

since it presents a lasting effect that fits better to the iron humate kinetics and so, it helps to make better use of the iron from the L/Fe^{3+}. Therefore, it would be possible to increase the soluble iron in the rhizosphere, avoiding the iron accumulation on roots, obtaining low costs and agricultural practices environmentally efficient.

4.1.6 References

Abadía, J., Vázquez, S., Rellán-Álvarez, R., El-Jendoubi, H., Abadía, A., Álvarez-Fernández, A., López-Millán, A. F. (2011): Towards a knowledge-based correction of iron chlorosis. *Plant Physiol. Biochem.* 49, 471–482.

Abros'kin, D. P., Fuentes, M., Garcia-Mina, J. M., Klyain, O. I., Senik, S. V., Volkov, D. S., Perminova, I. V., Kulikova, N. A. (2016): The effect of humic acids and their complexes with iron on the functional status of plants grown under iron deficiency. *Eurasian Soil Sci.* 49, 1099–1108.

Álvarez-Fernández, A., Pérez-Sanz, A., Lucena, J. J. (2001): Evaluation of effect of washing procedures on mineral analysis of orange and peach leaves sprayed with seaweed extracts enriched with iron. *Commun. Soil Sci. Plant Anal.* 32, 157–170.

Canellas, L. P., Olivares, F. L. (2014): Physiological responses to humic substances as plant growth promoter. *Chem. Biol. Technol. Agric.* 1, 3.

Canellas, L.P., Olivares, F.L., Aguiar, N.O., Jones, D.L., Nebbioso A., Mazzei, P., Piccolo, A. (2015): Humic and fulvic acids as biostimulants in horticulture. *Sci. Hort.* 196,15-27.

Cerdán, M., Sánchez-Sánchez, A., Juarez, M., Sánchez-Andreu, J. J., Jordá, J. D., Bermúdez, D. (2007): Partial replacement of Fe(*o,o*-EDDHA) by humic substances for Fe nutrition and fruit quality of citrus. *J. Plant Nutr. Soil Sci.* 170, 474-478.

Cesco, S., Römheld, V., Varanini, Z. and Pinton, R. (2000): Solubilization of iron by water-extractable humic substances. *J. Plant Nutr. Soil Sci.* 163, 285-290.

Chassapis, K., Roulia, M., Nika, G. (2010): Fe(III)–humate complexes from Megalopolis peaty lignite: A novel eco-friendly fertilizer. *Fuel* 89, 1480–1484.

Chen, Y. and Aviad, T. (1990)*:* Effects of humic substances on plant growth in Mac Carthy, P., Clapp, C. E., Malcolm, R. L., Bloom, P. R. (eds.): Humic Substances in Soil and Crop Science: Selected Readings. ASA, SSSA, Madison, FL, USA, pp. 161–186.

Cieschi, M. T., Benedicto, A., Hernández-Apaolaza, L., Lucena, J. J. (2016): EDTA Shuttle effect vs lignosulfonate direct effect providding Zn to navy bean plants (*Phaseolus vulgaris* L 'Negro polo') in a calcareous soil. *Front. Plant Sci.* 1767, 1-12.

Cieschi, M. T., Caballero-Molada, M., Menéndez, N., Naranjo, M. A., Lucena, J. J. (2017): Long-term effect of a leonardite iron humate improving Fe nutrition as revealed in silico, in vivo, and in field experiments. *J. Agric. Food Chem.* 65, 6554–6563.

Cieschi, M.T. and Lucena, J.J. (2018): Iron and humic acid accumulation in soybean roots fertilized with leonardite iron humates under calcareous conditions. *J. Agric. Food Chem.* 66, 13386-13396.

Cieschi, M. T., Polyakov, A. Y., Lebedev, V. A.., Volkov, D. S,, Pankratov, D. A., Veligzhanin, A. A.,. Perminova, I. V., Lucena, J. J. (2019): Eco-friendly iron-humic nanofertilizers synthesis for the prevention of iron chlorosis in soybean (*Glycine max*) grown in calcareous soil. *Front. Plant Sci.* 10, 1-17.

Colombo, C., Palumbo, G., He, J., Pinton, R., Cesco, S. (2014): Review on iron availability in soil: interaction of Fe minerals, plants, and microbes. *J. Soils Sediments.* 14: 538-548.

Gárate, A., Carpena Ruiz, R. O., Ramón, A. M. (1984): Influence of boron on manganese and other nutrients in juices of vascular tissues. *An. Edafol. Agrobiol.* 43.

Hernández-Apaolaza, L. and Lucena, J. J. (2011): Influence of the soil/solution ratio, interaction time, and extractant on the evaluation of iron sorption/desorption by soils. *J. Agric. Food Chem.* 59, 2493-2500.

Jeong, J. and Connolly, E. L. (2009): Iron uptake mechanisms in plants: Functions of the FRO family of ferric reductases. *Plant Sci*. 176, 709-714.

Kołodziej, B., Sugier, D., Bielińska, E. (2013): The effect of leonardite application and various plantation modalities on yielding and quality of roseroot (*Rhodiola rosea* L.) and soil enzymatic activity. *J. Geochemical Explor.* 129, 64–69.

Lindsay, W. L. and Schwab, A. P. (1982). The chemistry of iron in soils and its availability to plants. *J. Plant Nutr.* 5, 821–840.

López-Rayo, S., Hernández, D., Lucena, J. J. (2009): Chemical Evaluation of HBED/Fe^{3+} and the novel HJB/Fe^{3+} chelates as fertilizers to alleviate iron chlorosis. *J. Agric. Food Chem.* 57, 8504–8513.

Lucena, J.J. (2003): Fe chelates for remediation of Fe chlorosis in strategy I plants. *J. Plant Nutr.* 26, 1969–1984.

Lucena, J. J.; Chaney, R. L. (2006): Synthetic iron chelates as substrates of root ferric chelate reductase in green stressed cucumber plants. *J. Plant Nutr.* 29, 423−439.

Monreal, C., DeRosa, M., Mallubhotla, S., Bindraban, P., Dimpka, C. (2016): Nanotechnologies for increasing the crop use efficiency of fertilizer-micronutrients. *Biol. Fertil. Soils* 52, 423-437

Muscolo, A., Sidari, M. (2009): Carboxyl and phenolic humic fractions affect callus growth and metabolism. *Soil Sci. Soc. Am. J.* 73, 1119.

Nardi, S., Pizzeghello, D. (2002): Physiological effects of humic substances on higher plants. *Soil Biol. Biochem.* 34, 1527–1536.

Nardi, S, Ertani, A, Francioso, O. (2017): Soil-root cross-talking: the role of humic substances. *J. Plant Nutr. Soil Sci.* 180, 5-13.

Olaetxea, M., De Hitaa, D., Andrés Garcia, C., Fuentes, M., Baigorri, R., Mora, V., Garnica, M., Urrutia, O. , Erro, J., Zamarreño, A., Berbara, R. L., Garcia-Mina, J. M. (2018): Hypothetical framework integrating the main mechanisms involved in the promoting action of rhizospheric humic substances on plant root- and shootgrowth. *Appl. Soil Ecol.* 123, 521-537.

Rodríguez-Castrillón, J. Á., Moldovan, M., García Alonso, J. I., Lucena, J. J., García-Tomé, M. L., Hernández-Apaolaza, L. (2008): Isotope pattern deconvolution as a tool to study iron metabolism in plants. *Anal. Bioanal. Chem.* 390, 579–590.

Sánchez-Sánchez, a, Sánchez-Andreu, J., Juárez, M., Jordá, J., Bermúdez, D. (2002): Humic substances and amino acids improve effectiveness of chelate FeEDDHA in lemon trees. *J. Plant Nutr.* 25, 2433–2442.

Santos, C.S., Roriz, M., Carvalho, S.M.P., Vasconcelos, M.W. (2015): Iron partitioning at an early growth stage impacts iron deficiency responses in soybean plants (*Glycine max*. L.). *Front. Plant*

Sci. 6, 1-12.

Schenkeveld, W., Reichwein, A., Temminghoff, E., van Riemsdijk, W. (2014): Considerations on the shuttle mechanism of FeEDDHA chelates at the soil-root interface in case of Fe deficiency. *Plant Soil.* 379, 373-387.

Senesi, N., Griffith, S. M., Schnitzer, M, Townsend, M. G. (1977): Binding of Fe^{3+} by humic materials. *Geochim. Cosmochim. Acta.* 41, 969-976.

Shenker, M., Chen, Y. (2005): Increasing iron availability to crops: Fertilizers, organo-fertilizers, and biological approaches. *Soil Sci. Plant Nutr.* 51, 1–17.

Soltanpour, P. N., Schwab, A. P. (1977): A new soil test for simultaneous extraction of macro- and micro-nutrients in alkaline soils. *Commun. Soil Sci. Plant Anal.* 8, 195–207.

Stevenson, F. J. (1982): Humus chemistry: Genesis, composition, reactions, First edit. ed, A Willey Interscience Publication, John Willey & Sons, Inc. A Willey Interscience Publication, New York, USA.

Tagliavini, M., Rombolà, A. D. (2001): Iron deficiency and chlorosis in orchard and vineyard ecosystems. *Eur. J. Agron.* 15, 71–92.

Trevisan, S., Francioso, O., Quaggiotti, S., Nardi, S. (2010): Humic substances biological activity at the plant-soil interface: from environmental aspects to molecular factors. *Plant Signal. Behav.* 5, 635–43.

Vaccaro, S., Ertani, A., Nebbioso, A., Muscolo, A., Quaggiotti, S., Piccolo, A., Nardi, S. (2015): Humic substances stimulate maize nitrogen assimilation and amino acid metabolism at physiological and molecular level. *Chem. Biol. Technol. Agric.* 2, 5.

Varanini, Z., Pinton, R. (1995): Humic substances and plant nutrition, in Lüttge, U. (ed.): Progress in Botany, Vol. 56., Springer, Berlin, Germany, pp. 97–117.

Vasconcelos, M.W. and Grusak, M.A. (2014): Morpho-physiological parameters affecting iron deficiency chlorosis in soybean (*Glycine max*. L.) *Plant Soil* 374, 161-172.

Vasconcelos, M.W., Clemente, T.E., Grusak, M.A. (2014): Evaluation of constitutive iron reductase (AtFRO2) expression on mineral accumulation and distribution in soybean (*Glycine max*.L.). *Front. Plant Sci.* 5, 1-12.

Vallini, G., Pera, A., Avio, L., Valdrighi, M., Giovannetti, M. (1993): Influence of humic acids on laurel growth, associated rhizospheric microorganisms, and mycorrhizal fungi. *Biol. Fertil. Soils* 16, 1–4.

IV.2 Eco-friendly iron-humic nanofertilizers synthesis for the prevention of iron chlorosis in soybean (*Glycine* max) grown in calcareous soil

frontiers in Plant Science

ORIGINAL RESEARCH
published: 05 April 2019
doi: 10.3389/fpls.2019.00413

Eco-Friendly Iron-Humic Nanofertilizers Synthesis for the Prevention of Iron Chlorosis in Soybean (*Glycine max*) Grown in Calcareous Soil

María T. Cieschi[1], Alexander Yu Polyakov[2,3], Vasily A. Lebedev[4], Dmitry S. Volkov[4,5], Denis A. Pankratov[4], Alexey A. Veligzhanin[6], Irina V. Perminova[4] and Juan J. Lucena[1]**

[1] Department of Agricultural Chemistry and Food Science, Autonomous University of Madrid, Madrid, Spain, [2] Kurnakov Institute of General and Inorganic Chemistry, Russian Academy of Sciences, Moscow, Russia, [3] Department of Materials Science, Lomonosov Moscow State University, Moscow, Russia, [4] Department of Chemistry, Lomonosov Moscow State University, Moscow, Russia, [5] Department of Chemistry and Physical Chemistry of Soils, V.V. Dokuchaev Soil Science Institute, Moscow, Russia, [6] National Research Center "Kurchatov Institute", Moscow, Russia

OPEN ACCESS

Edited by:
Thomas J. Buckhout, Humboldt-Universität zu Berlin, Germany

Reviewed by:
Roberto Pinton, University of Udine, Italy
Zeno Varanini, University of Verona, Italy

***Correspondence:**
Irina V. Perminova
iperm@org.chem.msu.ru
Juan J. Lucena
juanjose.lucena@uam.es

Specialty section:
This article was submitted to Plant Nutrition, a section of the journal Frontiers in Plant Science

Received: *14 January 2019*
Accepted: *19 March 2019*
Published: *05 April 2019*

Citation:
Cieschi MT, Polyakov AY, Lebedev VA, Volkov DS, Pankratov DA, Veligzhanin AA, Perminova IV and Lucena JJ (2019) Eco-Friendly Iron-Humic Nanofertilizers Synthesis for the Prevention of Iron Chlorosis in Soybean (Glycine max) Grown in Calcareous Soil. Front. Plant Sci. 10:413. doi: 10.3389/fpls.2019.00413

Iron deficiency is a frequent problem for many crops, particularly in calcareous soils and iron humates are commonly applied in the Mediterranean basin in spite of their lesser efficiency than iron synthetic chelates. Development and application of new fertilizers using nanotechnology are one of the potentially effective options of enhancing the iron humates, according to the sustainable agriculture. Particle size, pH, and kinetics constrain the iron humate efficiency. Thus, it is relevant to understand the iron humate mechanism in the plant–soil system linking their particle size, characterization and iron distribution in plant and soil using ^{57}Fe as a tracer tool. Three hybrid nanomaterials (F, S, and M) were synthesized as iron-humic nanofertilizers (^{57}Fe-NFs) from leonardite potassium humate and ^{57}Fe used in the form of $^{57}Fe(NO_3)_3$ or $^{57}Fe_2(SO_4)_3$. They were characterized using Mössbauer spectroscopy, X-ray diffraction (XRD), extended X-ray absorption fine structure spectroscopy (EXAFS), transmission electron microscopy (TEM) and tested for iron availability in a calcareous soil pot experiment carried out under growth chamber conditions. Three doses (35, 75, and 150 μmol pot^{-1}) of each iron-humic material were applied to soybean iron deficient plants and their iron nutrition contributions were compared to ^{57}FeEDDHA and leonardite potassium humate as control treatments. Ferrihydrite was detected as the main structure of all three ^{57}Fe-NFs and the plants tested with iron-humic compounds exhibited continuous long-term statistically reproducible iron uptake and showed high shoot fresh weight. Moreover, the ^{57}Fe from the humic nanofertilizers remained available in soil and was detected in soybean pods. The Fe-NFs offers a natural, low cost and environmental option to the traditional iron fertilization in calcareous soils.

Keywords: iron nanoparticles, iron nutrition, humic substances, leonardite, ^{57}Fe, soybean, ferrihydrite

INTRODUCTION

Iron (Fe) is an essential micronutrient for humans and plants. Iron deficiency is very common in the human diet and affects an estimated two billion people in the world (Briat et al., 2015). Iron chlorosis is a widespread agricultural problem occurring in about 30–50% of cultivated soils (Cakmak, 2002) and one of the major limiting factor of crop production in calcareous soils. Farmers apply iron synthetic chelates to alleviate iron deficiency in cash crops. Despite the high costs of these fertilizers, they tend to lixiviate and the chelating agents may avoid the precipitation and enhance mobilization of heavy metals (Ylivainio, 2010). Many crops are sensitive to the iron chlorosis, such as citrus and fruit trees but soybean (*Glycine max* L.) is one of the most studied iron Strategy I plant (Fuentes et al., 2018). Moreover, soybean production reaches levels of about 230 million metric tons per year across the world (Vasconcelos and Grusak, 2014) and this legume is a highly nutritious crop which contains more protein (40%) and oil (20%) than any other ordinary food source (Bolon et al., 2010).

According to the United Nations [UN] (2013), the rapidly growing world population is projected to reach 9.6 billion by the year 2050 and Food and Agriculture Organization of the United Nations [FAO] (2017) has predicted that the global grain production is required to increase by 70% to meet these demands. Therefore, new approaches should be developed for alleviation of iron deficiency in plants and new ecofriendly fertilizers are needed in order to enhance crop environmental quality. Iron fertilizers based on HSs extracted from lignites, such as leonardite, are used in the Mediterranean area (as liquid concentrates) in drip irrigation (Kovács et al., 2013). This kind of iron fertilizers is more ecofriendly than synthetic iron chelates but they are less efficient in correcting iron chlorosis. Moreover, field experiments have demonstrated that the synthetic chelate has a fast effect while the iron humate fertilizers provide increasing iron availability in the root–soil interface resulting in slow uptake of Fe by the plants (Cieschi et al., 2017). Kulikova et al. (2017) have demonstrated that only iron from very small and amorphous nanoparticles of ferric polymers incorporated into humic matrix is readily taken up by plants. Therefore, the synthesis of iron humates should be optimized for developing efficient NFs.

According to Naderi and Danesh-Shahraki (2013), NFs are the most important products of nanotechnology with regard to agriculture. Nanosized active ingredients (from 1 to 100 nm in diameter) have a large specific surface area that can result in significantly enhanced reactivity, and this feature increases absorption of nutritional elements and essential compounds for plant growth and plant metabolism (Janmohammadi et al., 2016). Many attempts has been made to prepare inorganic Fe nanofertilizers. As example Sánchez-Alcalá et al. (2012) synthesized nanosiderite ($FeCO_3$) and demonstrated that it was highly effective in preventing iron chlorosis in chickpea and had a great residual effect. Ghafariyan et al. (2013) reported that low concentrations of superparamagnetic Fe-NPs significantly increased the chlorophyll contents in sub-apical leaves of soybeans in a greenhouse test under hydroponic conditions, suggesting that soybean could use this type of Fe-NPs as source of Fe and reduce chlorotic symptoms of Fe deficiency. However, the research on natural Fe nano-humate complexes is now in progress. Dholakia (2016) developed the preparation of nanoparticulate liquid organic fertilizers employing humic acids. In addition, Kulikova et al. (2017) have synthesized well-defined iron (hydr)oxide NPs of feroxyhyte stabilized by traces of HS (a model of iron-based engineered NPs) and water-soluble Fe-HS complexes of the proven high availability to plants tested their iron materials in wheat plants under hydroponic conditions. These promising results motivated us to follow the research on Fe NFs stabilized with humates.

According to Dimkpa and Bindraban (2017), up to now, the bulk of research in plant nanoscience either consists of experiments conducted in artificial media, such as nutrient solutions, agar, sand, or other non-soil media. Moreover, Liu and Lal (2015) recommend that micronutrient research should focus on enhancing the bioavailability (plant-uptake rate) of NFs to address the field leaching associated with the conventional micronutrient fertilizers and compare the beneficial effects of these micronutrient NFs with commercially available micronutrient counterparts [e.g., FeNPs vs. $FeCl_3$ or Fe(EDTA) as Fe sources] under the field condition. Therefore, it is of particular importance to test the ^{57}Fe-NFs in a soil system in a long-term experiment which would enable for completion of the full growth cycle crop in order to be closer to agronomical conditions. Since the efficacy of an iron fertilizer is related to the iron that the plants can take from the fertilizer, the use of iron isotopes is highly beneficial for monitoring iron uptake by plants (Cesco et al., 2002; Nikolic et al., 2003; Tomasi et al., 2013). The use of stable Fe isotopes instead of radioactive ones gives a high flexibility in the experimental designs and can include field studies, because special safety measurements and trained staff are not required. Moreover, long-term assays can be carried out without taking care of radioactivity decay over time. In addition, the generation of radioactive wastes is avoided (Benedicto et al., 2011). Many studies about ^{57}Fe application in soils experiments (Nadal et al., 2012; Martín-Fernández et al., 2017a,b) were reported, but this work is the first one in preparing ^{57}Fe-NFs and applying them in a calcareous soil.

Here, three ^{57}Fe-labeled humic nanomaterials (F, S, and M) were synthesized using potassium humate as a parent humic material and ^{57}Fe in the form of $^{57}Fe(NO_3)_3$ (product F) and $^{57}Fe_2(SO_4)_3$ (products S and M), characterized for iron speciation and phase composition of nanoparticles, and tested

Abbreviations: ^{57}Fe-NFs, iron-humic nanofertilizers isotopically labeled; ANOVA, analysis of variance; DAF, days after fertilizers applications; DTPA, diethylenetriaminepentaacetic acid; E.C., electrical conductivity; ED, electron diffraction; EELS, electron energy loss spectra; EXAFS, extended X-ray absorption fine structure spectroscopy; Fe-MCC, iron-maximum complexing capacity; Fe-Nps, iron nanoparticles; FeHBED, iron (III) *N*,*N*'-bis(*o*-hydroxybenzyl)-ethylenediamine-*N*,*N*'-diacetic acid complex; HEPES, *N*-(2-hydroxyethyl) piperazine *N*'-(2-ethanesulfonic acid); HS, humic substances; ICP-OES, inductively coupled plasma – optical emission spectrometry; ICP-MS, inductively coupled plasma mass spectrometry; L, leonardite potassium humate; NFs, nanofertilizers; *o*-*o*EDDHA, ethylenediamine-di (*o*-*o* hydroxyphenylacetic acid); OM, soil organic matter; SAED, selected area electron diffraction; SPAD, soil–plant analysis development; TEM, transmission electron microscopy; XANES, X-ray absorption near edge structure; XAS, X-ray absorption spectra; XRD, X-ray diffraction.

for bioavailability to soybean iron deficient plants grown in calcareous soils under growth chamber conditions. This was to establish a link between the Fe-NPs characteristics and their behavior in the soil–plant system using ^{57}Fe as a tracer tool.

MATERIALS AND METHODS

Reagents

All reagents used were of recognized analytical grade, and solutions were prepared with type-I grade water (ISO 3696:1987, 1987) free of organic contaminants (Millipore, Milford, CT, United States).

Synthesis of ^{57}Fe-NFs

Prior to the synthesis, a known weight of leonardite potassium humate (C 34.9%, H 3.89%, N 0.72%, S 0.06%, Fe 0.45%) (Powhumus, Humintech Ltd., Germany) was dissolved in distilled water and centrifuged at 10,000 min^{-1} for 10 min to separate and discard any insoluble mineral components. The obtained solution contained 70 g L^{-1} of leonardite potassium humate (L solution) and was used for the further NF synthesis.

A $^{57}Fe_2(SO_4)_3$ solution (0.20 M in ^{57}Fe) was prepared from metallic ^{57}Fe (Isoflex, 96.28% ^{57}Fe isotopic enrichment) by dissolving 0.4008 g in 34 mL 1M H_2SO_4 and heating till complete dissolution. After that, two products (S and M) were obtained by interaction of potassium humate with $^{57}Fe_2(SO_4)_3$ solution. In brief, the product S was synthesized as in Sorkina et al. (2014), 17 mL of 0.2M $^{57}Fe_2(SO_4)_3$ solution was added dropwise to 14.3 mL of the L solution and pH was maintained at a value of 10 by adding slowly 1M KOH when needed. For the synthesis of the product M, 17 mL of $^{57}Fe_2(SO_4)_3$ solution was slowly added to 40 mL of L solution, maintaining the pH at 9 with 1M KOH. The product M was prepared with the 90% of its maximum complexing capacity (Fe-MCC). Determination of Fe-MCC was conducted as described in Villén et al. (2007) and presented in the **Supplementary Figure SM1**. According to the obtained titration curve, an amount of 190 mg of Fe (III) per g org C^{-1} was necessary to obtain 200 mg of complexed Fe (III) per g org C^{-1} at the MCC.

Similarly, for the preparation of F product, a $^{57}Fe(NO_3)_3$ solution was prepared from the same metallic ^{57}Fe by dissolving 0.2004 g in 5 mL HNO_3 (70%, 1,401 g/mL density) and then diluted. The obtained solution was added dropwise to 32 mL of the L solution, maintaining the pH at 9 with 1M KOH.

In all syntheses described above, the final reaction mixtures were frozen "as is" using liquid N_2 and freeze-dried using Labconco FreeZone freeze dry system (-50°C, 0.03 mbar pressure).

It should be noted, that the high hydrolysis rate is required to obtain ultradispersed (nanosized) iron (hydr)oxide nanoparticles from iron (III) sulfate or nitrate solutions. For this, we added $^{57}Fe_2(SO_4)_3$ and $^{57}Fe(NO_3)_3$ dropwise but rapidly to the strongly alkaline medium of potassium humate solution and prevented the pH drop by simultaneous addition of KOH. The pH values between 9 and 10 were chosen to ensure formation of the disordered and chemically labile iron oxy-hydroxide phases instead of well-crystalline iron oxides like Fe_3O_4, Fe_2O_3 or rigid α-FeOOH.

The content of soluble iron in the synthesized fertilizers was determined using ICP AES. It was (in % mass) 2.9, 2.3, and 2.1 in the samples F, S, and M, respectively. The Fe:org C ratios were 0.27, 0.52, and 0.12 (g Fe g C org^{-1}) in the samples F, S, and M, respectively.

Characterization of ^{57}Fe-NFs

The freeze dried preparations of ^{57}Fe-NFs were exhaustively characterized using XRD, TEM with ED, EELS and energy filtered transmission electron microscopy (EFTEM), X-ray absorption spectroscopy (XANES and EXAFS) and Mössbauer spectroscopy. The XRD patterns were collected at CuKα on Rigaku D-MAX 2500 diffractometer in Theta/2Theta geometry. Reference samples, such as ferrihydrite and goethite were synthesized according to the procedure proposed by Schwertmann and Cornell (1992) and described by López-Rayo et al. (2015).

The TEM data were obtained with the use of Zeiss Libra 200MC microscope, equipped with monochromator and Omega-filter. For the TEM measurements, samples were dissolved in distilled water, dropped on the lacey-carbon coated copper grid for the few minutes with the following removal of the solution excess to reduce the concentration of mineral salts in the sample. Details of energy filtered TEM and SAED acquisition and processing are described in the corresponding part and in **Supplementary Materials**. Image processing was performed with the use of Gwyddion (Nečas and Klapetek, 2012), further data treatment – with the use of *scipy* and *matplotlib* (Hunter, 2007). The EELS spectra were acquired using the omega-filter, and integrated with DigitalMicrograph2 (DM2) software, Gatan. The variable slit of 3.5 eV width was placed in the Omega-filter to select the elastic part of scattered electrons. Two EFTEM images were collected with the background signal differing in intensity in the pre-edge energy area, and one image – with the combined signals of iron and background – was collected on the Fe M-line. Final iron distribution map was calculated using the DM2 software.

X-ray absorption spectra were measured at the STM beamline of Kurchatov Synchrotron Source facility, National Research Center "Kurchatov Institute", Moscow, Russia. The Si (111) channel-cut monochromator was used. Ionization chambers with length of 10 cm filled with argon were used as detectors of incidence and transmitted beams. The samples were used as dry powders mounted onto the kapton tape. Thickness of each sample was adjusted to yield the absorption value of 3. All spectra for the iron-containing NFs under study and the iron (hydr)oxide references were measured by absorption using Fe foil as a reference sample. XAS of the parent humate (L) was measured using fluorescence due to the low iron content in this sample. The Amptek X-123 SDD detector was used for this purpose. Six spectra were acquired for each sample and averaged. All spectra were handled with the use of Athena software. The further modeling and refinements were done using the Artemis software. Refinements were performed by k^2-weighted spectra in the range of 3–14 Å^{-1} in the k-space, and of 1–3.5 Å in the R-space, Hanning window

function was used. The value of S_0^2 = 1 was fixed during the refinements.

Mössbauer absorption spectra were obtained on MS1104EM Express Mössbauer spectrometer (Cordon GmbH, Rostov-on-Don). The radiation source with an activity of 6 mCi was ^{57}Co in a metal rhodium matrix (RITVERC GmbH, St. Petersburg, Russia). The spectra were obtained at room temperature (295 ± 3 K) and in a vacuumed cryostat at a liquid nitrogen temperature (77.5 ± 0.5 K). The spectra were collected until the signal to noise ratio was less than 1%. Mathematical processing was carried out for spectra with a high resolution (1,024 points) using SpectrRelax 2.4 (Lomonosov MSU, Russia) software. The isomer shift was determined relative to α Fe.

Soil Pot Experiment

Fertilizers

A stock solution (1,000 μmol Fe L^{-1}) of each ^{57}Fe-humic NF (F, S, and M) at pH 7 was prepared from the freeze dried products (^{57}Fe-NFs) previously obtained, as it was described above A stock solution of ^{57}FeEDDHA (1,000 μmol Fe L^{-1}) was prepared by chelation with Fe^{3+} from $Fe(NO_3)_3$ and *o-o*EDDHA [ethylenediamine-di (*o-o* hydroxyphenylacetic acid)] obtained from LGC Standards, Teddington, United Kingdom (93.12%), previously dissolved with three mol of NaOH per mol of chelating agent. The solution was adjusted at pH 7 with 1M KOH.

In order to test the ^{57}Fe-NFs as correctors of iron chlorosis, three doses (35, 75, and 150 μmol ^{57}Fe pot^{-1}) were applied to iron deficient soybean plants and compared to ^{57}FeEDDHA (50 μmol pot^{-1}), as a positive control, and L (providing 8.9 μmol Fe pot^{-1}). The treatments were applied over the soil surface 2 days after the soybean plants were transferred to the pots. Five replicates (five pots) per fertilizer were carried out.

Plant Material

Soybeans (*Glycine max AG1835* Asgrow Seed Co.) were germinated in the dark at room temperature on filter paper moistened with distilled water. After germination (7 days), seedlings were transferred to the growth chamber where they grew until the end of the experiment in a Dycometal-type CCK growth chamber provided with fluorescent and sodium vapor lamps with a 16 h, 25°C and 40% humidity day and 8 h, 20°C and 60% humidity night regime. Seedlings were placed on containers filled with 1/5 diluted nutrient solution of the full-strength solution with the following composition: macronutrients (mM) 1.0 $Ca(NO_3)_2$, 0.9 KNO_3, 0.3 $MgSO_4$, and 0.1 KH_2PO_4; cationic micronutrients (μM) 2.0 FeHBED, 2.5 $MnSO_4$, 1.0 $CuSO_4$, 10.0 $ZnSO_4$, 1.0 $CoSO_4$, 1.0 $NiCl_2$, and 115.5 $EDTANa_2$; anionic micronutrients (μM) 35.0 NaCl, 10.0 H_3BO_3, and 0.05 Na_2MoO_4 and 0.1 mM HEPES. The pH was adjusted to 7.5 with 1.0M KOH. After 8 days, the diluted nutrient solution was replaced by the full-strength solution without Fe. Seedlings were kept in this solution for 2 days in order to induce iron deficiency. In order to simulate calcareous conditions, $CaCO_3$ (0.1 g L^{-1}) was added to each pot. The deficient iron soybean plants (three plants per pot) were transferred into 600 g polystyrene pots filled in with the soil/sand 70/30% (w/w) mixture. The soil was obtained from the top 20 cm of a citrus farm at Picassent, Valencia, Spain (39°21′41.28″ N, 0°27′42.58″ W). Physicochemical characteristics of this soil are described in **Table 1**. Texture, pH, soil E.C., OM, C/N ratio, $CaCO_3$ were measured according to the official methods (MAPA, 1994) and micronutrients availability was determined as described by Soltanpour and Schwab (1977). Normalized calcareous sand (2–4 mm) was used. One day before transferring the seedlings, pots were irrigated till field capacity. Water and iron free nutrient solution were added every day. Two samplings were carried out, at 15 and 48 days after the fertilizers (DAF) were applied.

TABLE 1 | Physical and chemical properties of the soil used for both pot experiments.

Parameter	Picassent soil
[1]Sand (g · kg^{-1})	435
[1]Silt (g · kg^{-1})	80
[1]Clay (g · kg^{-1})	485
pH (H_2O)	7.9
E.C.$_{1:5}$ (dS m^{-1})	2.0
[2]OM (g kg^{-1})	9.2
[3]N Kjeldahl (g kg^{-1})	0.3
C/N	30.7
[5]$CaCO_3$ (g · kg^{-1})	380
[6]$CaCO_3$ active (g · kg^{-1})	89
[8]DTPA Zn (mg · kg^{-1})	3.00
[8]DTPA Fe (mg · kg^{-1})	5.3
[8]DTPA Mn (mg · kg^{-1})	4.5
[8]DTPA Cu (mg · kg^{-1})	1.1

E.C., electrical conductivity; OM, organic matter. [1]Densitometry Bouyoucos's method. [2]Walkley-Black's method. [3]Kjeldahl's method. [5]Williams's calcimeter. [6]Droinean's method. [7]Exchangeable cations extracted with NH_4Ac pH = 7. [8]Soltanpour and Swab's method.

Analytical Procedures

The sampled roots, stems, and leaves were separated, weighted, and washed with 0.1% HCl and 0.01% non-ionic detergent (Tween 80) solutions, rinsed with distilled water (Álvarez-Fernández et al., 2001) and dried in a forced air oven at 65°C for 3 days. Thereafter, samples were milled and calcined in a muffle furnace (480°C). The ashes were digested using 7M HNO_3 Suprapour.

Soil soluble fraction was obtained by washing the soil with distilled water (600 mL) by stirring for 10 min on a rotary shaker at 90 min^{-1}. An aliquot of 40 mL was centrifuged at 9,000 min^{-1} for 10 min (Sorvall Legend XFR, Thermo Fisher Scientific, United States), the supernatant was first filtered with ashless filters paper (Grade 1238, Filter Lab) and then, through syringe cellulose filters (0.45 μm) (OlimPeak, Teknokroma). Nitric acid (Suprapur, Merck) was added to achieve a 1% acid matrix.

Soil available fraction was obtained from the solid residue in the centrifuge tube by extraction for 20 min with 25 mL using Soltanpour and Schwab (1977) extractant (DTPA + ammonium bicarbonate). After that, the samples were filtered. The extraction was made in triplicate, the extracts joined in a single extract, and volume made up to 100.0 mL. An aliquot of 7.165 mL of 65% HNO_3 was added to eliminate the excess of bicarbonate and to allow an acid media for the analytical determinations.

Isotope quantification in the plant organs and soil fractions (soluble and available) were determined by ICP-MS (7500c, Agilent Technologies, Santa Clara, CA, United States) using ^{57}Fe standards and correcting Ca and Ar interferences by means of a collision cell quadrupole ICP-MS instrument.

The specific contribution of each iron fertilizer to the soil and plant nutrition was calculated by isotope pattern deconvolution analysis considering the two iron sources, with a modification of the method proposed by Rodríguez-Castrillón et al. (2008) In brief, the mass balance for the Fe natural isotope can be expressed as shown by matrix notation:

$$\begin{bmatrix} {}^{54}A_{Total} \\ {}^{56}A_{Total} \\ {}^{57}A_{Total} \\ {}^{58}A_{Total} \end{bmatrix} = \begin{bmatrix} {}^{54}A_{Fer} & {}^{54}A_{Nat} \\ {}^{56}A_{Fer} & {}^{56}A_{Nat} \\ {}^{57}A_{Fer} & {}^{57}A_{Nat} \\ {}^{58}A_{Fer} & {}^{58}A_{Nat} \end{bmatrix} \times \begin{bmatrix} x_{Fer} \\ x_{Nat} \end{bmatrix} + \begin{bmatrix} {}^{54}e \\ {}^{56}e \\ {}^{57}e \\ {}^{58}e \end{bmatrix}$$

where each A_{Total} is the isotope abundance of each Fe isotope in the plant sample. A_{Fer} is the corresponding isotope abundance in the tracer, and A_{Nat} is the natural isotope abundance. Moreover, x_{Fer} and x_{Nat} denote the molar fractions of Fe in the isotopically altered sample arising from the two different sources of the element (fertilizer or natural). The best values of x_{Nat} and x_{Fer} are found by least-squares fitting of the error vector e (minimizing the square sum of errors) using the SOLVER tool in Excel®.

To evaluate the influence of Fe on leaf chlorophyll, the SPAD Index was measured every 2 or 3 days, using a Minolta Chlorophyll Meter SPAD-502 (Minolta, Osaka, Japan) after the first application of the Fe fertilizers.

Statistical Analysis

In order to verify the homogeneity of the data, the Levene test was used first, prior to testing the differences between Fe treatments for significance by one-way ANOVA. Means were compared using the Duncan multiple range test ($P < 0.05$). Results of two-way ANOVA are expressed as ns (not significant), $^{*}P < 0.05$, $^{**}P < 0.01$, and $^{***}P < 0.001$. All the calculations were performed using SPSS v.24.0 software.

RESULTS

Characterization of ^{57}Fe-NFs

The main characterization tools used in this work were ^{57}Fe Mössbauer spectroscopy, XRD, EXAFS, and TEM. They were applied to identify the iron phases in the ^{57}Fe-NFs and to estimate the particle size. According to the XRD data, the major crystalline phases in all three samples of ^{57}Fe-NFs are mineral salts of potassium and sodium: nitrates in the product F, and sulfates in the products S and M, the collected data are shown in **Supplementary Figure SM2**. No iron-containing crystalline phases were observed in the obtained XRD patterns. The XRD data on the synthesized reference samples – ferrihydrite and goethite – are shown in **Supplementary Figure SM3**.

TEM data demonstrate that all ^{57}Fe-NFs samples contain large low density particles typical for HSs. Inside of these particles the nano-sized contrast variations can be observed, which correspond to the NPs with sizes < 5 nm (**Figures 1a,b**). Some aggregates of ∼20 nm were observed in the product S (**Figure 1c**). These NPs can be clearly seen in the zero loss images of the products F and M (**Supplementary Figure SM3**). **Figure 2** shows TEM images, Fe M-line EFTEM, EELS spectra and the scheme of EFTEM measurements for the F sample, which was of particular interest for this study, because its synthesis was specifically run under conditions favoring formation of ferrihydrite phase. The Fe M- and L-lines were clearly observed in the EELS spectrum of this sample (**Figure 2**). This confirmed the presence of iron in the region of interest. The spatial distribution of iron was investigated using three-point EFTEM, which yielded the pattern of iron-containing NPs (bright inclusions) in the darker matrix (HSs). The obtained results are indicative of the iron-containing composition of the formed NPs. In order to investigate the structures of the observed NPs, the SAED patterns were measured (**Supplementary Figure SM6**) and compared to the ED of the parent HS (L) and XRD pattern of the synthesized pure two-line ferrihydrite (Ferrihydrite). ED patterns of all iron containing samples were characterized with appearance of two additional reflexes as compared to the parent L sample (**Figure 3**). The smaller peak was observed at 0.15 nm, and the larger one – at 0.25–0.30 nm. Such a combination of reflexes is similar to the two-line ferrihydrite diffraction pattern. However, for refining this assignment additional information was desirable and obtained with the use of XANES and EXAFS spectroscopy.

The acquired XANES spectra of the samples obtained in this study are shown in **Supplementary Figure SM7** and their first derivatives are presented in **Figure 4A**. The spectra obtained for all samples under study were rather similar and demonstrated the presence of ferric ions in octahedral coordination (Manceau and Gates, 1997). EXAFS spectra of the same samples (**Figure 4B** and **Supplementary Figure SM8**) were fitted to the two-shell model (Maillot et al., 2011). It assumes that the first shell contains two different oxygen positions (Fe-O), whereas the second one- three iron position (Fe–Fe) with the same value of σ^2. The obtained results for ferrihydrite and goethite reference samples (**Table 2**) are in good agreement with the reported values for Fe–O and Fe–Fe distances (Maillot et al., 2011). For the samples under study, the values of Fe–Fe distances were very close to those of ferrihydrite (**Table 2**). For example, in the F sample (HS-ferrihydrite), they were 2.98 Å, 3.14 Å, and 3.53 Å, whereas in the reference sample – 2.91 Å, 3.06 Å, and 3.46 Å. These distances belong to face-sharing, edge-sharing, and corner-sharing octahedra in ferrihydrite, respectively (Manceau and Gates, 1997). Coordination number of iron at 2.91 Å and 3.06 Å for all three samples of the NFs are similar and indicative of ferrihydrite (Maillot et al., 2011). The high value of R-factor for the "S" sample results from the poorest quality of its approximation by the above two-shell model. This might be caused by heterogeneity of the S sample which contained different phases of iron (hydr)oxides. The iron in the parent humate resembles closely goethite phase. The differences in Fe–O distances between the reference ferrihydrite (1.82 Å and 1.97 Å) and the samples obtained in the presence of HS (1.94 Å and 2.11 Å) may be connected to very small size of the particles formed (<5 nm) and to respective surface effects. In the ideal

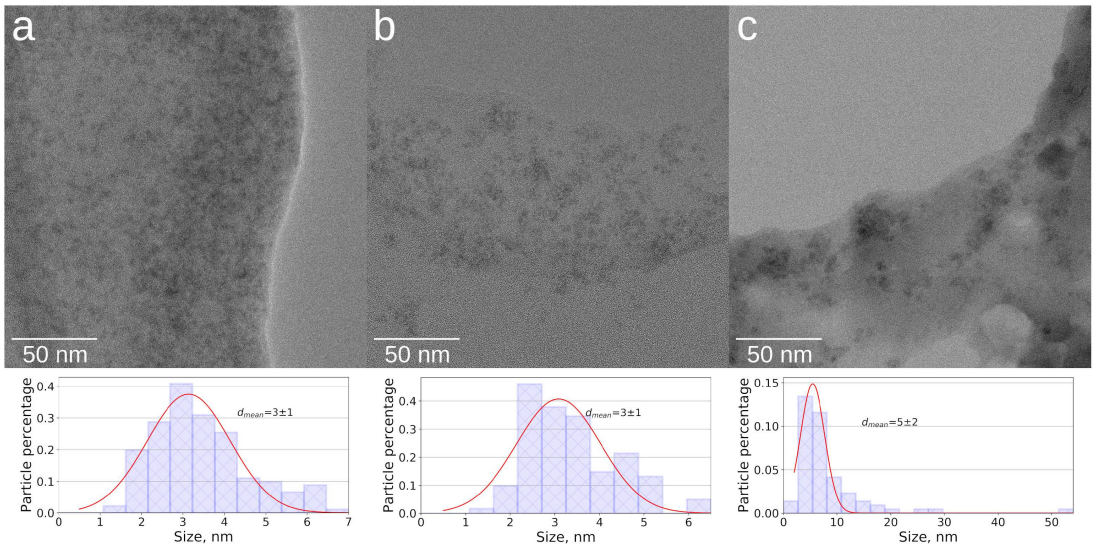

FIGURE 1 | TEM images and size statistics for the three ^{57}Fe-nanofertilizer samples under study: **(a)** F, **(b)** M, **(c)** S.

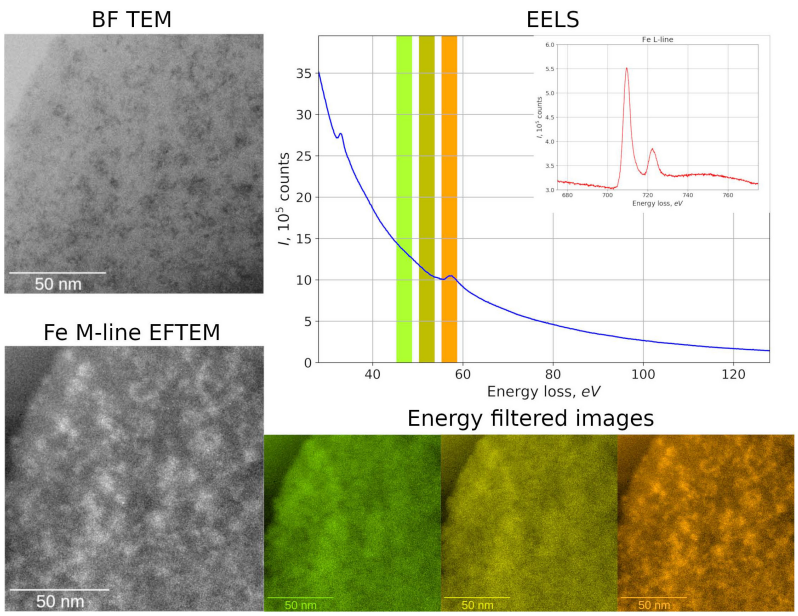

FIGURE 2 | TEM, Fe M-line EFTEM, EELS spectra and the scheme of EFTEM measurements for the product F.

ferrihydrite, the relation between tetrahedral Fe (IV Fe) and octahedral Fe (VI Fe) is 1:4. However, according to Michel et al. (2007), the size reduction of ferrihydrite particles leads to a decrease in IV Fe number. Moreover, Manceau and Gates (1997) demonstrated that 1.86Å Fe–O distance observed in the EXAFS spectra could not be directly assigned to the IV Fe due to the presence of short Fe–(O,OH) bonds on the surface. It means that the surface contamination and size reduction in the HS-stabilized ferrihydrite particles may lead to a decrease in a number of short Fe–O bonds as compared to the reference ferrihydrite. The applied EXAFS model involved only two Fe–O distances due to restriction on the amount of independent parameters, the most intense paths for each sample were chosen. The obtained data allow a conclusion that all three samples of the

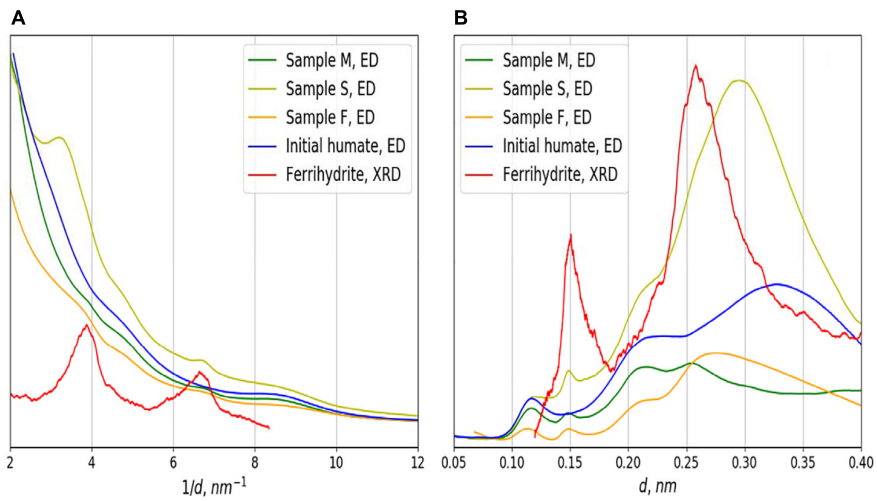

FIGURE 3 | Results of ED integration in reciprocal space **(A)** and in direct space, after background removal **(B)** for the products F, M, S. and initial humate (L) in comparison with the XRD data for ferrihydrite.

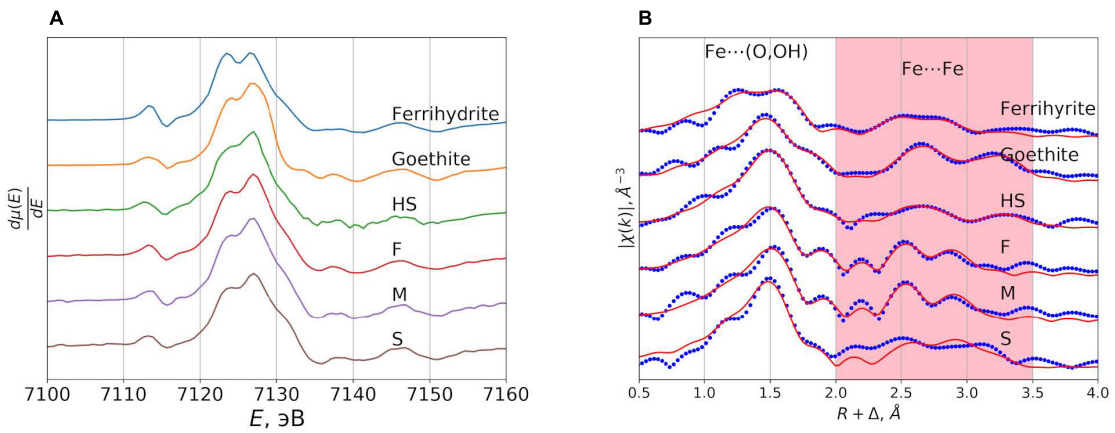

FIGURE 4 | The first derivatives of the XANES spectra shown in **Supplementary Figure SM7 (A)** and the results of model approximation of the EXAFS spectra in R-space **(B)** for the ^{57}Fe-labeled nanofertilizer samples under study.

synthesized NFs were very similar with regard to the iron phase and contained iron (hydr)oxide with the polyhedral arrangement motif of the ferrihydrite.

The results of Mössbauer spectroscopy investigation yielded additional support to this conclusion. The Mössbauer spectra of M and F samples recorded at room temperature and at liquid nitrogen showed broadened electric quadrupole doublets as it is demonstrated in **Figure 5A** on the example of M-sample. The Mössbauer spectra of F-sample is shown in **Supplementary Figure SM11**. This could be explained by the distribution of gradients of the electric field (**Supplementary Figure SM10**). For these samples, the distribution of quadrupole splittings has a bimodal character, similar to the distribution for high-temperature spectra of a reference sample of ferrihydrite (**Supplementary Figure SM10**). The small size of the particles under study and the low blocking temperature might be the reasons for a lack of substantial broadening of the resonance lines as well as the absence of a magnetically ordered fraction in the spectra at low temperature. Even for the reference sample of ferrihydrite with the larger particles as compared to the NPs stabilized by humate, the magnetic ordering (**Supplementary Figure SM10**) was not observed at the boiling point of liquid nitrogen (Schwertmann et al., 1999).

The spectra of S sample at these temperatures, in addition to very similar quadrupole doublets, contained extended absorption with low intensity, which can be conditionally described by a singlet line of a large width (**Figure 5B**). The relative area of extended absorption in the S sample did not

TABLE 2 | The model parameters calculated from the EXAFS spectra for three ^{57}Fe-NFs samples used in this study.

Sample	R_f (%)	ΔE (eV)		N	R (Å)	$\sigma^2 \times 10^3$
"L"	1.5%	−0.9	O	2.7 ± 0.9	1.94 ± 0.02	2 ± 2
			O	1.3 ± 0.4	2.08 ± 0.04	
			Fe	2.1 ± 0.8	3.05 ± 0.03	10*
			Fe	1.8 ± 1.2	3.24 ± 0.06	
			Fe	2.4 ± 0.9	3.48 ± 0.03	
Ferrihydrite	2.9%	-7	O	1.2 ± 0.4	1.82 ± 0.04	3 ± 3
			O	2.3 ± 0.8	1.97 ± 0.02	
			Fe	0.5 ± 0.3	2.91 ± 0.04	0 ± 6
			Fe	0.5 ± 0.4	3.06 ± 0.04	
			Fe	0.3 ± 0.2	3.46 ± 0.04	
Goethite	1.5%	−0.1	O	2.7 ± 0.6	1.94 ± 0.02	3 ± 2
			O	2.2 ± 0.4	2.09 ± 0.02	
			Fe	3.3 ± 1.4	3.07 ± 0.02	9 ± 3
			Fe	2.8 ± 1.6	3.30 ± 0.04	
			Fe	3.6 ± 1.3	3.47 ± 0.03	
"F"	3.0%	0.3	O	2.6 ± 0.8	1.94 ± 0.02	3 ± 3
			O	1.3 ± 0.4	2.11 ± 0.04	
			Fe	0.7 ± 0.4	2.98 ± 0.02	0 ± 4
			Fe	0.9 ± 0.5	3.14 ± 0.03	
			Fe	0.1 ± 10.2	3.49 ± 0.3	
"M"	2.9%	0.2	O	2.8 ± 1.1	1.94 ± 0.02	3 ± 3
			O	1.1 ± 0.5	2.10 ± 0.0C	
			Fe	0.9 ± 0.5	2.97 ± 0.02	0 ± 3
			Fe	0.9 ± 0.5	3.13 ± 0.03	
			Fe	0.2 ± 0.2	3.53 ± 0.09	
"S"	4.7%	3.2	O	1.4 ± 0.3	1.95 ± 0.02	0.5 ± 2.5
			O	2.0 ± 0.5	2.10 ± 0.03	
			Fe	0.9 ± 0.7	3.01 ± 0.03	2 ± 7
			Fe	1.1 ± 0.8	3.16 ± 0.04	
			Fe	0.4 ± 0.5	3.51 ± 0.07	

* *Fixed value.*

change with temperature indicating that it is not related to superparamagnetism. This can be connected with weak spin–spin interactions between iron (III) atoms in strongly inhomogeneous and disordered medium. These interactions could be precisely observed because of the use of ^{57}Fe (Pankratov et al., 2013). Distribution of quadrupole splitting in the S sample is unimodal and it has significantly larger dispersion as compared to those in the samples M and F. This might be indicative of the larger diversity of the local environments of iron atoms in the S sample. The further details on Mössbauer data can be found in the **Supplementary Table SM1** and Supplementary text. In general, the data of Mössbauer spectroscopy are in good agreement with the data of TEM and X-ray spectroscopy.

Soil Pot Experiment

In order to evaluate the ^{57}Fe-NFs effect in the plant growth, the SPAD index and the fresh weight of soybean shoots and roots at 48 DAF were measured and presented in **Table 3**. There was no leaf chlorosis observed and the plants presented SPAD indexes > 25, which is indicative of sufficient iron nutrition (Martín-Fernández et al., 2017b). The shoot biomass of the fertilized plants (in case of F3, S1, S2, S3, and M2) was larger as compared to FeEDDHA. There was no significant differences observed in the root biomass of the plants fertilized with the NFs under study (except for F3, which showed the largest fresh weight of roots). In our former studies, the plants fertilized with the leonardite humates accumulated slightly higher fresh weight than those fertilized with the iron chelate. According to Rose et al. (2014), the HSs generally increase the shoot and root growth by 15–25%. Canellas et al. (2015) reported that the growth response of monocotyledonous plants to exogenously applied HS is more sensitive as compared to for dicotyledonous plants, and the plant physiological responses to HS isolated from brown coal (e.g., lignite, leonardite, and subbituminous coals) are less than those observed in response to the addition of HS isolated from peat, composts or vermicomposts.

The ^{57}Fe tracer technique allowed monitoring Fe from the fertilizer (Fe_{Fer}) in the soil experiment and distinguishing it from the native Fe contained in the soil (Fe_{Nat}). The Fe_{Total} was calculated as the sum of Fe_{Fer} and Fe_{Nat}. A combination of ^{57}Fe isotope and mathematical deconvolution was a relevant tool to evaluate the efficacy between different NFs to correct iron deficiency.

The contents of Fe_{Fer}, Fe_{Nat}, and Fe_{Total} (μmol pot^{-1}) in soybean shoots were calculated as the sum of the first (15 DAF) and second samplings (48 DAF) and presented in **Figure 6**. The effect of type and doses of the ^{57}Fe-NFs on the contents of Fe_{Fer}, Fe_{Nat} and Fe_{Total} in soybean shoots was studied by ANOVA two-way statistical analysis and presented in **Table 4**. Significant differences were observed between ^{57}Fe-NFs types and doses. The product M provided the highest Fe_{Fer} content to the soybean shoots mainly when the third dose was applied (150 μmol ^{57}Fe pot^{-1}). The content of Fe_{Total} expressed as the sum of the Fe_{Fer} and Fe_{Nat} showed significant differences only between the doses, and the third dose seemed to be the most adequate. **Table 5** presents the Fe_{Total} (mg kg^{-1}) concentration in soybean leaves at 15 and 48 DAF. It ranged from 36.8 mg kg^{-1} (F1) to 53.6 mg kg^{-1} (M1) at 15 DAF and from 34.6 mg kg^{-1} (S1) to 39.9 (S3) mg kg^{-1} at 48 DAF. According to the iron concentration obtained in a previous work (Rodríguez-Lucena et al., 2010) and the SPAD index detected (**Table 4**), the soybean plants are sufficiently iron nourished and did not present symptoms of iron chlorosis. Moreover, the iron concentration in leaves decreased for the second sampling because iron was a priority for the pods production, even for plants fertilized with ^{57}FeEDDHA.

Differences in Fe_{Fer} uptake (nmol plant^{-1}) in soybean leaves between the first (15 DAF) and the second samplings (48 DAF) were calculated and plotted in **Figure 7**. The plants fertilized with the ^{57}Fe-NFs, nominally, with S2, M2 and F3, have taken up 93, 88, and 70 nmol Fe_{Fer} plant^{-1} in leaves in 33 days, whereas the plants fertilized with FeEDDHA stopped providing Fe_{Fer} to the leaves after the first sampling. The products S and M, prepared from $^{57}Fe_2(SO_4)_3$, at their second dose (75 μmol ^{57}Fe pot^{-1}) and the product F, prepared from $^{57}Fe(NO_3)_3$ at the third dose (150 μmol ^{57}Fe pot^{-1}) showed the highest Fe_{Fer} increase between sampling times. These results are consistent with our previous data (Cieschi et al., 2017) on

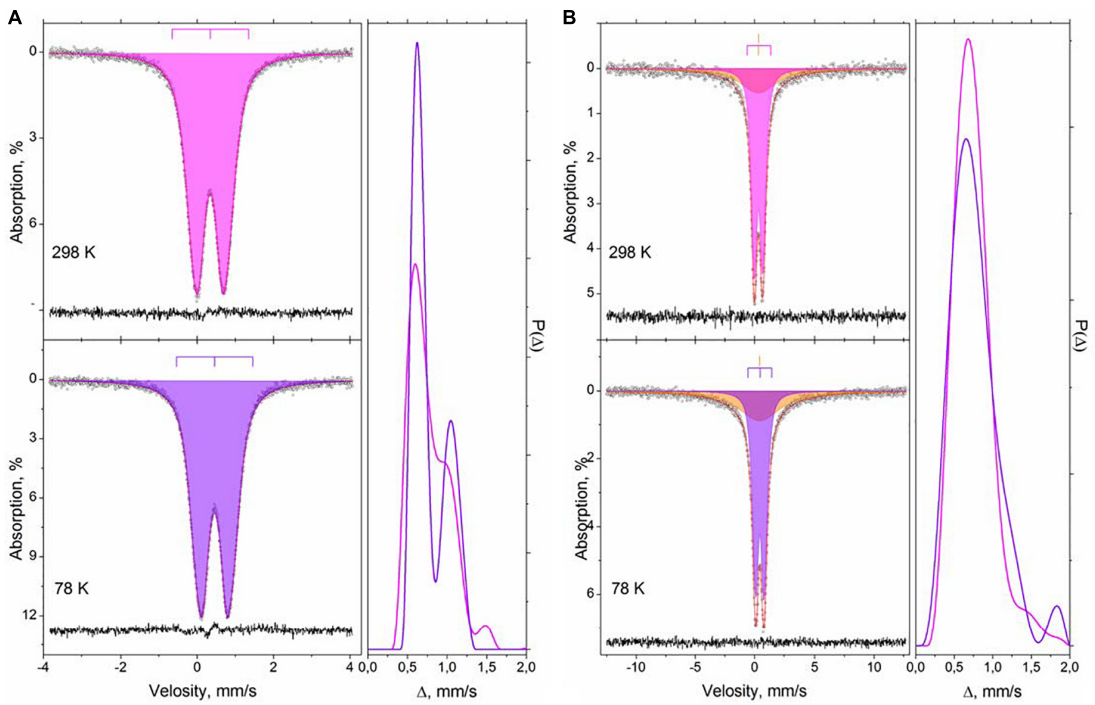

FIGURE 5 | Mössbauer spectra of the M and S samples (**A,B**, respectively) recorded at 295K and 78K and the quadrupole splitting distributions for these spectra.

fertilization with iron leonardite humate which sustained slow and increasing iron nutrition to citrus growth under conditions of calcareous soil and yielded results similar to FeEDDHA with regard to efficacy of iron deficiency correction during the first year of application.

TABLE 3 | SPAD index at the last level of trifoliate well developed soybean leaves and fresh weight (FW) of shoots and roots of soybean control (L) plants and plants fertilized with the ^{57}Fe products F, S, and M in three doses: (1) 35, (2) 75, and (3) 150 μmol ^{57}Fe pot^{-1} or 50 μmol ^{57}FeEDDHA pot^{-1} at 48 DAF.

Treatments	SPAD	Shoot FW (g pot^{-1})	Root FW (g pot^{-1})
L	41.8 ± 2.04^{abc}	13.9 ± 0.47^{a}	5.69 ± 0.62^{b}
F1	37.1 ± 1.55^{cd}	13.4 ± 0.50^{ab}	7.33 ± 0.61^{ab}
F2	39.2 ± 1.03^{bc}	13.8 ± 0.09^{a}	6.90 ± 0.22^{ab}
F3	45.9 ± 0.50^{ab}	14.6 ± 0.39^{a}	8.15 ± 0.60^{a}
S1	40.2 ± 1.75^{bc}	14.0 ± 0.73^{a}	6.80 ± 0.40^{ab}
S2	38.4 ± 1.98^{bc}	14.5 ± 0.55^{a}	7.03 ± 0.97^{ab}
S3	30.8 ± 4.75^{d}	13.9 ± 0.48^{a}	6.61 ± 0.32^{ab}
M1	39.1 ± 3.70^{bc}	13.4 ± 0.16^{ab}	6.81 ± 0.54^{ab}
M2	42.4 ± 2.84^{abc}	13.7 ± 0.45^{a}	6.34 ± 0.25^{ab}
M3	40.6 ± 2.44^{bc}	13.3 ± 1.13^{ab}	7.22 ± 0.79^{ab}
FeEDDHA	48.9 ± 1.53^{a}	11.5 ± 0.74^{b}	5.70 ± 0.45^{b}

For each series different letters denote significant differences among the treatments according to Duncan's Test ($p < 0.05$). Results are expressed as averages ± standard error, n = 5.

Of particular interest are the contents of Fe_{Fer}, Fe_{Nat} and Fe_{Total} (μmol pot^{-1}) in soybean pods at 48 DAF, which are presented in **Figure 8**. The Fe_{Fer} content in pods increased along with an increase in the dose of ^{57}Fe-NFs. The significant differences were observed between the doses and the ^{57}Fe-NF type when the obtained results were compared using ANOVA two-way statistical analysis (**Table 4**). As in case of the shoots, the product M provided the higher content of Fe_{Fer} as compared to the other two ^{57}Fe-NFs to the soybean pods and the third dose was the most efficient. Moreover, the similar Fe_{otal} contents in soybean pods were observed for the plants treated with ^{57}Fe-NFs (except for F2) or FeEDDHA, and the product M was the most efficient in providing Fe_{Total} to the soybean pods regardless of the dose applied. **Table 5** shows the Fe_{Total} concentration (mg kg^{-1}) in soybean pods at 48 DAF. It ranged from 32.6 mg kg^{-1} (F2) to 57.8 mg kg^{-1} (M2) for the plants fertilized with ^{57}Fe-NFs. According to Römheld and Nikolic (2007), the accumulation of total iron in pods for soybean plants reaches 50 mg kg^{-1} under conditions of sufficient nourishment. Nadal et al. (2012) and Martín-Fernández et al. (2017a) have observed ^{57}Fe in soybean fruit of plants fertilized with *o,o*EDDHA/$^{57}Fe^{3+}$ and HBED/$^{57}Fe^{3+}$. Still, this study is the first one when ^{57}Fe supplied by iron humates was detected in soybean pods. Shoots of plants fertilized with FeEDDHA showed the highest Fe_{Fer}, the lowest Fe_{Nat} and the highest Fe_{Total} contents. The pods showed similar results for Fe_{Fer} and Fe_{Nat} contents.

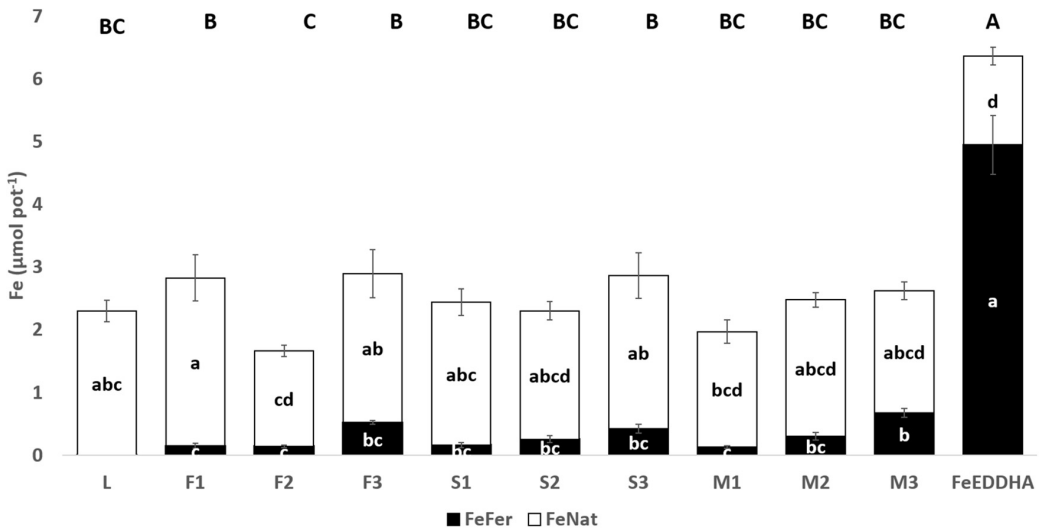

FIGURE 6 | Fe_{Fer} and Fe_{Nat} (µmol pot^{-1}) contents in soybean shoots of control plants (L) and plants fertilized with the ^{57}Fe products F, S, and M in three doses: (1) 35, (2) 75, and (3) 150 µmol ^{57}Fe pot^{-1} or 50 µmol $^{57}FeEDDHA$ pot^{-1}, calculated as the sum of the first (15 DAF) and second sampling (48 DAF). For each series different letters denote significant differences among the treatments according to Duncan's Test ($p < 0.05$). Lowercase letters correspond to Fe_{Fer} and Fe_{Nat} and capital letters correspond to Fe_{Total} statistical results. Results are expressed as averages ± standard error, $n = 5$.

TABLE 4 | Effect of doses (D) and nanofertilizers (NFs) related to the contents of Fe_{Fer}, Fe_{Nat}, and Fe_{Total} (µmol pot^{-1}) in soybean shoots, roots, pods, soluble and available soil fraction for soybean plants fertilized with the products F, S, and M with three doses (35, 75, and 150 µmol pot^{-1}) at 48 DAF.

					Nanofertilizers			Doses (µmol pot^{-1})		
		D	NFs	DxNFs	F	S	M	35	75	150
Shoots	Fe_{Fer}	***	*	*	0.27 ± 0.03^{b}	0.28 ± 0.03^{b}	0.35 ± 0.03^{a}	0.15 ± 0.03^{c}	0.23 ± 0.03^{b}	0.54 ± 0.03^{a}
	Fe_{Nat}	ns	ns	ns	2.19 ± 0.15	2.26 ± 0.15	1.99 ± 0.15^{ns}	2.27 ± 0.15	1.92 ± 0.15	2.25 ± 0.15^{ns}
	Fe_{Total}	*	ns	ns	2.44 ± 0.16	2.53 ± 0.16	2.36 ± 0.16^{ns}	2.41 ± 0.16^{ab}	2.15 ± 0.16^{b}	2.77 ± 0.16^{a}
Pods	Fe_{Fer}	***	*	ns	0.20 ± 0.04^{b}	0.19 ± 0.16^{b}	0.34 ± 0.16^{a}	0.11 ± 0.04^{c}	0.22 ± 0.04^{b}	0.40 ± 0.04^{a}
	Fe_{Nat}	ns	ns	ns	0.94 ± 0.09	0.97 ± 0.09	1.08 ± 0.09^{ns}	1.15 ± 0.09	0.94 ± 0.09	0.90 ± 0.09^{ns}
	Fe_{Total}	ns	*	*	1.14 ± 0.10^{b}	1.14 ± 0.11^{b}	1.42 ± 0.10^{a}	1.27 ± 0.10	1.22 ± 0.10	1.27 ± 0.10^{ns}
Roots	Fe_{Fer}	***	ns	ns	1.64 ± 0.29	1.21 ± 0.29	1.15 ± 0.29^{ns}	0.45 ± 0.30^{b}	0.75 ± 0.29^{b}	2.80 ± 0.27^{a}
	Fe_{Nat}	ns	ns	ns	77.7 ± 8.23	71.8 ± 8.23	77.8 ± 8.23^{ns}	67.6 ± 8.23	74.4 ± 8.23	85.2 ± 8.23^{ns}
	Fe_{Total}	ns	ns	ns	79.4 ± 8.34	73.1 ± 8.34	79.0 ± 8.34^{ns}	68.2 ± 8.34	75.2 ± 8.34	88.0 ± 8.34^{ns}
Soluble	Fe_{Fer}	**	*	*	0.16 ± 0.11^{b}	0.20 ± 0.11^{b}	0.53 ± 0.10^{a}	0.18 ± 0.10^{b}	0.06 ± 0.11^{b}	0.65 ± 0.11^{a}
	Fe_{Nat}	ns	ns	ns	5.24 ± 3.49	9.80 ± 3.49	15.6 ± 3.49^{ns}	10.6 ± 3.49	6.19 ± 3.49	13.8 ± 3.49^{ns}
	Fe_{Total}	ns	ns	ns	5.39 ± 3.43	10.0 ± 3.57	16.2 ± 3.43^{ns}	10.8 ± 3.43	6.36 ± 3.43	14.5 ± 3.57^{ns}
Available	Fe_{Fer}	***	***	***	27.3 ± 2.51^{a}	10.3 ± 2.51^{c}	17.7 ± 2.51^{b}	7.83 ± 2.51^{a}	17.3 ± 2.51^{b}	30.1 ± 2.51^{c}
	Fe_{Nat}	ns	*	ns	179 ± 55.8^{b}	169 ± 58.1^{b}	364 ± 55.8^{a}	255 ± 55.8	212 ± 55.8	245 ± 58.1^{ns}
	Fe_{Total}	ns	*	ns	207 ± 56.8^{b}	179 ± 59.2^{b}	382 ± 56.8^{a}	263 ± 56.8	230 ± 56.8	274 ± 59.2^{ns}

*Means (n = 5) in the same row followed by the same letter do not differ significantly according to the Duncan test (P < 0.05). Two-way ANOVA results. *P < 0.05, **P < 0.01, ***P < 0.001; ns, not significant.*

The content of Fe_{Fer} (µmol pot^{-1}) in soybean roots as well as the contents of soluble and available soil fractions at 48 DAF are presented in **Figure 9**. In general, an increase in the content of Fe_{Fer} in soybean roots was observed when the plants were treated with the ^{57}Fe-NFs (**Figure 9A**). The significant differences between the doses were confirmed by the ANOVA two-way statistical analysis (**Table 4**). The third dose was the most prone to store Fe_{Fer} in roots, in particular, in case of the F sample.

The Fe_{Fer} content in the soluble soil fraction was increasing along with the dose of the ^{57}Fe-NFs. The results obtained for F3, S3, M3, and FeEDDHA were similar, though the highest Fe_{Fer} content was observed in the pots treated with M3 (**Figure 9B**). The ANOVA two-way statistical analysis has confirmed these results when the effect of the ^{57}Fe-NF type and doses were compared (**Table 4**). Relating to the Fe_{Fer} content in the available soil fraction, the pots fertilized with the product F differed

TABLE 5 | Fe_{Total} (mg kg^{-1}) concentration in soybean leaves and pods of plants fertilized with the ^{57}Fe products F, S, and M in three doses: (1) 35, (2) 75, and (3) 150 μmol ^{57}Fe pot^{-1} or 50 μmol $^{57}FeEDDHA$ pot^{-1} at 15 and 48 DAF and soybean pods at 48 DAF.

Treatments	Leaves 15 DAF	Leaves 48 DAF	Pods
L	38.1 ± 2.85^{d}	48.3 ± 5.65^{b}	49.5 ± 5.40^{ab}
F1	36.8 ± 1.10^{d}	38.6 ± 3.52^{bc}	46.1 ± 9.53^{ab}
F2	41.3 ± 3.38^{cd}	37.5 ± 2.60^{bc}	32.6 ± 6.85^{b}
F3	40.2 ± 3.61^{d}	39.4 ± 2.40^{bc}	38.9 ± 4.00^{b}
S1	38.2 ± 3.11^{d}	34.6 ± 1.43^{c}	45.7 ± 5.38^{ab}
S2	38.9 ± 2.73^{d}	35.8 ± 1.97^{c}	45.7 ± 5.58^{ab}
S3	38.1 ± 2.59^{d}	39.9 ± 1.81^{bc}	45.9 ± 3.26^{ab}
M1	53.6 ± 4.29^{b}	35.4 ± 0.53^{c}	51.3 ± 2.90^{ab}
M2	46.1 ± 1.20^{bcd}	35.5 ± 2.61^{c}	57.9 ± 7.43^{a}
M3	50.7 ± 3.11^{bc}	39.5 ± 2.16^{bc}	49.8 ± 3.63^{ab}
FeEDDHA	139 ± 5.60^{a}	108 ± 6.99^{a}	46.7 ± 3.13^{ab}

For each series different letters denote significant differences among the treatments according to Duncan's Test ($p < 0.05$). Results are expressed as averages ± standard error, n = 5.

substantially from the others, in particular, in case of the third dose (**Figure 9C** and **Table 4**). In general, the Fe_{Fer} from the product F at the highest dose (150 μmol ^{57}Fe pot^{-1}) remained mostly available in soil (**Figure 9C**) or in the roots (**Figure 9A**).

Figure 10 shows the ^{57}Fe (%) distribution in soybean plants (shoots, pods and roots) of plants fertilized with the ^{57}Fe products F, S and M in three doses (35, 75 and 150 μmol ^{57}Fe pot^{-1}) and in the soil (soluble and available fraction). In general, the ^{57}Fe-NFs remained in soil and ranged from 80% (S1) to 95% (F1), mainly in the available soil fraction. With respect to the plant, the highest percentage of ^{57}Fe was detected in plants fertilized with S1 (18%), but mainly in roots. The ^{57}Fe content in shoots increased along with the dose for plants fertilized with F and M.

DISCUSSION

In our work, three ^{57}Fe-NFs (F, M, and S) were obtained and exhaustively characterized by XRD, TEM with ED, EELS and EFTEM, X-ray absorption spectroscopy (XANES and EXAFS) and Mössbauer spectroscopy. There were similarities among them with regard to the iron phase and iron (hydr)oxide content with the polyhedral arrangement motif of the ferrihydrite. Most agricultural soils contain natural ferrihydrite NPs, which may contribute to iron nutrition of plants. Many authors (Römheld and Nikolic, 2007; Colombo et al., 2012; Cieschi et al., 2017) reported ferrihydrite formation during the iron humate synthesis, they characterized and studied the relationship between the particle size, pH and stability. Angelico et al. (2014) and Colombo et al. (2015) have shown that the phase of iron (hydr)oxide formed in the presence of HS depends on pH, oxidation rate, and Fe:HS ratio.

Our pot experiments revealed that the ^{57}Fe-NFs were capable of supplying ^{57}Fe to the plants and it was transported from root to shoot and reached the pods (**Figures 6**, **8**, **9A**). In particular, we have observed that the plants fertilized with the product M presented the highest contents of ^{57}Fe in shoots, pods and the soil soluble fraction, according to the two-way ANOVA statistical analysis (**Table 4**). This iron humate was prepared taking into account its maximum complexing capacity in order to avoid the iron flocculation in calcareous conditions. Then, the Fe:HS ratio obtained after the synthesis was the lowest (0.12 g Fe g org. C^{-1})

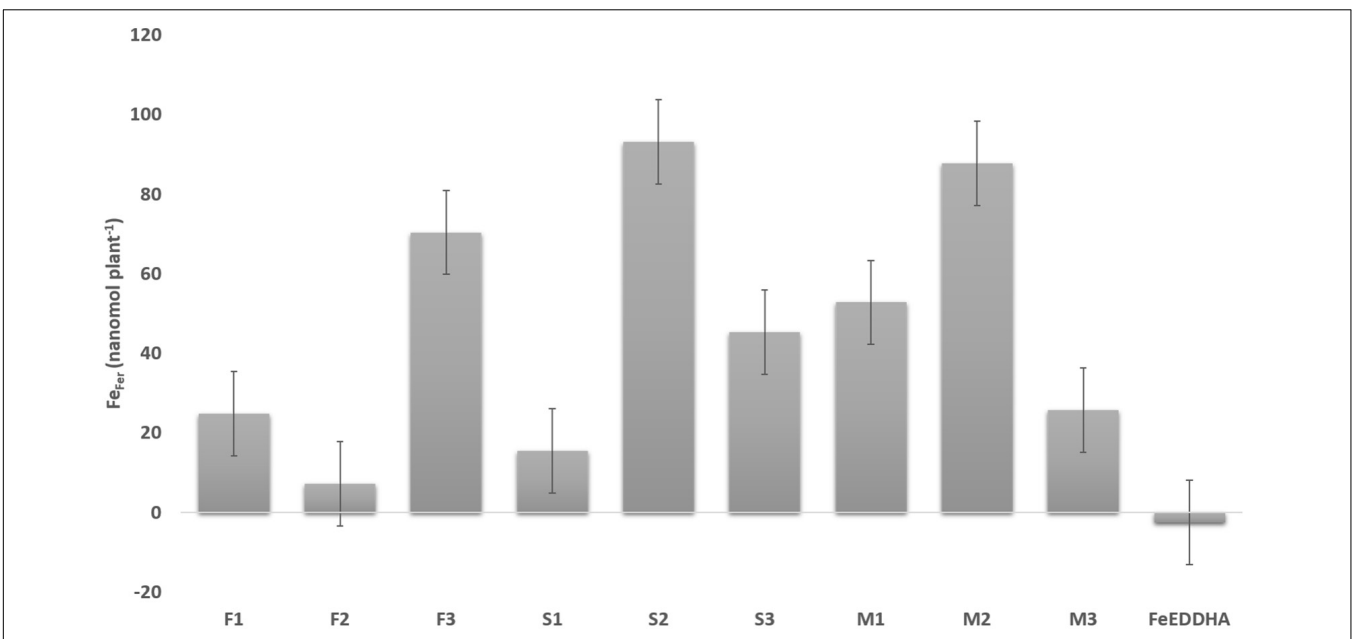

FIGURE 7 | Differences in Fe_{Fer} uptake (%) in soybean leaves of plants fertilized with the ^{57}Fe products F, S, and M in three doses: (1) 35, (2) 75, and (3) 150 μmol ^{57}Fe pot^{-1} or 50 μmol $^{57}FeEDDHA$ pot^{-1}, between the first (15 DAF) and the second sampling (48 DAF). Results are expressed as averages ± standard error, $n = 5$.

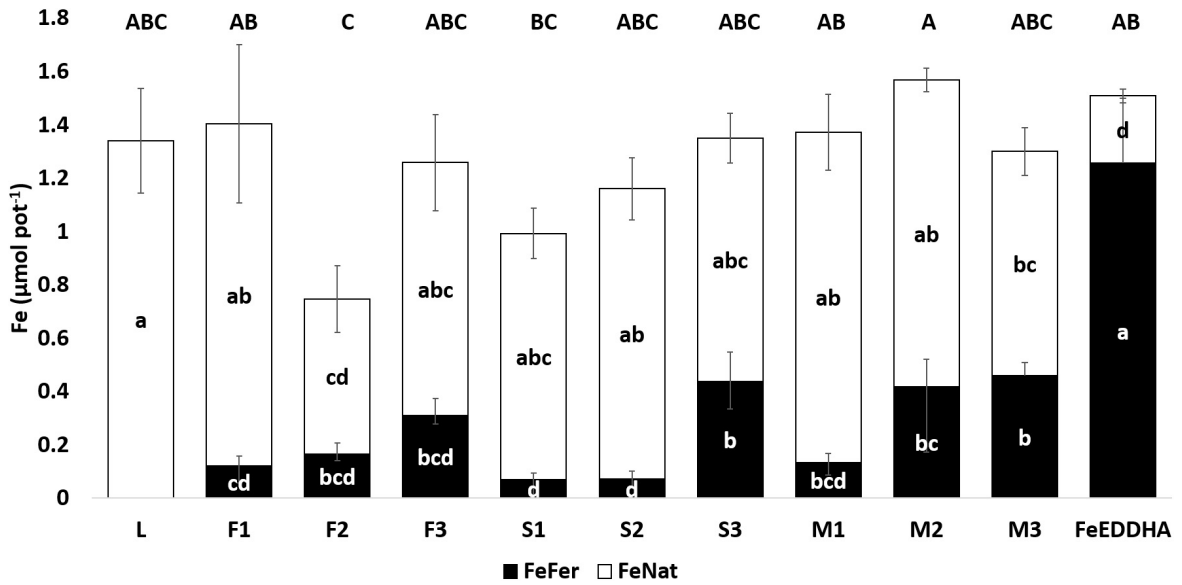

FIGURE 8 | Fe_{Fer} and Fe_{Nat} (µmol pot^{-1}) contents in soybean pods of control plants (L) and plants fertilized with the ^{57}Fe products F, S, and M in three doses: (1) 35, (2) 75, and (3) 150 µmol ^{57}Fe pot^{-1} or 50 µmol $^{57}FeEDDHA$ pot^{-1} at 48 DAF. For each series different letters denote significant differences among the treatments according to Duncan's Test ($p < 0.05$). Lowercase letters correspond to Fe_{Fer} and Fe_{Nat} and capital letters correspond to Fe_{Total} statistical results. Results are expressed as averages ± standard error, $n = 5$.

which suggested that the high content of HS has stabilized the poorly ordered ^{57}Fe structures entrapped into humic matrix and favored the iron uptake by the soybean plants. Similar results were obtained by Kulikova et al. (2017) for their product Fe-HA (4% Fe, 68% HA) which was tested with wheat plants grown under hydroponic conditions.

In soil, the ^{57}Fe-NFs presented an increasing tendency to remain available to the plant requirements for the different growth stages (**Figure 9C**). In addition, the slow and continuous iron release from these NFs has confirmed their long-term effect in providing iron in calcareous conditions in contrast to the short-term effect of the iron synthetic chelate (**Figure 7**), reported in the previous studies (Cieschi et al., 2017). Moreover, in a recent hydroponic assay (Cieschi and Lucena, 2018), plants fertilized with FeEDDHA presented the highest Fe contents in roots after 10 days but at longer term exposition (60 days) of the plants treated with iron humates yielded iron uptake similar to the plants fertilized with the iron synthetic chelate. We hypothesized that an increase in iron humate concentration in the rhizosphere might cause a decrease in the transcription level of the genes involved in the iron transport and shoot growth, and so the iron transport from root to shoot decelerated. Several authors (Aguirre et al., 2009; Tomasi et al., 2013; Olaetxea et al., 2015; Zamboni et al., 2016) suggested that the efficiency of the root transcriptional response to Fe supply depends on the nature (physicochemical characteristics) of the ligand and its capability to activate Fe uptake mechanisms and translocations. In particular, Zamboni et al. (2016) demonstrated that Fe complexed to water-extractable HSs from peat did not cause relevant changes in the root transcriptome of tomato plants with respect to Fe-deficient plants. However, Aguirre et al. (2009) observed that high doses of a purified humic acid from leonardite applied to cucumber plants promoted the upregulation of CsFRO1 and CsIRT1 gene expression for 48 and 72 h while these genes were downregulated for 96 h. The authors suggested that it may be associated to root iron accumulation and/or iron translocation. Olaetxea et al. (2018) proposed that it is very likely that the action of HS on plant mineral nutrition involves a coordinated functional crosstalk between indirect and direct HS effects on the soil–plant system. Soil and, in particular, the rhizosphere are extremely complex environments with a large degree of heterogeneity down to the nanoscale where the interactions between soil constituents, plant roots, and microorganisms take place (Mimmo et al., 2014). Thus, the long-term effect would be an expected result.

With respect to the uptake of nanoparticles by plants, Kulikova et al. (2014) have observed that particles of HA were transferred from root to shoot of wheat seedlings through the plant vascular system and Nardi et al. (2002) have previously observed the same mechanism for low molecular weight fraction of HA (<2.5 kDa). Furthermore, Pariona et al. (2016) have recently detected by 3D microscopic techniques, clusters of hematite and ferrihydrite NPs in endodermis, xylem, phloem vessels, and cell walls of the xylem vessels of maize stems of plants grown in hydroponic conditions. The extensive studies of R. Pinton and S. Cesco's group (Cesco et al., 2000, 2002; Nikolic et al., 2003; Colombo et al., 2012, 2014; Tomasi et al., 2013; Mimmo et al., 2014) modeled variety of interactions in soils of iron humate complexes according to the molecular weight of HS. They have demonstrated that low-molecular weight HS can form soluble complexes of Fe and move toward the root, acting as natural substrates for the membrane Fe (III)-chelate reductase

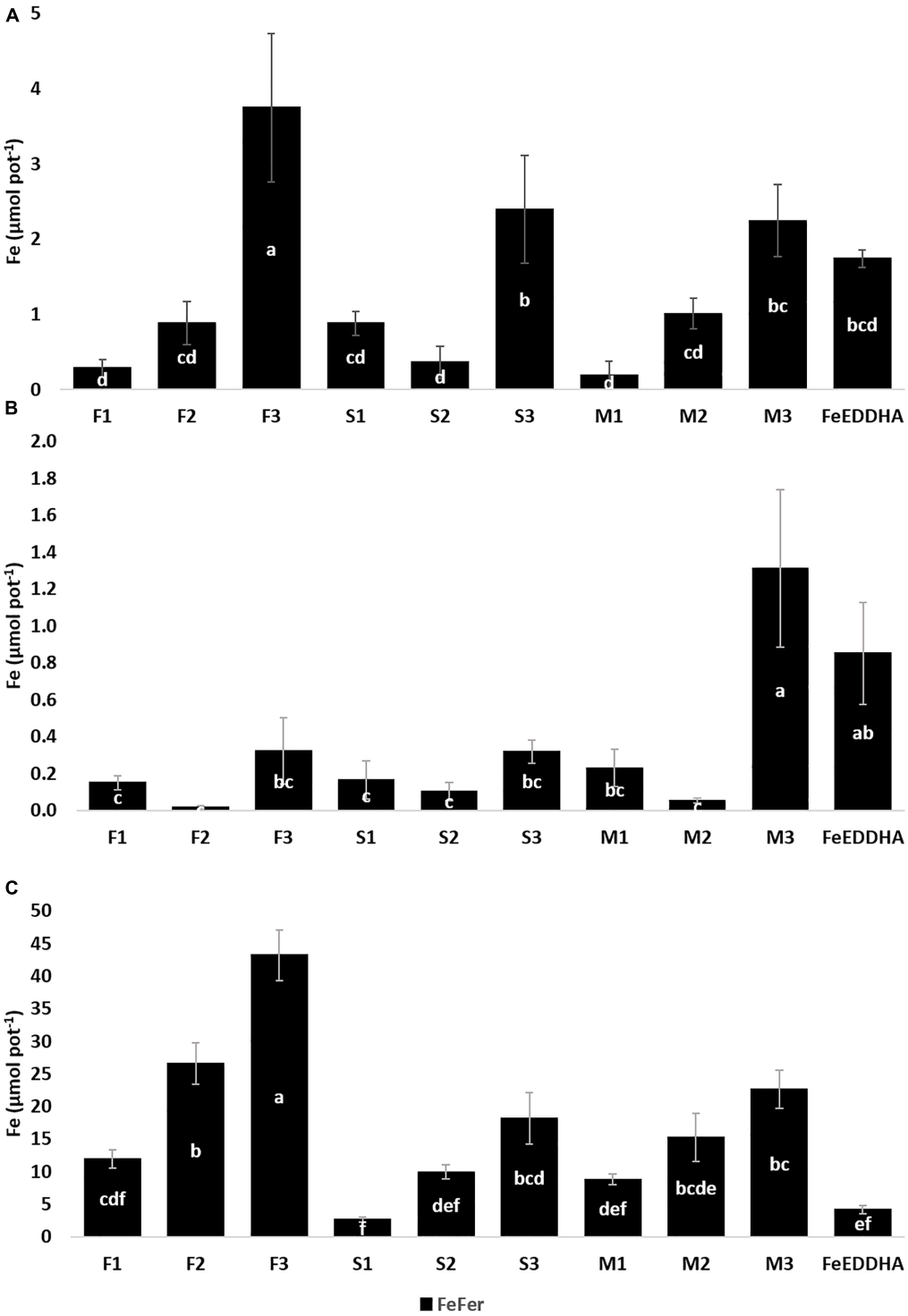

FIGURE 9 | Fe_{Fer} (µmol pot^{-1}) content in soybean roots of plants fertilized with the ^{57}Fe products F, S, and M in three doses: (1) 35, (2) 75, and (3) 150 µmol ^{57}Fe pot^{-1} or 50 µmol $^{57}FeEDDHA$ pot^{-1} **(A)**, soluble soil fraction **(B)**, and available soil fraction **(C)** at 48 DAF. For each series different letters denote significant differences among the treatments according to Duncan's Test ($p < 0.05$). Results are expressed as averages ± standard error, $n = 5$.

and stimulate the proton release promoting the Fe acquisition for Strategy I plants. Recently, Homonnay et al. (2016) have carried out a preliminary study about iron nanoparticles in plant nutrition and hypothesized that it would be possible to consider for plant nutrition supply in the soil iron-based oxide or oxy-hydroxide nanoparticles since storage of iron in cells

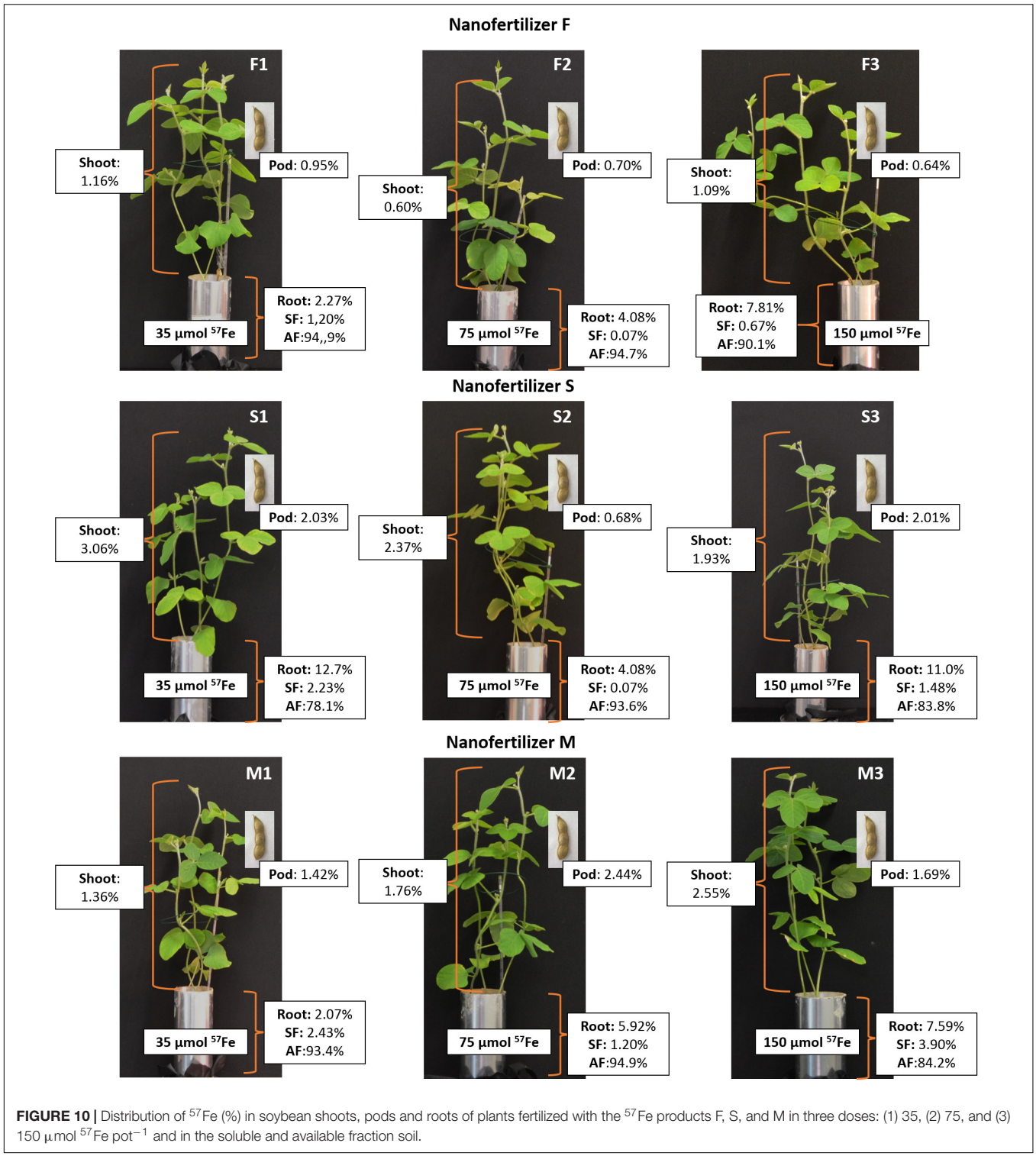

FIGURE 10 | Distribution of ^{57}Fe (%) in soybean shoots, pods and roots of plants fertilized with the ^{57}Fe products F, S, and M in three doses: (1) 35, (2) 75, and (3) 150 µmol ^{57}Fe pot^{-1} and in the soluble and available fraction soil.

usually implies formation of ferritin which has a certain similarity with ferrihydrite/ferric hydrous oxide nanoparticles with variable amounts of phosphate.

Further research is needed to redesign the classical model of the iron uptake by plant with more studies that consider uptake from the Fe-NPs.

CONCLUSION

According to Lal (2008), in the context of sustainable agriculture, applying innovative nanotechnology in agriculture is regarded as one of the promising approaches to significantly increase crop production. The Fe-NFs can be considered as a part of

a novel technology in line with the precision and sustainable agriculture. They are iron-natural complex NPs synthetized from leonardite and they contain ferrihydrite in their structures which was properly and widely characterized. Moreover, the ^{57}Fe-NFs used in this paper are capable of supplying Fe to the plants, transport it from root to shoot and reach the soybean pods. The slow and continuous iron release of these ^{57}Fe-NFs confirms their long-term effect in providing iron in calcareous conditions while in soil, they tends to remain available to the plant requirements for the different growth stages.

Although further research is needed about the contribution of iron nanoparticles in plant nutrition, the Fe-NFs offers a natural, low cost and environmental option to the traditional iron fertilization in calcareous soils.

AUTHOR CONTRIBUTIONS

MC: synthesis of ^{57}Fe-NFs, carried out of the soil experiment, data processing, and manuscript preparation. AP: synthesis of ^{57}Fe-NFs and manuscript preparation. VL: XRD, TEM, and EXAFS data processing. DV: ICP AES analysis of ^{57}Fe-NFs samples. DP: Mössbauer spectroscopy. AV: EXAFS spectroscopy. IP: design and supervision of the synthesis and characterization of the ^{57}Fe-NFs, data interpretation, and manuscript preparation. JL: design and supervision of the soil experiment, data interpretation, and manuscript preparation.

FUNDING

The Russian Science Foundation (16-14-00167), the Russian Foundation for Basic Research (18-29-25065), and the Spanish Ministry of Science and Innovation (AGL2013-44474-R) have financially supported this research.

ACKNOWLEDGMENTS

The authors would like to acknowledge generous help and professional assistance of Dr. Oleg Schlaykhtin with freeze-drying the samples of NFs. MC expresses acknowledgment to Erasmus+ International Credit Mobility Program Alliance 4 Universities (A-4U) KA-107 for an academic stay at the Lomonosov MSU devoted to synthesis of ^{57}Fe-labeled NFs. JL and MC acknowledge the financial support of the Spanish Ministry of Science and Innovation (grant AGL2013-44474-R). JL and MC also acknowledge to the Comunidad de Madrid (Spain) and Structural Funds 2014-2020 (ERDF and ESF) for the financial support (project AGRISOST-CM S2018/BAA-4330). AP, VL, DV, and IP acknowledge financial support of the Russian Science Foundation (grant # 16-14-00167) in part of the ICP-OES, XRD, TEM, and EFTEM measurements. VL and IP acknowledge support of Russian Foundation for Basic Research project 18-29-25065 for EXAFS measurements and interpretations of the obtained samples of ^{57}Fe-labeled NFs. The use of the Carl Zeiss Libra 200MC TEM is supported by Lomonosov Moscow State University Program of Development. XAS were measured at the unique scientific facility Kurchatov Synchrotron Radiation Source supported by the Ministry of Education and Science of the Russian Federation (project code RFMEFI61917X0007).

SUPPLEMENTARY MATERIAL

The Supplementary Material for this article can be found online at: https://www.frontiersin.org/articles/10.3389/fpls.2019.00413/full#supplementary-material

REFERENCES

Aguirre, E., Leménager, D., Bacaicoa, E., Fuentes, M., Baigorri, R., Zamarreño, A. M., et al. (2009). The root application of a purified leonardite humic acid modifies the transcriptional regulation of the main physiological root responses to Fe deficiency in Fe-sufficient cucumber plants. *Plant Physiol. Biochem.* 47, 215–223. doi: 10.1016/j.plaphy.2008.11.013

Álvarez-Fernández, A., Pérez-Sanz, A., and Lucena, J. J. (2001). Evaluation of effect of washing procedures on mineral analysis of orange and peach leaves sprayed with seaweed extracts enriched with iron. *Commun. Soil Sci. Plant Anal.* 32, 157–170. doi: 10.1081/CSS-100103000

Angelico, R., Ceglie, A., He, J. Z., Liu, Y. R., Palumbo, G., and Colombo, C. (2014). Particle size, charge and colloidal stability of humic acids coprecipitated with ferrihydrite. *Chemosphere* 99, 239–247. doi: 10.1016/j.chemosphere.2013.10.092

Benedicto, A., Hernandez-Apaolaza, L., Rivas, I., and Lucena, J. J. (2011). Determination of 67Zn distribution in navy bean (*Phaseolus vulgaris* L.) after foliar application of 67Zn-lignosulfonates using isotope pattern deconvolution. *J. Agric. Food. Chem.* 59, 8829–8838. doi: 10.1021/jf2002574

Bolon, Y. T., Joseph, B., Cannon, S. B., Graham, M. A., Diers, B. W., Farmer, A. D., et al. (2010). Complementary genetic and genomic approaches help characerize the linkage group I seed protein QTL. *BMC Plant Biol.* 10:41. doi: 10.1186/1471-2229-10-41

Briat, J. F., Dubos, C., and Gaymard, F. (2015). Iron nutrition, biomass production, and plant product quality. *Trends Plant Sci.* 20, 33–40. doi: 10.1016/j.tplants.2014.07.005

Cakmak, I. (2002). Plant nutrition research: priorities to meet human needs for food in sustainable ways. *Plant Soil* 247, 3–24. doi: 10.1007/978-94-017-2789-1_1

Canellas, L. P., Olivares, F. L., Aguiar, N. O., Jones, D. L., Nebbioso, A., Mazzei, P., et al. (2015). Humic and fulvic acids as biostimulants in horticulture. *Sci. Hortic.* 196, 15–27. doi: 10.1016/j.scienta.2015.09.013

Cesco, S., Nikolic, M., Römheld, V., Varanini, Z., and Pinton, R. (2002). Uptake of 59Fe from soluble 59Fe-humate complexes by cucumber and barley plants. *Plant Soil* 241, 121–128. doi: 10.1023/A:1016061003397

Cesco, S., Römheld, V., Varanini, Z., and Pinton, R. (2000). Solubilization of iron by water-extractable humic substances. *J. Plant Nutr. Soil Sci.* 163, 285–290. doi: 10.1002/1522-2624(200006)163:3<285::AID-JPLN285>3.0.CO;2-Z

Cieschi, M. T., Caballero-Molada, M., Menéndez, N., Naranjo, M. A., and Lucena, J. J. (2017). Long-term effect of a leonardite iron humate improving Fe nutrition as revealed in silico, in vivo, and in field experiments. *J. Agric. Food Chem.* 65, 6554–6563. doi: 10.1021/acs.jafc.7b01804

Cieschi, M. T., and Lucena, J. J. (2018). Iron and humic acid accumulation on soybean roots fertilized with leonardite iron humates under calcarous conditions. *J. Agric. Food Chem.* 66, 13386–13396. doi: 10.1021/acs.jafc.8b04021

Colombo, C., Palumbo, G., He, J. Z., Pinton, R., and Cesco, S. (2014). Review on iron availability in soil: interaction of Fe minerals, plants, and microbes. *J. Soils Sediments* 14, 538–548. doi: 10.1007/s11368-013-0814-z

Colombo, C., Palumbo, G., Sellitto, V. M., Cho, H. G., Amalfitano, C., and Adamo, P. (2015). Stability of coprecipitated natural humic acid and ferrous iron under oxidative conditions. *J. Geochem. Explor.* 151, 50–56. doi: 10.1016/j.gexplo.2015.01.003

Colombo, C., Palumbo, G., Sellitto, V. M., Rizzardo, C., Tomasi, N., Pinton, R., et al. (2012). Characteristics of insoluble, high molecular weight iron-humic substances used as plant iron sources. *Soil Sci. Soc. Am. J.* 76, 1246–1256. doi: 10.2136/sssaj2011.0393

Dholakia, P. V. (2016). Preparation of nanopartical liquid organic fertilizer and its effect on various crops. *Int. J. Sci. Res. Sci. Eng. Tech.* 2, 781–785.

Dimkpa, C. O., and Bindraban, P. S. (2017). Nanofertilizers: new products for the industry? *J. Agric. Food Chem.* 66, 6462–6473. doi: 10.1021/acs.jafc.7b02150

Food and Agriculture Organization of the United Nations [FAO] (2017). *The Future of Food and Agriculture. Trends and Challenges*. Rome: FAO.

Fuentes, M., Bacaicoa, E., Rivero, M., Zamarreño, ÁM., and García-Mina, J. M. (2018). Complementary evaluation of iron deficiency root responses to assess the effectiveness of different iron foliar applications for chlorosis remediation. *Front. Plant Sci.* 9:351. doi: 10.3389/fpls.2018.00351

Ghafariyan, M. H., Malakouti, M. J., Dadpour, M. R., Stroeve, P., and Mahmoudi, M. (2013). Effects of magnetite nanoparticles on soybean chlorophyll. *Environ. Sci. Technol.* 47, 10645–10652. doi: 10.1021/es402249b

Homonnay, Z., Tolnai, G., Fodor, F., Solti, Á, Kovács, K., Kuzmann, E., et al. (2016). Iron oxide nanoparticles for plant nutrition? A preliminary Mössbauer study. *Hyperfine Interact.* 237, 1–9. doi: 10.1007/s10751-016-1334-1

Hunter, J. D. (2007). Matplotlib: a 2D graphics environment. *Comput. Sci. Eng.* 9, 99–104. doi: 10.1109/MCSE.2007.55

ISO 3696:1987 (1987). *Water for Analytical Laboratory Use–Specification and Test Methods*. Available at: https://www.iso.org/standard/9169.html (accessed April, 1987).

Janmohammadi, M., Navid, A., Segherloo, A. E., and Sabaghnia, N. (2016). Impact of nano-chelated micronutrients and biological fertilizers on growth performance and grain yield of maize under deficit irrigation condition. *Biologija* 62, 134–147. doi: 10.6001/biologija.v62i2.3339

Kovács, K., Czech, V., Fodor, F., Solti, A., Lucena, J. J., Santos-Rosell, S., et al. (2013). Characterization of Fe-leonardite complexes as novel natural iron fertilizers. *J. Agric. Food Chem.* 61, 12200–12210. doi: 10.1021/jf404455y

Kulikova, N., Badun, G. A., Korobkov, V. I., Chernysheva, M. G., Tsvetkova, E. A., Abroskin, D. P., et al. (2014). Accumulation of coal humic acids by wheat seedlings: direct evidence using tritium autoradiography and occurrence in lipid fraction. *J. Plant Nutr. Soil Sci.* 177, 875–883. doi: 10.1002/jpln.201300648

Kulikova, N. A., Polyakov, A. Y., Lebedev, V. A., Abroskin, D. P., Volkov, D. S., Pankratov, D. A., et al. (2017). Key roles of size and crystallinity of nanosized iron hydr(oxides) stabilized by humic substances in iron bioavailability to plants. *J. Agric. Food Chem.* 65, 11157–11169. doi: 10.1021/acs.jafc.7b03955

Lal, R. (2008). Promise and limitations of soils to minimize climate change. *J. Soil Water Conserv.* 63, 113A–118A. doi: 10.2489/jswc.63.4.113A

Liu, R., and Lal, R. (2015). Potentials of engineered nanoparticles as fertilizers for increasing agronomic productions. *Sci. Total Environ.* 514, 131–139. doi: 10.1016/j.scitotenv.2015.01.104

López-Rayo, S., Di Foggia, M., Bombai, G., Yunta, F., Rodrigues Moreira, E., Filippini, G., et al. (2015). Blood-derived compounds can efficiently prevent iron deficiency in the grapevine. *Aust. J. Grape Wine Res.* 21, 135–142. doi: 10.1111/ajgw.12109

Maillot, F., Morin, G., Wang, Y., Bonnin, D., Ildefonse, P., Chaneac, C., et al. (2011). New insight into the structure of nanocrystalline ferrihydrite: EXAFS evidence for tetrahedrally coordinated Iron (III). *Geochim. Cosmochim. Acta* 75, 2708–2720. doi: 10.1016/j.gca.2011.03.011

Manceau, A., and Gates, W. (1997). Surface structural model for ferrihydrite. *Clays Clay Miner.* 45, 448–460. doi: 10.1346/CCMN.1997.0450314

MAPA (1994). *Métodos Oficiales De Análisis. Servicio De Publicaciones. Spanish Ministry of Agriculture, F. and F. MAPA Official Methods of Analysis*, Vol. III. Madrid: MAPA.

Martín-Fernández, C., López-Rayo, S., Hernández-Apaolaza, L., and Lucena, J. J. (2017a). Timing for a sustainable fertilisation of Glycine max by using HBED/Fe3+ and EDDHA/Fe3+ chelates. *J. Sci. Food Agric.* 97, 2773–2781. doi: 10.1002/jsfa.8105

Martín-Fernández, C., Solti, Á, Czech, V., Kovács, K., Fodor, F., Gárate, A., et al. (2017b). Response of soybean plants to the application of synthetic and biodegradable Fe chelates and Fe complexes. *Plant Physiol. Biochem.* 118, 579–588. doi: 10.1016/j.plaphy.2017.07.028

Michel, F. M., Ehm, L., Antao, S. M., Lee, P. L., Chupas, P. J., Liu, G., et al. (2007). The structure of ferrihydrite, a nanocrystalline material. *Science* 316, 1726–1729. doi: 10.1126/science.1142525

Mimmo, T., Del Buono, D., Terzano, R., Tomasi, N., Vigani, G., Crecchio, C., et al. (2014). Rhizospheric organic compounds in the soil-microorganism-plant system: their role in iron availability. *Eur. J. Soil Sci.* 65, 629–642. doi: 10.1111/ejss.12158

Nadal, P., García-Delgado, C., Hernández, D., López-Rayo, S., and Lucena, J. J. (2012). Evaluation of Fe-N,N'-Bis(2-hydroxybenzyl)ethylenediamine-N,N'-diacetate (HBED/Fe3+) as Fe carrier for soybean (*Glycine max*) plants grown in calcareous soil. *Plant Soil* 360, 349–362. doi: 10.1007/s11104-012-1246-z

Naderi, M. R., and Danesh-Shahraki, A. (2013). Nanofertilizers and their roles in sustainable agriculture. *Int. J. Agric. Crop Sci.* 5, 2229–2232.

Nardi, S., Pizzeghello, D., Muscolo, A., and Vianello, A. (2002). Physiological effects of humic substances on higher plants. *Soil Biol. Biochem.* 34, 1527–1536. doi: 10.1016/S0038-0717(02)00174-8

Nečas, D., and Klapetek, P. (2012). Gwyddion: an open-source software for SPM data analysis. *Cent. Eur. J. Phys.* 10, 181–188. doi: 10.2478/s11534-011-0096-2

Nikolic, M., Cesco, S., Römheld, V., Varanini, Z., and Pinton, R. (2003). Uptake of iron (59Fe) Complexed to water-extractable humic substances by sunflower leaves. *J. Plant Nutr.* 26, 2243–2252. doi: 10.1007/s11104-009-0091-1

Olaetxea, M., De Hitaa, D., Garcia, A., Fuentes, M., Baigorri, R., Mora, V., et al. (2018). Hypothetical framework integrating the main mechanisms involved in the promoting action of rhizospheric humic substances on plant root- and shootgrowth. *Appl. Soil Ecol.* 123, 521–537. doi: 10.1016/j.apsoil.2017.06.007

Olaetxea, M., Mora, V., Bacaicoa, E., Garnica, M., Fuentes, M., Casanova, E., et al. (2015). Abscisic acid regulation of root hydraulic conductivity and aquaporin gene expression is crucial to the plant shoot growth enhancement caused by rhizosphere humic acids. *Plant Physiol.* 169, 2587–2596. doi: 10.1104/pp.15.00596

Pankratov, D. A., Dolzhenko, V. D., Stukan, R. A., Al Ansari, Y. F., Savinkina, E. V., and Kiselev, Y. M. (2013). Investigation of Iron (III) complex with crown-porphyrin. *Hyperfine Interact.* 222, 1–11. doi: 10.1007/s10751-011-0378-5

Pariona, N., Martinez, A. I., Hdz-García, H. M., Cruz, L. A., and Hernandez-Valdes, A. (2016). Effects of hematite and ferrihydrite nanoparticles on germination and growth of maize seedlings. *Saudi J. Biol. Sci.* 24, 1547–1554. doi: 10.1016/j.sjbs.2016.06.004

Rodríguez-Castrillón, J. Á, Moldovan, M., García Alonso, J. I., Lucena, J. J., García-Tomé, M. L., and Hernández-Apaolaza, L. (2008). Isotope pattern deconvolution as a tool to study iron metabolism in plants. *Anal. Bioanal. Chem.* 390, 579–590. doi: 10.1007/s00216-007-1716-y

Rodríguez-Lucena, P., Hernández, D., Hernández-Apaolaza, L., and Lucena, J. J. (2010). Revalorization of a two-phase olive mill waste extract into a micronutrient fertilizer. *J. Agric. Food Chem.* 58, 1085–1092. doi: 10.1021/jf903185z

Römheld, V., and Nikolic, M. (2007). "Iron," in *Handbook of Plant Nutrition*, eds A. V. Barker and D. J. Pilbeam (Boca raton, FL: CRC Press).

Rose, M. T., Patti, A. F., Little, K. R., Brown, A. L., Jackson, W. R., and Cavagnaro, T. R. (2014). A meta-analysis and review of plant-growth response to humic substances: practical implications for agriculture. *Adv. Agron.* 124, 37–89. doi: 10.1016/B978-0-12-800138-7.00002-4

Sánchez-Alcalá, I., del Campillo, M. C., Barrón, V., and Torrent, J. (2012). Pot evaluation of synthetic nanosiderite for the prevention of iron chlorosis. *J. SCI. Food Agric.* 92, 1964–1973. doi: 10.1002/jsfa.5569

Schwertmann, U., and Cornell, R. (1992). *Iron Oxides in the Laboratory: Preparation and Characterization*. Hoboken, NJ: John Wiley & Sons.

Schwertmann, U., Friedl, J., and Stanjekl, H. (1999). From Fe (III) ions to ferrihydrite and then to hematite. *J. Colloid Interface Sci.* 209, 215–223. doi: 10.1006/jcis.1998.5899

Soltanpour, P. N., and Schwab, A. P. (1977). A new soil test for simultaneous extraction of macro- and micro-nutrients in alkaline soils. *Commun. Soil Sci. Plant Anal.* 8, 195–207. doi: 10.1080/00103627709366714

Sorkina, T. A., Polyakov, A. Y., Kulikova, N. A., Goldt, A. E., Philippova, O. I., Aseeva, A. A., et al. (2014). Nature-inspired soluble iron-rich humic compounds: new look at the structure and properties. *J. Soils Sediments* 14, 261–268. doi: 10.1007/s11368-013-0688-0

Tomasi, N., De Nobili, M., Gottardi, S., Zanin, L., Mimmo, T., Varanini, Z., et al. (2013). Physiological *and* molecular characterization of fe acquisition by tomato plants from natural Fe complexes. *Biol. Fertil. Soils* 49, 187–200. doi: 10.1007/s00374-012-0706-1

United Nations [UN] (2013). *World Population Prospects: The 2012 Revision*. Available at: https://population.un.org/wpp/Publications/Files/WPP2012_HIGHLIGHTS.pdf (accessed December 1, 2018).

Vasconcelos, M. W., and Grusak, M. A. (2014). Morpho-physiological parameters affecting iron deficiency chlorosis in soybean (*Glycine max* L.). *Plant Soil* 374, 161–172. doi: 10.1007/s11104-013-1842-6

Villén, M., Lucena, J. J., Cartagena, M. C., Bravo, R., García-Mina, J., and de la Hinojosa, M. I. M. (2007). Comparison of two analytical methods for the evaluation of the complexed metal in fertilizers and the complexing capacity of complexing agents. *J. Agric. Food Chem.* 55, 5746–5753. doi: 10.1021/jf070422t

Ylivainio, K. (2010). Effects of iron (III) chelates on the solubility of heavy metals in calcareous soils. *Environ. Pollut.* 158, 3194–3200. doi: 10.1016/j.envpol.2010.07.004

Zamboni, A., Zanin, L., Tomasi, N., Avesani, L., Pinton, R., Varanini, Z., et al. (2016). Early transcriptomic response to Fe supply in Fe-deficient tomato plants is strongly influenced by the nature of the chelating agent. *BMC Genomics* 17:35. doi: 10.1186/s12864-015-2331-5

Conflict of Interest Statement: The authors declare that the research was conducted in the absence of any commercial or financial relationships that could be construed as a potential conflict of interest.

Capítulo V: Discusión General

Chapter V: General Discussion

The physicochemical characteristics and origin of HA determine its efficiency in agronomical uses, so its characterization is crucial for the diagnosis of its efficiency and improvement in its agronomic application. Therefore, it is important to obtain a detailed description profile of the specific HS to be used. The diagenesis of each coal differs radically depending on biological residues and coal generating conditions (*Francioso et al*. 2005). The only way to characterize such HS is to apply a multiple-technique approach which can generally provide a more coherent picture of this complex molecular system. Moreover, the relationship between structure and biological activity of HS is of great importance in understanding the biological effects in plants and their use (*Nardi et al*. 2017).

In the present thesis, four humates were chemical and spectroscopically characterized: a leonardite iron humate (LIH in Chapter 3.1) and the iron humic nanofertilizers (^{57}Fe-NFs) named F (prepared with $^{57}Fe(NO_3)_3$), M and S (prepared with $^{57}Fe_2(SO_4)_3$ at different ratios, see Chapter 4.2. The leonardite potassium humate (LKH), used for the LIH synthesis (Chapter 3.2), was extracted with alkali from African deposits while the potassium humate used for the synthesis of the ^{57}Fe-NFs belonged to German mines. The LKH was also chemical and spectroscopically characterized while the German potassium humate was only spectroscopically characterized.

Moreover, it is relevant to identify the iron forms in iron humates in order to know what to expect with respect to iron solubility in soil, iron cations in solution (Fe^{2+} or Fe^{3+}) and so, to predict how iron humates will affect in the iron nutrition of plants. Therefore, many analytical techniques were applied as Mössbauer spectroscopy (Chapter 3.1, 3.2 and 4.2) or XRD (Chapter 3.1, 4.2 and 4.2), EXAFS, and TEM (Chapter 4.2) to identify iron phases in the ^{57}Fe-NFs and to estimate the particle size. All the products presented ferrihydrite and Fe^{3+} polynuclear forms in their structures which are sources of available iron for plants. Humic substances can affect ferrihydrite formation by an indirect mechanism involving the stabilization of ferrihydrite by high molecular weight humic fractions, which thus tend to stabilize the poorly crystalline iron precipitate (*Colombo et al*. 2014). Many authors (*Römheld and Nikolic* 2007, *Colombo et al.* 2012) reported ferrihydrite formation during the iron humate synthesis since they characterized and studied the relationship between the particle size, pH and stability. *Angelico et al.* (2014) and *Colombo et al.* (2015) have shown that the phase of iron (hydr)oxide formed in the presence of HS depends on pH, oxidation rate, and Fe:HS ratio. Moreover, fresh soybean root material of plants treated with LIH was analyzed by SEM (Figure 11, Chapter 3.2) and presented a distribution of crystals of jarosite deposited over the root surface. The jarosite deposits increased over time, indicating a possible source of available iron for the soybean plants under calcareous conditions. According to *Bigham and Kirk Nordstrom* (2000), jarosite tends to form

at low pH (<5), high sulfate ion concentrations (>3000 mg L^{-1}) and in the presence of base cations. Thus, the jarosite formation was not expected under calcareous conditions (nutrient solution at pH >7), although it was one of the components of the LKH. The jarosite deposits were evidence of acidic points on the root surfaces and probably a reserve of iron that is released slowly as the plant needed it. This pH decreases to 4,32 in the soybean rhizosphere (Figure 12, Chapter 3.2) and the jarosite nucleation may be favored on these acidic points of soybean roots by the presence of glycine (*Crabbe et al.* 2015), the main amino acid exudates by the *Glycine* max roots (*Kuzmicheva et al.* 2017).

The LIH (Chapters 3.1 and 3.2) and ^{57}Fe-NFs (Chapter 4.2) exerted a long-term effect in providing iron to citrus trees and soybean plants due to their kinetic limitations. The stability of LIH and its kinetic capacity to release Fe(III) in solution along time, in the presence of different chelating agents (o,oEDDHA + BPDS + LIH or HBED + BPDS + LIH) were studied indirectly. As the experiment progressed, EDDHA or HBED chelated the Fe(III) released by LIH and BPDS chelated Fe(II) obtained by the Fe(III) reduction at that pH condition (Chapter 3.1). So, LIH presented a slow kinetic behavior since it released after 97 days, 67% of Fe^{3+} in the presence of HBED and 85% of Fe^{3+} in the presence of *o,o*EDDHA. Then, a part of the Fe(III) was reduced to Fe(II) at pH 7 by the reducing capacity of humic substances and the Fe(II) chelated by BPDS. Under these experimental conditions, BPDS showed similar behavior independently of the Fe(III) chelating agent in solution. Moreover, the slow iron humate kinetic was confirmed with other ligand competition experiments (Figure 7, Chapter 4.1) which demonstrated that *o,o*EDDHA chelated the 50% of Fe(III) present in LIH in 17 days while HBED chelated the same percentage in almost 30 days. Both chelating agents are strong Fe(III) chelators with high stability constants. For FeEDDHA, log K is 35.09 (*Yunta et al.* 2003) and for FeHBED the log K is 39.02 (*López-Rayo et al.* 2009) while for an iron humate obtained through iron complexation of humic acids from leonardite the log K (apparent stability constant) is 4.67 (*Fuentes et al.* 2013). According to the high affinity of the chelating agent for Fe(III), a fast iron release was expected from the LIH, but in our study, the kinetics is quite slow. *Nuzzo et al.* (2013) demonstrated that the conformational structure of humic substance changes when it is complexed with iron. Fulvic acids tend to form a compact network of intra and intermolecular complexes with iron cations while humic acids used to form small aggregates and thermodynamically stable associations. Since the LIH is formed by 70% of humic acids and 30% of fulvic acids, the kinetic reaction would depend mainly on the ability of the chelating agents to produce the disaggregation of the humic acids to chelate the Fe(III). So, the most stable chelate (FeHBED) was formed slower than FeEDDHA.

Iron and humic acid accumulation on soybean roots were observed in a hydroponic bioassay (Chapter 3.2). High LIH doses frequently applied may have caused partial blockage of root cell-wall pores as other authors observed before (*Nardi et al.* 2002, *Asli and Neumann* 2010, *Kulikova et al.* 2014). Moreover, *Olaetxea et al.* (2015) concluded that the effect caused by a root-applied humic acid from leonardite on shoot growth (beneficial or detrimental) would depend on the humic acid concentration in the rhizosphere. In addition, the shoot growth may decreased because the transcription levels of the genes involved in the iron transport decreased, and so the iron transport from root to shoot decelerated as many authors (*Aguirre et al.* 2009, *Tomasi et al.* 2013, *Olaetxea et al.* 2015) observed for the transcription of genes encoding Fe(III) chelate reductase (LeFRO1) or encoding for Fe(II) transporters (LeIRT1 and LeIRT2). In fact, LIH (Figure 9, Chapter 3.1) has repressed among 40−50% of the expression genes involved in the iron transport system (FET3, FTR1, SIT1, and TIS11) of the *Saccharomyces cerevisiae* cells which suggests that the iron levels increased in the LIH treated cells due to the gene expression in the high-affinity iron transport system regulated for Aft1, a transcriptional factor whose activity increases in conditions of iron absence and decreases when the iron concentration in the cell increases. However, *Saccharomyces cerevisiae* cells treated with LIH has grown 5% less than with o,oEDDHA/Fe^{3+} (Figure 8, Chapter 3.1).

On the other hand, very low ferric chelate reductase (FC-R) activity was detected when LIH was applied to cucumber plants (Figure 6, Chapter 3.2) and no FC-R activity was noticed for soybean plants. Furthermore, several authors (*Aguirre et al.* 2009, *Tomasi et al.* 2013, *Olaetxea et al.* 2015, *Zamboni et al.* 2016) have suggested that the efficiency of the root transcriptional response to Fe supply depends on the nature (physicochemical characteristics) of the ligand and its capability to activate Fe uptake mechanisms and translocation. *Zamboni et al.* (2016) demonstrated that Fe complexed to water-extractable HS from peat did not cause relevant changes in the root transcriptome of tomato plants with respect to Fe-deficient plants. On the other hand, Aguirre et al. (2009) observed that high doses of a purified humic acid from leonardite applied to cucumber plants promoted the upregulation of CsFRO1 and CsIRT1 gene expression for 48 and 72 h while these genes were downregulated at 96 h. *Nardi et al.* (2017) and *Olaetxea et al*. (2018) have proposed that it is very likely that the action of HS on plant mineral nutrition involves a coordinated functional cross-talk between indirect and direct HS effects on the soil-plant system. Therefore, the long-term effect observed in the soil experiments would be a consequence of the iron humate concentration in the rhizosphere and its physicochemical characteristics, that may condition the iron transport up or downregulating the gene expressions.

A chlorotic orange (*Citrus clementine Hort. ex Tanaka*, ClemenRubı´PRI 23) orchard situated in Bétera (Valencia, Spain) was fertilized by drip irrigation with LIH and FeEDDHA from May to August 2014 (Chapter 3.1). LIH provided slow and increasing iron nutrition to citrus growth in calcareous conditions and corrected the iron deficiency for the first year of application with similar results to the FeEDDHA fertilization. However, trees treated with FeEDDHA showed the highest results at the first foliar sampling, indicating a short-term effect in correcting the deficiency while orange trees treated with LIH presented and incremented concentration tendency in each sampling, confirming the kinetic results.

Taking into account the kinetic constraints that limit the iron humate efficiency, this thesis studied three improvement possibilities:

1. Enhance of the iron humate dissolution in the rhizosphere.
2. Improvement of the iron humate kinetic by the help of iron synthetic chelates.
3. Decrease of the iron humate particle size.

Firstly, to enhance the iron humate dissolution in the rhizosphere and to avoid iron and humic acid accumulation on soybean roots caused by the weekly use of LIH, an one-time LIH application was carried out in a long-term hydroponic bioassay (Chapter 3.2). A circular effect of precipitation and dissolution of LIH that releases iron in the rhizosphere was proposed since the iron uptake by the plants was improved because of the amorphous iron (six lines ferrihydrite) and the jarosite crystals slow dissolution. The soybean plants treated with LIH250 (250 µmol Fe pot^{-1}) presented regreening of their leaves and no significant differences for the plants fertilized with FeEDDHA50 (50µmol Fe pot^{-1}).

Secondly, a possible synergic effect between mixtures of an iron leonardite humate (L/Fe^{3+}) with iron synthetic chelates (o,oEDDHA /Fe^{3+} or HBED/Fe^{3+}) was studied and the re-evaluation of the classical chelate shuttle effect model was done (Chapter 4.1). It was hypothesized that the labile iron bonded to the leonardite can be easily chelated by the synthetic ligand and transport it to the roots by the shuttle effect, ameliorating the soybean iron nutrition (*Lucena* 2003, *Schenkeveld et al.* 2014). The iron chelate shuttle effect was modeled for hydroponic or calcareous soil conditions when the iron humate/iron chelate mixtures are used. In the beginning, iron humate participates in the chelate shuttle mechanism providing available Fe to the chelating agent and then to the plants, showing a slight synergic effect. After a few days, the contribution of the chelates to the Fe nutrition decreases substantially, but the one from the humates is maintained. Similar behavior was observed for the ^{57}Fe-NFs (Figure 7, Chapter 4.2) and it was attributed to the long term effect exerted by iron humates.

The ratio with a better synergic effect was two parts of iron humates and one part of iron chelate and the most appropriate iron chelate that showed a better synergic effect was HBED/Fe^{3+} because of its lasting effect that fits better to the iron humate kinetics. The soluble iron in soil increased and the shoot to root iron translocation improved due to a synergic effect by a shuttle effect exerted by iron chelate in the mixture.

Finally, three ^{57}Fe humate nanofertilizers (^{57}Fe-NFs) were synthesized (Chapter 4.2) to improve iron humates efficiency in calcareous soils. The exhaustive characterization of ^{57}Fe-NFs demonstrated that products F and M contained large low-density particles typical for humic substances and inside of these particles the nano-sized contrast variations were observed, which correspond to the ferrihydrite nanoparticles with sizes <5 nm (Figures 1a,b, Chapter 4.2). According to *Baron-Epel et al.* (1988) only macromolecules with Stokes radii ≤3.3 nm may penetrate the soybean root cell wall unhindered and *Kulikova et al.* (2017) demonstrated that plants fertilized with iron humates only take up iron from very small and amorphous particles of ferric polymers incorporated into the HS matrix, whereas crystalline iron (hydr)oxide nanoparticles are readily adsorbed on roots but not translocated to the shoots. In particular, plants fertilized with the product M presented the highest contents of ^{57}Fe in shoots, pods and the soil soluble fraction (Table 4, Chapter 4.2). This iron humate was prepared to take into account its maximum complexing capacity to avoid the iron flocculation in calcareous conditions. Then, the Fe:HS ratio obtained after the synthesis was the lowest (0.12 g Fe g org. C^{-1}) which suggested that the high content of HS has stabilized the poorly ordered ^{57}Fe structures entrapped into the humic matrix and favored the iron uptake by the soybean plants.

In summary, this thesis contributes to the study of iron humates behavior in calcareous conditions. They are mainly high molecular weight humic acids with different particle sizes of which only macromolecules with Stokes radii ≤3.3 nm may penetrate the soybean root cell wall which means a minimum percentage. In addition, the iron humates usually contain Fe(III) as iron polynuclear structures, ferrihydrite and, in some cases, crystalline iron structures as jarosite. The iron dissolution is crucial for the iron release in the rhizosphere but, when the iron humate is applied in high concentrations, a dark brown coating covers the soybean roots that can blocks the cell wall pores and deactivates the Fe uptake mechanisms and translocations as iron genes expressions and iron transporters. Moreover, the iron humate preparation must be controlled to avoid iron flocculation and the Fe:HS ratio must be properly determined because the higher the iron content, the greater the humic aggregation. Therefore, as consequence of the above, the iron humates have a slow kinetic behavior and exert a long-term effect in providing slow and increasingly iron to the Strategy I plants during all the biological cycle and even reaching the pods. The possible iron humates improvements proposed in this thesis (enhance of the iron

humate dissolution, synthesis of iron humate nanofertilizers or mixtures of iron humate/iron synthetic chelates) indicates that the iron humate ameliorates its efficiency in hydroponic conditions if the iron humate is applied at once and its concentration is five times higher than the iron chelate. On the other hand, the efficiency in soil conditions enhances when iron humate/iron chelate mixtures are applied using the ratio 2:1 and HBED/Fe^{3+}. Finally, although the Fe-NFs synthetized did not enhance the iron humate efficiency, they are part of novel technology in line with precision and sustainable agriculture and so, further research is needed.

Capítulo VI: Conclusiones

Chapter VI: Conclusions

A partir de los resultados obtenidos en esta Tesis Doctoral y de su discusión, se concluye lo siguiente:

1. *Se establecieron relaciones entre algunas de las características fisicoquímicas de los humatos férricos procedentes de leonarditas y su eficiencia en la nutrición férrica de plantas de Estrategia I cultivadas en suelos calizos*

- Los humatos férricos de leonarditas estudiados, son principalmente ácidos húmicos de alta condensación, que tienden a formar agregados en condiciones de suelos calizos y depositarse sobre las raíces, ralentizando la absorción radicular de hierro y la translocación del hierro entre las raíces y la parte aérea de las plantas. Por lo tanto, afectan a la nutrición férrica de plantas de Estrategia I.
- El hierro se encuentra en los humatos férricos principalmente como compuestos polinucleares y cuasi-amorfos (ferrihidrita) estabilizados por la materia orgánica, y en algún caso, cristalinos como la jarosita. En experimentos hidropónicos la jarosita se biomineraliza en puntos ácidos de la rizosfera de plantas de soja (*Glycine* max), siendo una fuente extra de reserva de hierro de lenta liberación para la planta.
- Los humatos de hierro proporcionan hierro a las plantas de Estrategia I, tales como soja y mandarino, liberándolo lenta pero continuamente y con efecto a largo plazo debido a que su lenta liberación permite que la planta adquiera hierro durante todo su ciclo vital.

2. *Se pueden proponer posibilidades de mejora en la eficiencia de los humatos férricos en la nutrición de plantas de Estrategia I cultivadas en suelos calizos*

- La nutrición férrica de plantas de soja en hidroponía mejora cuando se aplica una sola dosis de humato férrico en vez de dosis bajas y frecuentes, promoviendo un efecto cíclico de deposición y disolución del mismo en la rizosfera.
- La aplicación de mezclas de humato férrico con quelatos de hierro, en particular HBED/Fe^{3+}, en relación de dos partes de humato férrico por cada parte de quelato

sintético de hierro, presenta ventajas en la nutrición férrica. De este modo se favorece la sinergia entre ambos productos a través del efecto de recarga del agente quelante y se aumenta el contenido de hierro soluble en el suelo.

- Se ha identificado en todos los órganos de la planta, incluso en las vainas, el hierro aportado por los nanofertilizantes de humatos de ^{57}Fe. Se demuestra, por tanto, que el uso de este tipo de fertilizantes es una vía alternativa de nutrición férrica. Las nanopartículas de humatos férricos, aunque no resultaron ser una mejora en la eficiencia, son parte de una nueva tecnología agrícola que precisa ser investigada en mayor profundidad.

According to the results of this Doctoral Thesis and after their discussion, the conclusions are:

1. *Some physicochemical characteristics and the efficiency of leonardite iron humates in Strategy I plant iron nutrition in calcareous soils were linked*

- The studied leonardite iron humates are mainly high condensed humic acids that tend to make aggregates in calcareous soils conditions and cover the root surface, restraining the iron uptake and translocation from shoot to root. So, they affect the iron nutrition in Strategy I plants.
- Iron humates usually contain iron as polynuclear, quasi-amorphous (ferrihydrite) stabilized by the organic matter and, sometimes, crystalline components as jarosite. In hydroponics, jarosite is biomineralized in the rizhospheric acidic points of soybean (*Glycine* max) and acting as a slow release pool of iron for the plant.
- Iron humates provide iron slowly but continuously to Strategy I plants, like soybean or tangerine, and they exert a long-term effect in iron nutrition because their slow release allows plants to take up iron during all their biological cycle.

2. *Methods for improvements of iron leonardite humate efficiency in iron nutrition of Strategy I plants grown in calcareous soils can be proposed*

- Soybean iron nutrition under hydroponic conditions is enhanced when a one-time dose is applied instead of low and regular doses and so, promoting the iron release in the rhizosphere by a circular effect of precipitation and dissolution of the iron humates.
- The application of mixtures of iron humates with iron synthetic chelates, in particular, HBED/Fe^{3+}, with a ratio of two parts of iron humate and one part of iron synthetic chelate, offers advantages in iron nutrition. The iron humate efficiency is improved by the synergy between the iron humate and the iron synthetic chelate and favored by the chelate agent shuttle effect and the increment of the iron content in the soil soluble fraction.

- The iron provided by the leonardite ^{57}Fe humate nanofertilizers was detected in all plant tissues and in particular in soybean pods. So, it has been demonstrated that the use of this type of fertilizers is an alternative in Strategy I plants iron nutrition. Although the leonardite iron humate nanoparticles did not improved the iron humate efficiency, they are part of a new agricultural technology that deserves further research.

Capítulo VII: Bibliografía

Chapter VII: References

Abad, I., Livi, K., Nieto, F. (2001): Espectroscopia de pérdida de energía de electrones (EELS): Fundamentos y aplicaciones en filosilicatos. Nuevas tendencias en el estudio de las arcillas pp. 14-18. Sociedad Española de Arcillas.

Amils, R., de la Fuente, V., Rodríguez, N., Zuluaga, J., Menéndez, N., Tornero, J. (2007): Composition, speciation and distribution of iron minerals in *Imperata Cylindrica*. *Plant Physiol. Biochem.* 45, 335−340

Alva, A K. (1992): Solubility and iron release characteristics of iron chelates and sludge products. *J. Plant Nutr*. 15, 1939−1954

Alva, A.K. and Obreza, T.A. (1998): By-product iron-humate increases tree growth and fruit production of orange and grapefruit. *Hort. Science*. 33, 71−74

Angelico, R., Ceglie, A., He, J. Z., Liu, Y. R., Palumbo, G., Colombo, C. (2014): Particle size, charge and colloidal stability of humic acids coprecipitated with ferrihydrite. *Chemosphere* 99, 239–247

Aguirre, E., Leménager, D., Bacaicoa, E., Fuentes, M., Baigorri, R., Zamarreño, A. M., García-Mina, J. M. (2009): The root application of a purified leonardite humic acid modifies the transcriptional regulation of the main physiological root responses to Fe deficiency in Fe sufficient cucumber plants. *Plant Physiol. Biochem.* 47, 215−223

Akinremi, O.O., Janzen, H.H., Lemke, R. L. and Larney, F.J. (2000): Response of canola, wheat and green beans to leonardite additions. *Can. J. Soil Sci*. 80, 437-443

Asli, S.; Neumann, P. M. (2010): Rhizosphere humic acid interacts with root cell walls to reduce hydraulic conductivity and plant development. *Plant Soil*. 336, 313−322

Ayuso, M., Moreno, J. L., Hernández, T., García, C. (1997): Characterization and evaluation of humic acids extracted from urban waste as liquid fertilisers. *J. Sci. Food Agric.* 75, 481–488

Backx, C., De Groot, C.P.M., Biloen, P. (1980): Electron energy loss spectroscopy and its applications. *Appl. Surf. Sci*. 6, 256-272

Baron-Epel, O.; Gharyal, P. K.; Schindler, M. (1988): Pectins as mediators of wall porosity in soybean cells. Planta. 175, 389−395

Barone, V., Bertoldo, G., Magro, F., Broccanello, C., Puglisi, I., Baglieri,A., Cagnin, M., Concheri, G., Squartini, A., Pizzeghello, D., Nardi, S. y Stevanato, P. (2019): Molecular and morphological changes induced by leonardite-based biostimulant in *Beta vulgaris* L. *Plants.* 8,181

Bigham, J. M.; Kirk Nordstrom, D. (2000): Iron and aluminum hydroxysulfates from acid sulfate waters. *Rev. Mineral. Geochem.* 40, 351−403

Boiteau, R.M., Shaw, J.B., Pasa-Tolic, L., Koppenaal, D.W., Jansson, J.K. (2018): Micronutrient metal speciation is controlled by competitive organic chelation in grassland soils*. Soil Biol. Biochem.* 120, 283–291

Bolea, E., Gorriz, M. P., Bouby, M., Laborda, F., Castillo, J. R., Geckeis, H. (2006): Multielement characterization of metal-humic substances complexation by size exclusion chromatography, asymmetrical flow field-flow fractionation, ultrafiltration and inductively coupled plasma-mass spectrometry detection: A comparative approach. *J. Chromatogr. A.* 1129, 236–246

Briat, J. F., Dubos, C., Gaymard, F. (2015): Iron nutrition, biomass production, and plant product quality. *Trends Plant Sci.* 20, 33–40

Canellas, L. P., Olivares, F. L., Aguiar, N. O., Jones, D. L., Nebbioso, A., Mazzei, P., Piccolo, A. (2015): Humic and fulvic acids as biostimulants in horticulture. *Sci. Hortic. (Amsterdam).* 196, 15–27

Canellas, L.P. and Olivares, F.L. (2014): Physiological responses to humic substances as plant growth promoter. *Chem. Biol. Technol. Agric*. 1, 1–11

Canellas, L. P., Olivares, F. L., Canellas, N. O. A., Mazzei, P., and Piccolo, A. (2019): Humic acids increase the maize seedlings exudation yield. *Chem. Biol. Technol*. Agric. 6:3

Casierra-Posada, F., Fischer, G. (2009): Reducing negative effects of salinity in tomato (*Solanum lycopersicum* L .) plants by adding leonardite to soil reducing negative effects of salinity in tomato (*Solanum lycopersicum* L .) Plants by adding leonardite to soil. *Acta Hortic.* 821, 133–140

CE:2003/2003 Reglamento del Parlamento Europeo y del Consejo relativo a los abonos.

CE:1009/2019 Reglamento del Parlamento Europeo y del Consejo por el que se establecen disposiciones relativas a la puesta a disposición en el mercado de los productos fertilizantes UE.

Cerdán, M., Sánchez-Sánchez, A., Juárez, M, Sánchez-Andreu, J.J., Jordá, J.D., Bermúdez, D. (2007): Partial replacement of Fe(o,o-EDDHA) by humic substances for Fe nutrition and fruit quality of citrus. *J. Plant Nutr. Soil Sci.* 170, 474–478

Cesco, S., Nikolic, M., Römheld, V., Varanini, Z., Pinton, R. (2002): Uptake of ^{59}Fe from soluble

59Fe-humate by cucumber and barley plants. *Plant Soil* 241, 121–128

Cesco, S., Neumann, G., Tomasi, N., Pinton, R., Weisskopf, L. (2010): Release of plant-borne flavonoids into the rhizosphere and their role in plant nutrition. *Plant Soil.* 329, 1–25

Chassapis, K., Roulia, M., Nika, G. Fe(III)–humate complexes from Megalopolis peaty lignite: A novel eco-friendly fertilizer. *Fuel*. 89, 1480-1484

Chen, Y.; Senesi, N., Schnitzer, M. (1977). Information provided on humic substances by E4/E6 ratios. *Soil. Sci. Soc. Am. J*. 41: 352-358

Chen, Y., Clapp, C. E., Magen, H. (2004): Mechanisms of plant growth stimulation by humic substances: The role of organo-iron complexes. *Soil Sci. Plant Nutr.* 50, 1089–1095

Colangelo, E.P., Guerinot, M.L. (2004): The essential basic helix-loop-helix protein FIT1 is required for the iron deficiency response. *Plant Cell* 16, 3400–3412

Colombo, C., Palumbo, G., Sellitto, V. M., Rizzardo, C., Tomasi, N., Pinton, R., Cesco, S. (2012): Characteristics of insoluble, high molecular weight iron-humic substances used as plant iron sources. *Soil Sci. Soc. Am. J.* 76, 1246–1256

Colombo, C., Palumbo, G., Ji-Zheng, H., Pinton, R., Cesco, S., (2014)*:* Review on iron availability in soil: interaction of Fe minerals, plants, and microbes. *J. Soils Sediments* 14, 538–548

Colombo, C., Palumbo, G., Sellitto, V. M., Cho, H. G., Amalfitano, C., Adamo, P. (2015). Stability of co-precipitated natural humic acid and ferrous iron under oxidative conditions. *J. Geochem. Explor. 151, 50–56.*

Cornell, R., Schwertmann, U. (2003): The iron oxides: structure, properties, reactions ocurrences and uses. Wiley-VCH Verlag GMBH & Co. KGaA, Weinheim. Germany

Crabbe, H.; Fernandez, N.; Jones, F. (2015): Crystallization of jarosite in the presence of amino acids. *J. Cryst. Growth* 416, 28–33.

Curie, C., Panaviene, Z., Loulergue, C., Dellaporta S.L., Briat, J.F., Walker, E.L. (2001): Maize yellow stripe1 encodes a membrane protein directly involved in Fe(III) uptake. *Nature*. 409, 346–349

De Santiago, A., Delgado, A. (2007): Effects of humic substances on iron nutrition of lupin. *Bio.l Fertil. Soils* 43, 829–836

Di Iorio, E., Colombo, C., Angelico, R., Terzano, R., Porfido, C., Valentinuzzi, F., Pii, Y., Mimmo, T., Cesco, S. (2019): Iron oxide-humic acid coprecipitates as iron source for cucumber plants. *J. Plant Nutr. Soil Sci*. 000, 1–13

Filipponi, A. Di Cicco, A., Natoli, C.R. (1995): X-ray-absorption spectroscopy and n-body distribution functions in condensed matter. I. Theory. *Phys. Rev. B* 52, 15122-15134

Filipponi, A. (2001): EXAFS for liquids. J. Phys.: Condens. Matter 13, R23–R60

Fourcroy, P., Sisó-Terraza, P., Sudre, D., Savirón, M., Reyt, G., Gaymard, F., Abadía, A., Abadía, J., Álvarez-Fernández, A., Briat, J.F. (2013): Involvement of the ABCG37 transporter in secretion of scopoletin and derivatives by *Arabidopsis* roots in response to iron deficiency. *New Phytol.* 201, 155–167

Francioso, O., Montecchio, D., Gioacchini, P., Ciavatta, C. (2005): Thermal analysis (TG–DTA) and isotopic characterization (^{13}C–^{15}N) of humic acids from different origins. *Appl. Geochem.* 20, 537–544

Frimmel, F.H., Abbt-Braun, G. (2009): Chapter 10. Dissolved organic matter (DOM) in natural environments. En Biophysico-chemical processes involving natural nonliving organic matter in environmental systems pp 367-406. Edited by Nicola Senesi, Baoshan Xing, and Pan Ming Huang. John Wiley & Sons, Inc.

Fuente, V., Rufo L., Juárez B.H., Menéndez, N., García-Hernández, M., Salas-Colera, E., Espinosa, A. (2016): Formation of biomineral iron oxides compounds in a Fe hyperaccumulator plant: *Imperata cylindrica* (L.) P. Beauv. *J. Struct. Biol*. 193, 23-32.

Fuentes, M., Olaetxea, M., Baigorri, R., Zamarreño, A. M., Etienne, P., Laîné, P., Ourry, A., Yvin, J.C., Garcia-Mina, J. M. (2013): Main binding sites involved in Fe(III) and Cu(II) complexation in humic based structures. *J. Geochem. Explor.* 129, 14–17

Fuentes, M., Baigorri, R., González-Gaitano, G., García-Mina, J.M. (2018): New methodology to assess the quantity and quality of humic substances in organic materials and commercial products for agriculture. *J. Soil Sediment*. 18, 1389-1399

García, A.C., Olaetxea, M., Azevedo Santos, L., Mora, V., Baigorri, R., Fuentes, M., Zamarreño, A.M., Louro Berbara, R.L., García-Mina, J.M. (2016): Involvement of hormone and ROS signaling pathways in the beneficial action of humic substances on plant growing under normal and stressing conditions. *Bio. Med. Res. Int.* 2016:3747501

García-Mina, J.M., Antolín, M.C., Sanchez-Diaz, M. (2004): Metal-humic complexes and plant micronutrient uptake: a study based on different plant species cultivated in diverse soil types. *Plant Soil* 258. 57-68

García-Mina, J.M. (2006): Stability, solubility and maximum metal binding capacity in metal-

humic complexes involving humic substances extracted from peat and organic compost. *Org. Geochem*. 37, 1960-1972

Gattullo, C.E., Pii, Y., Allegretta, I.,Medici, L., Cesco, S., Mimmo, T., Terzano, R. (2018): Iron Mobilization and mineralogical alterations induced by iron-deficient cucumber plants (*Cucumis sativus L.*) in a calcareous soil. *Pedosphere* 28, 59–69

González-Guerrero, M., Escudero, V., Saéz, Á., Tejada-Jiménez, M. (2016): Transition metal transport in plants and associated endosymbionts: Arbuscular mycorrhizal fungi and rhizobia. *Front. Plant Sci*. 7, 1088

Gonzalez-Vila, F.J., del Rio, JC., Almendros, G., Martin, F. (1994): Structural relationship between humic fractions from peat and lignites from the Miocene Granada basin. *Fuel* 73, 215-221

Goodman, B.A. and DeKock P.C. (1982): Mössbauer studies of plant materials. I. Duckweed, stocks, soyabean and pea. *J Plant Nutr* 5:345–353

Grillet, L., Mari, S., Schmidt,W. (2014): Iron in seeds–loading pathways and subcellular localization. *Front. Plant Sci.* 4, 535

Guo, N., Fingland, B.R, Williams, W.D., Kispersky, V.F., Jelic, J., Delgass, W.N., Ribeiro, F.H., Meyerc, R.J., Miller, J.T. Determination of CO, H2O and H2 coverage by XANES and EXAFS on Pt and Au during water gas shift reaction. *Phys. Chem. Chem. Phys.* 12, 5678–5693

Hell, R., Stephan, U.W. (2003): Iron uptake, trafficking and homeostasis in plants. *Planta* 216, 541-555

Inoue, H., Kobayashi, T., Nozoye, T., Takahashi, M., Kakei, Y., Suzuki, K., Nakazono, M., Nakanishi, H., Mori, S., Nishizawa, N.K. (2009): Rice OsYSL15 is an iron-regulated iron(III)-deoxymugineic acid transporter expressed in roots and is essential for iron uptake in early growth of the seedlings. *J. Biol. Chem.* 284, 3470–3479

IHSS 2007: International Humic Substances Society: What are humic substances? IHSS. http://humic-substances.org/what-are-humic-substances-2/. Consultado Agosto 2019.

IHSS 2019a: International Humic Substances Society. Elemental composition and stable isotopic ratios of IHSS samples. http://humic-substances.org/elemental-compositions-and-stable-isotopic-ratios-of-ihss-samples/ Consultado Julio 2019.

IHSS 2019b*:* International Humic Substances Society. Acidic functional groups of IHSS samples http://humic-substances.org/acidic-functional-groups-of-ihss-samples/ Consultado

Julio 2019.

IHSS 2019c: International Humic Substances Society. F-TIR, 13CNMR and Fluorescense sectrum. http://humic-substances.org/ftir-13c-nmr-and-fluorescence-spectra/ Consultado Julio 2019.

Irving, H, Williams R.J.P. (1953): The stability of the transition-metal complexes. *J. Chem. Soc*. 3192–3210

Isoflex 2019: Isotopes for Science, Medicine and Industry https://www.isoflex.com/iron Consultado Julio 2019.

Jannin, L., Arkoun, M., Ourry, A., Laîné, P., Goux, D., Garnica, M., Fuentes, M., San Francisco, S., Baigorri, R., Cruz, F., Houdusse, F., Garcia-Mina, J. M., Yvin, J.C., Etienne, P. (2012): Microarray analysis of humic acid effects on Brassica napus growth: involvement of N, C and S metabolisms. *Plant Soil* 359, 297–319

Jean, M.L., Schikora, A., Mari, S., Briat, J.F., Curie, C. (2005): A loss-of-function mutation in AtYSL1 reveals its role in iron and nicotianamine seed loading. *Plant J.* 44, 769–782

Jin, C.W., You, G.Y., He, Y.F., Tang, C., Wu, P., Zheng, S.J. (2007): Iron deficiency-induced secretion of phenolics facilitates the reutilization of root apoplastic iron in red clover. *Plant Physiol.* 144, 278–285

Jindo, K., Soares, T.S., Peres, L.E. P., Azevedo, I.G., Aguiar, N.O.,Mazzei, P., Spaccini, R., Piccolo, A., Lopes Olivares, F., Canellas, L.P. (2016): Phosphorus speciation and high-affinity transporters are influenced by humic substances. *J. Plant Nutr. Soil Sci*. 179, 206–214

Juárez-Sanz, M., Sánchez-Andreu, J., Sánchez-Sánchez, A. (2006): Capítulo 5: Fracción orgánica del suelo, humus, origen, composición y dinámica. pp. 145-207. En Química del suelo y medio ambiente. Publicaciones de la Universidad de Alicante. España.

Karpukhina, E., Mikheev, I., Perminova, I., Volkov, D., Proskurnin, M. (2018): Rapid quantification of humic components in concentrated humate fertilizer solutions by FTIR spectroscopy. *J. S* 1–11

Kasatochkin, V.I., Kononova, M.M., Larina, N.K., Jgorova, O.I. (1964): Spectral and X-ray investigations of the chemical structure of humic substances in soils. Trans. 8th Intern. Congr. Soil Sci. 3:81 Bucarest.

Kilcoyne, S.H., Bentley, P.M., Thongbai, P., Gordon, D.C., Goodman, B.A. (2000): The application

of ^{57}Fe Mössbauer spectroscopy in theinvestigation of iron uptake and translocation in plants. Nucl. Instr. and Meth. in Phys. Res. B 160,157-166

Kobayashi, T., Nishizawa, N. K. (2012): Iron uptake, translocation, and regulation in higher plants. *Ann. Rev. Plant Biol*. 63, 131–152

Kononova, M. (1982). Bioquímica del proceso de formación del humus. En: La materia orgánica del suelo. Su naturaleza, propiedades y métodos de investigación. Editorial, Oikos-Tau. Barcelona (España). p. 63-109

Kovács, K. Kuzmann, Tatá, E., Vértes, A., Fodor, F. (2009): Investigation of iron pools in cucumber roots by Mössbauer spectroscopy: direct evidence for the Strategy I iron uptake mechanism. *Planta.* 229: 271-278

Kovács, K., Czech, V., Fodor, F., Solti, A., Lucena, J.J., Santos-Rosell, S., Hernández-Apaolaza, L. (2013): Characterization of Fe-leonardite complexes as novel natural iron fertilizers. *J. Agric. Food Chem.* 61, 12200−12210

Kovács, K., Pechousek, J., Machala, L., Zboril, R., Klencsár, Z., Solti, A., Tóth, B., Müller, B., Pham, H.D., Kristóf, Z., Fodor, F. (2016): Revisiting the iron pools in cucumber roots: identification and localization. *Planta*. 244, 167-179

Kulikova, N.; Badun, G. A.; Korobkov, V. I.; Chernysheva, M. G.; Tsvetkova, E. A.; Abroskin, D. P.; Konstantinov, A. I.; Zaitchik, B. T.; Ruzhitsky, A. O.; Perminova, I. V. (2014): Accumulation of coal humic acids by wheat seedlings: direct evidence using tritium autoradiography and occurrence in lipid fraction. *J. Plant Nutr. Soil Sci.* 177, 875−883

Kulikova, N. A.; Polyakov, A. Y.; Lebedev, V. A.; Abroskin, D.P.; Volkov, D. S.; Pankratov, D. A.; Klein, O. I.; Senik, S. V.; Sorkina,T. A.; Garshev, A. V.; Veligzhanin, A. A.; Garcia Mina, J. M.; Perminova, I. V. (2017): Key roles of size and crystallinity of nanosized iron hydr(oxides) stabilized by humic substances in iron bioavailability to plants. *J. Agric. Food Chem.* 65, 11157−11169

Kuzmicheva, Y.V., Shaposhnikov, A.I., Petrova, S.N., Makarova, N.M., TychinskayaJan, I.L., Puhalsky, V., ParahinIgor, N.V., Tikhonovich, A., Belimov, A.A. (2017): Variety specific relationships between effects of rhizobacteria on root exudation, growth and nutrient uptake of soybean. *Plant Soil* 419, 83−96

Kyriacou, B., Moore, K.L., Paterson, D., de Jonge, M.D., Howard, D.L., Stangoulis, J., Tester, M., Lombi, E., Johnson, A.A. (2014): Localization of iron in rice grain using synchrotron X-ray

fluorescence microscopy and high resolution secondary ion mass spectrometry. *J. Cereal Sci.* 59, 173–180

Lamar, R., Olk, D., Mayhew, L., Bloom, P. (2014): A new standardized method for quantification of humic and fulvic acids in humic ores and commercial products. *J. AOAC Int*. 97, 721-730

Lindsay, W. L. (1979): Chemical equilibrium in soils. Wiley. New York. USA

Lee, P.A., Beni, G. (1977): New method for the calculation of atomic phase shifts: Application to extended x-ray absorption fine structure (EXAFS) in molecules and crystals. *Phys. Rev. B* 15, 2862-2883

Lindsay, W. L., Schwab, A. P. (1982): The chemistry of iron in soils and its availability to plants. *J. Plant Nutr.* 5, 821–840

Liñan, C. (2001 y 2019): Correctores de carencia de hierro. En: Vademecums de productos fitosanitarios y nutricionales. Agrotécnicas S. L. Madrid. España

López-Rayo, S.; Hernández, D.; Lucena, J. J. (2009): Chemical evaluation of HBED/Fe^{3+} and the novel HJB/Fe^{3+}. Chelates as fertilizers to alleviate iron chlorosis. *J. Agric. Food Chem.* 57, 8504−8513

López-Rayo, S., Di Foggia, M., Bombai, G., Yunta, F., Rodrigues- Moreira, E., Filippini, G., Pisi, A., Rombolà, A.D. (2015): Blood-derived compounds can efficiently prevent iron deficiency in the grapevine. *Aust. J. Grape Wine Res.* 21, 135–142

Lucena, J.J. (2003): Fe chelates for remediation of Fe chlorosis in strategy I plants. *J. Plant Nutr.* 26, 1969–1984

Ma, J. F. (2005): Plant root responses to three abundant soil minerals: Silicon, aluminum and iron. *CRC. Crit. Rev. Plant Sci.* 24, 267–281

Mao, J.D., Hu, W.G., Schmidt-Rohr, K., Davies, G., Ghabbour, E.A., Xing, B. (2000): Quantitative characterization of humic substances by solid-state carbon-13 nuclear magnetic resonance. *Soil Sci. Soc. Am*. J. 64, 873-884

Marschner, H., Römheld, V. (1994): Strategies of plants for acquisition of iron. *Plant Soil* 165, 261–274

Mimmo, T., Del Buono, D., Terzano, R., Tomasi, N., Vigani, G., Crecchio, C., Pinton, R., Zocchi, G., Cesco, S. (2014): Rizhospheric organic compounds in the soil-microorganism-plant system: their role in iron availability. *Eur. J. Soil Sci.* 65, 629-642

Mira, L., Fernandez, M.T., Santos, M., Rocha, R., Florencio, M.H., Jennings, K.R. (2002):

Interactions of flavonoids with iron and copper ions: A mechanism for their antioxidant activity. *Free Radic Res*. 36, 1199–1208

Mora, V., Bacaicoa, E., Zamarreño, A. M., Aguirre, E., Garnica, M., Fuentes, M., García-Mina, J. M. (2010): Action of humic acid on promotion of cucumber shoot growth involves nitrate-related changes associated with the root-to-shoot distribution of cytokinins, polyamines and mineral nutrients. *J. Plant Physiol.* 167, 633–642

Mora, V., Baigorri, R., Bacaicoa, E., Zamarreño, A. M., García-Mina, J. M. (2012): The humic acid-induced changes in the root concentration of nitric oxide, IAA and ethylene do not explain the changes in root architecture caused by humic acid in cucumber. *Environ. Exp. Bot.* 76, 24–32

Muscolo, A., Sidari, M., Nardi, S. (2013): Humic substance: Relationship between structure and activity. Deeper information suggests univocal findings. *J. Geochemical Explor.* 129, 57–63

Nardi, S.; Pizzeghello, D.; Muscolo, A.; Vianello, A. (2002): Physiological effects of humic substances on higher plants. *Soil Biol. Biochem*. 34, 1527–1536

Nardi, S., Ertani, A., Francioso, O. (2017): Review Article Soil – root cross-talking : The role of humic substances. *J. Plant Nutr. Soil Sci*. 180, 5–13

Neilands, J.B. Chapter 2: Iron in biology. Manthey J, Luster D, Crowley DE (eds) (1994) Biochemistry of metal micronutrients in the rhizosphere pp 15–28. CRC Press. Boca Raton. USA

Newton,M.A., Dent, A.J., Evansa, J. (2002): Bringing time resolution to EXAFS: recent developments and application to chemical systems. *Chem. Soc. Rev.* 31, 83-95

Nikolic, M., Cesco, S., Römheld, V., Varanini, Z., Pinton, R. (2003): Uptake of iron (^{59}Fe) complexed to water-extractable humic substances by sunflower leaves. *J. Plant Nutr*. 26, 2243-2252

Norvell, W. A., Lindsay, W. L. (1982): Estimation of the concentration of Fe^{3+} and the $(Fe^{3+})(OH^{-})_3$ ion product from equilibria of EDTA in soil. *Soil Sci. Soc. Am. J.* 46, 710–715

Nuzzo, A.; Sánchez, A.; Fontaine, B., Piccolo. A. (2013) Conformational changes of dissolved humic and fulvic superstructures with progressive iron complexation. *J. Geochem. Explor.* 129, 1–5

Olaetxea, M., Mora, V., Bacaicoa, E., Garnica, M., Fuentes, M., Casanova, E., Zamarreño, A. M., Iriarte, J. C., Etayo, D., Ederra, I., Gonzalo, R., Baigorri, R., García-Mina, J. M. (2015): Abscisic acid regulation of root hydraulic conductivity and aquaporin gene expression is

crucial to the plant shoot growth enhancement caused by rhizosphere humic acids. *Plant Physiol.* 169, 2587–2596

Olaetxea, M., De Hitaa, D., Andrés Garcia, C., Fuentes, M., Baigorri, R., Mora, V., Garnica, M., Urrutia, O. , Erro, J., Zamarreño, A., Berbara, R. L., Garcia-Mina, J. M. (2018): Hypothetical framework integrating the main mechanisms involved in the promoting action of rhizospheric humic substances on plant root- and shootgrowth. *Appl. Soil Ecol.* 123, 521-537.

Oliver, S., Barber, S. A. (1966): Mechanisms for the movement of Mn, Fe, B, Cu, Zn Al and Sr from one soil to the surface of soybean roots (Glycine max). *Soil Sci. Soc. Am. J.* 30, 468–470

Panorama Minero (2017): Publicación del Instituto Geológico y Minero de España. Ministerio de ciencia, innovación y universidades. http://www.igme.es/PanoramaMinero/actual/PANORAMA_MINERO_2017(BU24)(BR).pdf (Consultado Julio 2019).

Pansou, M., Gautheyrou, J. (2007): Handbook of soil analysis: mineralogical, organic and inorganic methods. Springer. Paris. Francia.

Parfitt, R.L., Childs, C.W. (1988): Estimation of forms of Fe and Al: a review, and analysis of contrasting soils by dissolution and Moessbauer methods. *Aust. J. Soil Res*. 26, 121-44

Peña-Méndez, E., Havel, J., Patočka, J. (2005): Humic substances-compounds of still unknown structure: applications in agriculture, industry, environment, and biomedicine. *J. Appl. Biomed.* 3, 13-24

Pérez-Sanz, A., Álvarez-Férnandez, A., Casero, T., Legaz, F., Lucena, J.J. (2002): Fe enriched biosolids as fertilizers for orange and peach trees grown in field conditions. *Plant Soil*. 241, 145–153

Pettit, R.E. (2004): Organic matter, humus, humate, humic acid, fulvic acid, and humin: Their Importance in soil fertility and plant health.

http://www.humates.com/pdf/ORGANICMATTERPettit.pdf Consultado Agosto 2019

Piccolo, A. (2001): The supramolecular structure of humic substances. *Soil Sci.* 166, 810–832.

Piccolo, A. (2002): The supramolecular structure of humic substances: A novel understanding of humus chemistry and implications in soil science. *Adv. Agron.* 75, 57–134

Pinton, R., Cesco, S., Santi, S., Agnolon, F., Varanini, Z. (1999): Water-extractable humic substances enhance iron deficiency responses by Fe-deficient cucumber plants. *Plant Soil*

210, 145–157

Polyakov, A.Yu., Goldt, A.E., Sorkina, T.A., Perminova, I.V., Pankratov, D.A., Goodilin, E.A., Tretyakov, Y.D. (2012): Constrained growth of anisotropic magnetic δ-FeOOH nanoparticles in the presence of humic substances. *Cryst. Eng. Comm*. 14. 8097-8102

Polyakov, A.Yu., Sorkina, T.A., Goldt, A. E, Pankratov, D.A., Perminova, I. V., Goodilin, E.A. (2013): Mössbauer spectroscopy of frozen solutions as a stepwise control tool in preparation of biocompatible humic-stabilized feroxyhyte nanoparticles. *Hyperfine Interac*. 219, 113-120

Qian, S., Ding, W., Li, Y., Liu, G., Sun, J., Ding, Q. (2015): Characterization of humic acids derived from Leonardite using a solid-state NMR spectroscopy and effects of humic acids on growth and nutrient uptake of snap bean 2299

Rajniak, J., Giehl, R.F.H., Chang, E., Murgia, I., Von Wiren, N., Sattely, E.S. (2018): Biosynthesis of redox-active metabolites in response to iron deficiency in plants. *Nat. Chem. Biol*. 14, 442–450

Rellán-Álvarez, R., Giner-Martínez-Sierra, J., Orduna, J., Orera, I.; Rodríguez-Castrillón, J.Á., García-Alonso, J.I., Abadía, J.; Álvarez-Fernández, A. (2010): Identification of a tri-iron(iii), tri-citrate complex in the xylem sap of iron-deficient tomato resupplied with iron: New insights into plant iron long-distance transport. *Plant Cell Physiol*. 51, 91–102

RD506/2013: Real Decreto sobre productos fertilizantes. Boletin Oficial del Estado Nº 164.

Rice, J.A., Mac Carthy, P. (1991): Statistical evaluation of the elemental composition of humic substances. *Org. Geochem.* 17, 635-648.

Robinson, N.J. Procter, C.M. Connolly, E.L. Guerinot, M.L. (1999): A ferric-chelate reductase for iron uptake from soils. *Nature* 397, 694–697

Rodríguez-Castrillón, J.A., Moldovan, M., García Alonso, J.I., Lucena, J.J., García-Tomé, M.L., Hernández-Apaolaza, L. (2008): Isotope pattern deconvolution as a tool to study iron metabolism in plants. *Anal. Bioanal. Chem*. 390: 579-590

Rodríguez-Celma, J., Vázquez-Reina, S., Orduna, J., Abadía, A., Abadía, J., Álvarez-Fernández, A., Lopez-Millan, A.F. (2011): Characterization of flavins in roots of Fe-deficient strategy I plants, with focus on *Medicago truncatula*. *Plant Cell Physiol.* 52, 2173–2189

Rodríguez-Celma, J., Lin, W.D., Fu, G.M., Abadía, J., López Millán, A.F.; Schmidt, W. (2013): Mutually exclusive alterations in secondary metabolism are critical for the uptake of

insoluble iron compounds by *Arabidopsis* and *Medicago truncatula*. *Plant Physiol.* 162, 1473–1485

Rodríguez-Lucena, P., Benedicto, A., Lucena, J.J., Rodríguez-Castrillón, J.A., Moldovan, M., García-Alonso., J.I., Hernández-Apaolaza, L. (2011): Use of the stable isotope ^{57}Fe to track the efficacy of the foliar application of lignosulfonate/Fe^{3+} complexes to correct Fe deficiencies in cucumber plants. *J. Sci. Food Agric.* 91, 395-704

Römheld, V., Nikolic, M. (2007): "Iron," in Handbook of Plant nutrition A. V. Barker and D. J. Pilbeam , eds. CRC Press. Boca Raton. USA

Roschzttardtz, H., Conéjéro, G., Curie, C., Mari, S. (2009): Identification of the endodermal vacuole as the iron storage compartment in the *Arabidopsis* embryo. *Plant Physiol*. 151, 1329–1338

Salma, I., Mészáros, T., Maenhaut, W., Vass, E., Majer, Z. (2010): Chirality and the origin of atmospheric humic-like substances. *Atmos. Chem. Phys.* 10, 1315–1327

Sänchez-Sánchez, A., Sánchez-Andreu, J., Juárez, M., Jordá, J., Bermúdez, D. (2002): Humic substances and amino acids improve effectiveness of chelate FeEDDHA in lemon trees. *J. Plant Nutr.* 45, 2433-2442

Santi, S., Schmidt, W. (2009): Dissecting iron deficiency-induced proton extrusion in Arabidopsis roots. *New Phytol*. 183, 1072–1084

Schenker, M., Chen, Y. (2005): Increasing iron availability to crops: fertilizers, organo-fertilizers, and biological approaches. *Soil Sc. Plant Nutr*. 51. 1-17

Schenkeveld, W., Reichwein, A., Temminghoff, E., van Riemsdijk, W. (2014): Considerations on the shuttle mechanism of FeEDDHA chelates at the soil-root interface in case of Fe deficiency. *Plant Soil.* 379, 373-387

Schmidt, H., Günther, C., Weber, M., Spörlein, C., Loscher, S., Böttcher, C., Schobert, R., Clemens, S. (2014): Metabolome analysis of Arabidopsis thaliana roots identifies a key metabolic pathway for iron acquisition. *PLoS One* 9, e102444

Schnitzer, M., Khan, S.U. (1972). Humic substances in the environment. Marcel Dekker, New York. Pp. 57-60

Schnitzer, M. (1978): Chapter 1: Humic Substances: Chemistry and Reactions. pp 1-64. En Soil organic matter. Dev. Soil Sci. Editors: M. Schnitzer S.U. Khan. Elsevier. Amsterdam. Netrerlands.

Shulten H.R. (1996): A new approach to the structural analysis of humic substances in water and soils: humic acid oligomers. En Humic and fulvic isolation, structure, and environmental role. pp 42-56. ACS symposium series. American Chemical Society. Washington. USA

*Shulten H.*R., Leinweber (2000): New insights into organic-mineral particles: composition, properties and models of molecular structure. *Biol. Fert. Soils* 30, 399-432

Schulten, H.R., Schnitzer, M. (1993): A state of the art structural concept for humic substances. *Naturwissenschaften* 80, 29-30

Schwertmann, U., Taylor, R.M. (1977): Iron Oxides. In J. B. Dixon and S. B. Weed (eds.), Minerals in Soil Environments. Soil Science Society of America, Madison. USA

Schwertmann, U., Wagner, F., Knicker, H. (2005): Ferrihydrite–humic associations: magnetic hyperfine interactions. *Soil Sci. Soc. Am. J.* 69, 1009–1015

Sisó-Terraza, P., Rios, J.J., Abadía, J., Abadía, A., Álvarez-Fernández, A. (2015): Flavins secreted by roots of iron-deficient *Beta vulgaris* enablemining of ferric oxide via reductive mechanisms. *New Phytol*. 209, 733–745

Sivitz, A.B., Hermand, V., Curie, C., Vert, G. (2012): Arabidopsis bHLH100 and bHLH101 control iron homeostasis via a FIT-independent pathway. *PLoS One* 7, e44843

Sorkina, T.A., Polyakov, A.Y., Kulikova, N.A., Goldt, A.E., Philippova, O.I., Aseeva, A.A., Veligzhanin, A.A., Zubavichus, Y.V., Pankratov, D.A., Goodilin, E.A., Perminova, I.V. (2014): Nature-inspired soluble iron-rich humic compounds: New look at the structure and properties. *J. Soils Sediments*. 14, 261−268

Stevenson, F. J. (1982) and (1994): Humus chemistry: Genesis, composition, reactions. A Willey A Willey Interscience Publication, New York, USA

Sugier, D., Kołodziej, B., Bielińska, E. (2013): The effect of leonardite application on *Arnica montana* L. yielding and chosen chemical properties and enzymatic activity of the soil. *J. Geochemical Explor.* 129, 76–81

Sutton, R., Sposito, G. (2005): Critical review molecular structure in soil humic substances : The New View. *Environ. Sci. Technol.* 39, 9009–9015

Swift, R. S. (1999): Macromolecular properties of soil humic substances: fact, fiction, and opinion. *Soil Sci*. 164, 790-802

Terés, J., Busoms, S., Pérez-Martín, L., Luís-Villarroya, A., Flis, P., Álvarez-Fernández, A., Tolrà, R.,

Salt, D.E., Poschenrieder, C. (2019): Soil carbonate drives local adaptation in *Arabidopsis thaliana*. *Plant Cell Environ*. 42, 2384–2398

Terzano, R., Cuccovillo, G., Gattullo, C.E., Medici, L., Tomasi, N., Pinton, R., Mimmo, T., Cesco, S. (2015): Combined effect of organic acids and flavonoids on the mobilization of major and trace elements from soil. *Biol Fertil Soils*. 51, 685–695

Tsai, H.H., Schmidt, W. (2017a): One way. Or another? Iron uptake in plants. *New Phytol*. 214, 500–505

Tsai, H.H., Schmidt, W. (2017b): Mobilization of iron by plant-borne coumarins. *Trends Plant Sci*. 22, 538-548

Tipping, E. (2002): Cation binding by humic substances. Cambridge University Press, 1–434. Cambridge. UK

Tomasi, N., Weisskopf, L., Renella, G., Landi, L., Pinton, R., Varanini, Z., Nannipieri, P., Torrent, J., Martinoia, E., Cesco, S. (2008): Flavonoids of white lupin roots participate in phosphorus mobilization from soil. *Soil Biol Biochem*. 40, 1971–1974

Tomasi, N., De Nobili, M., Gottardi, S., Zanin, L., Mimmo, T., Varanini, Z.., Römheld, V., Pinton, R., Cesco, S. (2013): Physiological and molecular characterization of Fe acquisition by tomato plants from natural Fe complexes. *Biol. Fertil. Soils* 49, 187–200

Trevisan, S., Botton, A., Vaccaro, S., Vezzaroa, A., Quaggiotti, S., Nardi, S. (2011): Humic substances affect *Arabidopsis* physiology by altering the expression of genes involved in primary metabolism, growth and development. *Environ. Exp. Bot. 74, 45–55*

UNE-EN 15962:2011 Fertilizers: Determination of the complexed micronutrient content and of the complexed fraction of micronutrients; AENOR: Madrid, Spain

UNE-EN 16962:2018 Fertilizers - Extraction of water soluble micro-nutrients in fertilizers and removal of organic compounds from fertilizer extracts; AENOR: Madrid. Spain

Vert, G., Grotz, N., Dedaldechamp, F., Gaymard, F., Guerinot, M.L., Briat, J.F., Curie, C. (2002): IRT1, an *Arabidopsis* transporter essential for iron uptake from the soil and plant growth. *Plant Cell* 14, 1223–1233

Villén, M.; Lucena, J. J.; Cartagena, M. C.; Bravo, R.; García Mina, J. M.(2007): Comparison of two analytical methods for the evaluation of the complexed metal in fertilizers and the complexing capacity of complexing agents. *J. Agric. Food Chem.* 55, 5746–5753

Yarkova, T.A. (2011): Chemical modification of humic acids by the introduction of indole-containing fragments. Solid Fuel Chem. 45, 261-266

Yi, Y., Saleeba, J., Guerinot, M.L. Chapter 19: Iron uptake in *Arabidopsis thaliana*. Manthey, J., Luster, D., Crowley, D.E. (eds) (1994): Biochemistry of metal micronutrients in the rhizosphere. pp 295–307. CRC Press, Boca Raton. USA

Yunta, F.; García-Marco, S.; Lucena, J. J.; Gómez-Gallego, M.; Alcázar, R.; Sierra, M. A. (2003): Chelating agents related to ethylenediamine bis (2-hydroxyphenyl) acetic acid (EDDHA): Synthesis, characterization, and equilibrium studies of the free ligands and their Mg^{2+}, Ca^{2+}, Cu^{2+}, Fe^{3+} chelates. *Inorg. Chem.* 42, 5412−5421.

Zamboni, A., Zanin, L., Tomasi, N., Avesani, L., Pinton, R., Varanini, Z., Cesco, S. (2016). Early transcriptomic response to Fe supply in Fe-deficient tomato plants is strongly influenced by the nature of the chelating agent. *BMC Genomics.* 17:35.

Zandonadi, D.B, Santos, M.P., Dobbss, L.B., Olivares, F.L., Canellas, L.P., Binzel, M.L., Okorokova-Façanha, A.l., Façanha, A.R. (2010): Nitric oxide mediates humic acids-induced root development and plasma membrane H^+-ATPase activation. *Planta.* 231, 1025-1036.

Zandonadi, D.B., Santos, M.P., Caixeta, L.S., Marinho, E.B., Peres, L.E.P., and Façanha, A.R. (2016): Plant proton pumps as markers of biostimulant action. *Sci. Agric.* 73, 24–28

Zanin, L., Tomasi, N., Zamboni, A., Sega, D., Varanini, Z., Pinton, R. (2018): Water-extractable humic substances speed up transcriptional response of maize roots to nitrate. *Environ. Exp. Bot.* 147, 167–178

Zanin, L., Tomasi, N., Cesco, S., Varanini, Z., Pinton, R. (2019): Humic substances contribute to plant iron nutrition acting as chelators and biostimulants. *Front. Plant Sci*. 10:675

Zhu, X.F., Wang, B., Song, W.F., Zheng, S.J., Shen, R.F. (2016): Putrescine alleviates iron deficiency via NO-dependent reutilization of root cell-wall Fe in Arabidopsis. *Plant Physiol.* 170, 558–567

Zieliñska-Dawidziak, M. (2015): Plant ferritina source of iron to prevent its deficiency. *Nutrients* 1184–1201

Anexo I

Annex I

Supporting Information belonging to

Long term effect of a leonardite iron humate improving Fe nutrition as revealed *in silico*, *in vivo* and in field experiments

María T. Cieschi[1], Marcos Caballero-Molada[2], Nieves Menéndez[3], Miguel A. Naranjo[2] and Juan J. Lucena[1*]

[1] Department of Agricultural Chemistry and Food Science. Autonomous University of Madrid. c/ Francisco Tomás y Valiente, 7. Ciudad Universitaria de Cantoblanco, 28049, Madrid. Spain.

[2]Institute for Plant Molecular and Cellular Biology. CSIC. Polytechnic University of Valencia. Camino de Vera s/n, 46022 Valencia. Spain.

[3]Department of Applied Physical Chemistry. Autonomous University of Madrid. c/ Francisco Tomás y Valiente, 7. Ciudad Universitaria de Cantoblanco, 28049, Madrid. Spain.

Corresponding author: juanjose.lucena@uam.es, +34 914973968, Fax +34 914973826.

1- Methods for LIH Characterization

- Moisture was measured after heating the humic material overnight at 105ºC[1]

- Ash was determined by weight loss after calcination for 4h at 540ºC

- Oxidizable organic matter (OM) was analyzed by wet oxidation with potassium dichromate[2].

- Elemental composition (C, H, N and S) was carried out by total oxidation of the sample through a fast and complete combustion in a LECO CHNS-932 elemental analyzer.

- Total humic extract (THE), humic (HA) and fulvic acids (FA) content were measured in the soluble fraction of LIH. For THE, the sample was extracted in 0.1M NaOH and 0.1M $Na_2P_2O_7$. The HA was then obtained by precipitation with H_2SO_4 at pH 1.0. The carbon content in THE and HA were determined after oxidation with $K_2Cr_2O_7$ and determination of excess $Cr_2O_7^{2-}$ with $Fe(NH_4)_2(SO_4)_2.6H_2O$. Conversion of C to THE and HA was made using 1.724 as factor. The FA content was estimated by the difference between THE and HA[3].

- pH and the EC (electrical conductivity) were measured in a humic material/water mixture at a ratio of 1:2.5.

- The ratio of absorbance at 465nm and 665nm (E4/E6 ratio) was determined by dissolving 3.0mg of LIH in 10.0mL of 0.05 M $NaHCO_3$ and adjusting the pH to 8.3 with 0.02M NaOH. Absorbance at 465 and 665nm were measured using a Jasco V650 spectrophotometer[4].

- Macro and micronutrients concentration in LIH was analyzed by ICP MS (NEXIon 300XX Perkin Elmer).

- Complexed iron was determined by EN 15962:2011[5]. In brief, 0.1g of LIH was dissolved in type I water and the volume made up to 250.0ml. Two drops of H_2O_2 (33%, P.A.) were added to 20.0mL of sample solution, and the pH increased to 9.0 with 0.5M NaOH. The pH was readjusted to 9.0 after 30min and then after 1 day. Sample was then transferred to a 100.0mL volumetric flask and diluted to the mark with type I water. The solution was filtered through a 0.45µm Millipore filter. The complexed element in the fertilizer was determined after removal of organic compound by HCl-H_2O_2 digestion to allow the assessment of the element by Atomic Absorption Spectrophotometry (AAS) with an

AAnalyst 800 Spectrophotometer (Perkin-Elmer, Madrid, Spain) according to the EU method 9.3[6].

- The LIH was characterized by FT-IR and the spectra of a mixture of LIH and KBr (1.0mg of sample+ 99.0mg of dry KBr) from 7000 to 560cm^{-1} was recorded on a Bruker IFS66v FTIR spectrophotometer fitted with an instrument measuring diffuse reflectance. An X-Ray diffraction pattern and Mössbauer spectra of solid LIH were obtained. Mössbauer spectra was recorded in triangular mode using a conventional spectrometer with ^{57}Co(Rh) source. The analysis of the spectra was made by a non-linear fit using the NORMOS program and the energy calibration was made using a-Fe (6mm) foil. The diffraction pattern was obtained using a Panalytical X'Pert PRO with a Ge (111) as a primary monochromator and graphite as a secondary monochromator, which allows the selection of the CuK α1 radiation that was analyzed with an X'Celerator detector.

2- Soils and soil components used in the interaction experiment

The solid phases and amounts used in the interaction experiments were

- 0.2g acid peat (Tolsa, Buyos, Spain), Commercial black peat was provided by Tolsa S.A. (Buyos, Lugo, Spain). Chemical characteristics[3]: pH (H_2O) = 4.0, oxidizable organic matter (g·kg^{-1}) = 854; total organic matter (dry ashed) (g·kg^{-1}) = 995, carbon in humic acids (g·kg^{-1}) = 302, carbon in fulvic acids (g·kg^{-1}) = 183. Nitrogen (Kjeldahl) (g·kg^{-1}) = 14, C/N = 35.4, CEC ($cmol_c$·kg^{-1}) = 150. Fe and Mn extracted by the Lindsay and Norvell[7] method were 295 mg· L^{-1} and 8.2 mg· L^{-1} respectively

- 0.1g of synthetic Ferrihydrite, Synthetic Ferric Hydroxide prepared in the laboratory following the procedure of Sims et al.[8]. A solution of $FeCl_3$·$6H_2O$ (Probus) is treated with NaOH (Fe^{3+}/OH^- = 1/3) at room temperature. The precipitate is first washed with distilled water for 24 h and then with ethanol (80%) until the pH is 6.0. The brown precipitate is dried in oven at 65º C for 24 h and then ground in a mortar till a fine powder is obtained. Such material is X Ray identified as a 6 lines ferrhydrite with high specific surface (220 m^2·g^{-1}) that allows a high interaction with the chelates.

-0.2g of Ca-montmorillonite (STx-1, Clay Minerals Repository, USA), from Gonzales County (Texas, USA)

-2.0g of calcium carbonate (Probus),

-2.0g of a calcareous soil from Picassent (Valencia, Spain), Picassent soil (sandy clay soil, 380.0g kg^{-1} total calcium carbonate, 89.0g kg^{-1} active lime, 9.2g kg^{-1} organic matter, pH in water of 7.7) was characterized previously by López-Rayo et al.[9]

-2.0g of a calcareous soil from La Almunia (Zaragoza, Spain). La Almunia soil (sandy loam soil, 238.0g kg^{-1} total calcium carbonate, 139.0g kg^{-1} active lime, 12.6g kg^{-1} organic matter, pH in water of 8.6) was characterized by Álvarez-Fernández et al.[10]

3- Procedures used in the experiments using a *Saccharomyces cerevisiae* strain

Cell growth rate: The cell growth rate was evaluated during the exponential phase (48 hours later) by measuring the optical density with a Bioscreen C bioanalyzer Thermic Labsystems, Turku, Finland. Optical density readings every 30 minutes at wavelength range (420-580nm) were carried out in order to reduce the background contributions. Pre inoculum saturated SD media YNB without iron, was first diluted 150 times in appropriate media before being placed in the multi-well plate. The iron treatments applied were the followings: Control (without iron application), FeEDDHA and LIH. The doses for the iron treatments were 0.5, 1.0, 5.0 and 10.0µg mL^{-1}. Three replicates were done and the mean data were subsequently corrected to avoid losing of optical densities linearity with high cell densities[11].

Quantification of mRNA using RT-qPCR: *Sacharomyces cerevisiae* strain was growth up to exponential phase (Abs_{660} ≈ 0.4) in SD media and treated with LIH and FeEDDHA (10.0mg L^{-1}). Yeast RNA was isolated according to Li et al.[12]. Thereafter, RNA was purified using the Nucleo Spin RNA kit (Macherey-Nagel, Düren, Germany). For the reverse transcription a RT-qPCR Maxima First Strand cDNA Synthesis kit (Thermo Scientific, Massachusetts, USA) was used and the 5× Pyro Taq Eva Green qPCR Mix Plus kit (ROX) (Cultek Molecular Bioline, Madrid, Spain) was used for the quantitative RT-PCR analysis. Genes analyzed and relative primers are listed in Table S.1. As a reference gene, UBC6 was used. Real-Time PCR quantification was performed in a 7500 Real-Time PCR System (Applied Biosystems, Foster City, CA, USA), in three technical replicates.

Determination of iron intra-cellular content: Cells grown up to medial exponential phase (150.0ml) in SD media YNB without iron, treated with Fe EDDHA and LIH (1.0mg L^{-1}) and untreated (Control) were collected and washed by centrifugation with 50.0mM Tris-HCl, pH 6.5, 10.0mM EDTA. Cell pellets were digested in 1.0ml of 5:2 nitric acid: perchloric acid at 80°C for $1h^{13}$. After digestion, the samples were diluted to 4.0ml with deionized water and then measured by AAS (GBC Scientific Equipment Pty Ltd, Victoria, Australia). All samples were measured in triplicate, and the experiment was repeated at least three times.

Table S.1. Specific forward and reverse primer sequences used in quantitative RT-PCR

Gene	Primer forward (5'-3')	Primer reverse (5'-3')
FET3	TTCAGCATGCCTTCATTCCTAC	TTCGGTCGCATCTTCCATATC
FTR1	GAGACAACTGTTTGCCAAGATG	CGAGGAATGACTGGTAGTTTGC
SIT1	CGGTATCATTGGCTCTTTGTG	GAGGTTACTACCGCCATTCTTG
TIS11	ACGGACTCGGCGAATTAAAG	CTGCCATAAGGACAATAACCTAGT
UBC6	CGGCAAATACAGGTGATGAAAC	TTCAGCGCGTATTCTGTCTTC

References:

(1) AFNOR. *NF U44-171 Sludge. Organic soils conditioners. Growth media. Determination of dry matter.* 1982; p 3. Association Française de Normalisation Editions. Paris. France.

(2) AFNOR. *NF U44-160 Organic soil conditioners and organic material for soil improvement. Determination of total organic matter. Calcination method.*; 1985; p 3. Association Française de Normalisation Editions. Paris. France.

(3) Royal Decree 1110/1991 *Oficial methods for organic fertilizers analysis.* (In spanish). BOE (Official Bulletin of the State).**1991**, *170*, 23725-23730.

(4) Chen, Y.; Senesi, N.; Schnitzer, M. Information provided on humic substances by E4/E6 ratios. *Soil Sci. Soc. Am. J.* **1977**, *41*, 352–358.

(5) UNE-EN 15962:2011. Fertilizers. Determination of the complexed micronutrient content and of the complexed fraction of micronutrients. **2011**. AENOR Editions. Madrid. Spain

(6) Regulation (EC) No 2003/2003 of the European Parliament and of the Council of 13 October **2003** relating to fertilizers. Official Journal of the European Union L304, 1–194.

(7) Lindsay, W. L. and Norvell, W. A. Development of a DTPA soil test for zinc, iron, manganese, and copper. *Soil Sci. Soc. Am. J*. **1978**, 42, 421–428.

(8) Sims, J. and Bingham, F. Retention of boron by layer silicates, sesquioxides and soil materials. II. Sesquioxides. *Soil Sci. Soc. Amer*. **1968**. 32:364-369.

(9) López-Rayo, S.; Hernández, D.; Lucena, J. J. Chemical evaluation of HBED/Fe^{3+} and the novel HJB/Fe^{3+}. Chelates as fertilizers to alleviate iron chlorosis. *J. Agric. Food Chem.* **2009**, *57*, 8504–8513.

(10) Álvarez-Fernández, A.; Paniagua, P.; Abadía, J.; Abadía, A. Effects of Fe deficiency chlorosis on yield and fruit quality in peach (*Prunus persica* L. Batsch). *J. Agric. Food Chem.* **2003**, *51*, 5738–5744.

(11) Warringer, J. and Blomberg, A. Automated screening in environmental arrays allows analysis of quantitative phenotypic profiles in Saccharomyces cerevisiae. *Yeast* **2003**, *20*, 53–67.

(12) Li, J.; Liu, J.; Wang, X.; Zhao, L.; Chen, Q.; Zhao, W. A waterbath method for preparation of RNA from *Saccharomyces cerevisiae. Anal. Biochem.* **2009**, *384*, 189–190.

(13) Li, L. and Kaplant, J. Defects in the yeast high affinity iron transport system result in increased metal sensitivity because of the increased expression of transporters with a broad transition metal specificity. *J. Biol. Chem.* **1998**, *273*, 22181–22187.

Anexo II

Annex II

Supplementary Materials

Eco-Friendly Iron-Humic Nanofertilizers Synthesis for the Prevention of Iron Chlorosis in Soybean (*Glycine max*) Grown in Calcareous Soil

María T. Cieschi[1], Alexander Yu. Polyakov[2, 3], Vasily A. Lebedev[4], Dimitry S. Volkov[4, 6], Denis A. Pankratov[4], Alexey A. Veligzhanin[5], Irina V. Perminova[4*], Juan J. Lucena[1*]

[1]Autonomous University of Madrid. Department of Agricultural Chemistry and Food Science. Madrid. Spain.

[2]Kurnakov Intitute of General and Inorganic Chemistry. Russian Academy of Sciences, Moscow. Russia

[3]Department of Materials Science, Lomonosov Moscow State University, Moscow. Russia

[4] Department of Chemistry, Lomonosov Moscow State University Moscow. Russia

[5]National Research Center "Kurchatov Institute", Akademik Kurchatov Square 1, 123098 Moscow, Russia

[6] V.V. Dokuchaev Soil Science Institute, Moscow, Russia

Determination of the Fe-MCC

Maximum complexing capacity corresponds to the maximum iron content, Fe (III) that can be bound to the potassium humate structure without clotting. To determine the Fe-MCC of the potassium humate, based on the work of Villén et al. (2007) and modified for us, was used. In brief, increasing volumes of a c_{Fe} = 200 g L^{-1} solution of $FeSO_4 \cdot 7H_2O$ for Fe (II) were added to 15 ml of a potassium humate solution (28 g C org L^{-1}). The pH was raised to 9.0 with KOH 1M solution. After one day in the dark, the pH was increased again to 9.0. After 2 h, the solutions were transferred to a 50-ml volumetric flask and the volume made up to 50 ml. The solutions were subsequently centrifuged at 10000 min^{-1} at room temperature for 10 min, and the supernatants filtered using 0.45 µm filters of cellulose acetate (Schleicher & Schuell). The complexed element was determined by inductively coupled plasma - optical emission spectrometry (ICP-OES) with a 5110 ICP-OES (Agilent Technologies, U.S.A.).

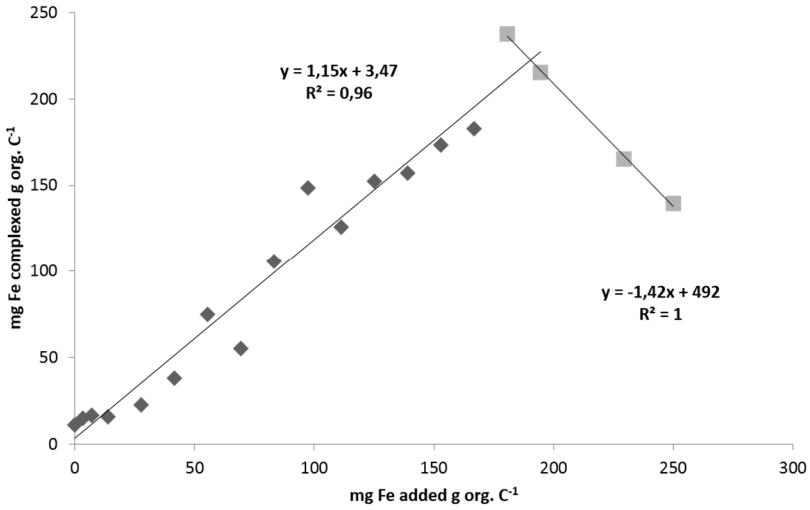

Figure SM1: Typical tritation curve for the determination of the maximum complexing capacity (Fe-MCC) of the potassium humate used with Fe (III).

Reference

Villén, M., Lucena, J.J., Cartagena, M.C., Bravo, R., García-Mina, J. and de la Hinojosa, M.I.M. (2007). Comparison of two analytical methods for the evaluation of the complexed metal in fertilizers and the complexing capacity of complexing agents. *J. Agric. Food Chem* 55, 5746–5753. doi.org/10.1021/jf070422t

Determination of Fe using ICP AES spectroscopy

An axial ICP-AES 5100 spectrometer with an SPS4 auto sampler (Agilent Technologies, USA) was used for ICP-AES measurements with a low flow axial quartz torch with 2.4 mm inner diameter injector tube, a double-pass glass cyclonic spray chamber, a glass pneumatic nebulizer (Agilent Technologies, USA), and a Trident Internal Standard Kit (Glass Expansion, Australia). A peristaltic pump used the white/white polyvinyl chloride pump tube for feeding and the blue/blue one for drain. A Sc (20 mg/L) internal standard solution was added online (orange/blue polyvinyl chloride pump tube) to increase the accuracy of measurements. Conditions of ICP–AES measurements are presented in Table 1. Results were collected and processed by ICP Expert software 2.0.5 (Agilent Technologies, USA).

Table SM1. The conditions of ICP–AES measurements

Conditions for all lines registrations	
RF power (kW)	1.40
Plasma flow (L/min)	18.0
Axial flow (L/min)	1.50
Nebulizer flow (L/min)	0.95
Replicate read time (s)	20
Instrument stabilization delay (s)	25
Replicates	6
Sample introduction settings	
Sample uptake delay (s)	25
Pump rate (rpm)	12

Deionized water (18.2 MΩ × cm from a Milli-Q Academic system, Millipore, France) was used for the preparation of all the solutions and washing. An iron standard solution, 1000 mg/L (High Purity Standards) was used for calibration in the range 0.01–100 mg/L. An internal standard solution of Sc (20 mg/L) was prepared from Sc standard solution, 1000 mg/L (High Purity Standards).

XRD characterization of ^{57}Fe-NFs

According to the XRD data, no iron-containing phases were observed in the obtained samples. Sample F contains niter (alpha-KNO_3, #71-1558) as a major crystalline phase, sample M – $K_3Na(SO_4)_2$ and Na_2SO_4 , sample S - arcanite (K_2SO_4).

Obtained XRD patterns and results of leBail refinement are demonstrated on

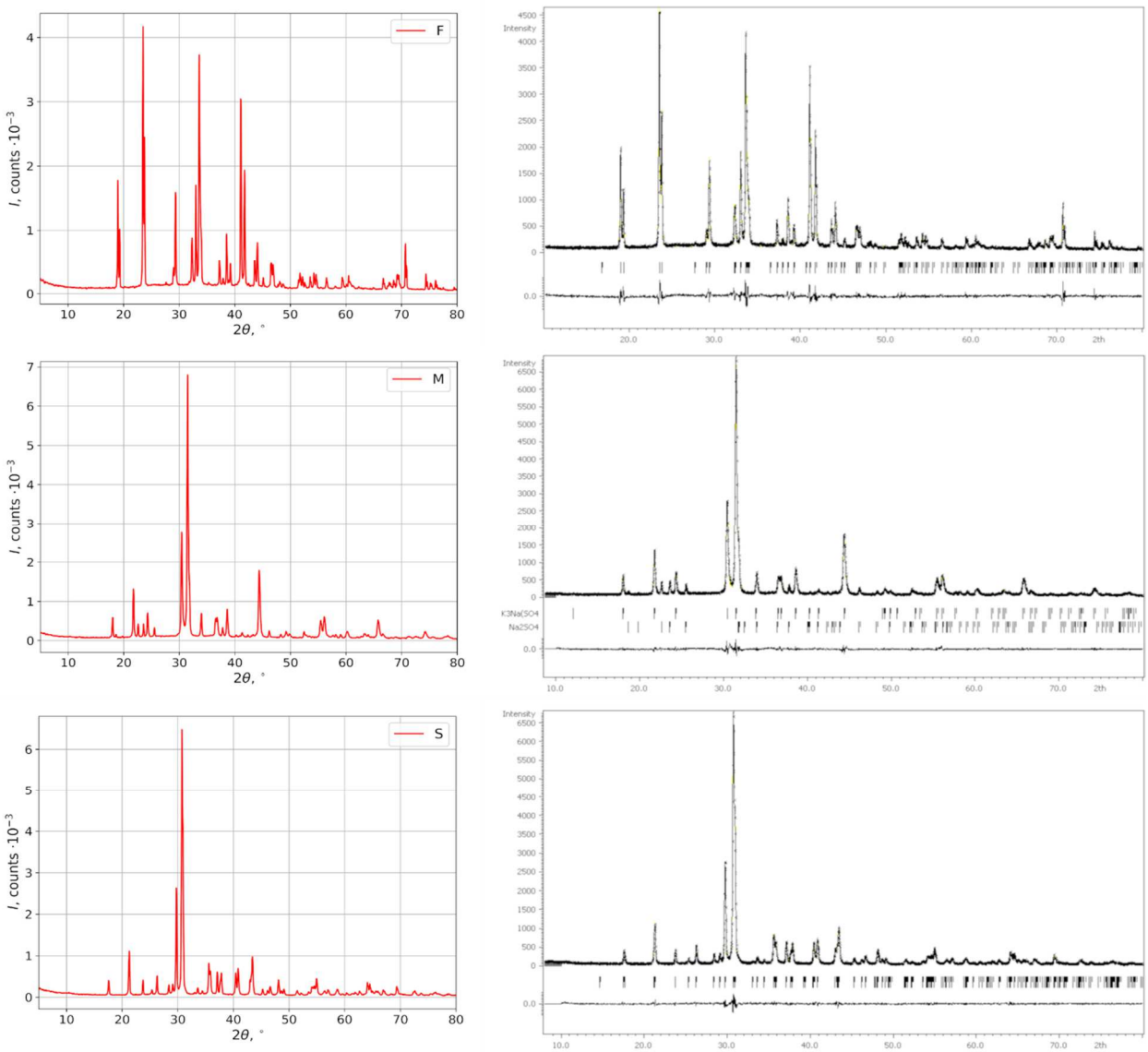

Figure SM2. XRD pattern of the product F compared to the KNO_3 pattern (a), XRD pattern of the product M compared to $K_3Na(SO_4)_2$ and Na_2SO_4 patterns (b), XRD pattern of the product S compared to the $K_2(SO_4)$ pattern

XRD of the reference samples

According to the XRD data, the reference sample of goethite contains pure goethite (*Pmcn*, a 5.4182, b 9.1694, c 6.4389). Samples of ferrihydrite (Fh), obtained with pH value of 7 and 8, demonstrate XRD patterns, usual for the 2-line ferrihydrite.

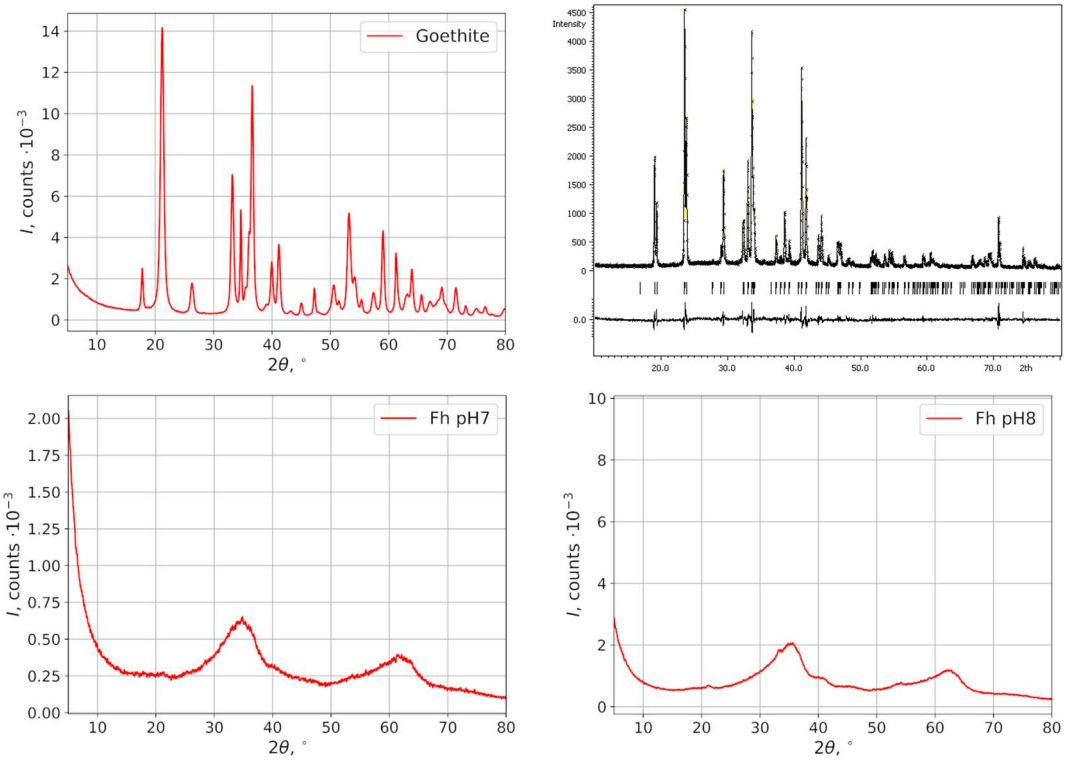

Figure SM3. XRD patterns of goethite and Fh preparations

Electron Energy Loss Spectra

The observed core loss lines of iron for the sample F are shown in Fig S4. For EFTEM imaging the M-line was chosen due to its high relative intensity.

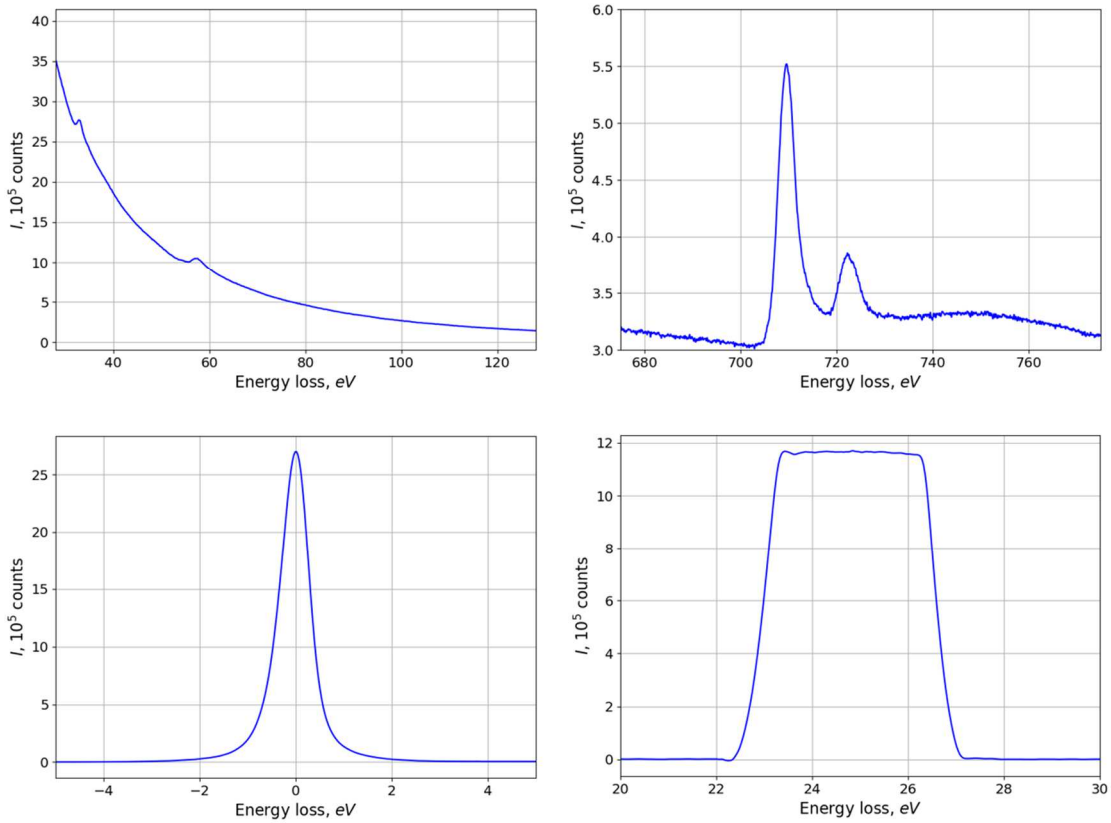

Figure SM4: EELS of the product F in different energy ranges, zero loss peak and the selected energy range (slit size) for the EFTEM.

Zero-loss images

In order to increase the contrast of iron-containing NP, the elastic (zero-loss) imaging was used. Obtained images for F and M samples are exemplified at Figure SM5.

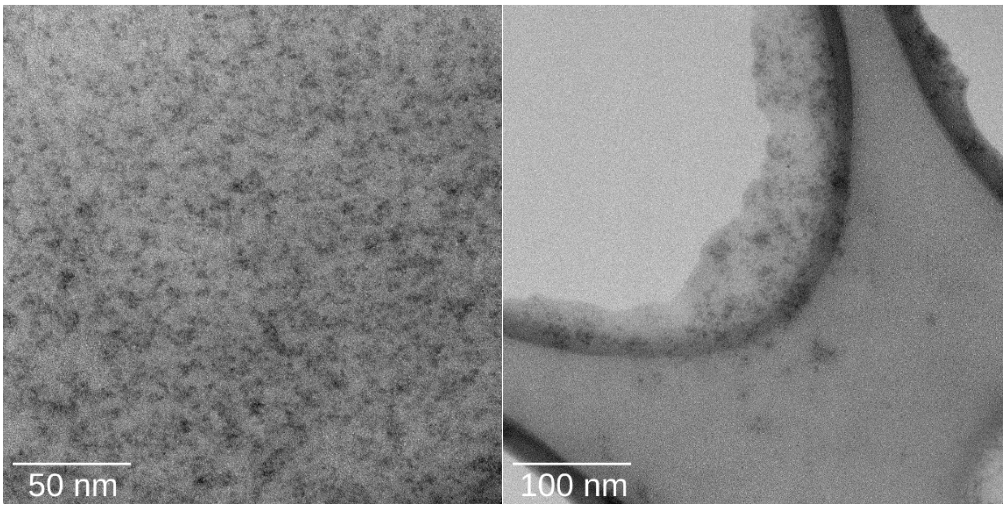

Figure SM5. Zero-loss EFTEM images of the F and M samples, respectively

Electron diffraction data

The selected areas and corresponding ED patterns are shown in Figure SM6.

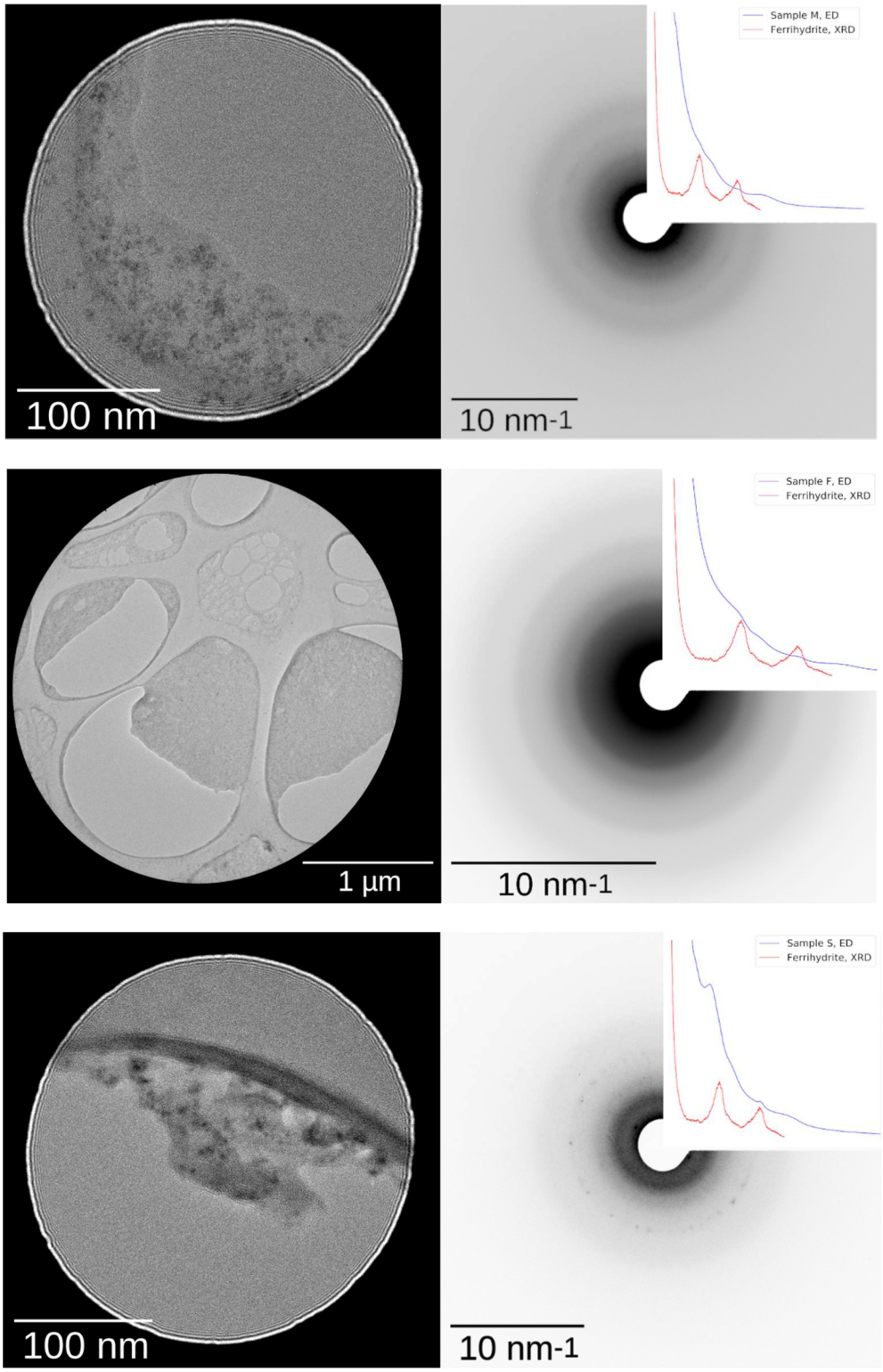

Figure SM6. SAED of F, M, and S samples: the selected area for the ED, and collected ED pattern with the integration result and XRD pattern of ferrihydrite inn the inset.

XANES and EXAFS studies

Fe K-line XANES spectra of F, M, S and reference samples are demonstrated in Figure SM9.

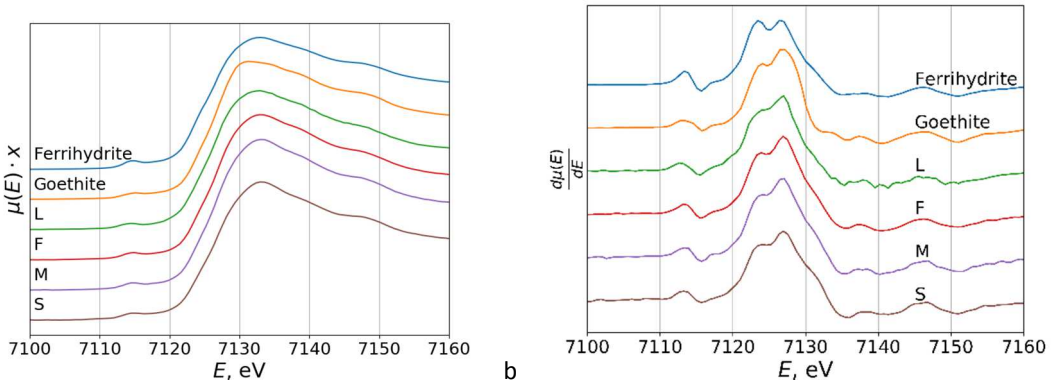

a b

Figure SM7. Fe K-line XANES spectra (a) and the first derivatives of the XANES spectra (b) of three ^{57}Fe-labelled nanofertilizers and reference samples of ferrihydrite, goethite, and the parent humate (L) (a)

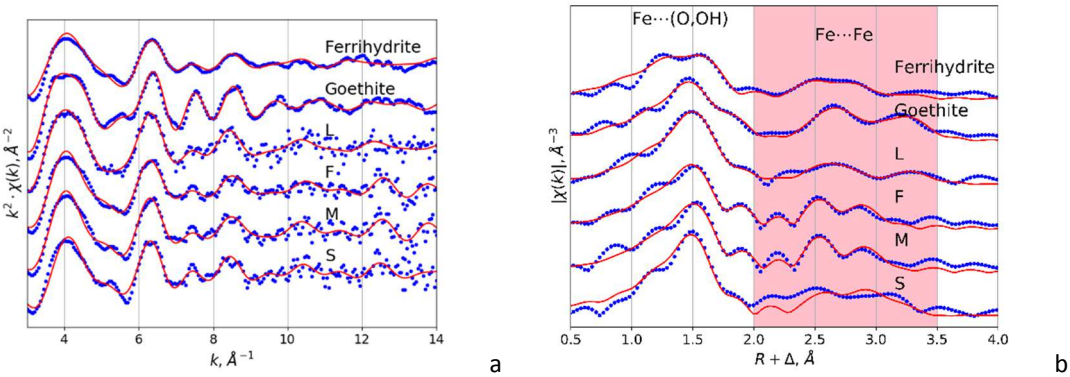

a b

Figure SM8. EXAFS spectra in k- (a) and R-space (b) of three ^{57}Fe-labelled nanofertilizers and reference samples of ferrihydrite, goethite, and the parent humate (L).

Mössbauer spectroscopy characterization of reference samples (goethite and ferrihydrite) and ^{57}Fe-NFs.

The Mössbauer spectrum at room temperature for a reference goethite sample is a distorted sextet with asymmetrically broadened lines characteristic for microcrystalline of magnetically ordered substances with a high blocking temperature. The Mössbauer spectrum is satisfactorily described by the sextet by the many-state superparamagnetic relaxation model (Jones and Srivastava 1986) with parameters: δ=0.37 mm/s, Δ=-0.26 mm/s, H_{hf}= 38.5 T (Figure SM9a). From the data obtained, taking the value of magnetic anisotropy energy constant equal to 10^3 J/m^3 (Shinjo 1966), one can estimate the size of goethite crystallites as 34.6 nm. The amount of the paramagnetic impurity phase was about 4%. At the boiling point of liquid nitrogen, the width of sextet lines is significantly reduced, which made it possible to describe the ferromagnetic part of the spectrum by a superposition of two sextets with hyperfine parameters corresponding to goethite (Mørup et al. 1983): δ_1=0.47 mm/s, Δ_1=-0.24 mm/s, H_{hf1}= 49.6 T, S_1=72%; δ_2=0.48 mm/s, Δ_1=-0.22 mm/s, H_{hf1}= 48.0 T, S_1=25%. The content of the paramagnetic phase of the impurity does not exceed 3% (Figure SM9b).

The Mössbauer spectrum of a control sample of ferrihydrite at room temperature is a symmetric paramagnetic doublet with markedly broadened lines. The description of the experimental spectrum using the quadrupole splitting distribution functions shows that the quadrupole splitting has a bimodal distribution (Figure SM10a). When the temperature drops to the boiling point of liquid nitrogen, due to the appearance of magnetic ordering in the structure of the ferrihydrite, the paramagnetic doublet increases noticeably, the distribution of quadrupole splitting turns into a unimodal representation with a simultaneous significant increase in the dispersion of the distribution. (FigureSM10b). In addition, at low temperature about 3% of a magnetically ordered phase is observed, with a magnetic hyperfine field H_{hf} = 48.2 T, corresponding to that observed in low-temperature spectra for ferrihydrite (Zhao et al. 1994). The results of the model description of the paramagnetic part of experimental spectra using a pair of nested symmetric doublets are presented in Table SM2.

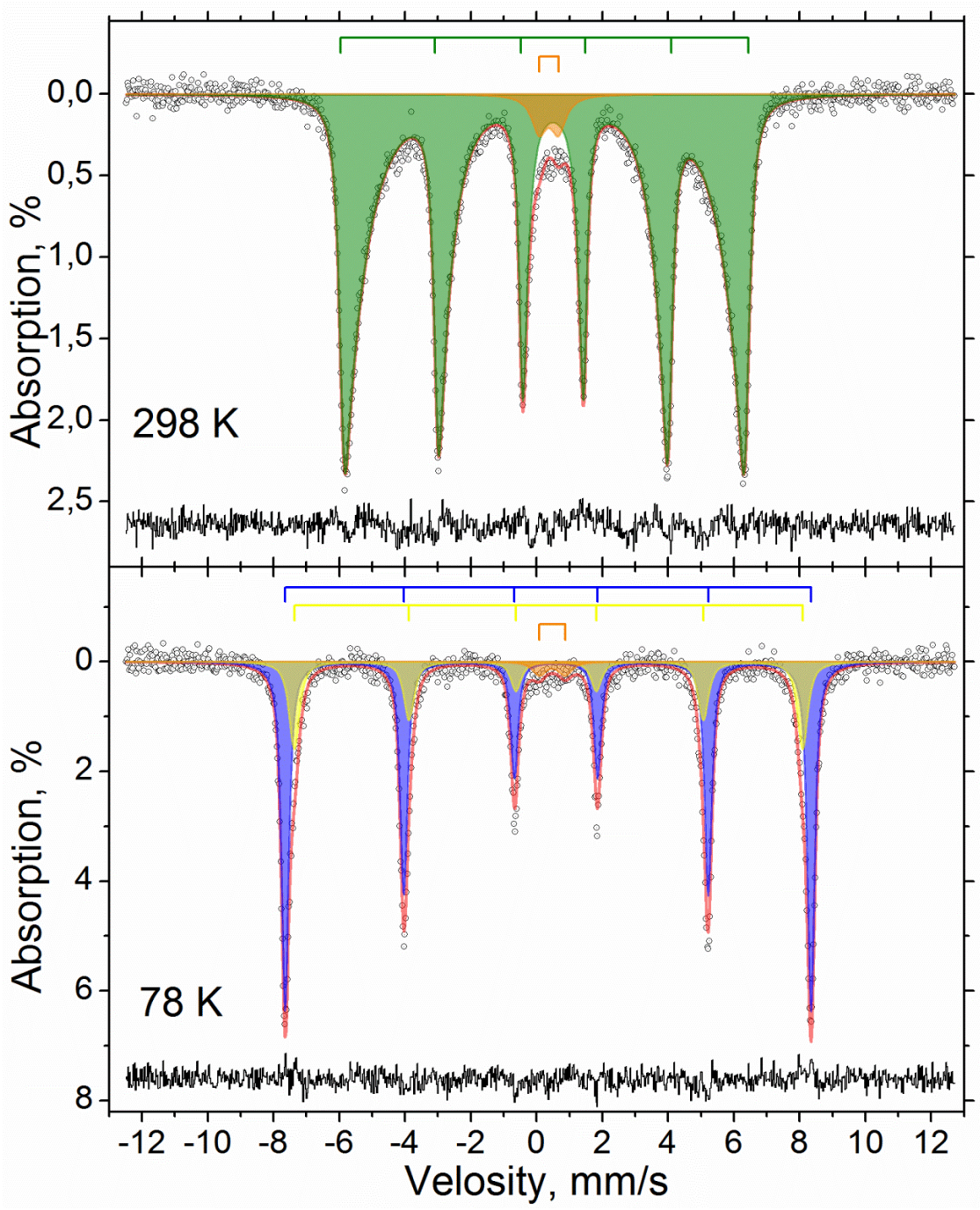

Figure SM9. Mössbauer spectra of the goethite sample recorded at 298 (a) and 78 (b) K.

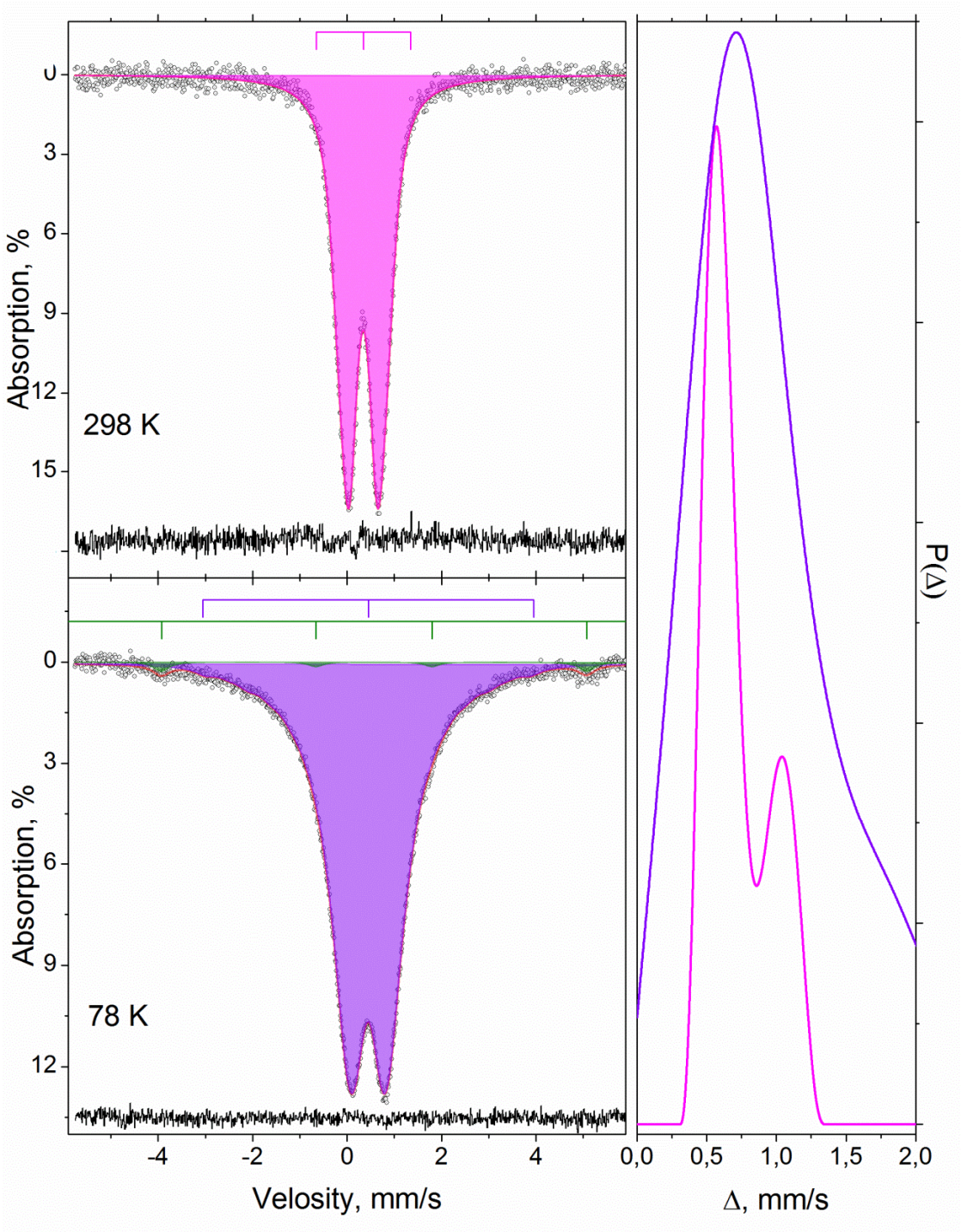

Figure SM10. Mössbauer spectra of the ferrihydrite sample recorded at 298 (a) and 78 (b) K and the quadrupole splitting distributions (c) for these spectra.

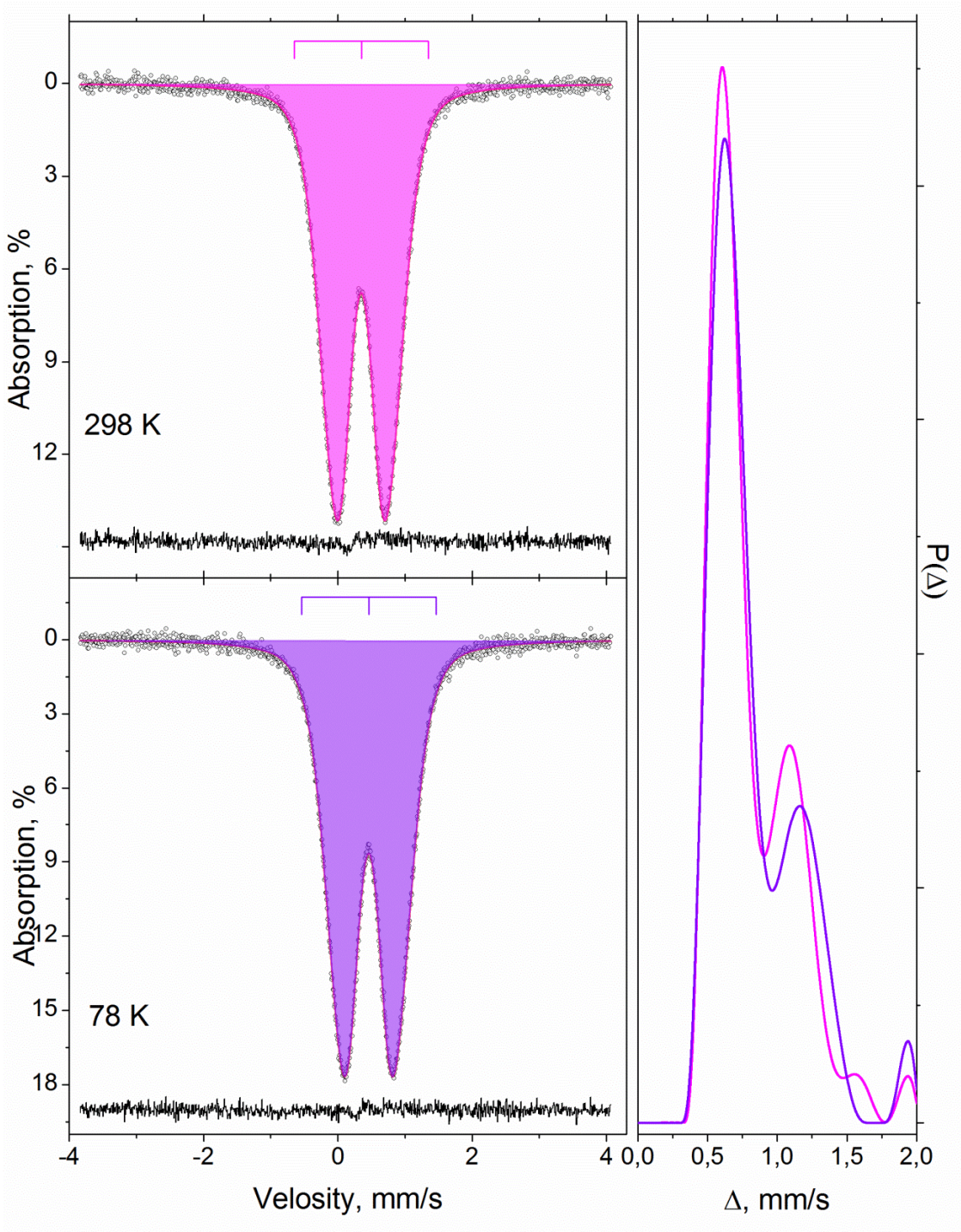

Figure SM11. Mössbauer spectra of the F sample recorded at 298 (a) and 78 (b) K and the quadrupole splitting distributions (c) for these spectra.

In addition to the non-model description of the paramagnetic part of the Mössbauer spectra for the three samples, a description of the model in the form of by superposition of two embedded symmetrical quadrupole doublets can be proposed (Table SM2).

Table SM2. Data of the Mössbauer spectra recorded at different temperatures

Temperature, K		298				78			
Sample	Subspectrum	δ*	Δ	Γ_{exp}	S	δ	Δ	Γ_{exp}	S
		mm/s			%	mm/s			%
Ferrihydrite	1	0.35±0.01	0.82±0.03	0.55±0.01	75±8	0.45±0.01	1.2±0.3	1.7±0.1	42±16
	2	0.35±0.01	0.50±0.01	0.34±0.03	25±8	0.45±0.01	0.78±0.01	0.74±0.07	55±16
M	1	0.35±0.01	0.85±0.03	0.56±0.01	80±9	0.46±0.01	0.87±0.05	0.57±0.01	78±11
	2	0.34±0.01	0.52±0.02	0.35±0.04	20±9	0.46±0.01	0.54±0.02	0.35±0.05	22±11
F	1	0.35±0.01	0.91±0.06	0.55±0.01	70±12	0.46±0.01	0.94±0.06	0.57±0.01	69±12
	2	0.35±0.01	0.56±0.02	0.37±0.03	30±12	0.46±0.01	0.57±0.02	0.38±0.03	31±12
S	1	0.34±0.01	0.86±0.05	0.54±0.03	42±10	0.44±0.01	0.82±0.04	0.67±0.01	53±7
	2	0.34±0.01	0.53±0.03	0.40±0.03	23±9	0.46±0.01	0.54±0.02	0.38±0.07	11±7
	3	0.28±0.02		4.0±0.3	36±2	0.52±0.04		6.9±0.4	36±1

*δ, isomer shift; Δ, quadrupole splitting; Γ_{exp}, line width; S, relative area of a subspectrum.

The hyperfine parameters of quadrupole doublets for all samples correspond to iron (III) atoms in the octahedral coordination environment of oxygen (Pankratov 2014). They are similar to one another, and are statistically poorly distinguishable (see Table SM2). Analyzing the hyperfine parameters of quadrupole doublets at two temperatures for all samples, we note a linear correlation of the width of the resonance lines of the quadrupole splitting (Figure SM12), which almost coincides with the previously observed for oxo-hydroxy compounds obtained in the presence of nanohydroxyapatite (Pankratov 2017).

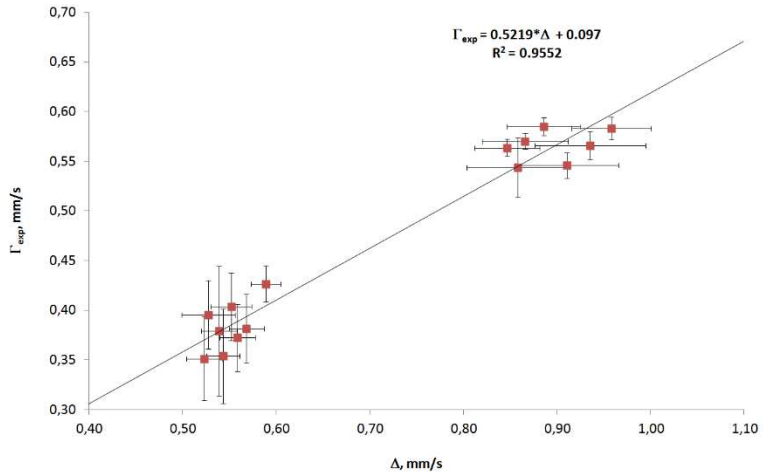

Figure SM12. Correlation of quadrupole splittings and widths of resonance lines for quadrupole doublets for Mössbauer spectra of the samples studied (data for different temperatures are combined, data for the first doublet of the S sample at 78 K were not taken into account).

In this paper, we came to the conclusion that the reason for this dependence is a partial contribution of the molecular-ion fragments of the series H_2O-OH^--O^{2-} surrounding the iron atoms to the parameters of the Mössbauer spectra associated with their dynamic properties and electromagnetic interactions.

References

Jones, D.H. and Srivastava, K.K.P. (1986). Many-state relaxation model for the Mossbauer spectra of superparamagnets. *Phys. Rev. B: Condens. Matter Mater*. *Phys*. 34, 7542−7548. doi.org/10.1103/PhysRevB.34.7542

Mørup, S., Bo Madsen, M., Franck, J., Villadsen, J. and Koch, C.J.W. (1983). A new interpretation of Mössbauer spectra of microcrystalline goethite: "Super-ferromagnetism" or "super-spin-glass" behavior? *J. Magn. Magn. Mater.* 40, 163-174. doi.org/10.1016/0304-8853(83)90024-0

Pankratov, D.A. (2014). Mössbauer study of oxo derivatives of iron in the Fe_2O_3-Na_2O_2 system. *Inorg. Mater*. 50, 82-89. doi.org/10.1134/S0020168514010154

Pankratov, D.A., Dolzhenko, V.D., Ovchenkov, E.A., Anuchina, M.M. and Severin, A.V. (2017). Properties of iron-containing nanohydroxyapatite-based composites. *Inorg. Mater*. 53, 89–98. doi.org/10.1134/S0020168517010125

Shinjo, T. (1996) Mössbauer effect in antiferromagnetic fine particles. *J. Phys. Soc. Jpn*. 21, 917-922 doi.org/10.1143/JPSJ.21.917

Zhao, J, Huggins, F.E., Feng, Z. and Huffman, G. (1994). Ferrihydrite: surface structure and its effects on phase transformation. *Clays. Clay. Miner*. 42, 737-746 doi.org/10.1346/CCMN.1994.0420610